1986

A SIMULATION PROGRAM FOR MULTIPLE TUBE-ROW TWO-PHASE THERMOSIPHON COIL LOOP HEAT EXCHANGERS.

GURSARAN DAS. MATHUR
University of Windsor

CANADIAN THESES

THÈSES CANADIENNES

NOTICE

The quality of this microfiche is heavily dependent upon the quality of the original thesis submitted for microfilming. Every effort has been made to ensure the highest quality of reproduction possible.

If pages are missing, contact the university which granted the degree.

Some pages may have indistinct print especially if the original pages were typed with a poor typewriter ribbon or if the university sent us an inferior photocopy.

Previously copyrighted materials (journal articles, published tests, etc.) are not filmed.

Reproduction in full or in part of this film is governed by the Canadian Copyright Act, R.S.C. 1970, c. C-30.

AVIS

La qualité de cette microfiche dépend grandement de la qualité de la thèse soumise au microfilmage. Nous avons tout fait pour assurer une qualité supérieure de reproduction.

S'il manque des pages, veuillez communiquer avec l'université qui a conféré le grade.

La qualité d'impression de certaines pages peut laisser à désirer, surtout si les pages originales ont été dactylographiées à l'aide d'un ruban usé ou si l'université nous a fait parvenir une photocopie de qualité inférieure.

Les documents qui font déjà l'objet d'un droit d'auteur (articles de revue, examens publiés, etc.) ne sont pas microfilmés.

La reproduction, même partielle, de ce microfilm est soumise à la Loi canadienne sur le droit d'auteur, SRC 1970, c. C-30.

THIS DISSERTATION
HAS BEEN MICROFILMED
EXACTLY AS RECEIVED

LA THÈSE A ÉTÉ
MICROFILMÉE TELLE QUE
NOUS L'AVONS REÇUE

NL-339 (r. 86/06)

Canada

A SIMULATION PROGRAM FOR MULTIPLE TUBE-ROW TWO-PHASE THERMOSIPHON COIL LOOP HEAT EXCHANGERS

A Dissertation
Submitted to the Faculty of Graduate Studies through the Department of Mechanical Engineering in Partial Fulfillment of the Requirements for the Degree of Doctor of Philosophy at the University of Windsor

By

Mathur, Gursaran Das

ISBN 0-315-31993-3

ABSTRACT

A computer algorithm has been developed to simulate two-phase thermosiphon coil loop heat exchanger systems in which each coil consists of parallel rows of tubes running between common headers. The coils may be oriented in any arbitrary fashion relative to the gravitational field, subject to the limitation that the condensate must be able to return by gravity to the evaporator and may be subject to different external flow and thermal conditions. The developed program requires the operator to specify the source and sink fluid approach temperature and face velocities; various source, sink, and working fluid properties; the source and sink fluid to coil inner surface heat transfer coefficients; and the size and orientation of the various system components.

The simulated performance was compared to each of the following three very different experimental systems:

1. The evaporator and condenser coils used by Raza (12) each consisted of three coplanar independently water jacketed tubes. The plane of each coil could be inclined from the vertical to simulate the operating conditions of an inclined, one-row coil. They could also be rotated in a vertical plane to simulate the effect of unequal charges in the tube rows of an inclined three-row evaporator coil. The effect

of static charge, temperature difference, unequal heating of each evaporator tube row and unequal charge in each evaporator tube row was studied on the performance of the system. The working fluid was R-11.

2. An air-to-air heat exchanger system which consisted of four thermosiphon loops arranged in a counter flow configuration in the air ducts. Each of the coils in each loop consisted of two rows of tubes with wavy plate fins. In this system, studied by Stauder (17) and by Kosnik & Bertoni (15) the evaporator tubes were vertical and the condenser tubes were inclined at 45 degrees. The evaporator and the condenser coils had the same face area and were installed in warm and cold ducts having the same mass flow rates. The effect on the performance of the system of different air mass flow rates, various static charges and of sequentially increasing and decreasing the overall temperature difference was studied. The working fluid used in the system was R-11.

3. Bergevin et al. (23) studied a system using R-113 in which a single tube evaporator was subject to a constant heat flux boundary condition. The evaporator tube was inclined at an angle of 60 degrees from the horizontal. The condenser was water jacketed. The working fluid was in a subcooled state at the entry to the evaporator tube. The effect of the heat flux was studied on the performance of the system.

For these systems, the results predicted by the computer simulation program agreed very well in most cases with the experimentally determined values of the overall heat transfer rate, the average heat transfer coefficient for each tube, the loop conductance and the wall superheat for either the heating or the cooling mode. A major limitation at present is the need for a correlation to determine the conditions under which boiling will initiate during the system startup.

ACKNOWLEDGEMENTS

The author wishes to express his profound gratitude to Dr. T.W. McDonald for his invaluable guidance, encouragement, keen interest and patience throughout the course of this study.

The author would like to thank to Mr.S. Raza, Mr. F.A. Stauder, Miss M.A. Kosnik & Miss G. Bertoni for providing their experimental data for the comparison with the author's computer generated data.

Acknowledgement is made to the National Research Council of Canada for providing financial support.

The author would like to thank his parents, who were a great source of inspiration without which this study could not have been possible.

To my parents

TABLE OF CONTENTS

LIST OF FIGURES

LIST OF TABLES

NOMENCLATURE

A - Surface area (sq m)

A_x - Cross-sectional area (m^2)

Bo - Boiling number ($q/G\ h_{fg}$)

Cp - Specific heat (kj/kg K)

Csf - A constant on Rohsenow's pool boiling correlation

D - Tube diameter (m)

E - Effectiveness

f - Friction factor (Btu/hr/sq.ft/F)

F - Fouling factor

Fl - Froude number

G - Mass flux ($Kg/m^2/s$)

Gn - Graetz number (Re Pr D/z)

g - Gravitational constant

h - Heat transfer coefficient ($W/m^2/K$)

h_{fg} - Latent heat of vaporization ($_KJ/kg$)

J - Superficial velocity (m/s)

K - Thermal conductivity (W/m K) , Velocity head factor

L - Tube length (m)

M - Entrance effect factor, Mach number , Number of tubes per row

$\dot{m}$ - Mass flow rate (kg/sec)

N - Number of tube rows

Nu - Nusselt number (h D/K)

p - Pressure (N/m^2)

Pe - Peclet number (Re Pr)

Pr - Prandtl number (μ Cp/ K)

Q - Heat flow rate (W)

q - Heat flux (W/m^2)

R - Thermal resistance (m^2 K/W)

r - A constant in Rohsenow's pool boiling correlation

Re - Reynolds number (ρ V D / μ)

R - Liquid holdup , liquid fraction

S - Slip ratio , given by equation 3.7

St - Stanton number (h/ρC V)

T - Temperature (c)

U - Velocity (m/s), Conductance (W/m^2 K)

V - Velocity (m/s)

We - Weber number

x - Quality

X - Lockhart-Martinelli parameter

xc - Critical quality

z - Distance along the tube axis (m)

z^* - Dimensionless parameter (2z/D)/Pe

GREEK SYMBOLS:

σ - Surface tension (N/m)

ρ - Density (kg/m^3)

μ - Dynamic viscosity (kg/m s)

δ - Superheated boundary layer thickness (m)

ξ - Eddy diffusivity (m^2/s)

α - Void fraction

ϕ - Parameter defined in section 3.2.6

β - Inclination angle of evaporator from the horizontal, degrees

γ - Inclination angle of condenser from the horizontal , degrees

λ - Latent heat of vaporization (kJ/Kg)

SUBSCRIPT:

a - acceleration , approach

av - average

b - bulk, boiling, bottom

c - condenser, cold, critical conditions, condensation

ce - condenser external

ci - condenser internal

co - condenser outside

cw - condenser wall

cr - critical conditions

d - based on diameter, downstream

e - evaporator, exit, element

ee - evaporator external

ei - evaporator inside

eo - evaporator outside

ew - evaporator wall

eȝ - effective h in the dryout region, defined by equation 3.61

eq - equivalent

f - fluid, frictional

g - vapour

gs - vapour superficial

h - hydrostatic, hot

he - heat exchanger

ib - incipient boiling condition

l - liquid

lp - liquid phase

ls - liquid superficial

m - mean, metal

pb - pool boiling

r - recirculation

s - surface condition

sat - saturation condition

scb - sub cooled boiling

t - total, transport

tp - two-phase

v - vapour

vp - vapour phase

w - wall

z - point value

2e - effective h in subcooled boiling region, defined by equation 3.44

CHAPTER I

INTRODUCTION

1.1 GENERAL

Until several years ago, energy sources had been both inexpensive and abundant. Today's situation, however, is drastically different. Fuel costs have risen dramatically and are continuing on the rise. The increase in the cost of the energy has brought about a desire on the part of the consumers to use energy as efficiently as possible. According to the projections made by the Federal Government, 53 % of Canada's total energy consumption in the 1980's will be rejected in the form of waste. Because this waste will generally be in the form of thermal energy, heat reclaming equipment and systems have become very important and thus are receiving increased attention.

Heat reclamation can be divided into three major categories: (1) heat which is recovered from process flue gases and then recycled directly into the process for reuse; (2) recovered waste heat from process exhausts which is used to preheat make up air during heating seasons; and (3) the use of comfort exhaust to preheat ventilation fresh air during the heating season, and to precool it during the summer months.

Several different classes of air-to-air heat exchangers are currently used for waste heat recovery. If the two air streams are adjacent to one another , compact heat exchangers, rotary regenerative heat exchangers or heat pipe heat exchangers may be effectively used. If the two air streams are not close to each other then liquid coupled forced circulation run around loops may be utilized. The latter system is a highly flexible one but requires a pump to circulate the working fluid.

The waste heat recovery system discussed in this thesis has the features of a combination of heat pipe heat exchangers and liquid coupled forced circulation run around loop systems. The resulting system illustrated in figure 1.1 has been termed a two-phase thermosiphon loop to characterize its shape and to distinguish this system from gravity heat pipes and counter-flowing thermosiphon systems. These systems may also be used to cool electronic and electrical equipment, and to heat hot water in solar systems.

Thermosiphon loop heat exchangers offer a number of significant advantages over other types of heat exchangers. These advantages can be summarized as :

1. Require no external power to circulate the working fluid - the temperature difference between the two air streams acts as the activating mechanism for the fluid circulation.

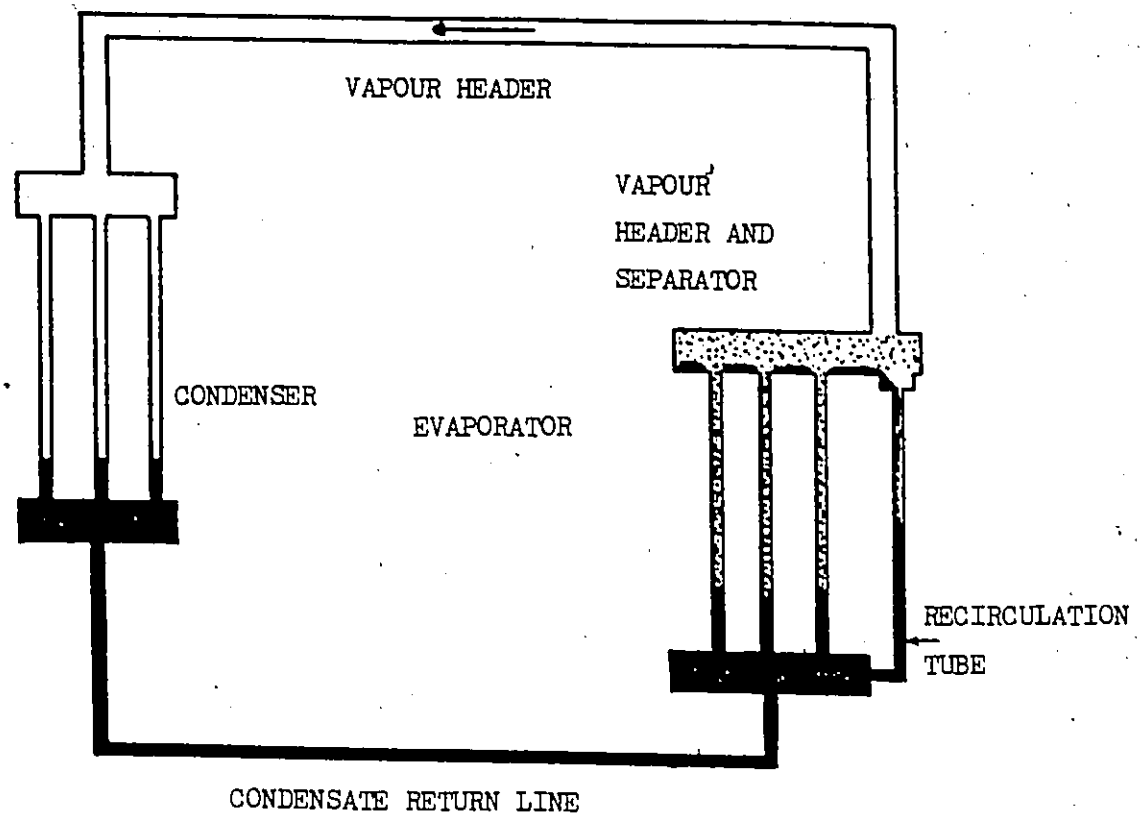

FIG. 1.1 TWO-PHASE THERMOSIPHON LOOP HEAT EXCHANGER

2. No moving parts in the system - only the working fluid circulates in the loop.

3. Long life - since there are no moving parts and the system is sealed, the system can operate indefinitely within the design temperature range.

4. No cross contamination - the two air streams are separated and the system is sealed so there is no problem of contamination of the streams; only heat is transferred from one air stream to another.

5. Reversibility - heat can be transferred in either direction.

6. Less weight - two-phase thermosiphon systems are only partially filled with liquid and hence are less heavy than single-phase circulation heat exchangers.

1.2 PRINCIPLE OF OPERATION OF TWO-PHASE THERMOSIPHON LOOP HEAT EXCHANGERS

A thermosiphon loop heat exchanger transfers energy from a heat source to a heat sink by the natural circulation of an intermediate working fluid between the two regions. A two-phase loop utilizes the difference in the saturation pressure between the evaporator and the condenser to cause the vapour to flow from the hot evaporator coil

through a separator to the cold condenser coil. The geometric configuration must be such that the condensate can flow back to the bottom of the evaporator by gravity.

In the two-phase thermosiphon loop heat exchanger system shown in figure 1.1 the liquid removed in the separator is recirculated to the evaporator coil liquid header. The presence of a separator allows more working fluid to be present in the evaporator, and hence helps to suppress dryout; it also ensures that little liquid is carried over to the condenser and hence improves the condensation film coefficient in the condenser.

If liquid working fluid is present in both coils at all times as shown in figure 1.2(a) then either coil can act as an evaporator, and the system is said to be bidirectional (i.e. it can transfer heat in either direction). For a system to operate in a bidirectional mode, recirculation tubes must be provided in both the heat exchanger coils. If the liquid working fluid drains completely from one of the coils when the system is inoperative as shown in figure 1.2(b), then only the flooded coil can act as an evaporator and heat can be transferred in only one direction. Such a system is said to be unidirectional.

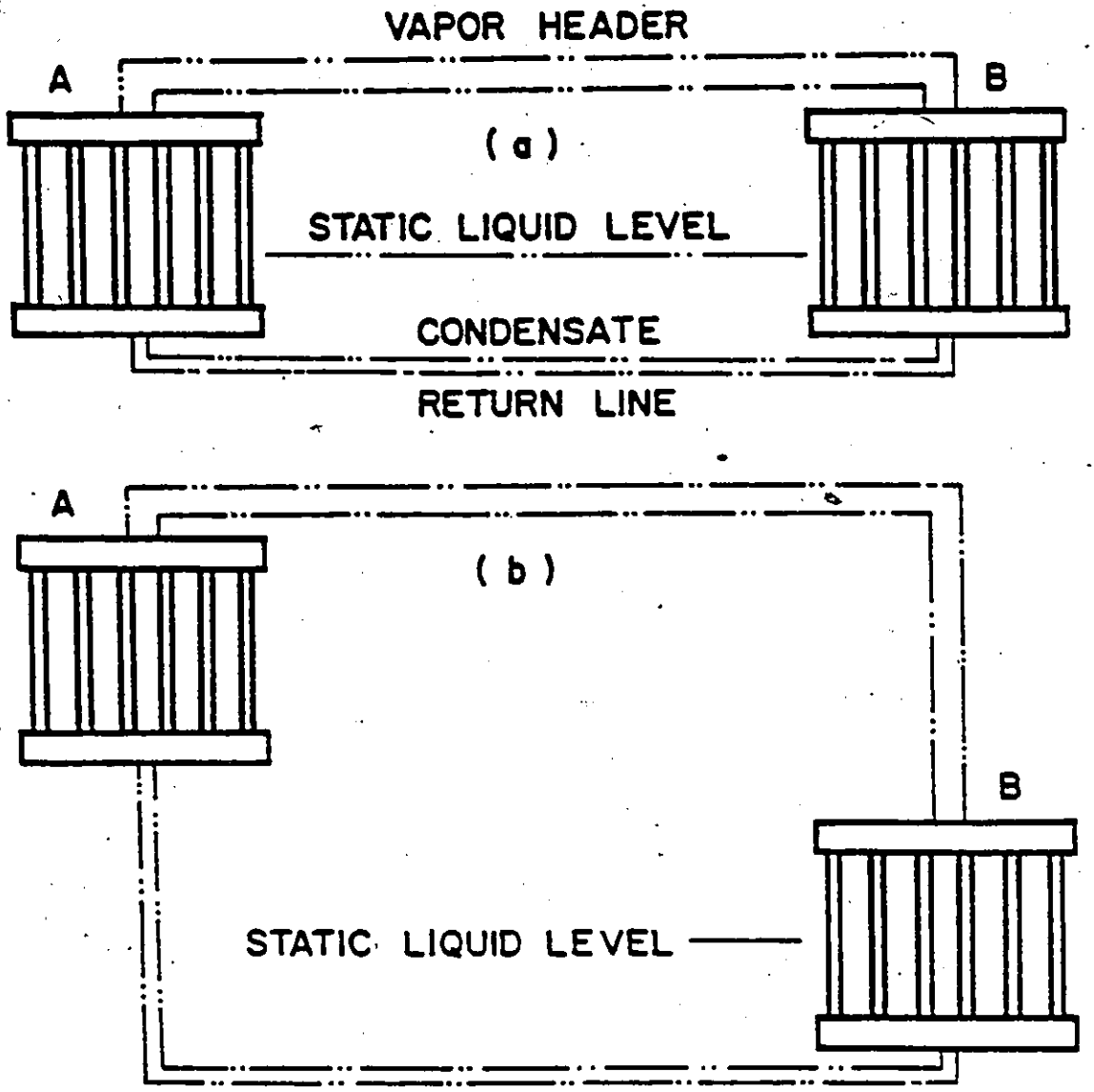

Figure 1·2 SCHEMATIC ELEVATION VIEW OF COIL LOOP THERMOSIPHON HEAT EXCHANGERS

(a) Bidirectional configuration. Loop can transfer heat in either direction, A to B or B to A.

(b) Unidirectional configuration. Loop can transfer heat only from B to A.

1.3 FLOW PATTERNS & HEAT TRANSFER REGIONS ENCOUNTERED IN TWO-PHASE THERMOSIPHON LOOP HEAT EXCHANGERS

A two-phase mixture flowing in a pipe can exhibit several flow geometries, such as bubbles, slugs, and films. Large variations in heat transfer occur when the flow geometry changes from one to another e.g. bubbly to slug and slug to annular. The flow pattern and the heat transfer are interrelated and they affect the hydrodynamics of the flow. Figures 1.3 & 1.4 show the various flow patterns and the heat transfer regions encountered in a vertical evaporator tube. The fluid reaches the heat exchanger portion of the evaporator as a liquid in a subcooled state. The liquid enters the evaporator tube from the header and in the entrance region both the thermal and the momentum boundary layers develop as the working fluid flows up the tube. Initially, both the bulk fluid temperature and the wall temperature remain below that necessary for nucleation and the heat transfer process is single-phase convective heat transfer to the liquid phase (region A). At some point along the tube, nucleation takes place in the presence of subcooled liquid (region B) which is known as subcooled nucleate boiling. The bubbles produced in the superheated wall region condense as they move away into the subcooled liquid. In this region, the wall temperature is higher than the saturation temperature and the bulk fluid temperature is still below the saturation temperature. The transition between region B & C is the point at which the bulk fluid temperature

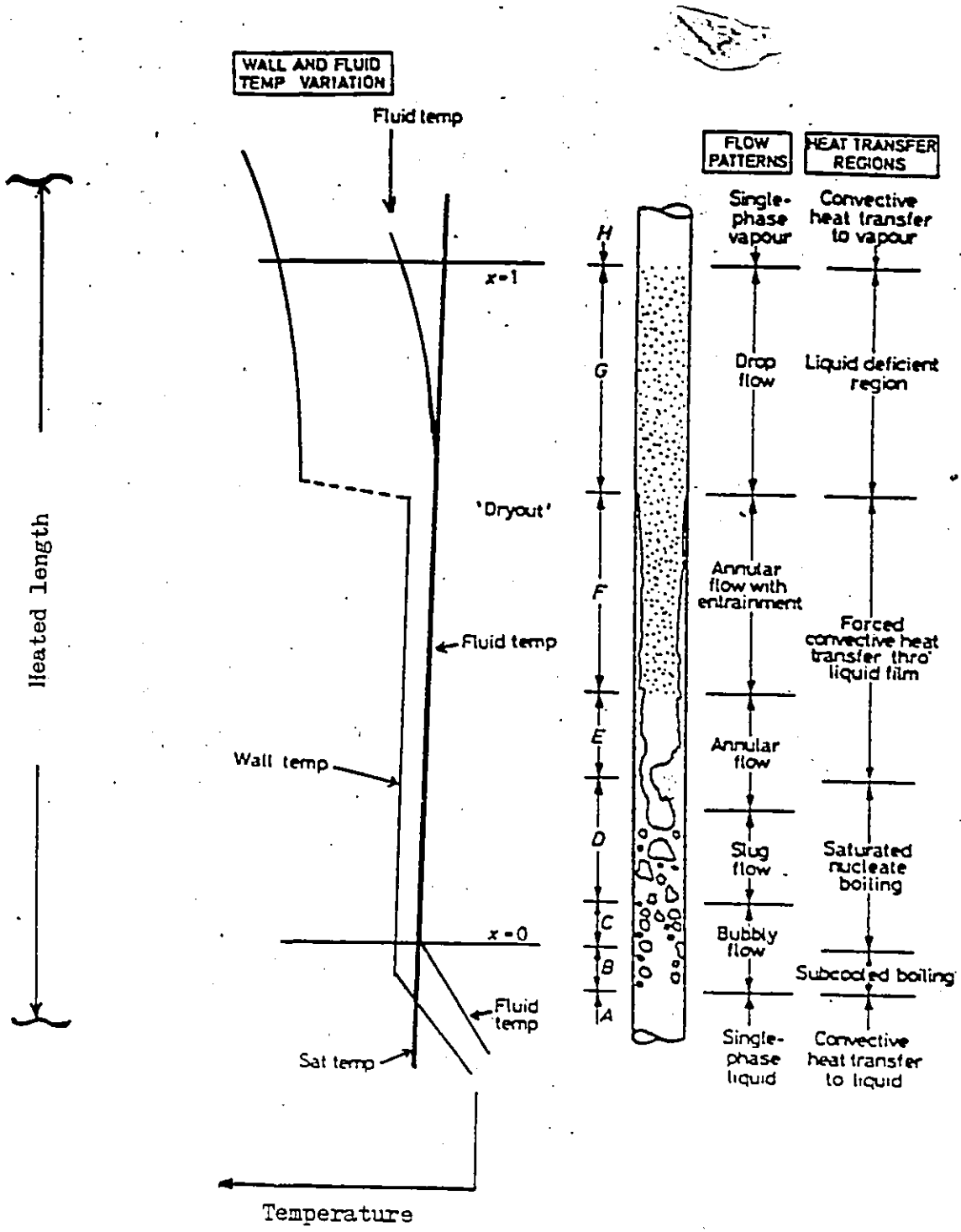

FIG. 1.3 REGIONS OF HEAT TRANSFER IN CONVECTIVE BOILING

	TUBES	
	VERTICAL FLOW	HORIZONTAL FLOW
BUBBLE FLOW	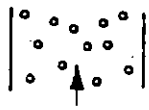	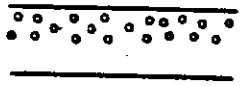
PLUG FLOW		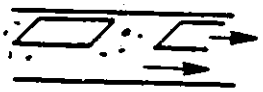
STRATIFIED FLOW		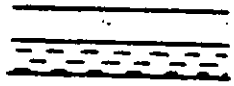
WAVY FLOW		
SLUG FLOW		
ANNULAR FLOW		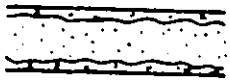

FIG. 1.4 FLOW PATTERNS IN VERTICAL & HORIZONTAL TUBES

equals the saturation temperature and saturated nucleate boiling (also known as bulk boiling) starts. As bubbles accumulate (region C) and coalesce the flow pattern changes from bubbly to slug flow (region D) and then to annular flow (regions E & F). As the quality and the vapour fraction increase, the resulting higher vapour velocities and higher two-phase heat transfer coefficients cause nucleate boiling to be replaced by surface vapourization. At some critical value of the quality dryout starts to occur on the tube wall and causes a significant rise in the wall temperature, an increase which could lead to tube failure in a constant heat flux boundary condition (burnout). Region G, between the dryout point and the transition to single phase vapour is termed the liquid deficient region. In this region, the vapour temperature increases above that of the liquid droplets which are at the saturation state. The heat transfer coefficients for region H are the lowest of all of the heat transfer regions.

The vapour generated in the evaporator reach the condenser either as saturated vapour or as wet mixture through a vapour header. If there is a heat loss from the vapour header, some of the vapour will condense and the condensate is removed in a separator and is circulated back to the evaporator liquid header. If the pressure drop in the vapour header is substaintial, the vapour would be in a

superheated state at the inlet to the condenser.

In the condenser the heat transfer can take place by either dropwise condensation or by film condensation. If the condenser is partially flooded, the mode of heat transfer in the flooded region would be by single phase liquid forced convection. The condensed liquid flows by gravity to the evaporator bottom through a liquid header and thus the cycle is completed.

1.4 PROBLEM IDENTIFICATION

The experimental studies of Hwang (1), Diciccio (2) & Sampath (3) and the simulation study of Ali (4) carried out at the University of Windsor established the basic performance characteristics of single tube coil loops and of multiple tube evaporator and condenser coil loops where all of the evaporator and the condenser coil tubes were subjected to the same source and sink temperatures and where the charge present in all the evaporator tubes were the same.

For many applications, the boundary conditions of the evaporator tubes are not the same and there may be different amounts of charge present in the evaporator tube rows. The present work deals with the development of a program which can be used to simulate the performance of two-phase thermosiphon loops in wich the evaporator

coil consists of straight tubes running between a common liquid and a common vapour header and where the tubes may be inclined from the vertical and where each tube row may be subject to different thermal boundary conditions. The program can also be used to calculate the effectiveness of commercial finned two-phase thermosiphon loop heat exchanger systems.

The program also takes into consideration the hysteresis effect for boiling of fluids in forced convection vertical flow. This hysteresis occurs due to the fact that a much greater wall superheat is required to initiate nucleate boiling than to maintain it. The boiling characteristics of a surface at low wall superheats is dependent on its past history, i.e. whether the surface nucleation sites are being initiated or quenched. Different correlations must be used for the quenching mode, where a high temperature difference between the surface and the working fluid has already established all the nucleation sites than for the site initiation mode where each successive run is for a greater overall temperature differences.

Figure 1.5(a) shows a thermosiphon loop where the tube rows in the evaporator coil are subjected to unequal heating due to the cooling of the exterior gas as it passes through the coil. Figure 1.5(b) shows an inclined evaporator coil in which each tube row has an unequal charge. Figure 1.6 shows a commercial finned thermosiphon loop heat exchanger.

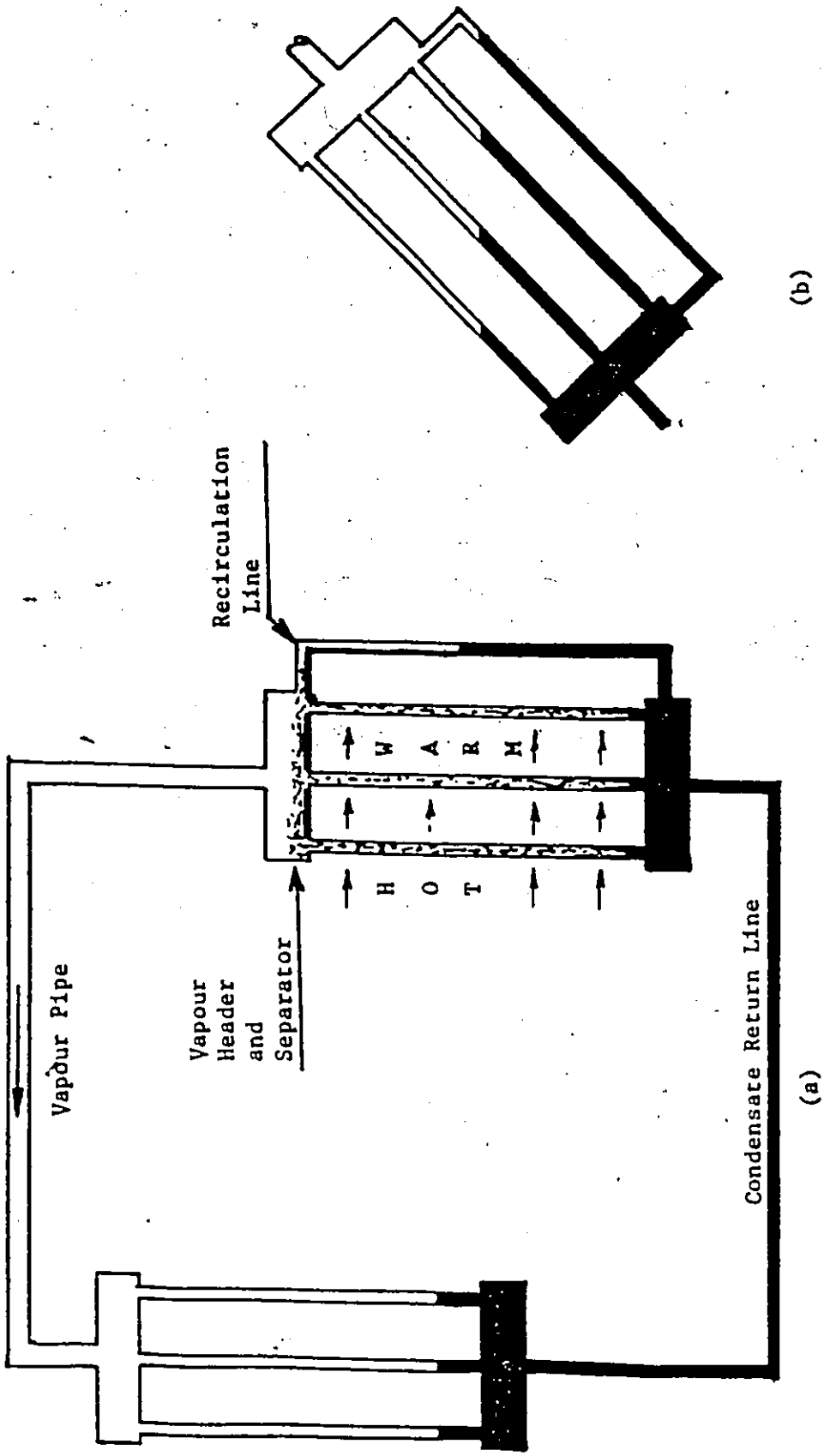

FIG. 1.5 Schematic elevation of coil loop thermosiphon showing evaporator with (a) unequal tube heating and (b) unequal tube charge

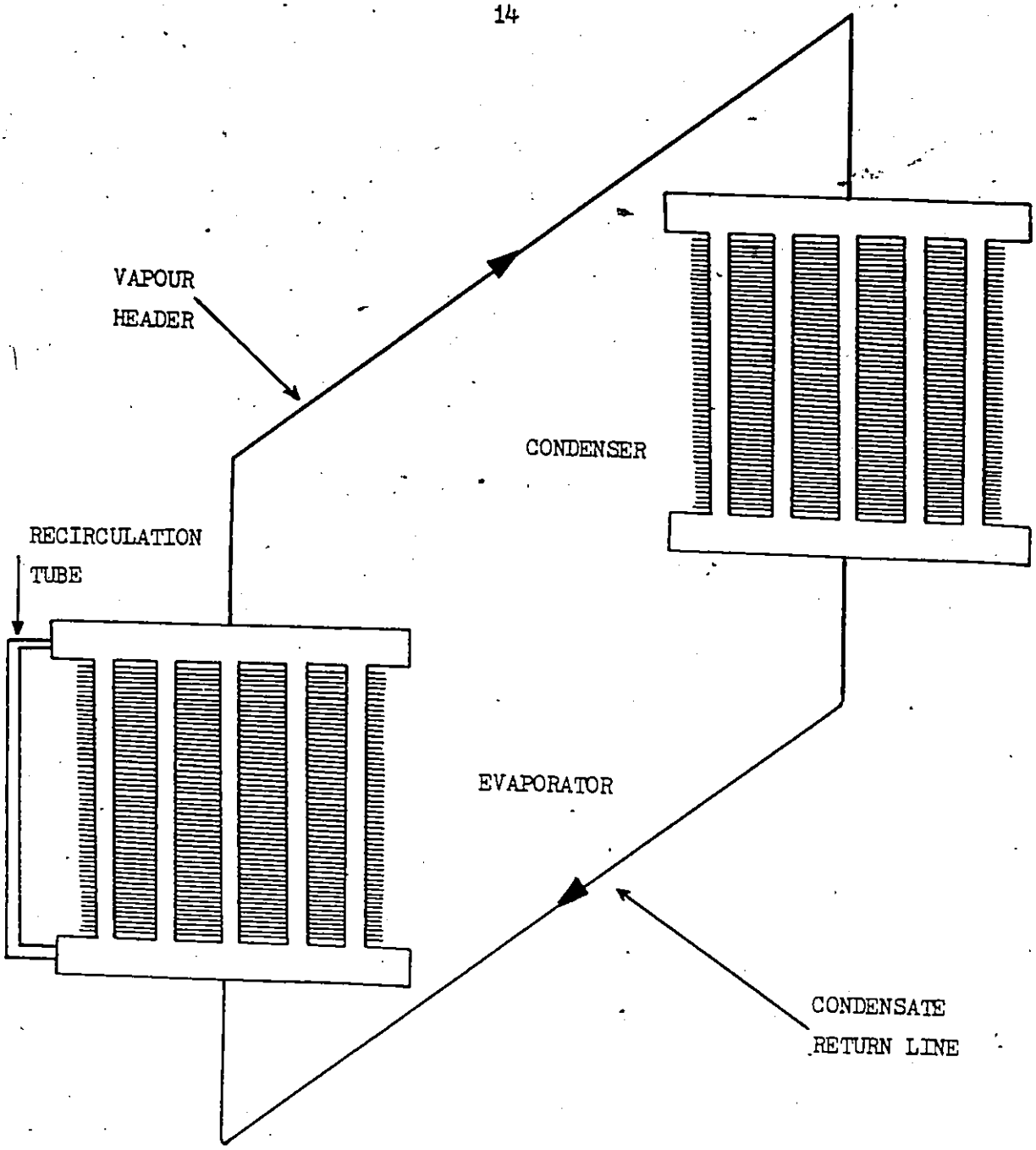

FIG 1.6 A COMMERCIAL FINNED TWO-PHASE THERMOSIPHON LOOP HEAT EXCHANGER

CHAPTER II

LITERATURE SURVEY

2.1 INTRODUCTION

A closed loop thermosiphon is a commonly employed device for heat transfer in various industrial applications. Extensive work has been done on single phase natural circulation loops, where the working fluid does not change phase. For these systems temperature differences around the loop produce the buoyancy effect which causes the working fluid to circulate. On the other hand, in a two-phase thermosiphon loop the vapour generated in the evaporator flow to the condenser due to the difference in the saturation pressure between the evaporator and the condenser. Two-phase thermosiphons are getting a lot of attention these days since they have lot of advantages over the conventional forced circulation heat exchanger systems.

The object of the present work deals with the utilization of two-phase thermosiphon loop heat exchanger systems for waste heat recovery. To the best of author's knowledge the work on this topic has mainly been done at the University of Windsor.

In the following section a literature survey is done on thermosiphons.

2.2 LITERATURE SURVEY ON THERMOSIPHONS

In the following section a literature survey is presented on two- phase thermosiphon loops.

Hwang (1), Diciccio (2), Ali (4), McDonald et al. (5), Ali & McDonald (6) and McDonald & Ali (7) studied the performance of two-phase thermosiphon waste heat recovery systems. Their studies indicated that the optimum performance may be expected from a thermosiphon loop when the evaporator and condenser tubes are oriented in such a way that the condenser is nowhere flooded, no dryout occurs in the evaporator and negligible liquid is carried into the condenser. Sampath (3), McDonald et al. (8) and McDonald & Sampath (9) investigated multiple tube evaporators and condensers with recirculation for both bidirectional & unidirectional two-phase coil loop thermosiphon heat exchangers both experimentally and by computer simulation.. Their results showed that single tube two-phase thermosiphon loops may be designed to provide peak performance over a modest range of operating temperature differences. Unidirectional loops offer a higher performance than the bidirectional loops but are more sensitive to changes in the imposed temperature differences. The

condenser is not flooded in the case of a unidirectional loop which results in a better performance. A two-phase thermosiphon heat exchanger without and with a recirculation tube is shown in figure 2.1. The final reports of these studies were submitted to ASHRAE by McDonald (10,11). The experimental rigs of Hwang, Diciccio & Sampath are shown in figures 2.2 & 2.3. Raza (12) used Sampath's apparatus to investigate the effect of unequal heating and unequal charge conditions for the evaporator tubes, as shown in figure 1.5. Each tube had a separate water jacket to produce the non uniform heating of the evaporator tubes. Raza & McDonald (13), McDonald & Raza (14) found that, for the conditions tested, the overall heat transfer rate and the overall average evaporator heat transfer coefficients were insensitive to these effects for static charges between 40% and 90%. They also noted that the performance of each tube row was changed significantly. Kosnik & Bertoni (15) and McDonald et al. (16) investigated the performance of a finned commercial thermosiphon loop heat exchanger with R-11 as the working fluid. The condenser and the evaporator coils each consisted of 8 rows of tubes. The evaporator tubes were vertical and the condenser tubes were inclined at 45 deg. from the vertical. The test apparatus could be arranged to study 8, 4, 2 or 1 loop system configurations. They used 4 loops for their studies comprising of 2 rows of tubes per loop. The static charge, overall temperature difference and the coil face velocity were varied and their effect on effectiveness was studied. They found that the

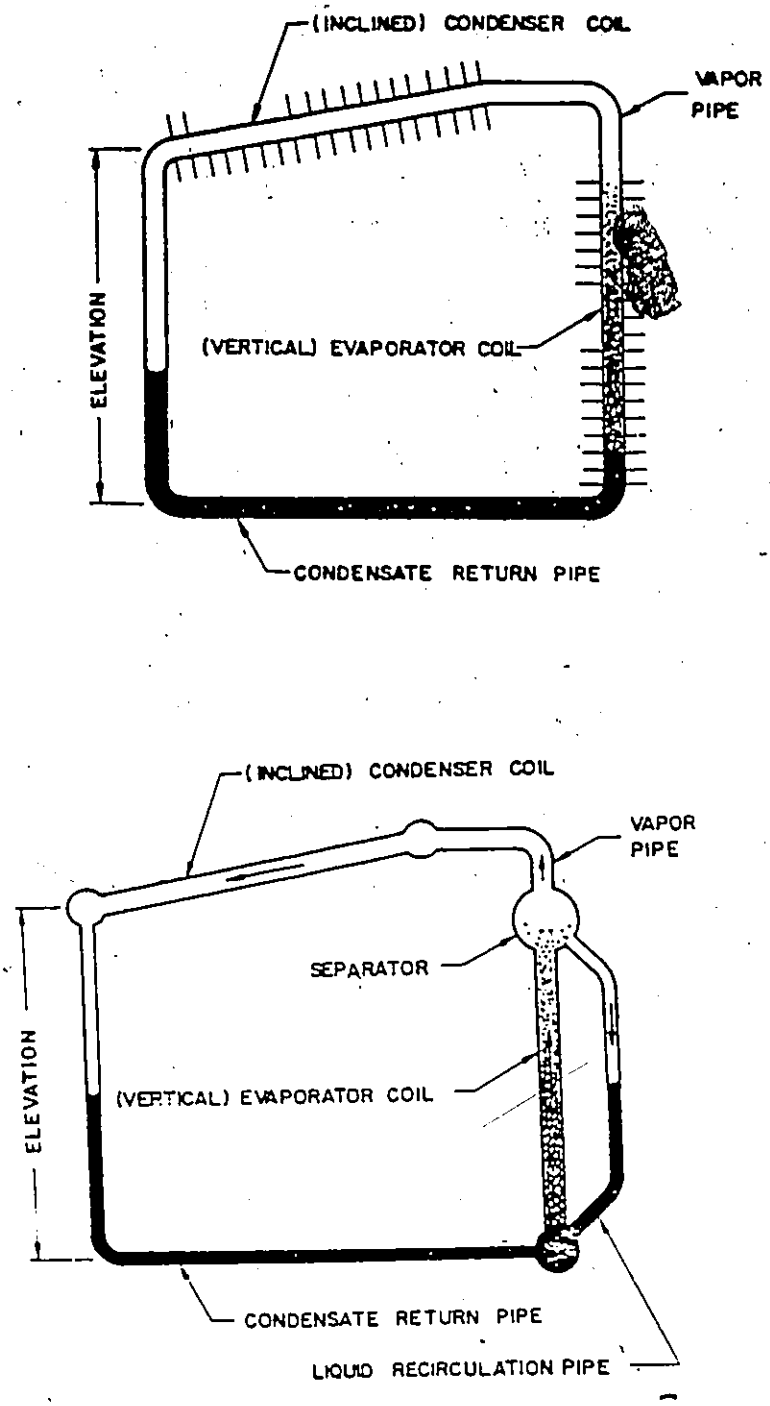

FIG. 2.1 THERMOSIPHON LOOP HEAT EXCHANGERS WITHOUT & WITH A RECIRCULATION TUBE

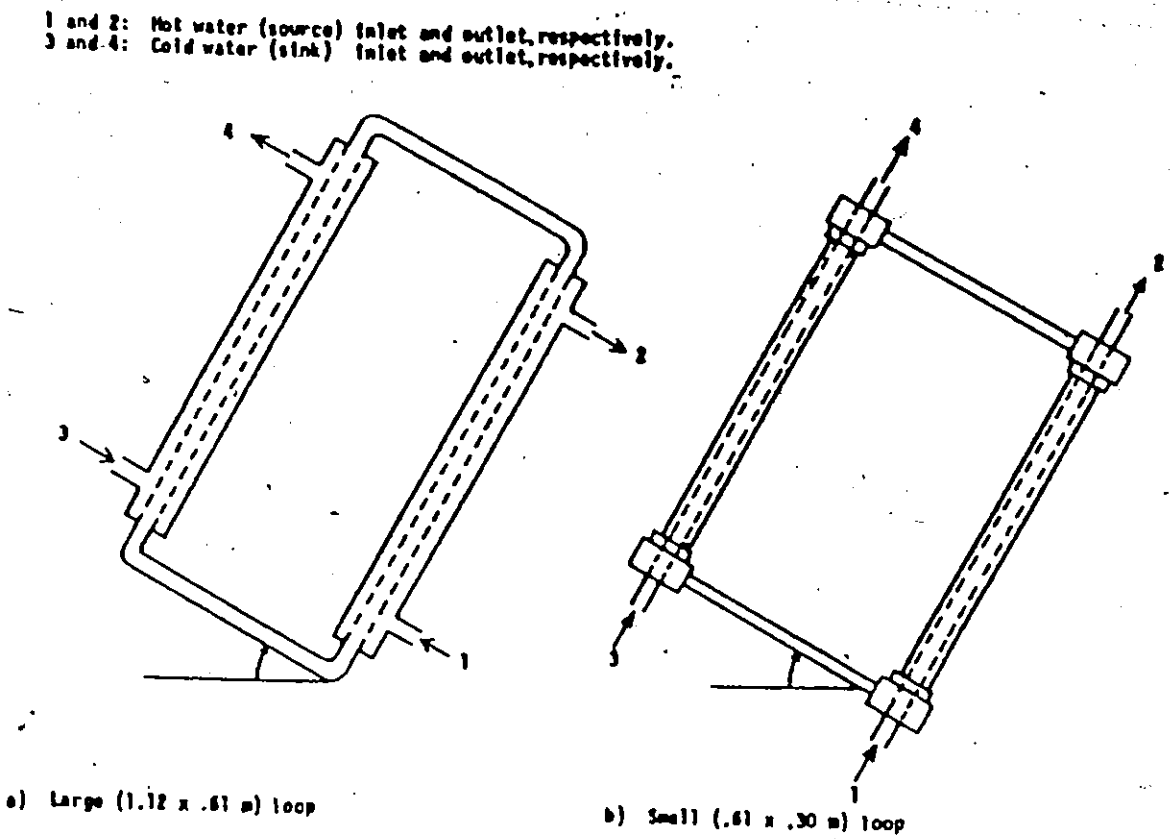

FIG 2.2 EXPERIMENTAL THERMOSIPHON LOOPS OF (A) HWANG (1) & (B) DICICCIO (2)

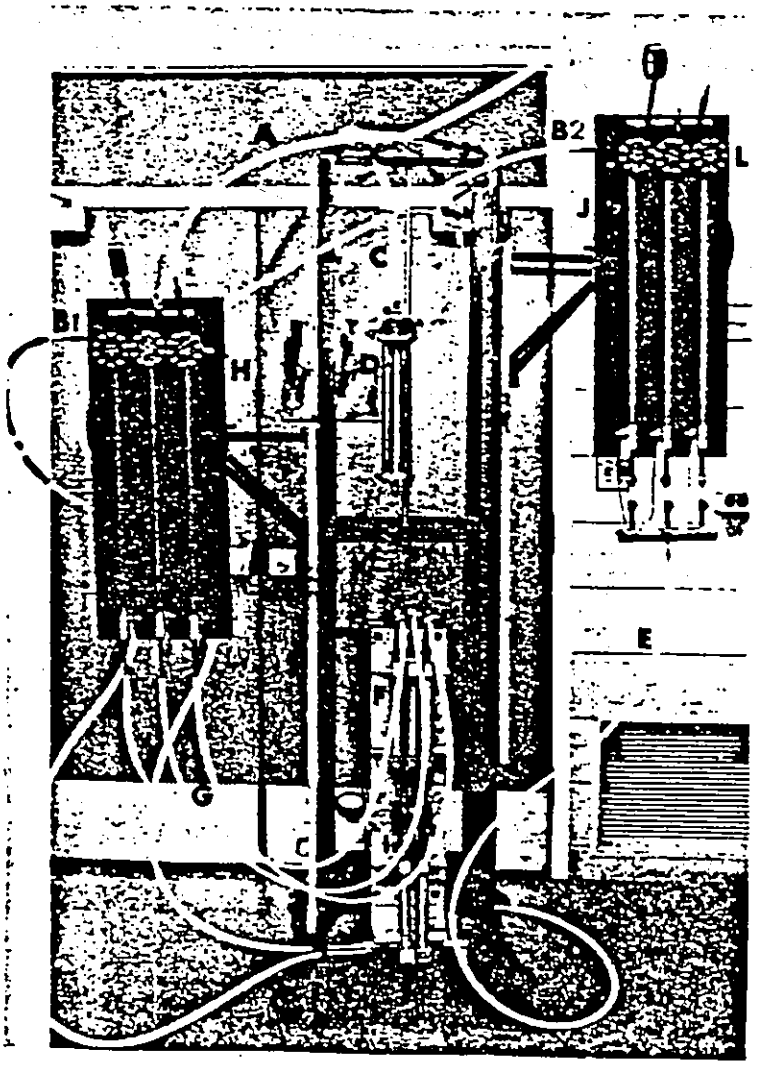

Fig. Uninsulated multiple tube evaporator and condenser apparatus

A	Vapor header
B1, B2	Evaporator and condenser liquid bypass lines, respectively
C	Vapor line to reservoir
D	Working fluid reservoir
E	Condensate return line
F	Bypass, condensate and evaporator tube flow meters
G	Liquid return lines to the evaporator tubes
H	Evaporator assembly
J	Condenser assembly
K	Liquid line to reservoir (with valve at connection to the loop)
L	Tube wall thermocouple terminals
X	Reservoir vapor line valve

FIG. 2.3 EXPERIMENTAL THERMOSIPHON LOOP OF SAMPATH (REF. 3)

effectiveness of the system was insensitive to the quantity of charge in the evaporator, except when dryout occurred; it increased with the hot to cold air duct temperature difference and decreased as the airflow rates increased. Their 4 loop system operated best between static charge of 60 to 90 % with optimum performance achieved near 80 %. Recently, Stauder (17) made an exhaustive experimental study on the experimental rig used by Kosnik & Bertoni and found that a hysteresis effect occurs in such systems which can severely reduce the performance of two-phase thermosiphon loop heat exchangers. He found that wall superheats of approximately 12-14 C were required to initiate the boiling process for the R-11/copper interface used. Figure 2.4a and 2.4b shows the schematics of the experimental rig used by Kosnik & Bertoni and Stauder. Figure 2.5 shows at a glance, the research work done at the University of Windsor on two-phase thermosiphon loop heat exchangers.

Mendler et al. (18) investigated experimentally and by theoretical model the performance of natural circulation & forced circulation loops with water at 800 to 2000 psia under nonboiling, local boiling and bulk boiling conditions. They used single rectangular channel test sections of three different dimensions and without a liquid-vapour separator. Heat fluxes ranged from 50,000 Btu/hr-sq.ft to burnout with inlet subcoolings of 20, 20 and 100 F. The results showed that single and two-phase pressure drop, burnout heat flux, and riser density measured under natural circulation were

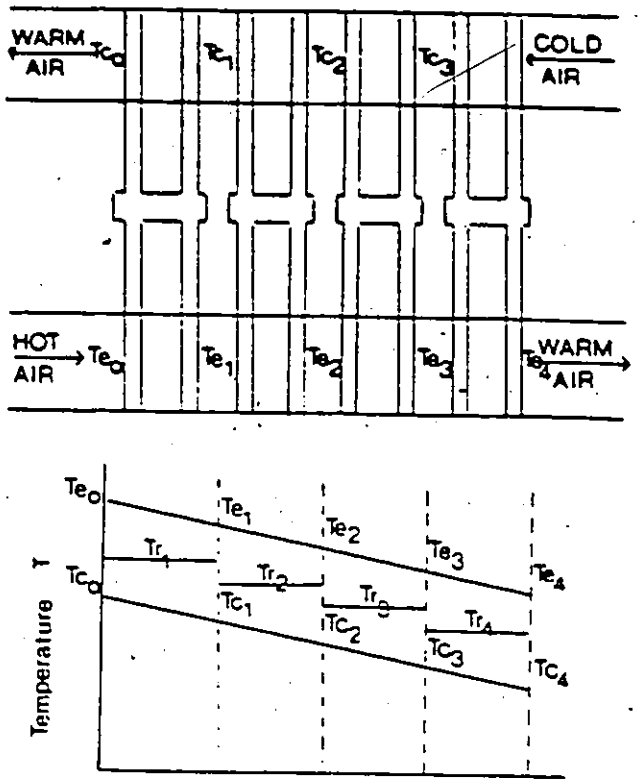

FIG. 2.4a

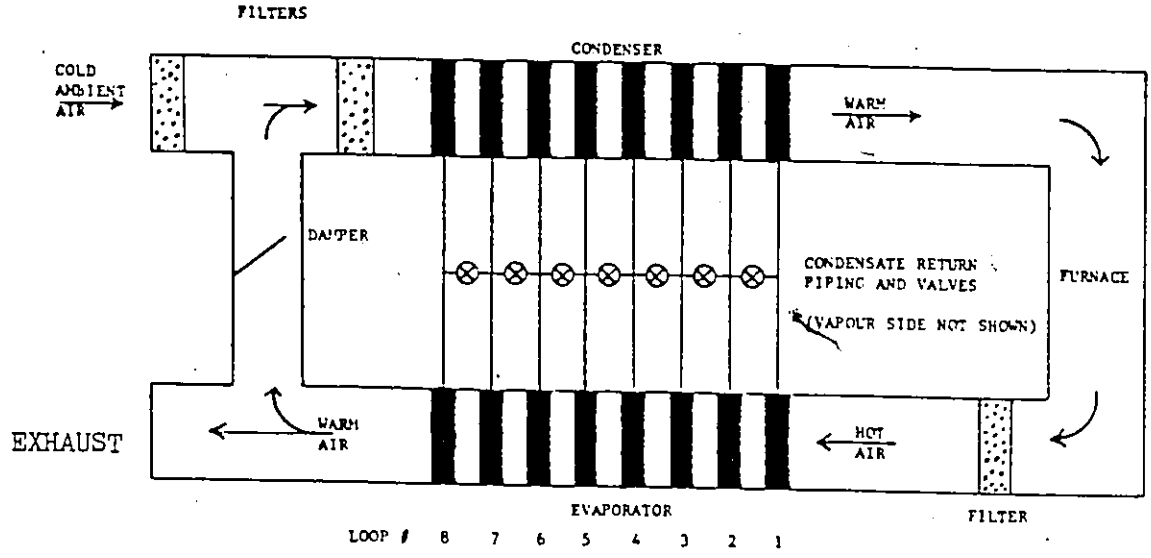

FIG. 2.4b SCHEMATIC REPRESENTATION OF THE THERMOSIPHON TEST FACILITY

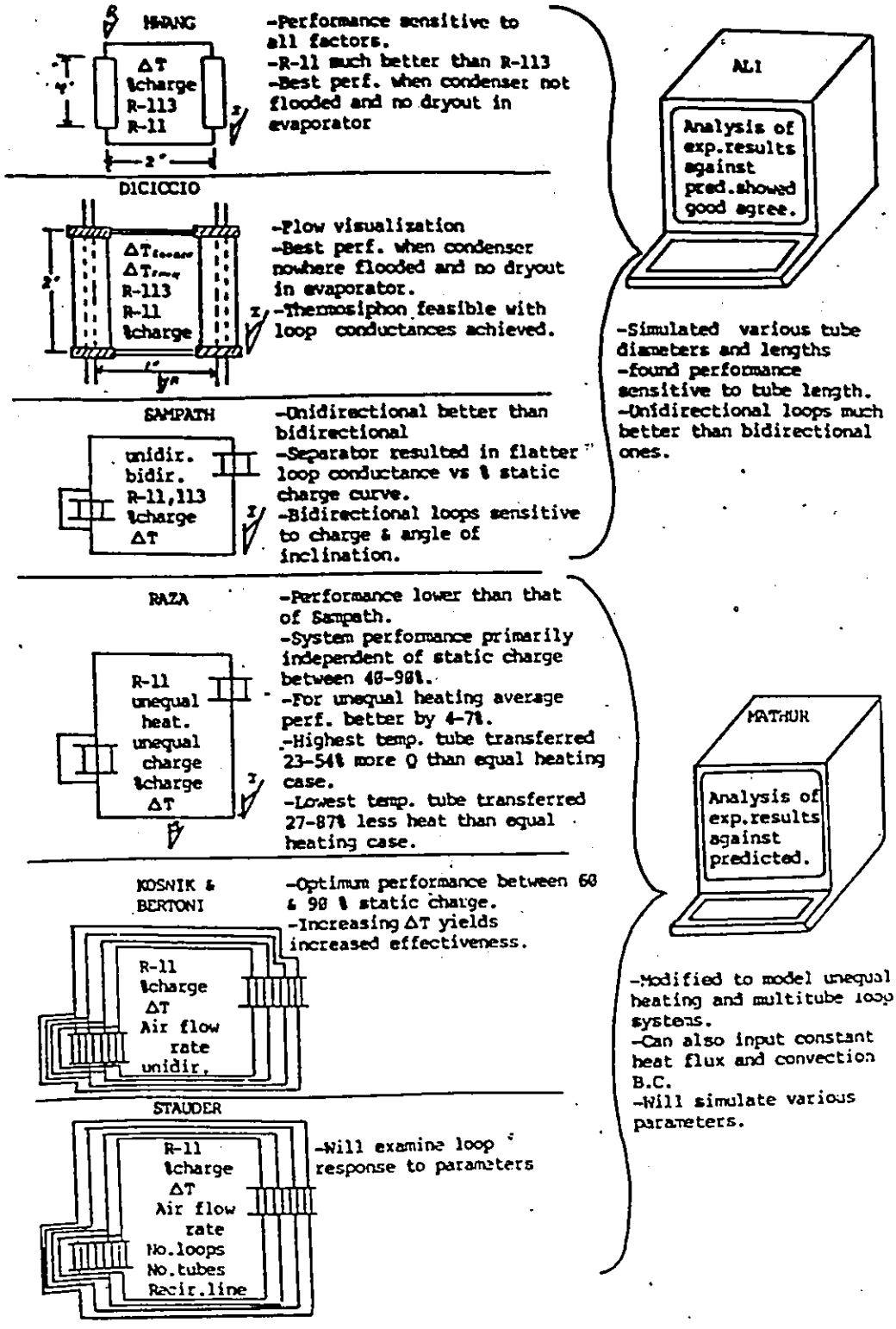

FIG. 2.5 UNIVERSITY OF WINDSOR THERMOSIPHON LOOP RESEARCH HISTORY

no different from those measured with forced circulation at the same thermal and fluid flow conditions. For the loop studied, natural circulation flow rates were predicted within 10.%.

Bandy et al. (19) investigated maximization of heat rejection rate to a natural circulation boiling channel by experiments and theroetical model. Water and Freon-113 were used as the working fluid. Variable area and constant area evaporator tubes were used for their studies for non uniform and uniform heat fluxes. The authors found out that the burnout power could be increased significantly by using a variable area heated section. The model was able to predict the theoretical flowrates within 23% and burnout powers within 16%.

Soin et al. (20) investigated the performance of flat plate solar collector with fluid undergoing phase change for natural circulation. They used acetone and petroleum ether (40-60 C) as the working fluids for their experiments. They found that the collector efficiency increases linearly with liquid level measured in the recirculation tube.

Tanger et al. (21) studied heat transfer to sulfur hexafluoride near the thermodynamic critical region in a natural circulation loop without a liquid-vapour separator. Local and average heat transfer coefficients along the test section were calculated from the experimental data. They reported that maximum heat transfer

coefficients were obtained at pressures slightly above the critical state.

Cheng & Rovang (22) investigated the steady state operation and heat transfer characteristics of a two-phase closed thermosiphon system for low grade energy recovery. The working fluid used was water. The parameters which were varied are - the liquid charge level, liquid source and sink temperatures 55-95 C, 14-19 C and their flow rates 30-35 ml/s, 10-70 ml/s, and with or without a liquid-vapour separator. The evaporator pressure was held constant at 34 kPa. The evaporator and condenser coils were fabricated from spiral copper tubes. The flow rates of the working fluid were found to be in the range of 14-36 ml/s and the heat recovered was in the range of 1000-4600 W.

Bergevin et al. (23) investigated the performance of a phase-change solar collector. The solar collector channel was simulated by means of a uniformly heated glass pipe which was supplied with a liquid below its saturation temperature. The channel was inclined at an angle of 60 degrees from the horizontal with a diameter and length of 5 mm and 143 cm respectively. The condenser was water jacketed and was 400 cm long. The water inlet temperature was 25 C with a flow rate of 50-69 gram/minute. The heat flux was varied between 600 to approx. 3400 W/sq.m and the working fluid used was Freon-113. Their

experimental system is shown in figure 2.6. The results of their study is shown on figure 2.7, which is a plot of the average heat transfer coefficient for two-phase and single-phase region as a function of the heat flux. They correlated their local experimental data for both the single- and two-phase regions with the following equations.

$$h_l = q\left[T_m - T_l\right]^{-1} \qquad \text{---- (1)}$$

$$h_{tp} = 0.023\, k_l\, D^{-1} \left(\rho_l/\rho_g\right)^{0.25} \left[Re(1-x)\right]^{0.8} Pr^{0.33} \qquad \text{---- (2)}$$

References 24 to 43 deal with the studies of two-phase heat pipes operating in a thermosiphon mode. The basic mechanism of operation of a two-phase heat pipe is entirely different than that of a two-phase loop and hence the detailed discussion of these references is not directly relevent to this thesis and will not be presented. References 44 to 63 deal with the studies of single-phase thermosiphon loops. Since the nature of operation of these loops is also different than that of two-phase thermosiphon loops a detailed discussion of these references is omitted. These papers (from 24 to 63) have been included in the list of references in order to provide a more complete literature survey, which the reader might find useful.

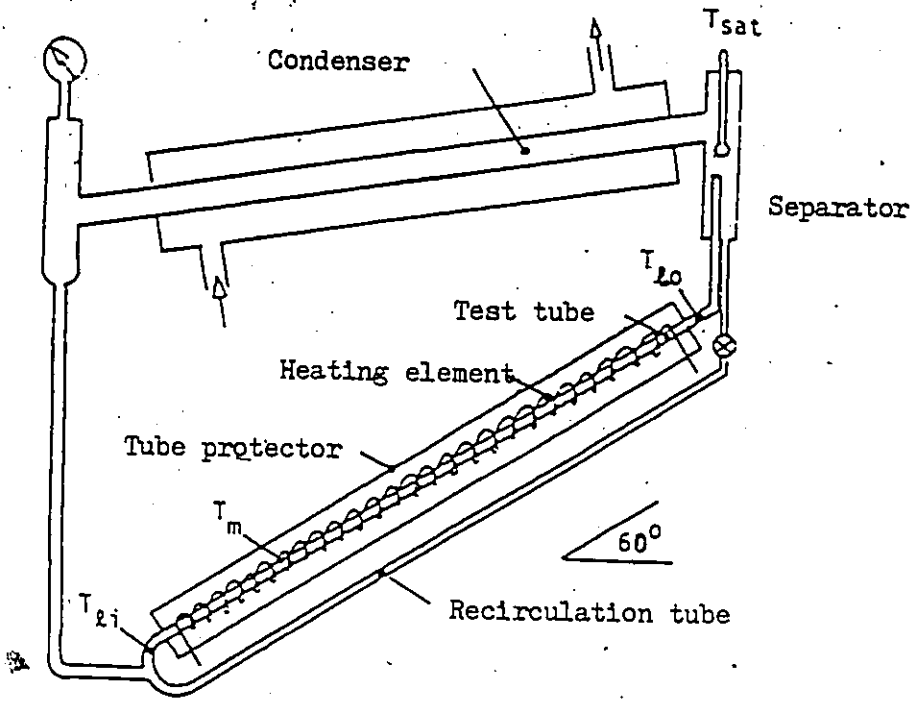

Figure 2.6 Experimental set up of reference 23

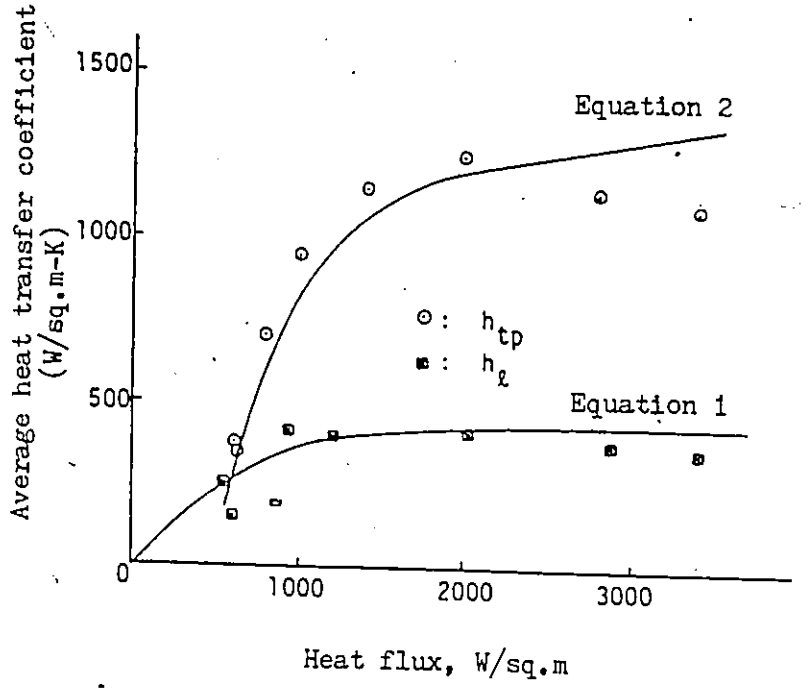

Figure 2.7 Effect of heat flux on the average heat transfer coefficient for two-phase (h_{tp}) and single-phase (h_l) region

2.3 TWO-PHASE FLOW REGIMES

The determination of which flow regime will occur for any given set of conditions is one of the problems facing a designer of two-phase flow devices. The flow regime depends upon the following factors;

1. Volumetric flow rates of each phase
2. Pressure
3. Heat flux at the wall
4. Densities and viscosities of each phase
5. Surface tension
6. Pipe geometry
7. Angle of pipe with respect to the horizontal plane
8. Flow direction (upward, downward, cocurrent, countercurrent)
9. Inlet length
10. Phase injection devices

Traditionally, flow regimes are identified from a flow regime map obtained from experimental observations. Many flow regime maps have been proposed using dimensional coordinates based on the liquid and gas superficial velocities (64-90). Other investigators have attempted to correlate the transition boundaries by non-dimensional groups. There have also been theoretical works to predict the flow regimes. These conventional flow regime maps are based on the liquid and gas superficial velocities or the total mass flux and quality.

Figure 2.8 shows the flow regime map by Hewitt & Roberts (67) for vertical flows. It is the most widely used chart for air-water and steam-water flows. It was originally established for an air-water mixture flowing in a pipe 31.2 mm in diameter at a pressure varying from 1.4 to 5.4 bar. Figure 2.9 shows the modified flow regime map of Baker (89) by Scott (90) for the horizontal flows. Flow pattern map of Mandhane (85) for gas-liquid in horizontal pipes is shown in figure 2.10. Figure 2.11 shows Soliman's (87) flow regime map for transition from mist-to-annular flow condensation.

The correlations to predict the transitions in a two-phase flow are given in table 2.3 of appendix A.

2.4 HEAT TRANSFER IN EVAPORATOR TUBES

In an evaporator tube, the heat transfer may take place in various forms, as the working fluid is transformed from a subcooled liquid at the entrance to the evaporator tubes to either a wet or a superheated vapour at its exit. Each of these mechanisms will be reviewed in order in which they would normally be expected to occur in the evaporator and a summary of the literature survey is presented in tabular forms.

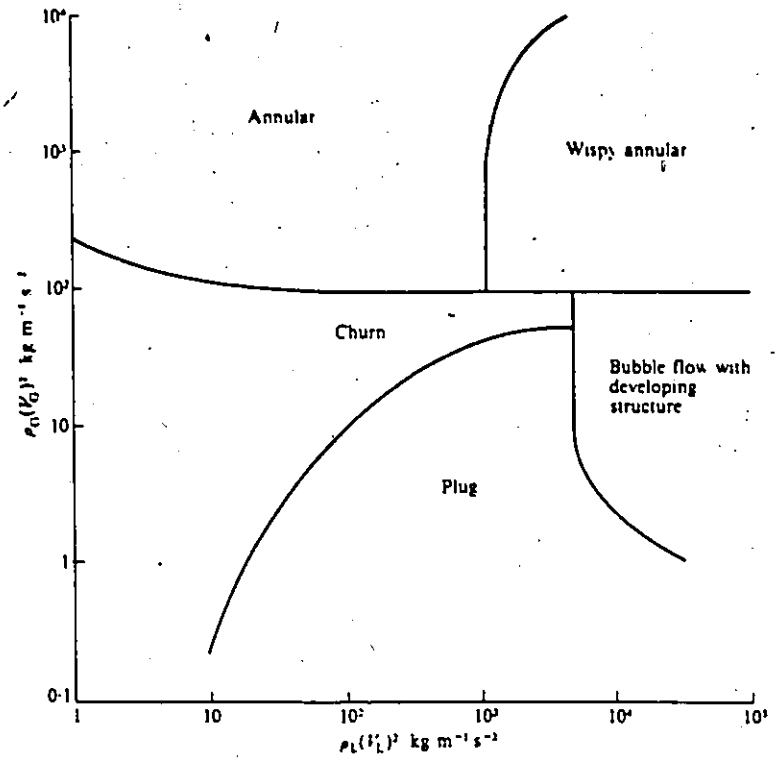

FIG. 2.8 MAP OF HEWITT & ROBERTS FOR VERTICAL TWO-PHASE FLOW (REF. 67)

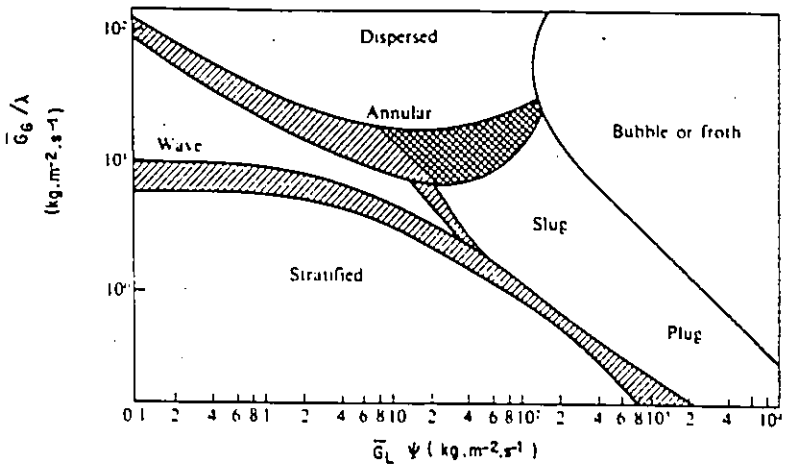

$$\lambda \triangleq \left(\frac{\rho_G}{\rho_A}\frac{\rho_L}{\rho_W}\right)^{1/2}$$

$$\psi \triangleq \frac{\sigma_{WA}}{\sigma}\left[\frac{\mu_L}{\mu_W}\left(\frac{\rho_W}{\rho_L}\right)^2\right]^{1/3}$$

FIG. 2.9 FLOW PATTERN MAP OF BAKER AS MODIFIED BY SCOTT (REF. 90)

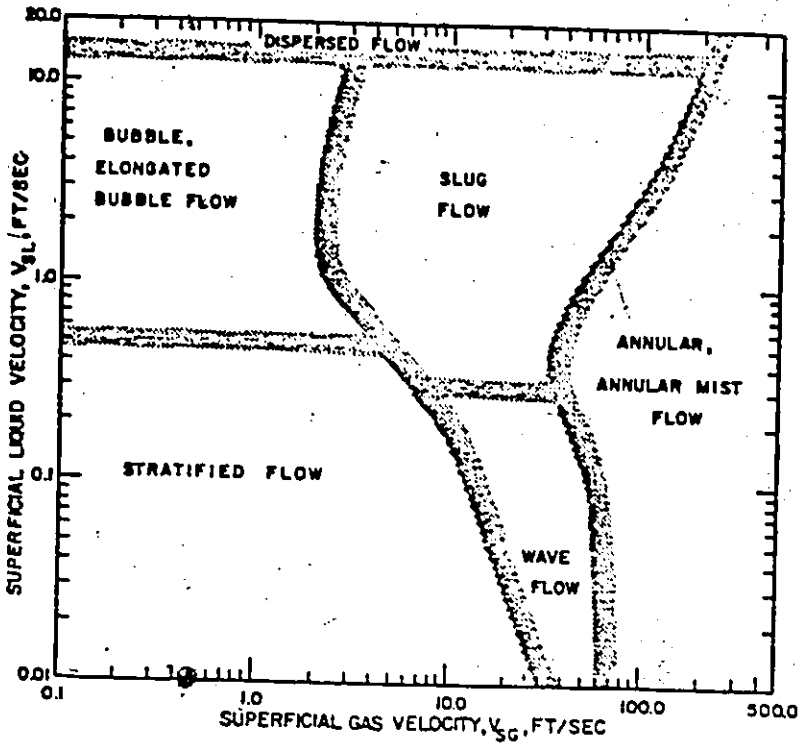

FIG. 2.10 FLOW PATTERN MAP PROPOSED BY MANDHANE (REF. 85)

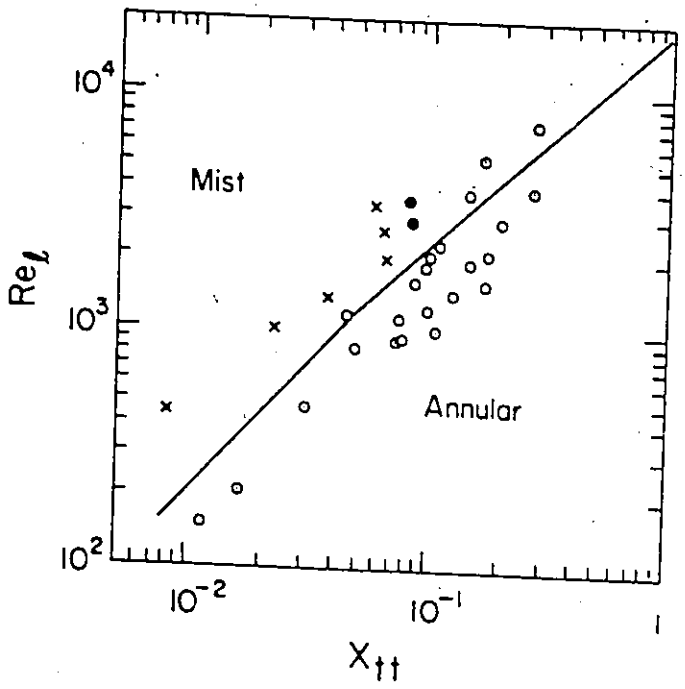

FIG. 2.11 SOLIMAN'S FLOW REGIME MAP FOR TRANSITION FROM MIST-TO-ANNULAR FLOW CONDENSATION (REF. 87). X MIST, ● MIST-ANNULAR, O ANNULAR

2.4.1 Single-phase liquid forced convection

Heat transfer by single-phase convection will occur when the fluid is flowing inside a tube either in laminar or in turbulent flow condition. There are many correlations available for this mode of heat transfer and a summary is presented in table 2.4.1 (appendix A) for laminar fully developed flow, turbulent fully developed flow and for the entrance region.

2.4.2 Transition from single-phase forced convection to nucleate boiling

An understanding of the factors which influence the onset of boiling is of importance in the design and operation of the equipment used for heat transfer in various processes. Transition from single-phase convection to nucleate boiling occurs when the liquid layer adjacent to a heating surface becomes superheated. It is now an accepted fact that the presence of nucleation cavities is required to establish boiling on a metal surface. Many investigators have presented correlations to predict an "incipient boiling" point. Most of these investigators assumed a linear temperature profile in the superheated layer and that the bubbles would grow and detach from the nucleation sites only when the superheated layer is such that a net heat flux into the developing bubble is realized when taking into

consideration the pressure and hence saturation temperature difference across the bubble boundary due to surface tension. Most of these investigators studied the phenomenon of wall superheat during incipient boiling in tubes. A summary of the correlations to predict this "incipient boiling" point is presented in table 2.4.2 (appendix A). The heat flux or the wall superheat can be calculated from these correlations for this condition.

Corty & Foust (118) observed that the past history of the boiling surface had a pronounced effect on the superheat required to initiate nucleate boiling. They described and classified the phenomenon for ether, normal pentane and R-113 and reported wall superheats far in excess of those required to maintain boiling once initiated. Turton (119) reported large wall superheat - as high as 100 to 120 F for R-11 boiling on a stainless steel tube at pressures above atmospheric and under the influence of increased gravity. Abdelmessih et al. (120) found that a wall superheat of 25 - 30 F was required to initiate boiling of R-11 on a stainless steel tube under forced flow conditions. The superheat was found to be independent of the fluid velocity in the range tested. Hodgson (121) investigated the hysteresis effect in forced convection, subcooled boiling with water. Marto & Rohsenow (122) reported temperatures as high as 135 F for the onset of nucleate boiling for liquid sodium in pool boilng and found that the value of the wall superheat required to initiate boiling depended on the surface finish. Similar overshoots in

temperatures have been reported by Chen (117) for flow boiling of liquid potassium. Joudi & James (123) reported wall superheats far in excess of normal boiling temperature differences were required to initiate boiling of R-113 and methanol. Clarke & Robertson (124) reported that the onset of convective boiling in a boiling channel of an industrial heat exchanger would be considerabely delayed beyond the point where the bulk fluid reached local saturation temperature. Recent work reported by Stauder (17) has shown that the performance of a two-phase thermosiphon loop heat exchanger using R-11 can be seriously affected by this hysteresis phenomenon. Excessive wall superheats were also reported by Bankoff et al. (125) and by Sakurai & Shiotsu (126).

Figure 2.12, a and b shows this effect for the experimental data of Abdelmessih et al. (120) for R-11. Figure 2.12a is for increasing heat flux and 2.12b is for decreasing heat flux. Figure 2.13 shows the hysteresis effect at the inception of flow boiling at two different positions an the test section. Figure 2.14 shows a similar effect investigated by Murphy & Bergles (114). Figure 2.15 shows the hysteresis effect for R-113 and methonal at atmospheric and subatmospheric pressures investigated by Joudi & James (123). Turton's results for Arcton 11 (Fr-11) is shown in figure 2.16.

Yin & Abdelmessih (127) investigated the boiling characteristics

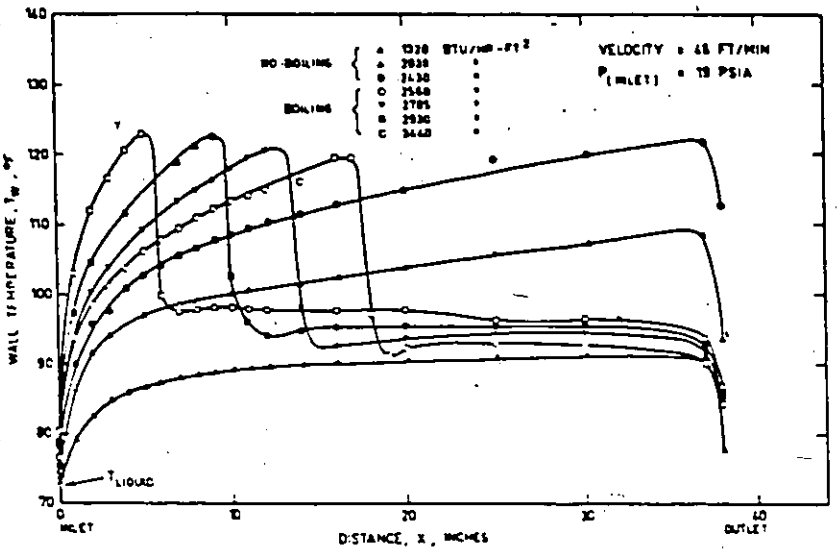

(a) INCREASING HEAT FLUX

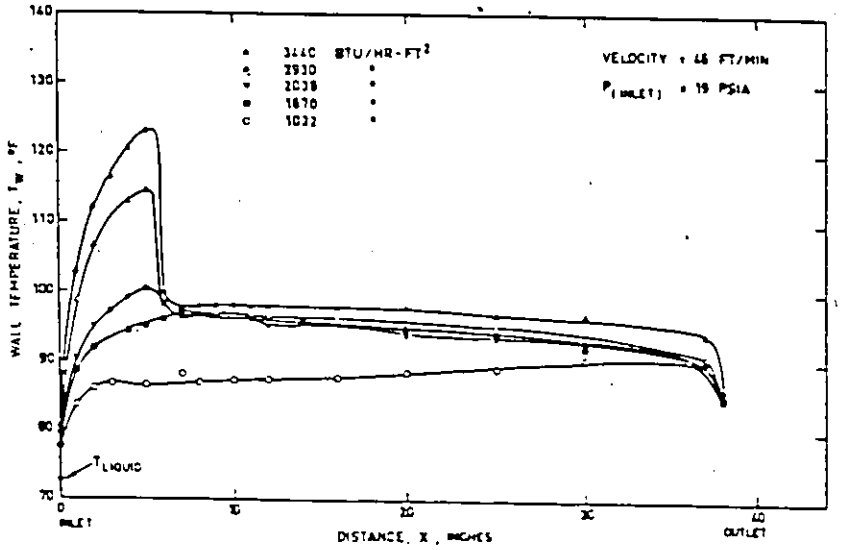

(b) DECREASING HEAT FLUX

FIGURE 2.12 WALL TEMPERATURES ALONG A TEST SECTION

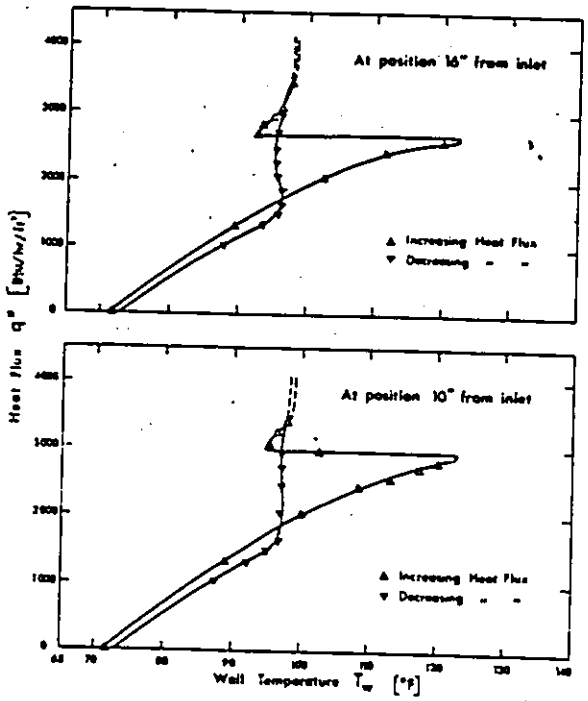

FIGURE 2.13 The hysteresis effect at the inception of flow boiling at two different positions on the test section. V=46 ft/min P_{in}= 19.0 psia

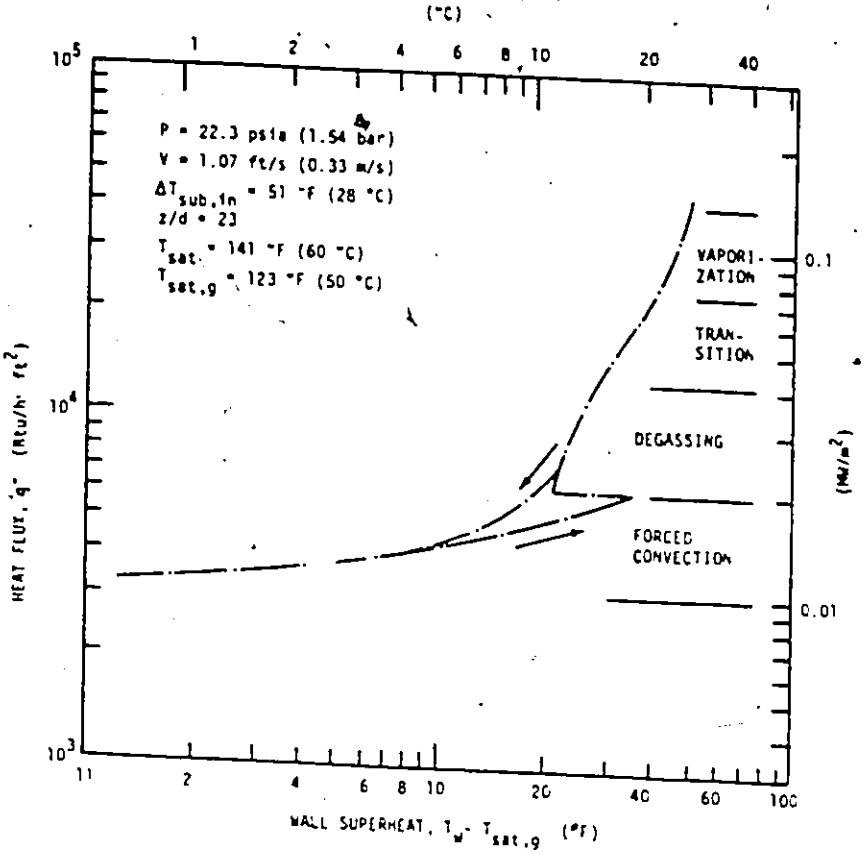

FIGURE 2.14 Boiling curve obtained with gassy coolant by Murphy and Bergles (114) showing hysteresis around the incepient boiling point.

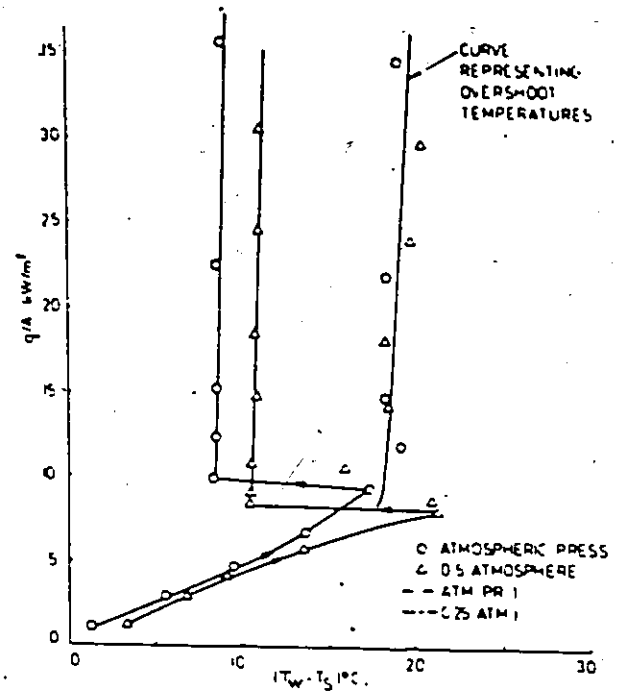

Incipient boiling and temperature overshoots for R-113

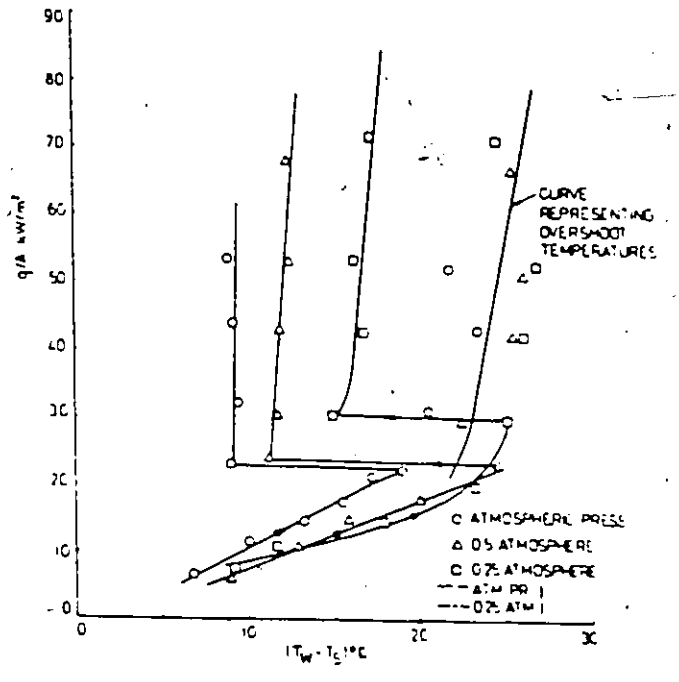

Incipient boiling and temperature overshoots for methanol

FIG. 2.15 INCIPIENT BOILING SUPERHEATS FOR R-113 & METHANOL (REF.123)

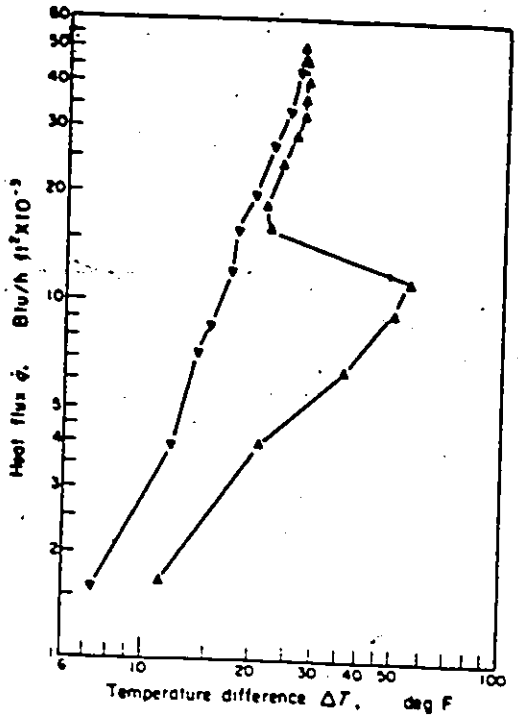

run No 32. Pressure, 90 lbf/in^2, acceleration, a = 16·3 g.

▲ increasing heat flux
▼ decreasing heat flux
ΔT_{sub} = 1·1 degF

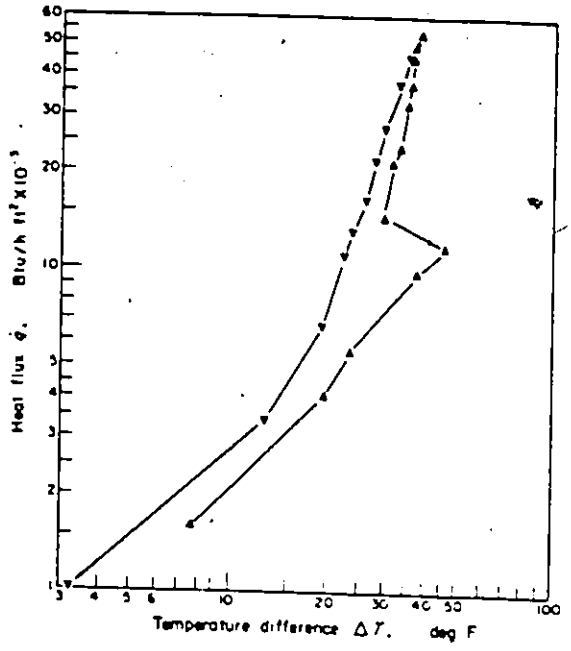

run No 33. Pressure, 95 lbf in^2, acceleration, a = 65·3 g

▲ increasing heat flux
▼ decreasing heat flux
ΔT_{sub} = 4·5 degF

FIG. 2.16 INCIPIENT BOILING SUPERHEATS FOR R-11 UNDER THE INFLUENCE OF INCREASED GRAVITY (REF.119)

of R-11, and they correlated their experimental data with the following equations for increasing and decreasing heat fluxes.

For increasing heat flux (for incipience of boiling process)

$$(T_w - T_{sat})^2 = (7 - q/6500)^2 \frac{2 \sigma T_{sat}}{K_l h_{fg} \rho_v} q$$

For decreasing heat flux (for maintaining the boiling process)

$$(T_w - T_{sat})^2 = 5 \frac{\sigma T_{sat}}{K_l h_{fg} \rho_v} q$$

The values of all the variables in these two equations are in SI units. The experimental data of Yin and Abdelmessih for increasing and decreasing heat fluxes is shown in appendix B.

2.4.3 Nucleate boiling

Various regimes in a typical case pool boiling are shown in figure 2.17, which is the conventional log-log representation of heat flux versus wall superheat. This curve is for pool boiling of water at atmospheric pressure. In the range B-C, the liquid near the wall is superheated forming bubbles. The bubbles transport the latent heat of the phase change and also increase the convective heat transfer by agitating the liquid near the heating surface. The mechanism in this

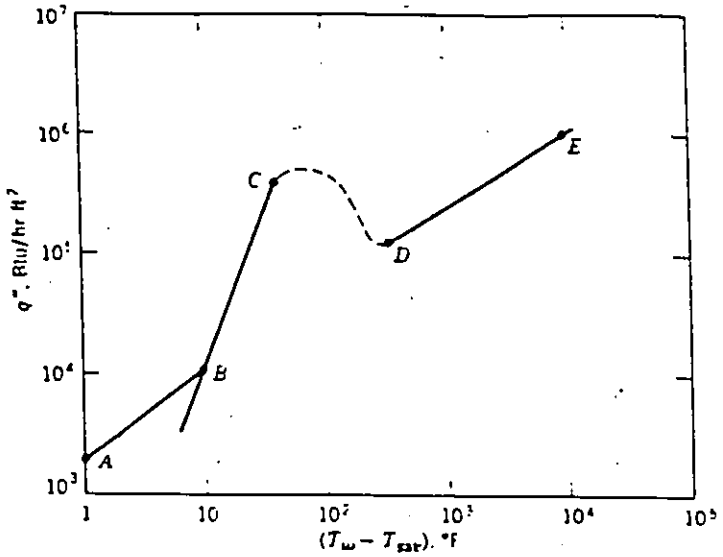

FIG. 2.17 Pool boiling regimes. *A-B*, natural convection; *B-C*, nucleate boiling; *C-D*, partial film boiling. *D-E*, stable film boiling

range is called nucleate boiling and is characterised by a very high heat transfer rate for only a small temperature difference. There are two subregimes in nucleate boiling;

1. local boiling or subcooled boiling
2. bulk boiling or saturated boiling

Local boiling is nucleate boiling in a subcooled liquid, where the bubbles formed at the heating surface tend to condense locally. Bulk boiling is nucleate boiling in a saturated liquid; in this case, the bubbles do not collapse. When the population of bubbles becomes too high at some high heat flux point C, the outgoing bubbles may obstruct the path of the incoming fluid. The vapour thus forms an insulating blanket covering the heating surface and thereby raising the surface temperature. In the range C-D the surface is alternately covered with a vapour blanket and a liquid layer, resulting in oscillating surface temperature. Boiling in this range is known as the transition boiling or partial film boiling.

There are numerous factors which affect the boiling mechanism e.g. number of active boiling sites, cavity size, mouth radius and depth, heated surface orientation, contact angle, growth and departure of bubbles, fluid-surface combination, initial liquid velocity, fluid properties, subcooling etc. There is a marked change in the heat transfer rate if any of the above variables are changed. Many

investigators (128-142) have studied the effect of the above mentioned variables on nucleate boiling. Detailed information is also available in books on two-phase flow heat transfer (143-147). Table 2.4.3 (appendix A) gives the details of the correlations available to predict the heat transfer rate in nucleate boiling regime.

2.4.4 Transition from nucleate boiling to two-phase forced convection

Nucleate flow boiling occurs in tubes when the quality is low. When the quality increases a transition occurs from nucleate boiling to two-phase forced convection. The quality plays an important role in determining the onset of this transition. Unforfunately, there is no published data to predict the onset of such a transition.

2.4.5 Two-phase forced convection

This is the most important heat transfer regime when the fluid is undergoing a change of phase in an evaporator tube. A literature survey on this topic reveals that there are numerous correlations available for this mechanism of heat transfer. These correlations were derieved for different sets of physical conditions and for a variety of working fluids.

As suggested by Martinelli (145), many of the correlations which have been proposed for two-phase convective heat transfer are in the form

$$(h_{tp}/h_{lo}) \text{ or } (h_{tp}/h_l) = a\ (1/X_{tt})^b \qquad \text{--- (I)}$$

where h_{tp} is the two-phase heat transfer coefficient, h_{lo} is the heat transfer coefficient if the total fluid were flowing with liquid properties in the tube, and h_l is the heat transfer coefficient if the liquid were flowing alone in the tube. The parameter X_{tt} is the Lockhart & Martinelli parameter and is given by

$$X_{tt} = ((1-x)/x)^{0.9}\ (\rho_g/\rho_l)^{0.5}\ (\mu_l/\mu_g)^{0.1}$$

A number of authors have extended the above equation to the following form

$$(h_{tp}/h_l) = C1[\ Bo + C2\ (1/X_{tt})^{n1}\ ]^{n2} \qquad \text{--- (II)}$$

where Bo is the boiling number and is given by $(q/G\ h_{fg})$. This equation gives the heat transfer coefficient for saturated convective heat transfer with simultaneous nucleate boiling. Tables 2.4.5 A and B (appendix A) show emperical values for the multipliers and exponents in equations I and II respectively and table 2.4.5C (appendix A)

gives the literature survey of the other correlations available to predict the two-phase forced convection heat transfer coefficient.

2.4.6 Transition from two-phase forced convection to liquid deficient region

During the process of evaporation inside tubes several flow pattern occur. Generally annular flow prevails over most of the tube length. Prior to the complete evaporation, the liquid film vanishes from the heating surface due to a complex hydrodynamic and heat transfer phenomenon causing dryout. This marks the change from annular to mist flow. The mass vapour fraction at the onset of dryout may be termed critical fraction or critical quality. Table 2.4.6 (appendix A) gives the details of the correlations which may be used to predict the onset of dryout in flow boiling.

2.4.7 Heat transfer in the liquid deficient region

In this region the magnitude of the heat transfer coefficients continue to drop as the quality increases. Table 2.4.7 (appendix A) gives a list of the correlations which may be used to calculate the heat transfer coefficients in this regime. Some of the investigators (201-206) have studied this region by experiments.

2.4.8 Heat transfer in single-phase vapour region

When the tube wall ceases to be wetted (no droplets impinging on the walls), the heat transfer coefficient becomes a mimimum. This results in an increase in the wall temperature of the heated surface. After this point onwards, the heat transfer coefficient is governed by the correlations listed in table 2.4.1 (appendix A). The vapour properties should be used to evaluate the heat transfer coefficients.

2.5 HEAT TRANSFER IN THE CONDENSER

Condensation occurs when the temperature of a vapour is reduced below its saturation temperature. In practice, the process generally occurs when the vapour comes in contact with a cool surface. The latent energy of the vapour is released, and there is heat transfer to the surface. Condensation may be divided into two categories as follow;

1. Film condensation
2. Dropwise condensation

Film condensation is generally characteristics of clean, uncontaminated surfaces and is very common in any engineering process. In the film condensation process the surface is blanketed by the film, which grows in thickness as it moves down the plate or a tube. A

temperature gradient exists in the film, and the film represents a thermal resistance to heat transfer. In dropwise condensation a large portion of the area of the plate or a tube is directly exposed to the vapour; there is no film barrier to heat flow, and higher heat transfer rates are experienced. The heat transfer rates in dropwise condensation may be as much as ten times higher than in film condensation. Because of the higher heat transfer rates, dropwise condensation would be preferred to film condensation, but it is extremely difficult to maintain since most surfaces become wetted after exposure to a condensing vapour over an extended period of time. Various surface coatings and vapour additives have been used in attempts to maintain dropwise condensation, but these methods have not met with general success to date.

A literature survey on this topic reveals that there are a number of correlations available to predict the heat transfer coefficients for the condensation process. However, most of these correlations are for falling film i.e. for film condensation. A number of investigators (207-233) have studied film and dropwise condensation and a summary of the correlations to predict the condensation coefficients inside a tube are presented in table 2.5 of appendix A.

2.6 PRESSURE DROP & VOID FRACTION CORRELATIONS

In any evaporating and condensing heat exchanger system, the working fluid undergoes a phase change and it may exist in either single-or two-phase. In the following section a literature survey is presented on the correlations available to predict the pressure drop and the void fraction for single-phase and two-phase regions.

2.6.1 Single-phase region

In single-phase flow the frictional pressure drop can be calculated by the following relation

$$\Delta P_f = f \frac{L}{2 g D} V^2 \rho_l$$

where f is the Blasius (234) friction factor and is a function of the Reynolds number.

$f = 64/Re$ for laminar flow

$f = 0.316/Re^{0.25}$ for turbulent flow

Hydrostatic pressure drop can be calculated from the following relation

$$\Delta P_h = \rho g Z \sin\gamma$$

where γ is the inclination angle from the horizontal.

The void fraction for this region is either 1 or 0 depending on the type of flow.

$\alpha = 0$ for single-phase liquid flow

$\alpha = 1$ for single-phase vapour flow

2.6.2 Two-phase region

The correlations of two-phase pressure drop and void fraction for isothermal and non-isothermal flow is of importance in many technical flow problems and has been the subject of numerous investigations (235-271) in the past. A literature survey on the correlations available is presented in table 2.6.2 (appendix A) for the calculation of two-phase frictional pressure drop, total pressure drop and the void fraction. The methods proposed have varied from semi-theoretical to empirical correlations without any one being completely successful, although the proposed method of Lockhart & Martinelli (250) has perhaps been the most widely used, where the use of two-phase frictional multipliers, whose actual values have been

determined empirically, have allowed helpful predictions to be made for certain flow regimes. Detailed checks with extensive data have shown that the correlation overpredicts the frictional pressure drop or stratified flow regime; is quite reasonable for slug and plug flow; and for annular flow it underpredicts for small diameter pipes but overpredicts for larger pipes (ref 241).

The hydrostatic pressure drop for this region may be calculated by first evaluating the density of two-phase mixture which is a function of void fraction and densities of both phases.

$$\Delta P_{tp,h} = \rho_m \; g \; Z \; \sin\gamma$$

where

$$\rho_m = \alpha \rho_v + (1-\alpha)\rho_l$$

The third kind of pressure loss occurs because of the acceleration of fluids due to vapour generation. The acceleration pressure drop can be calculated from the following relations.

For homogenous flow model

$$\Delta P_a = G_t^2/\rho_l \left[(1-x) + x\,(\rho_l/\rho_v) - 1\right]$$

For separated flow model

$$\Delta P_a = G_t^2/\rho_l \left[(1-x)^2/(1-a) + (x^2/a)\ (\rho_l/\rho_v) - 1\right]$$

CHAPTER III

MODEL DEVELOPMENT

3.1.1 INTRODUCTION

In the last chapter, various aspects of a two-phase flow systems were discussed and various correlations were presented for the flow regimes that are encountered in a such a system. In this chapter, a model will be developed by using the correlations listed in chapter 2.

The original model (see appendix C) developed by Ali (4) showed good agreement with earlier experiments (6,8,9). However, Ali's program was not able to simulate the more recent experiments done by Raza (12), where the overall performance was much lower than the results reported by Sampath (8). The lower performance obtained by Raza could be due to the fact that at the time he carried out his experiments, he was not aware of the presence of a hysteresis effect resulting from fluids boiling on a heated surface. Thus Raza's results may be for the heating process instead of cooling where a larger wall superheat is needed to initiate the boiling process.

In order to obtain better agreement with the data obtained by

Raza several correlations had to be changed. In addition some mistakes found in Ali's program were corrected. These mistakes were of a minor nature and would not have affected the previous results. The new model developed not only agrees with the data of Raza but also does a good job in simulating the experimental data obtained by Stauder (17), Kosnik & Bertoni (15) and Bergevin et al.(23). The reasons for selecting the various correlations are also discussed in this chapter.

3.1.2 Definitions

In this section some of the important parameters are defined as follows.

Vapour quality

By assuming thermal equlibrium in two-phase flow, the vapour quality is defined as

$$x = \frac{(h - h_f)}{h_{fg}} = \frac{\dot{m}_v}{(\dot{m}_v + \dot{m}_l)} \qquad \text{--- (1)}$$

Void fraction

The void fraction is defined as the ratio of the flow area occupied by vapour to the total flow area.

$$\alpha = \frac{A_v}{A_v + A_l} \qquad \text{--- (2)}$$

Mean density

Mean density of a two-phase mixture is given by the following relation.

$$\rho_m = \alpha \rho_v + (1-\alpha)\rho_l \qquad \text{--- (3)}$$

Phase velocities

For one-dimensional flow the area-averaged velocity of liquid and vapour phases are defined as follows.

$$V_l = \frac{\dot{m}_l}{\rho_l A_x (1-\alpha)} \qquad \text{--- (4)}$$

$$V_v = \frac{\dot{m}_v}{\rho_v A_x \alpha} \qquad \text{--- (5)}$$

Slip ratio

Slip ratio is defined as the ratio of the vapour phase velocity to the liquid phase velocity.

$$S = V_v/V_l \qquad \text{--- (6)}$$

from equations 4, 5 & 6

$$S = [x/(1-x)]\ (\rho_l/\rho_v)\ [(1-\alpha)/\alpha] \qquad \text{--- (7)}$$

3.1.3 Conservation equations

In this section the conservation equations are given, which should be satisfied for the loop.

Mass conservation

For steady state the conservation of mass equation must be satisfied.

$$\frac{d\dot{m}}{dz} = 0 \qquad \text{--- (8)}$$

Momentum conservation

For steady state the momentum equation is

$$-\frac{dp}{dz} = \frac{dG}{dt} + \frac{1}{A}\frac{d}{dz}\left[\frac{G^2 A}{\rho}\right] + \frac{P}{A}\tau_w + \rho g \cos\theta \qquad \text{--- (9)}$$

Equation (9) represents the acceleration pressure drop, frictional pressure drop, hydrostatic pressure drop and the pressure drop in bends, fittings. etc.

$$-dP_t = dP_a + dP_f + dP_h + dP_l \qquad \text{--- (10)}$$

The terms dP_a, dP_f, dP_h and dP_l are acceleration pressure loss, frictional pressure loss, hydrostatic pressure loss and pressure drop in valves, bends, fittings, etc. respectively.

For a closed system the summation of the pressure drops around the loop must be zero.

$$\Delta P_t = 0 \qquad \text{--- (11)}$$

Energy conservation

The amount of heat transferred to a mixture per unit length, q', is equal to the rate of change of enthalpy of mixture with respect to z, neglecting the changes in potential and kinetic energies.

$$q' = \frac{d}{dz}(\dot{m}_l h_l) + \frac{d}{dz}(\dot{m}_v h_v) \qquad \text{--- (12)}$$

$$q' \, dz = d(\dot{m}_l h_l) + d(\dot{m}_v h_v) \qquad \text{--- (13)}$$

3.1.4 Program logic

In this section the model used for the development of a computer simulation program is described which is capable of simulating the performance of fluid-to-fluid, two-phase thermosiphon loop heat exchanger systems, using any working fluid. The model developed is based on the assumption of one-dimensional steady state equlibrium flow in the tubes. The equations used in the model were taken from the literature discussed in chapter 2, and the detailed description of the correlations is presented in sections 3.2 to 3.6. Due to many possible modes of heat transfer that can occur along the length of the evaporator tubes, as discussed in chapter 2, the evaporator was analyzed by subdividing each tube into shorter elemental lengths for which average values provide a good approximation.

Figure 3.1 shows a flow diagram for the program which illustrates the program logic and the type of information which the operator must supply. Before using the program the operator must ensure that the appropriate property subroutines for the working fluids and the source and the sink fluids are incorporated (see appendix D). To run the program, the operator must specify the hot

FIG. 3.1 SIMULATION PROGRAM FLOW DIAGRAM - CONT. ON NEXT PAGE

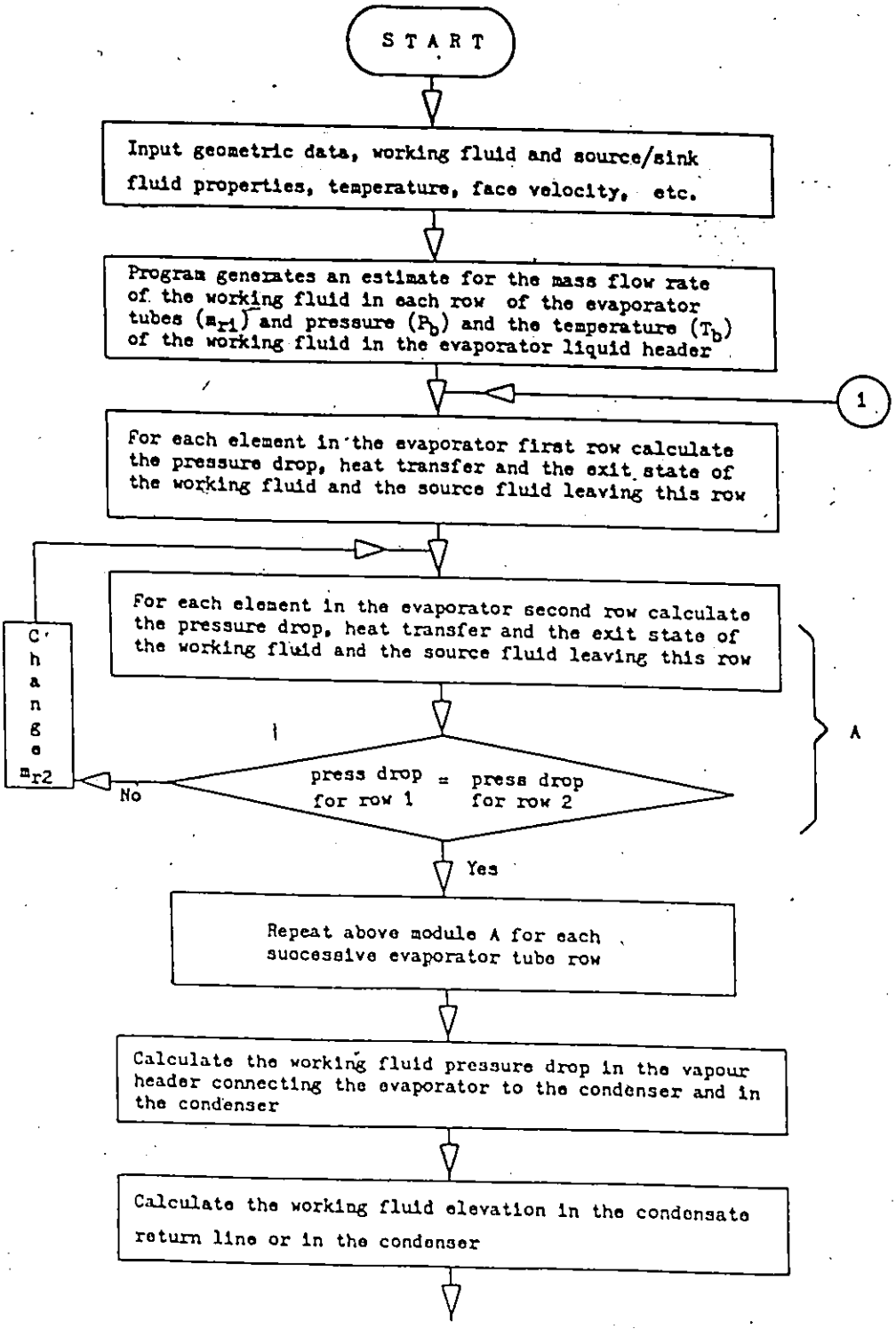

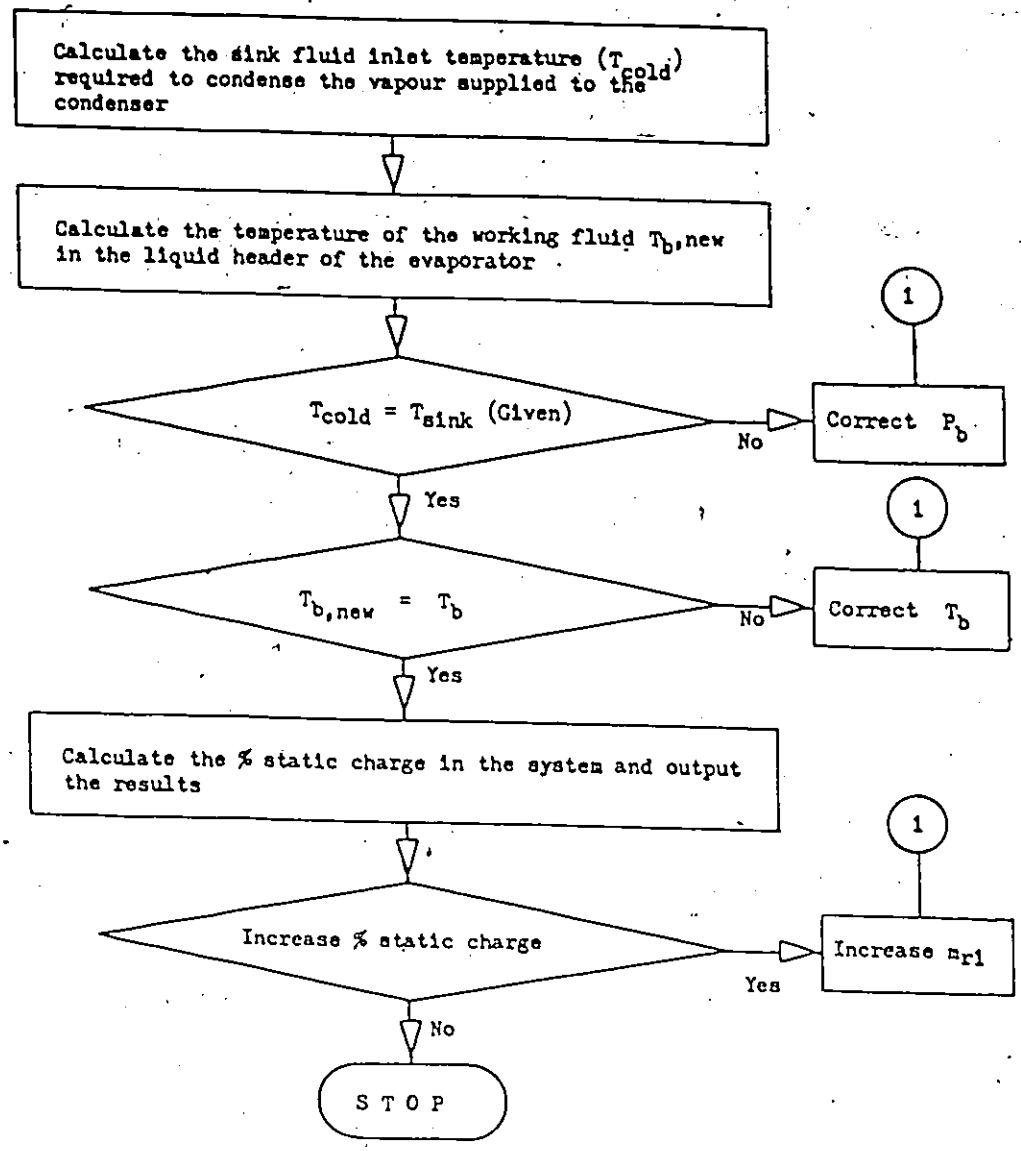

FIG. 3.1 SIMULATION PROGRAM FLOW DIAGRAM

and cold supply duct temperatures (T_h) and (T_c); the geometric configuration and the size information necessary to describe the system and the number of elements into which the length of each evaporator tube is to be subdivided (the default value is 10). Appendix H2 "User's manual" gives the precise form of the subroutines which should be used.

The program estimates an initial pressure and temperature in the evaporator liquid header and the mass flow rate per tube in the first row of tubes , then proceeds to calculate the heat transfer, the exit state of the working fluid and the source fluid temperature downstream of the evaporator element for each tube element in the first row. Similar calculations are done for each subsequent row of evaporator tubes. For each of these rows the flow rate is varied until its exit pressure agrees with that from the first row of tubes. The pressure drop across and the heat loss from the vapour header is calculated. Assuming a negligible pressure drop across the condenser tubes, and by knowing the inlet and the exit states of the condenser, the heat transfer in condenser and the sink fluid temperature is calculated. The inlet pressure of the evaporator liquid header is varied until the given cold duct supply temperature is achieved. Once this convergence is reached an energy balance applied to the evaporator liquid header yield a new value for the fluid temperature at the bottom of the evaporator. This new value is used to generate final data including the static liquid level which would exist in the loop upon shutdown.

The program outputs the overall results and the calculated static charge in the evaporator as a percentage of the total tube volume. To generate a set of results for a higher or a lower static charge in the evaporator, the mass flow rate of the working fluid per tube in the first row of evaporator tubes must be increased or decreased respectively.

3.1.5 Heat transfer relationships

In order to calculate the rate of heat transfer through any element, a relationship must be developed between the heat flux, the temperature difference between the source fluid temperature and the working fluid and the thermal properties of the element. This may be easily done with the help of an electrical analog of the system.

Figure 3.2 shows such an electrical analog for an evaporator heat exchanger transferring heat from a source fluid at a constant temperature T_h to a working fluid at a temperature of T_f. The various resistances to the flow of heat from the source to a working fluid are shown and identified below:

1. Evaporator resistance, R_e, the thermal resistance between evaporator wall and the working fluid.
2. Evaporator external resistance, R_{ee}, the resistance between the evaporator tube wall and the source fluid.
3. Evaporator wall resistance, R_{ew}
4. Evaporator fouling factors; Inside, F_{ei} & Outside, F_{eo}

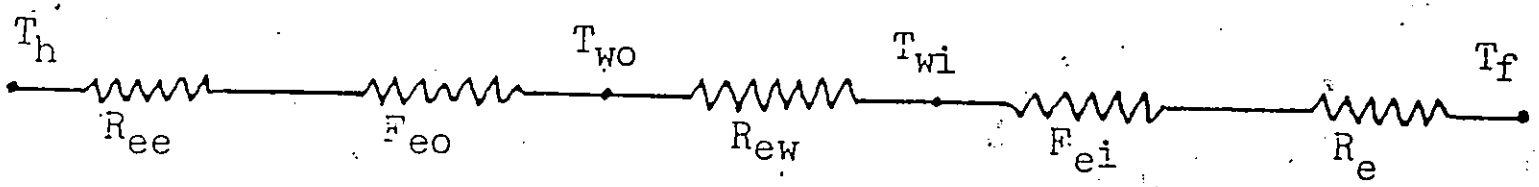

FIGURE 3.2 ELECTRICAL ANALOG FOR AN EVAPORATOR ELEMENT

exchanger depends largely on the resistances listed 1 and 2.

The heat transfer rate at any point can be calculated as follows:

$$Q_z = \frac{(T_h - T_f)}{R_{tot}} \qquad \text{--- (14)}$$

where T_h is the average source fluid temperature for an element.

and $$R_{tot} = R_{ee} + F_{eo} + R_{ew} + F_{ei} + R_e \qquad \text{--- (15)}$$

$$R_{tot} = 1/(U_z A_i) \qquad \text{--- (16)}$$

$$1/U_z = 1/U_o\ (A_i/A_o) + F_{eo} + [\Delta A_i\ \ln(r_o/r_i)/2\pi k\ z] + F_{ei} + 1/h_{lp} \qquad \text{--- (17)}$$

The first term on the right hand side of equation 17 is the evaporator outside resistance (including the effect of external fins etc.), the second and fourth terms are the outside and inside fouling factors respectively, the third term is the wall resistance and the last term is the evaporator inside resistance. The values of F_{ei} & F_{eo} must be obtained from the literature. Once U_o is supplied for a particular geometry and fin configuration, and h_{lp} is calculated in the program then heat transfer rate may be evaluated. See appendix E & F for the evaluation of U_o for annulus and cross flow finned tube configurations.

For the case where the source fluid temperature is varying (as in the case of air flowing over finned tubes) the effectiveness may be calculated from

$$E_z = 1 - e^{(-NTU_z)} \qquad \text{--- (18)}$$

where $$NTU_z = ((U_z \ A_i)/(\Delta\dot{m}\ Cp)_{air}) \qquad \text{--- (19)}$$

$\Delta\dot{m}$ is the mass flow rate of hot air flowing past the tube element, and $(U_z A_i)$ may be calculated using equation 17.

The rate of heat transfer for the element may be calculated by

$$Q_z = E_z\ (\Delta\dot{m}\ Cp)_{air}\ (T_a - T_f) \qquad \text{--- (20)}$$

where T_a is the approach air temperature for the element.

For a prescribed heat flux boundary condition

The rate of heat transfer for the element was calculated by

$$Q_z = q_z \ A_i \qquad \text{--- (21)}$$

and the wall temperature was calculated by

$$T_w = T_f + Q_z/(h_i \ A_i) \qquad \text{--- (22)}$$

3.2 EVAPORATOR CALCULATIONS

In this section, the correlations used for the various flow regimes are discussed in details. In the beginning of this section, the estimation of the working fluid state in the evaporator liquid header is discussed.

3.2.1 Estimation of an initial state of the working fluid in evaporator liquid header

Input data is used to estimate the state of the working fluid (pressure & temperature).

(a) Estimation of pressure & temperature

The source and the sink temperatures T_h & T_c govern the maximum and minimum pressure limits in a two-phase thermosiphon loop. The maximum pressure ,P_{max}, would correspond to the saturation pressure at T_h and the minimum pressure, P_{min}, would correspond to the saturation pressure at T_c. The initial starting pressure in the evaporator liquid header was set equal to the average of these two pressures plus the pressure head corresponding to the evaporator tube filled with liquid. Hence, the following relation was used in determination of the first estimation of pressure in the evaporator liquid header.

$$P_{evap,b} = (P_{max} + P_{min})/2 + H_e \rho_l g \qquad \text{--- (23)}$$

where H_e is the difference in elevation between the vapour and the liquid headers of the first row of evaporator tubes.

The working fluid enters the bottom of the evaporator from the condenser in a subcooled state and hence the temperature of the working fluid in the evaporator inlet would be less than the saturation temperature corresponding to $P_{evap,b}$. The following relation was used to estimate the temperature of the working fluid.

$$T_{evap,b} = T_{sat}(P_{evap,b}) - C\,[\,T_{sat}(P_{evap,b}) - T_{cold}] \qquad \text{--- (24)}$$

where T_{cold} is the cold fluid temperature. A value of 0.045 for C was found to agree with the converged results obtained by the computer program.

The estimated values of pressure and temperature from equations 23 and 24 resulted in convergence in 2 or 3 iterations.

(b) Estimation of mass flow rate in the evaporator tube

The mass flow rate for the evaporator tube may be estimated by the following method.

The heat added in the evaporator tube may be estimated by

$$Q_e = h_{e,av}\, A_e\, (T_{ew,av} - T_{eb,av}) = \dot{m}\, h_{fg}\, x_e \qquad \text{--- (25)}$$

where $h_{e,av}$ is the average heat transfer coefficient for the evaporator, $T_{ew,av}$, $T_{eb,av}$, x_e & A_e are the average evaporator wall temperature, average bulk fluid temperature, the evaporator exit quality and the evaporator surface area. Solving for $\dot{m}$

$$\dot{m} = \frac{h_{ev,av}\, A_e\, (T_{ew,av} - T_{eb,av})}{h_{fg}\, x_e} \qquad \text{--- (26)}$$

From the experience of running the computer program it was found that when x_e is taken as 0.45, a good initial estimate is produced.

Once the evaporator inlet pressure, temperature and the mass flow rate are estimated, the program proceeds to calculate the heat transfer & pressure drop for each evaporator element. In the following sections the correlations which were used for the calculations are discussed.

3.2.2 Single-phase flow

The working fluid enters the evaporator in a subcooled state and hence is all liquid at the entrance. Heat transfer takes place by single phase forced convection and the pressure decreases as the fluid progresses up the tube. The heat transfer and the pressure drop for the first element were determined as follows:

3.2.2.1 Heat transfer calculations

The correlations of Sieder & Tate (96) were used to determine the local heat transfer coefficient for single-phase developing flow. The following correlations were used to determine the heat transfer coefficient for this single-phase liquid region.

For laminar flow

$$Nu_z = 1.24\,[Re\ Pr/(L/D)]^{1/3}\,(\mu/\mu_s)^{0.14} \quad \text{---} \quad (27)$$

For turbulent flow

$$Nu_d = 0.027\ Re^{0.8}\ Pr^{0.33}\ (\mu/\mu_s)^{0.14} \qquad \text{--- (28)}$$

Once the value of h_{lp} is known, the heat transfer rate into the element can be calculated from equation 14.

3.2.2.2. Pressure drop calculation

The frictional and the hydrostatic pressure drops were calculated from the following relations.

$$\Delta P_{fz} = f\ \frac{\Delta z\ V_l^2}{2\ D}\ \rho_l \qquad \text{--- (29)}$$

$$\Delta P_{hz} = \Delta z\ \rho g\ \sin\gamma \qquad \text{--- (30)}$$

where, for Laminar flow (Re < 2000)

$$f = 64/Re \qquad \text{--- (31)}$$

and for Turbulent flow (Re > 2000)

$$f = 0.316/Re^{0.25} \qquad \text{--- (32)}$$

As the flow progresses up the evaporator tube, the pressure drops and hence the saturation temperature decreases. The bulk fluid temperature and the wall temperature increase along the length of this section of the evaporator tube. When the wall temperature exceeds the local saturation temperature by a sufficient amount (even when the bulk fluid temperature is below the saturation temperature) the first nucleation site becomes activated. If boiling takes place when the

bulk fluid temperature is below the saturation temperature, it is termed subcooled nucleate boiling.

3.2.3 Subcooled boiling

The correlations available to predict the conditions necessary for boiling are listed in table 2.4.2. These correlations may be used to predict the minimum heat flux required to maintain subcooled boiling in a flow boiling situation. The correlation of Sato & Matsumura (112) for turbulent flow, and their modification introduced by Ali for laminar flow were used to predict the mimimum heat flux necessary to sustain boiling.

For laminar flow

$$q = \frac{k_L \lambda}{8\sigma T_s (v_g - v_L)} \left[\frac{(D\nu_L Z)^{1/3} q}{1.86\, v_L^{0.33}\, Pr_L^{0.33}\, k_L} - (T_s - T) \right]^2 \quad (33)$$

For turbulent flow

$$q = \frac{k_L \lambda}{8\sigma T_s (v_g - v_L)} \left[\frac{D^{0.2}\, \nu_L^{0.8}\, q}{0.023\, Pr_L^{0.4}\, k_L\, v_L^{0.8}} - (T_s - T) \right]^2 \quad (34)$$

However, when no vapour bubbles are present as in the case of the system startup, a much greater wall superheat is required to initiate the bubble growth. Abdelmessih et al.(120) investigated this incipient boiling effect for R-11 flowing in a heated stainless steel 10.92 mm inside diameter tube with a mass flow range of 2.44

kg/min to 18.29 kg/min. They found that for the startup process the wall superheats were in the range of 13.9 - 16.7 C. For the present studies for R-11 boiling in copper tubes, Stauder (17) found that wall superheats of 12 - 14 C were required to initiate the boiling for the system startup. To investigate this effect a flag can be set in the program which requires the system to have a wall superheat of 13.3 C before any boiling was allowed to take place.

3.2.3.1. Effective heat transfer coefficient in the subcooled boiling region

Once subcooled nucleate boiling has been initiated, vapour bubbles formed at the wall detach and move into the bulk of the fluid. Since the bulk fluid temperature is less than the saturation temperature, the bubbles condense in the fluid and give up their latent heat. Figure 3.3 illustrates different models suggested to estimate the effective heat transfer coefficient for this region. In this region highly localized nucleate boiling is initially superimposed on the heat flux due to forced convection at the wall. The effective heat transfer coefficient for this region was evaluated from the following relation, which was developed by Ali (4)

$$h_{el} = [\, h_b^{\,p} + h_{lp}^{\,p} \,]^{(1/p)} \qquad \text{--- (35)}$$

where the power p is given by

$$p = 2 - \frac{(T_s - T_f)}{(T_s - T_f)_{ib}} \qquad \text{--- (36)}$$

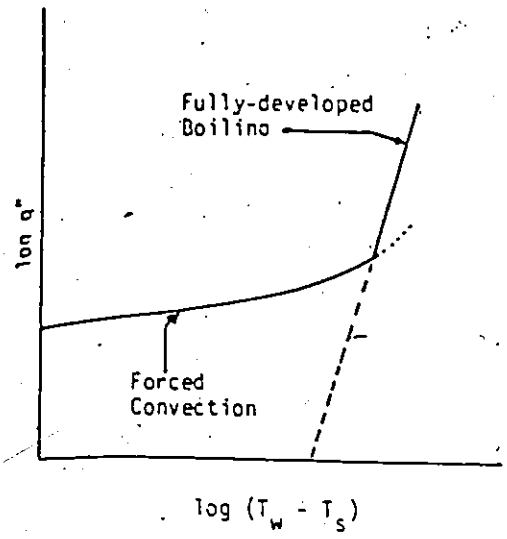

Procedure of McAdams et al.

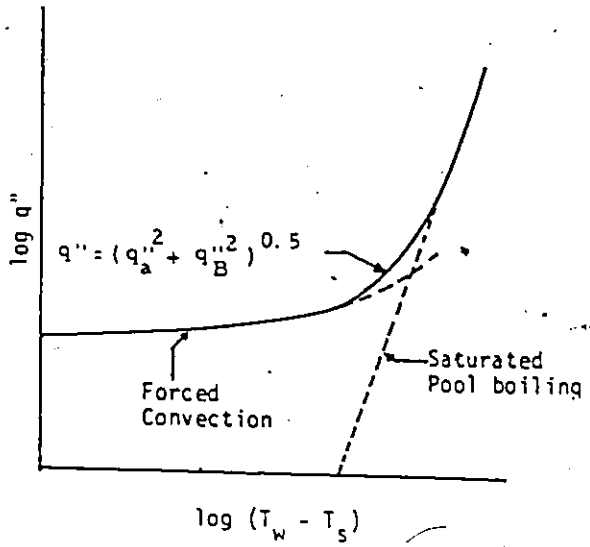

Procedure of Kutateladze

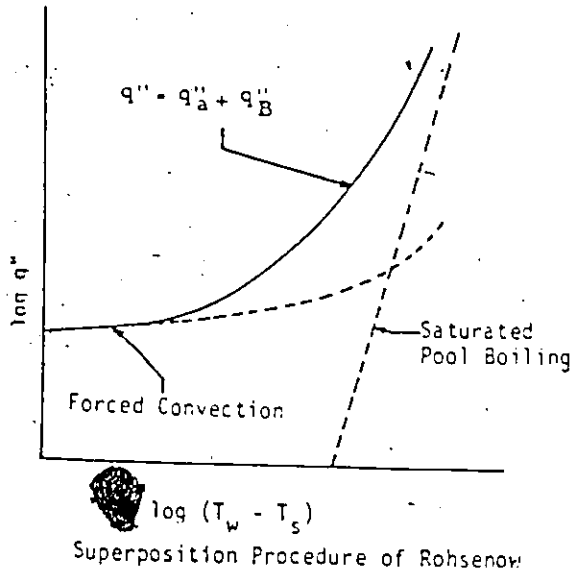

Superposition Procedure of Rohsenow

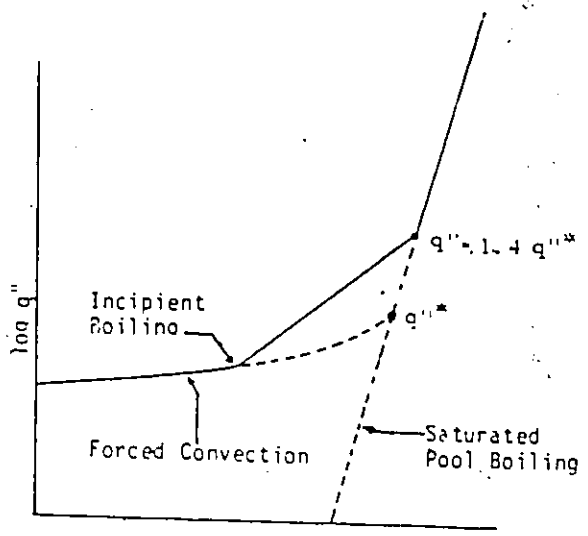

Procedure of Forster and Grief

FIG. 3.3 ESTIMATION PROCEDURE IN TRANSITIONAL BOILING

p is unity at the point of incipient boiling , therefore additive (Rohsenow), then approaches the value two as the degree of subcooling ($T_s - T_f$) approaches zero (agreeing with Kutateladze).

In the subcooled nucleate boiling region the vapour quality is zero (based on the enthalpy), even though the void fraction may be sufficient to cause an increase in the velocity of the fluid.

For this region, the single-phase forced convection coefficient was calculated from equation 27 or 28 with the modified Reynolds number as follows;

$$Re_{scb} = V_l \; D \; \rho_m / \mu_l \qquad \text{--- (37)}$$

where ρ_m is given by equation 3.

In the subcooled nucleate boiling region it is presumed that the fluid is throughly mixed due to condensing of the vapour bubbles and hence a void fraction was calculated based on the homogenous model.

$$\alpha = 1 \; / \; [\, 1 + (\, 1 - x_{scb})/x_{scb} \; (\rho_v / \rho_l)] \qquad \text{--- (38)}$$

The following quality was used in equation 38 to calculate the void fraction.

$$x_{scb} = q_b / (m_t \; h_{fg}) \qquad \text{--- (39)}$$

where q_b is the heat transfer due to boiling. Once q_b is calculated from Rohsenow's (152) pool boiling correlation (discussed in 3.2.4),

the Reynolds number was calculated from equation 37 by using equations 38 & 39 and thus h_{el} was calculated from equation 35.

3.2.3.2. Pressure drop calculation

Even though the void fraction and the quality in the subcooled region are of very small magnitude, the pressure drop would be lower in comparison to that of single-phase liquid flow. The method of estimation of the pressure drop is discussed in 3.2.5.2.

3.2.4. Flow boiling

As the fluid progresses up the evaporator tube, the bulk fluid temperature would eventually be equal to the saturation temperature, when saturated nucleate boiling starts.

3.2.4.1. Determination of boiling heat transfer coefficient h_b

Rohsenow's pool boiling correlation is the most widely used correlation in the determination of the nucleate boiling coefficient, even though numerous correlations are available in the literature. The following is Rohsenow's correlation (152)

$$q_b = \mu_L \lambda \left[\frac{g(\rho_L-\rho_g)}{\sigma}\right]^{\frac{1}{2}} \left[\frac{C_L(T_w-T_s)}{\lambda(CSF)\ Pr^{1.7}}\right]^r \quad \text{--- (40)}$$

where Csf and r are constant for a given working fluid/heating surface combination.

Once the heat flux q_b is known, the boiling heat transfer coefficient can be calculated from

$$h_b = q_b/\Delta T_b \qquad \text{--- (41)}$$

where $\Delta T_b = T_w - T_s$

The following values of Csf and r were used by Ali.

$$\left.\begin{array}{l} Csf = 0.01 \\ r = 1.31 \end{array}\right| \qquad \text{--- (42)}$$

Initially, the program was run with the values used by Ali. But it was found that the boiling heat transfer coefficient h_b was greater than the two-phase heat transfer coefficient even at high vapour qualities, where nucleate boiling should have been suppressed. Literature shows that various values for r in Rohsenow's boiling equation have been used with a range of 0.33 to 3.0. In order to accurately model the experimental data of Raza, so that the simulated wall temperature and the heat transfer rate agreed with the corresponding experimental data it was found nessary to correct the value of r. The following values of Csf and r were used in the present studies.

$$\left.\begin{array}{l} Csf = 0.01 \\ r = 1.80 \end{array}\right| \qquad \text{--- (43)}$$

The same values of these constants were also used to simulate

the experimental data provided by Stauder, Kosnik & Bertoni and the experimental data of Bergevin et al.

3.2.4.2 Boiling suppression

The quality and the vapour fraction increases with the heat addition resulting in higher vapour velocities and higher two-phase heat transfer coefficients. As the quality and vapour fraction continue to increase, the flow inside the evaporator becomes annular and nucleate boiling is suppressed. The following relation, which was used to calculate the effective heat transfer coefficient in two-phase flow region, shows the domination of two-phase heat transfer coefficient at higher qualities (when $h_{tp} > h_b$), where the effect of h_b diminish.

$$h_{2e} = [\, h_{tp}{}^{p} + h_b{}^{p} \,]^{(1/p)} \qquad \text{--- (44)}$$

3.2.4.3 Pressure drop calculations

In flow boiling region the working fluid is in two-phase state and the procedure for calculation of the pressure drop is discussed in section 3.2.5.2.

3.2.5 Two-phase forced convection

3.2.5.1 Heat transfer calculations

At the point where the bulk fluid temperature reaches the

saturation temperature, a two-phase flow coefficient h_{tp}, based on the correlation of Davis & David (161) was calculated. Ali used Sachs & Long (173) correlation for the determination of the two-phase flow coefficient which was used to simulate the experimental data of Hwang (1) & Sampath (3). The agreement between the simulated results and the experimental data was excellent. Since, Raza used the same experimental rig which was used by Sampath, the author used the correlation used by Ali to simulate the experimental studies done by Raza. Surprisingly, the overall heat transfer rates and the wall temperatures did not match with the experimental values provided by Raza. The simulated overall heat transfer rate, on average, was 20 - 25 % greater than that was obtained from the experiments. The temperatures of the evaporator wall on the average were 2 C lower than the experimental values. One of the major cause for this lower performance obtained by Raza could be due to the fact that the experimental set up was sitting in the lab for more than 3 years and the boiling characteristics could have been changed due to deposition of foreign matter resulting in destroying some of the nucleation sites. The other reason could be that Raza was not aware of the presense of a hysteresis effect resulting from fluids boiling on a heated surface. Hence, it was necessary to increase the inside evaporator resistance which would result in a lower heat transfer rate and a higher wall temperature for the evaporator. It was logical to use a correlation which would yield a lower heat transfer

coefficient in comparison to that of Sachs & Long. It was found that the correlation proposed by Davis & David yielded a good agreement of the simulated and the experimental results. However, it should be noted that their correlation was derived for water-steam mixtures flowing in a horizontal duct. The following is the correlation of Davis & David.

$$h_{tp} = 0.0333 \left(\frac{K_l}{D}\right) \left(\frac{D\, G_t}{\mu_{tp}}\right)^{0.87} Pr_l^{0.4} \qquad \text{--- (45)}$$

where

$$\frac{1}{\mu_{tp}} = \frac{x}{\mu_v} + \frac{1 - x}{\mu_l} \qquad \text{--- (46)}$$

In the two-phase region the effective heat transfer coefficient was calculated from equation 44 with the power p = 4.0. Ali used a value of 2 for p for his model, which had to be changed to 4.0 to bring the wall temperatures in to agreement with the experimental values. The model used by the author in this region to combine h_b and h_{tp} is shown in figure 3.4. By using p = 4 in equation 44, the effective heat flux in the transitional boiling region follow very close to the true boiling curve, as can be seen from figure 3.4.

3.2.5.2 Pressure drop & void fraction calculations

The Lockhart & Martinelli (249) correlations were used to relate the two-phase frictional pressure drop to the single-phase frictional pressure drops for the vapour and liquid phases flowing separately.

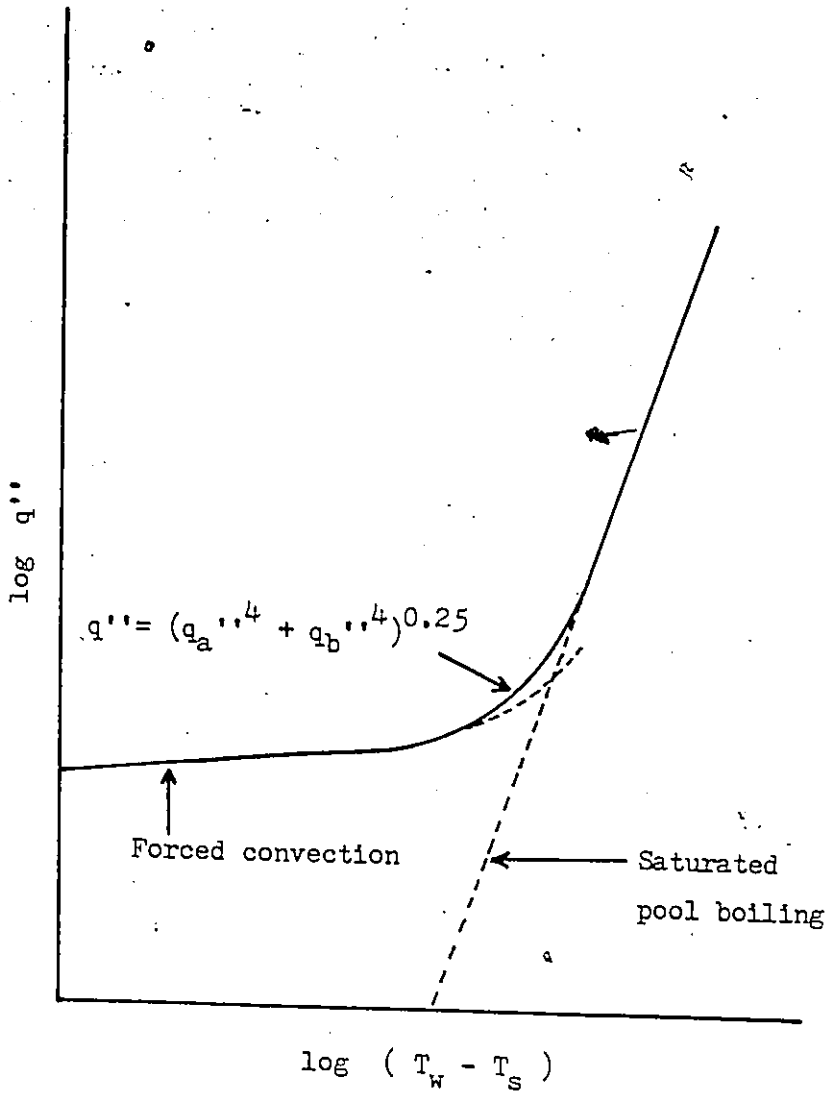

Figure 3.4 Author's proposed method of estimation effective heat flux in transitional boiling

$$\Delta P_{tp}/\Delta P_{lp} = \phi_{ij}^2 \qquad \text{--- (47)}$$

The parameter ϕ is emperically determined in terms of Lockhart-Martinelli parameter X. Subscript i j represents the conditions of liquid and the vapour phases respectively. Four such conditions exist for the mixture.

1. liquid phase laminar and vapour phase laminar
2. liquid phase laminar and vapour phase turbulent
3. liquid phase turbulent and vapour phase laminar
4. liquid phase turbulent and vapour phase turbulent

For case 1

$$X_{ll} = \left(\frac{1-x}{x}\right)\left(\frac{\rho_v}{\rho_l}\right)\left(\frac{\mu_l}{\mu_v}\right)^{0.5} \qquad \text{--- (48)}$$

$$\phi_{ll} = \left(1 + X_{ll}^{-0.70}\right)^{1.43} \qquad \text{--- (49)}$$

For case 2

$$X_{lt} = 18.65\ Re_v^{-0.4}\left(\frac{1-x}{x}\right)\left(\frac{\rho_v}{\rho_l}\right)\left(\frac{\mu_l}{\mu_v}\right)^{0.5} \qquad \text{--- (50)}$$

$$\phi_{lt} = \left(1 + X_{lt}^{-0.56}\right)^{1.80} \qquad \text{--- (51)}$$

For case 3

$$X_{tl} = 0.054\ Re_l^{0.4}\ \left(\frac{1-x}{x}\right)\left(\frac{\rho_v}{\rho_l}\right)\left(\frac{\mu_l}{\mu_v}\right)^{0.5} \quad \text{--- (52)}$$

$$\Phi_{tl} = \left(1 + X_{tl}^{-0.56}\right)^{1.80} \quad \text{--- (53)}$$

For case 4

$$X_{tt} = \left(\frac{1-x}{x}\right)^{0.9}\ \left(\frac{\rho_v}{\rho_l}\right)^{0.5}\ \left(\frac{\mu_l}{\mu_v}\right)^{0.1} \quad \text{--- (54)}$$

$$\Phi_{tt} = \left(1 + X_{tt}^{-0.49}\right)^{2.05} \quad \text{--- (55)}$$

The hydrostatic pressure drop was calculated from the following relation

$$\Delta P_{h,tp} = \Delta z\ \rho_m\ \sin\gamma \quad \text{--- (56)}$$

where ρ_m is given by equation 3 and γ is the inclination angle from the horizontal.

The acceleration pressure drop was calculated (249) from the following relation.

$$\Delta P_a = G_t^2/\rho_l\ [(1-x)^2/(1-\alpha) + (x^2/\alpha)(\rho_l/\rho_v) - 1] \quad \text{--- (57)}$$

The empirical correlation of Lockhart & Martinelli (66) was used for the calculation of the void fraction.

$$\alpha = \left(1 + x^{0.8}\right)^{-0.378} \quad \text{--- (58)}$$

3.2.7 Transition from two-phase forced convection to the liquid deficient region

The correlation of Lavin & Young (180), which was used by Ali, was used at first for the present studies. But it was found that it did not predict dryout even at lower static charges of approximately 25 %, which was clearly observed from the experimental data of Raza. Hence correlations proposed by Sthapak et al. (193), Roko et al. (194), Rhee & Young (181) and Jones & Altman (195) were tried. It was found that the correlation proposed by Rhee & Young predicted this transition point accurately. Dryout occurred if the quality exceeded the critical quality defined as

$$x_c = \left[\frac{We \cdot \sigma \rho_g}{G_L \mu_L \{Re_L/(1-\alpha)\}^{0.125}} \right]^{0.5} \quad \text{--- (59)}$$

where We is given by Rhee & Young

$$We = 1.87 \times 10^{-7} Re_g \left(\frac{\rho_\ell}{\rho_g}\right)^{0.6} \left(\frac{D}{0.0608}\right)^{-0.48} \quad \text{--- (60)}$$

where the diameter, D, is in feet.

3.2.7.1 Effective heat transfer coefficient in the dryout region

In this region the heat transfer coefficient decreases as the quality increases and reaches a minimum equal to that of single phase vapour when x = 1. The effective heat transfer for this region was calculated as follows;

$$h_{e3} = A\, h_v + B\, h_{e2} \qquad \text{--- (61)}$$

where $A = [(x - x_c)/(1 - x_c)]^m$ --- (62)

$B = (1 - A)$ --- (63)

At first, the author used a linear variation (m=1) for the heat transfer coefficient for the dryout region. It was found that for m = 1; the simulated wall temperatures and the heat transfer rate did not agree with the corresponding experimental results. A value of 0.5 for m was tried, which yielded good agreement with the experimental data.

The single phase vapour heat transfer coefficient was calculated under the assumption that vapour alone occupied the tube.

3.2.7.2 Pressure drop calculations

The pressure drop in this region decreases as the quality increases. The following method was adopted from reference 9, where the frictional pressure drop was calculated as a function of x_c. The following is the relation used in the program to calculate the frictional pressure drop for the dryout region.

$$\Delta p_{f,do} = (C\, \Delta p_{f,g} + D\, \Delta p_{f,tp}) \qquad \text{--- (64)}$$

where $C = (x - x_c)/(1 - x_c)$ --- (65)

$D = (1 - C)$ --- (66)

at $x = x_c$; $\Delta p_{f,do} = \Delta p_{f,tp}$

and at $x = 1$; $\Delta p_{f,do} = \Delta p_{f,g}$

The pressure drop decreases linearly with the increase of x_c between the above two limits.

The hydrostatic and acceleration pressure drops were calculated in a manner similar to that described in section 3.2.5.2.

3.2.8 Single-phase vapour flow

3.2.8.1 Heat transfer calculation

When the magnitude of the quality reaches 1, the flow is all vapour and the heat transfer coefficient for this region was calculated from the relations described in section 3.2.2.1 by using vapour properties instead of the liquid properties.

3.2.8.2 Pressure drop calculation

Since the flow is all vapour, the pressure drop was calculated from the relations as indicated in section 3.2.2.2 by using vapour properties.

3.2.9. Calculations for evaporator second and successive tube rows

3.2.9.1 Estimation of the mass flow rate of the working fluid through the tubes

The source fluid temperature decreases as it passes over the evaporator tube rows and hence the evaporator tube rows are subjected

to unequal heating. Hence, for a given mass flow rate for the evaporator coil first row, the mass flow rate in the second tube row is calculated, which would be different from the first row (due to unequal heating). The flow rate in the second row is varied until the pressure drop for the second row equals to the pressure drop of row 1. Similar calculations may be done for the successive evaporator tube rows. The mass flow rate and the pressure drop are related by the following (see appendix G for the derivation).

$$\dot{m} = f(\Delta P)^n \qquad \text{--- (67)}$$

where $n = 1.0$ for laminar flow

& $n = 0.571$ for turbulent flow

Equation 67 was used to calculate the mass flow rate in the second and the successive rows

$$\dot{m}_{2\ row} = \dot{m}_{1\ row} [\Delta P_{2\ row} / \Delta P_{1\ row}]^n \qquad \text{--- (68)}$$

3.2.9.2 Heat transfer calculations

Since the source fluid temperature decreases as it passes over the evaporator tube rows, the downstream source fluid temperatures for the elements of the evaporator first row were stored in a dimensional form. The variation of the downstream source fluid temperature for the evaporator first row along the length of the tube is shown in figure

3.5 (assuming that the first row of the evaporator is not dried up). These temperatures were used as the source fluid temperatures for the calculations of the heat transfer rate for the evaporator second tube row. Similar calculations could be done for each successive evaporator tube rows.

3.3 SEPARATOR CALCULATIONS

When the fluid reaches the evaporator top, it goes into the vapour header and then through a separator from which the liquid is recirculated to the evaporator liquid header by gravity. The recirculation flow rate and the vapour header flow rate were calculated assuming perfect separation and equlibrium conditions.

Hence

$$\dot{m}_r = \dot{m}_t \ (1 - x) \qquad \text{--- (69)}$$

$$\dot{m}_v = \dot{m}_t \ x \qquad \text{--- (70)}$$

and thus the quality of the vapour entering the vapour header is one.

3.4 VAPOUR HEADER CALCULATIONS

The vapour header interconnects the top of the evaporator to the top of the condenser. Heat loss from the vapour header was calculated from the following equations.

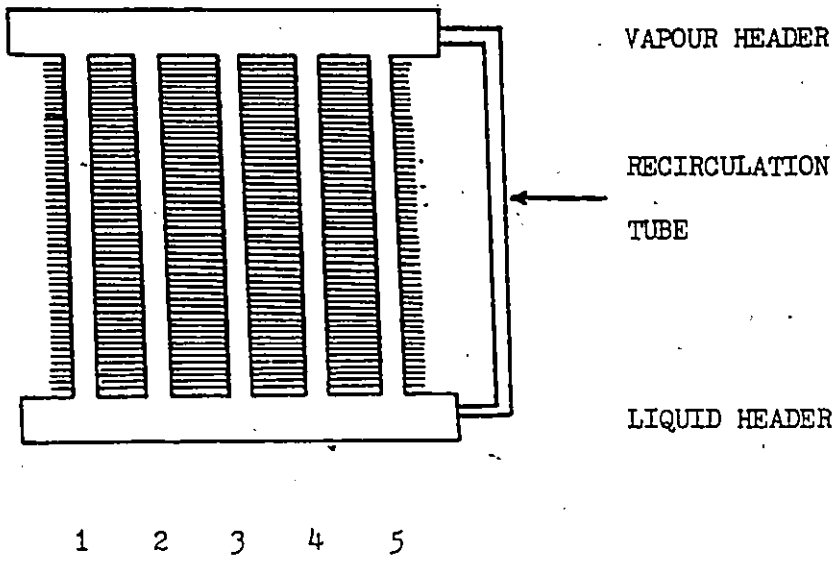

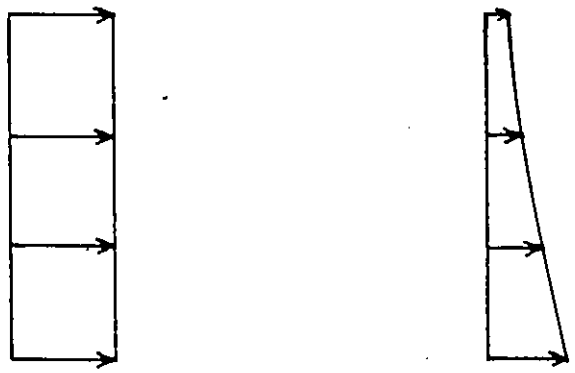

FIGURE 3.5 Temperature profiles for the source fluid approaching evaporator (a) row # 1 (b) row # 2

$$E = 1 - \exp\ (-L_{vh}/R\ \dot{m}_v\ Cp_v) \qquad \text{---- (71)}$$

$$Q = E\ \dot{m}_v\ Cp_v\ (T_f - T_s) \qquad \text{---- (72)}$$

where E, L_{vh}, R, $\dot{m}_v$, Cp_v, T_f and T_s are the effectiveness, length of the vapour header (m), the resistance per unit length (m K/W), the mass flow rate of vapour (kg/s), the specific heat of the vapour (kj/kg K), the inlet working fluid temperature (C) & the surrounding temperature (C) respectively. The amount of insulation on the vapour header must be accounted for by the user when he specifies the external thermal resistance per unit length, R, (m K/W) for the vapour header.

In order to select suitable properties for the pressure drop calculations, an average state in the header was estimated by calculating an exit quality (or superheat) assuming no pressure drop. This average state was used to calculate the frictional and hydrostatic pressure drops for the vapour header either by the method discussed in section 3.2.5.2, when the working fluid is in a wet state at the exit of the vapour header, or by the method discussed in section 3.2.8.2, when the working fluid is in single phase vapour state. The entrance and exit pressure losses and the pressure drop due to bends and elbows were also calculated using velocity head factors for each which are incorporated in the program.

3.5 CONDENSER

3.5.1 Condensation

If the vapour is in a superheated state at the entrance to the condenser, vapour desuperheating takes place and the wall temperature is calculated using single-phase vapour heat transfer correlations. When the wall temperature drops below the saturation temperature of the vapour, heat transfer takes place by condensation.

Numerous correlations were presented in table 2.5 to determine the condensation coefficient. The correlation proposed by Ali & McDonald (228) was used in the determination of the condensation coefficient. The following is their correlation.

$$\bar{h}_c = B_1 \left[\frac{K_l^3 \rho_l^2 h_{fg} g}{\mu_l D (T_s - T_w)} \right]^{1/4} \qquad \text{--- (73)}$$

for $0^\circ < \beta < 40^\circ$; $B_1 = 0.727$

for $40^\circ < \beta < 90^\circ$; $B_1 = 0.727 \left[\cos \left(\frac{\beta - 40}{50} \right) 90 \right]^{0.25}$

For partly flooded condensers, the heat transfer and the pressure drop were calculated as indicated in section 3.2.2.2.

3.5.2 Calculations for condenser tube rows

The sink fluid temperature increases as it passes over the condenser tube rows ,as shown in figure 3.6 (assuming saturated state of vapour in the vapour header) , and hence the tube rows are subjected to unequal heating. The vapour flow rate for the condenser tube rows were calculated as follows:

The flow rate of vapour for one tube in the condenser first row was initially estimated by taking the average of the total vapour ($\dot{m}_{t,e}$) generated in the evaporator.

$$\dot{m}_{1,row} = \dot{m}_{t,e}/(N * M) \qquad \text{--- (74)}$$

where N and M are the number of tube rows and tubes per row for the condenser.

Calculations for the heat transfer were made for the condenser first row by using this vapour flow rate by the following equation

$$Q_{1,row} = \dot{m}_{1,row} * (h_{c,in} - h_f) \qquad \text{--- (75)}$$

where $h_{c,in}$ and h_f are the enthalpies (Btu/lb) at the top and the bottom of the condenser.

The cold fluid (sink) temperature approaching this row and the downstream sink temperatures were calculated as follows.

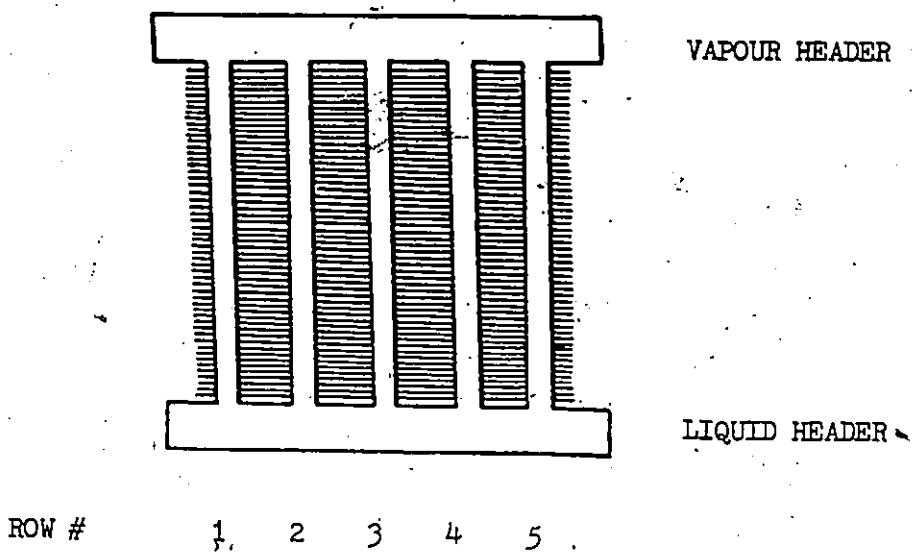

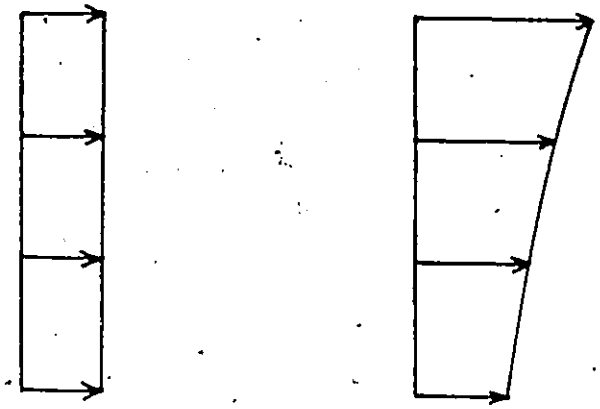

FIGURE 3.6 Temperature profiles for the sink fluid approaching condenser (a) row # 1 (b) row # 2

$$T_a = T_s - Q_{1,row}/((\dot{m}\ Cp)_{air} * E) \qquad \text{--- (76)}$$

$$T_d = T_a + Q_{1,row}/(\dot{m}\ Cp)_{air} \qquad \text{--- (77)}$$

This downstream temperature was used to estimate the rate of heat transfer for the second row by initially assuming $h_{c,2} = h_{c,1}$.

$$Q_{2,row} = E\ (\dot{m}\ Cp)_{air}\ (T_s - T_d) \qquad \text{--- (78)}$$

$$m_{2,row} = Q_{2,row}/h_{fg} \qquad \text{--- (79)}$$

By knowing the value for $Q_{2,row}$, the condenser wall temperature was calculated followed by the condensation coefficient $h_{c,2}$. This new value of condensation coefficient was used to calculate the overall "U" value and hence the effectiveness, E. Convergence was obtained for $h_{c,2}$ and equations 78 and 79 were used to calculate the heat transfer and the mass flow rate for the vapour.

Similar calculations were done for each of the successive condenser rows. The total flow rate of the vapour through the condenser ($\dot{m}_{t,c}$) was calculated and it was then compared to $\dot{m}_{t,e}$. If both these flow rates did not match, the flow rate for the condenser first row was varied until $\dot{m}_{t,c}$ equalled to $\dot{m}_{t,e}$. The flow diagram shown in figure 3.7 explains this logic with the for a condenser consisting of two rows of tubes.

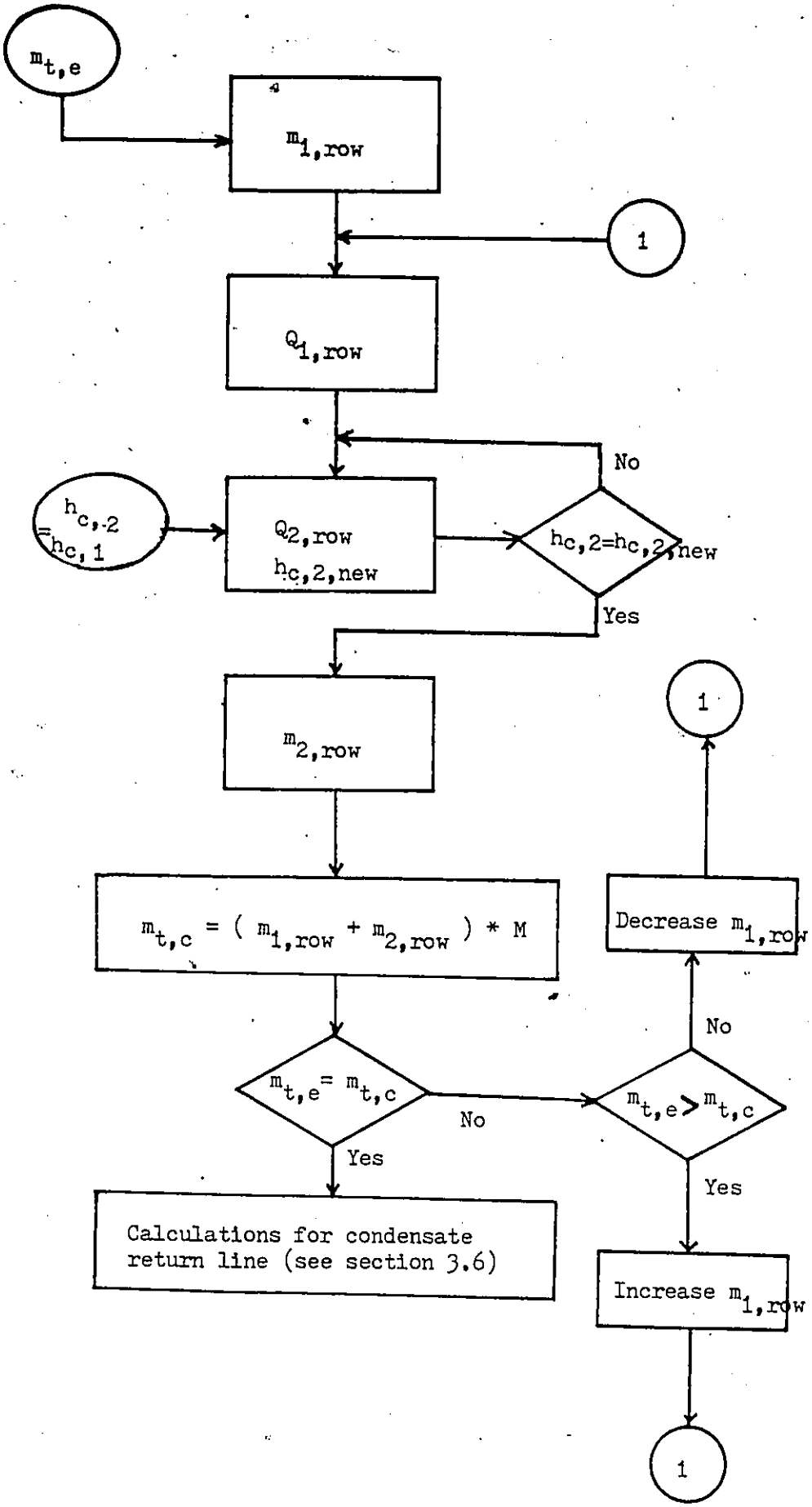

FIGURE 3.7 Flow diagram for condenser calculations

3.6 CONDENSATE RETURN LINE

The condensate coming out of the condenser liquid header flows into the condensate return line. The amount of insulation on the condensate return line may be accounted for by the user when he specifies the external thermal resistance per unit length (m K/W) for the condensate return tube. The heat transfer was calculated in a manner similar to that discussed in section 3.4 for the vapour header. The frictional pressure drop in the condensate return line was calculated by the method described in 3.2.8.2. The configuration model used in the program for the condensate return line is shown below. The elevation of the liquid vapour interface in the condensate return line can be calculated from the following, by assuming a negligible pressure drop in the condenser.

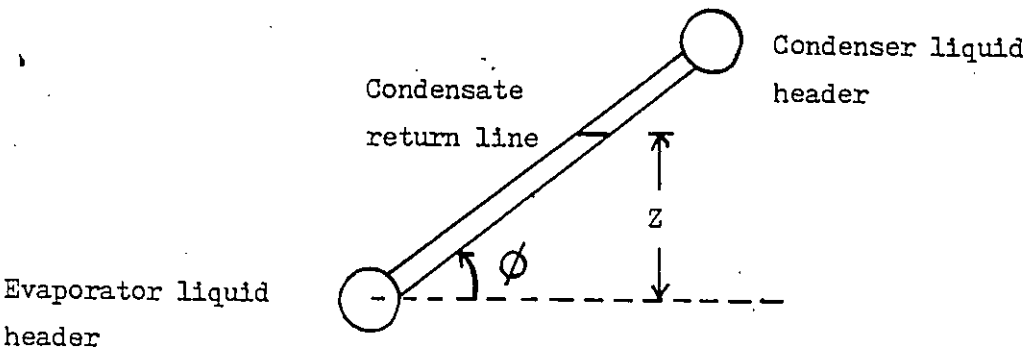

$$(P_{evap,b} - P_{cond,b}) = \rho\, g\, Z + \left[\frac{f\,(Z/\sin\phi) + \Sigma K_i}{D} \right] (V^2/2\, g) \qquad \text{--- (80)}$$

For flooded condeners, different lengths and diameters should be used in equation 80 to calculate Z.

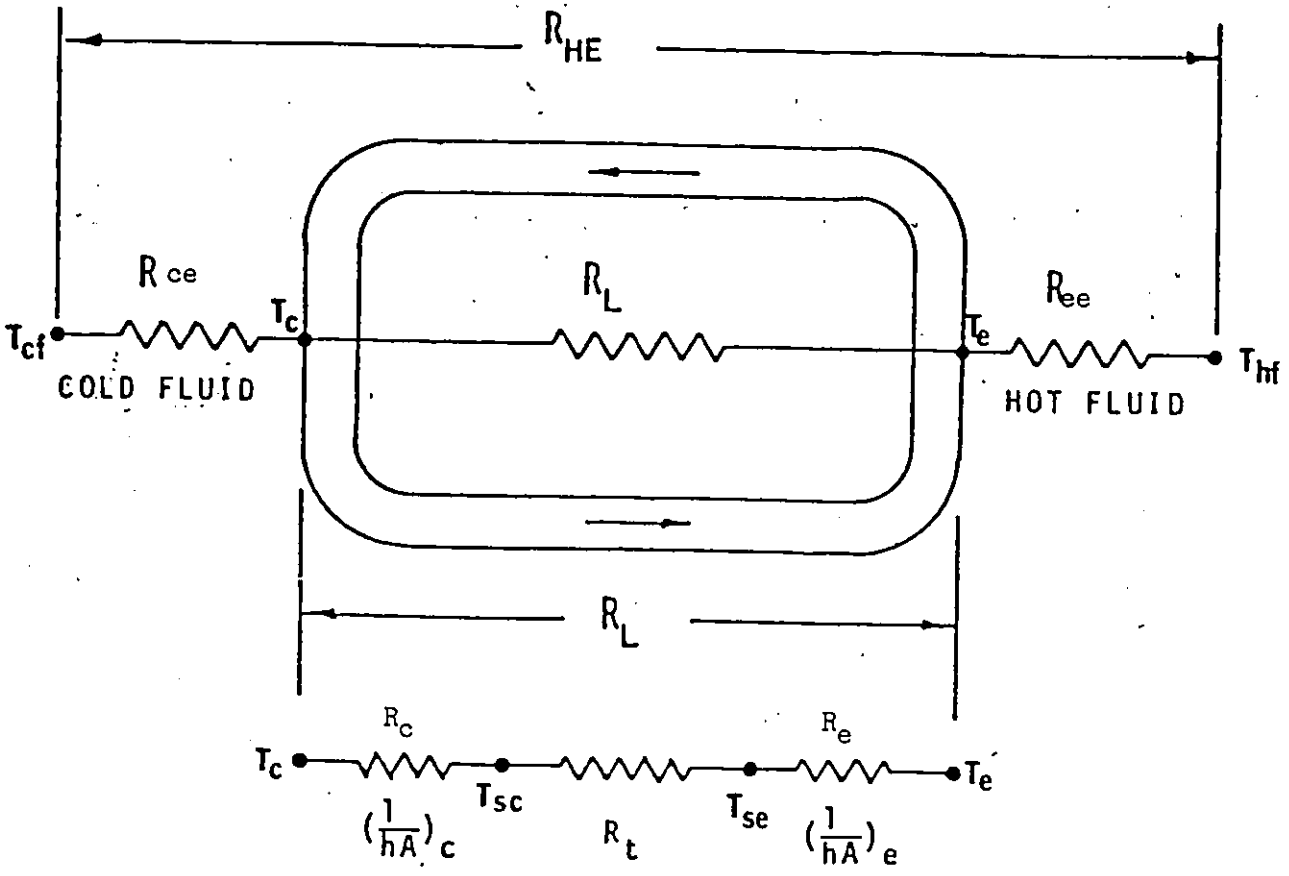

HEAT EXCHANGER CONDUCTANCE $(UA)_{HE} = R_{HE}^{-1}$

THERMOSIPHON LOOP CONDUCTANCE $(UA)_L = R_L^{-1}$

FIGURE 3.8 : ELECTRICAL ANALOG OF IDEALIZED THERMOSIPHON LOOP

The flow is all liquid in the condensate return line , and the fluid then enters the evaporator liquid header, thus completing a cycle.

3.7 PERFORMANCE RATING

Figure 3.8 shows an idealized electrical analog of a two-phase thermosiphon loop heat exchanger and identifies the various resistances.

The performance for a thermosiphon loop heat exchanger is characterized by defining its effectiveness as the ratio of the heat transferred to the maximum possible heat transfer.

The effectiveness of a heat exchanger is dependent on the outside source, outside sink and the loop resistances which are identified as R_{ee}, R_{ce} and R_L respectively.

In order to isolate the effect of the outside resistances in studying the effect of variable parameters on the performance of the loop it is convinient to concentrate on $R_L = (UA)$, and ignore R_{ee} and R_{ce}. The overall loop conductance (UA) for a two-phase thermosiphon heat exchanger is defined as the amount of heat transferred per unit temperature difference between the source and the sink fluids.

The loop resistance has three components: evaporator, condenser and the transport resistances given by R_e, R_c and R_t respectively. The

resistance of the evaporator and condenser can be expressed in terms of their average heat transfer coefficients which are defined as the heat transfer rate per unit tube inner surface area and per unit temperature difference between the average wall temperature and the saturation temperature in the evaporator vapour header.

In some cases it is useful to study the effect of the local heat transfer coefficient.

CHAPTER IV

RESULTS & DISCUSSIONS

4.1 INTRODUCTION

This chapter presents a comparison of experimental and corresponding simulated results for a number of experimental investigations (12, 15, 17, 23) which were carried out on three very different systems.

R-11 was used by reference 12, 15 & 17; and R-113 was used by reference 23 as the working fluid for their respective systems , and the systems were oriented in such a way that they could only operate in an unidirectional mode.

In all of the following figures, the curves shown represent the simulated values whereas the points shown represent experimental results.

4.2 COMPARISON WITH WATER-TO-WATER SYSTEM

For this study, the simulated values of the heat transfer rate, average heat transfer coefficients, conductance etc. have been

compared with the corresponding results obtained by Raza (12).

The system used in this study was a well instrumented three tube evaporator and three tube condenser system especially designed for studying thermosiphon loop behaviour. Each of the three coplanar tubes in each heat exchanger was independently water jacketed, 0.61 m long copper tubes. Each heat exchanger could be translated vertically, rotated in a plane about a horizontal axis, and be inclined from the vertical with its header remaining horizontal. The inside diameter of the evaporator and condenser coil tubes was 7.9 mm and 4.8 mm respectively. The tube spacing in the evaporator coil was 8.0 cm. A complete description of the system is given by Raza and McDonald (13).

Figures 4.1 and 4.2 show , respectively , a comparison of the total heat transfer rate and the average evaporator inner tube surface heat transfer coefficient versus the evaporator static charge when all three evaporator tubes are vertical and equally charged. The system was run with source to sink temperature differences of 20 C and 10 C and with an average source/sink temperature of 30 C. Both the figures show a good agreement with the experimental results.

A comparison of plots of the heat transfer rate and the average evaporator inner tube surface heat transfer coefficient versus evaporator static charge when the tubes are inclined from the vertical and are equally heated is shown in figures 4.3, 4.4, 4.5 & 4.6 for 20

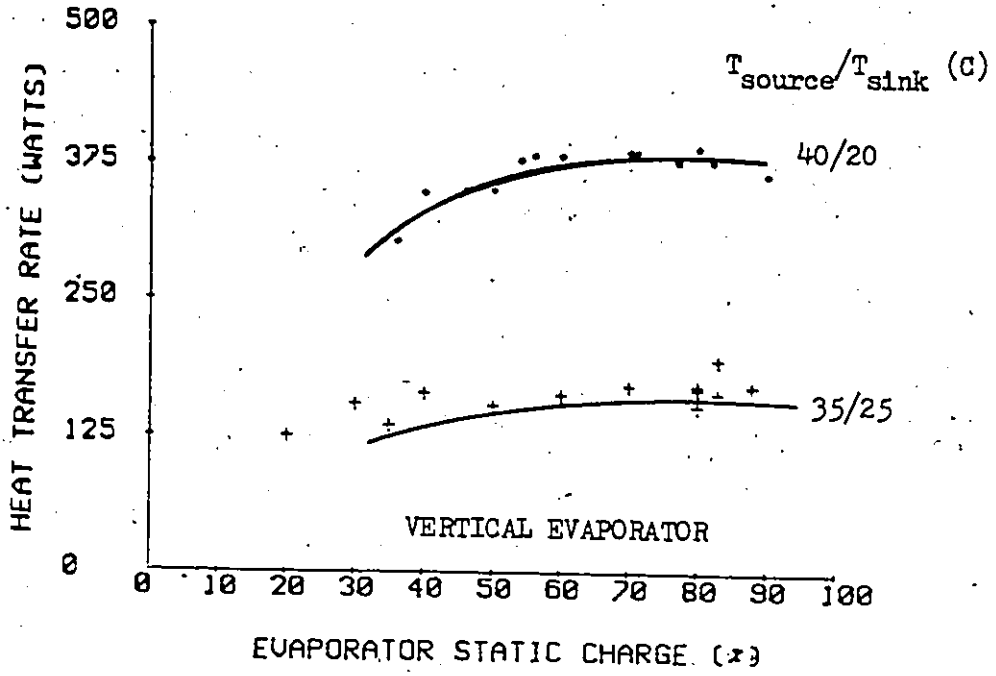

FIG. 4.1 HEAT TRANSFER RATE VERSUS STATIC CHARGE FOR VERTICAL EVAPORATOR, T_{mean} = 30 C

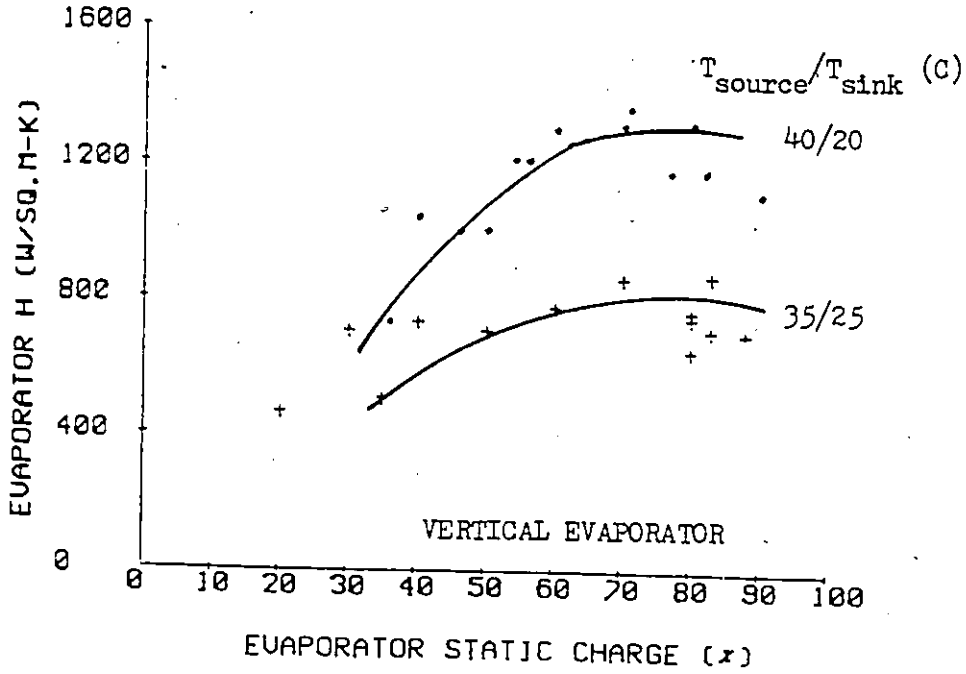

FIG. 4.2 AVERAGE EVAPORATOR HEAT TRANSFER COEFFICIENT VERSUS STATIC CHARGE, T_{mean} = 30 C

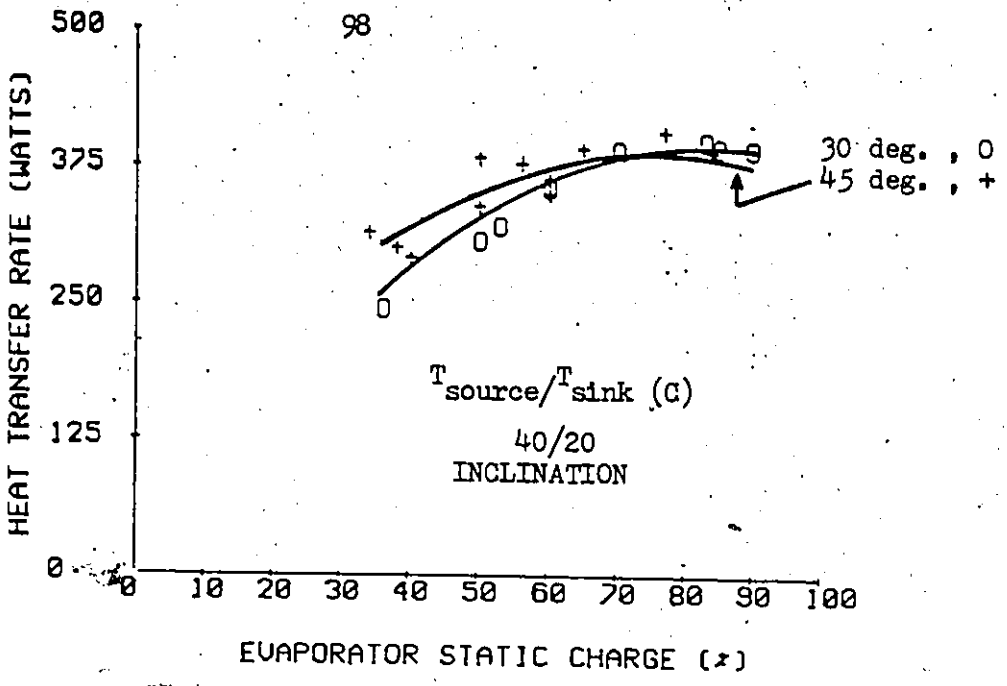

FIG. 4.3 HEAT TRANSFER RATE VERSUS STATIC CHARGE FOR INCLINED EVAPORATOR TUBES, T_{mean} = 30 C

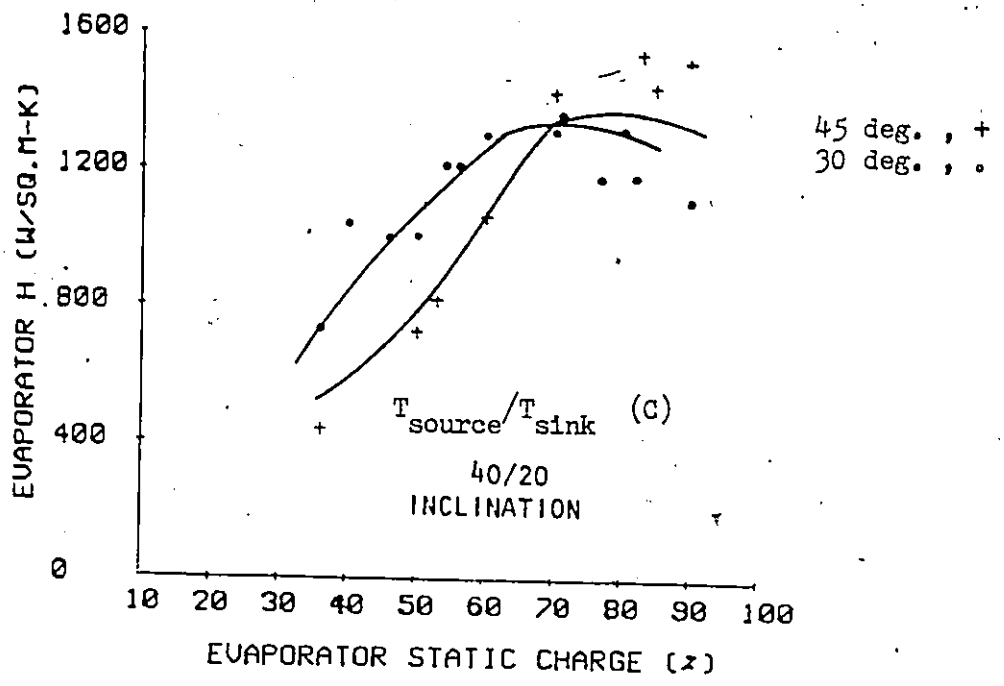

FIG. 4.4 AVERAGE EVAPORATOR HEAT TRANSFER COEFFICIENT VERSUS STATIC CHARGE FOR INCLINED EVAPORATOR TUBES , T_{mean} = 30 C

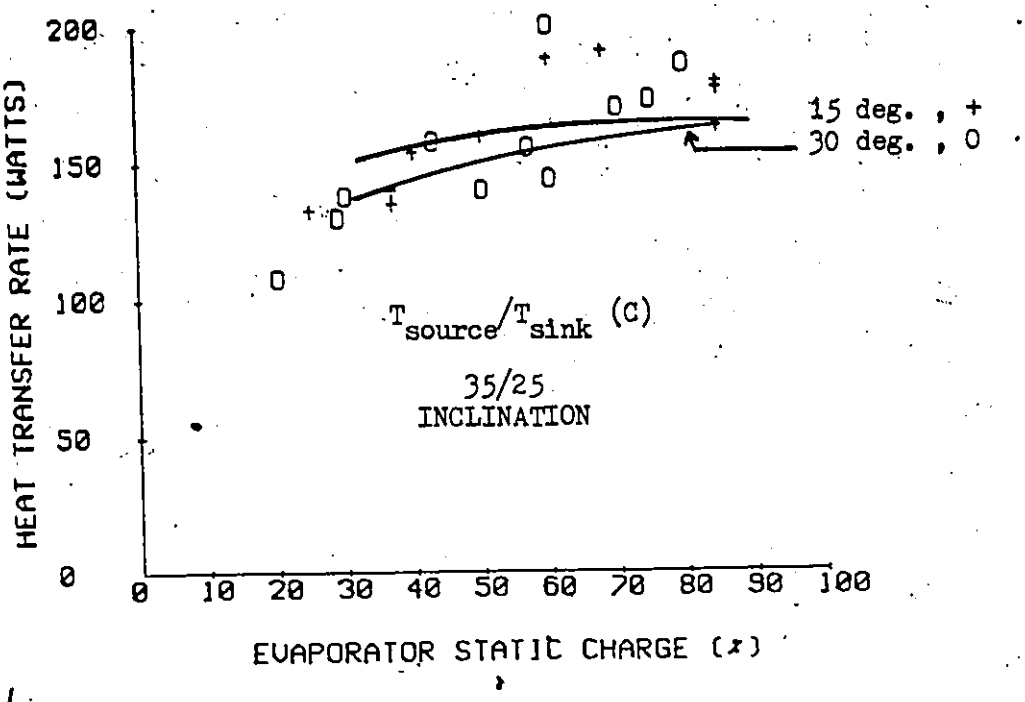

FIG. 4.5 HEAT TRANSFER RATE VERSUS STATIC CHARGE FOR INCLINED EVAPORATOR TUBES , Tmean = 30 C.

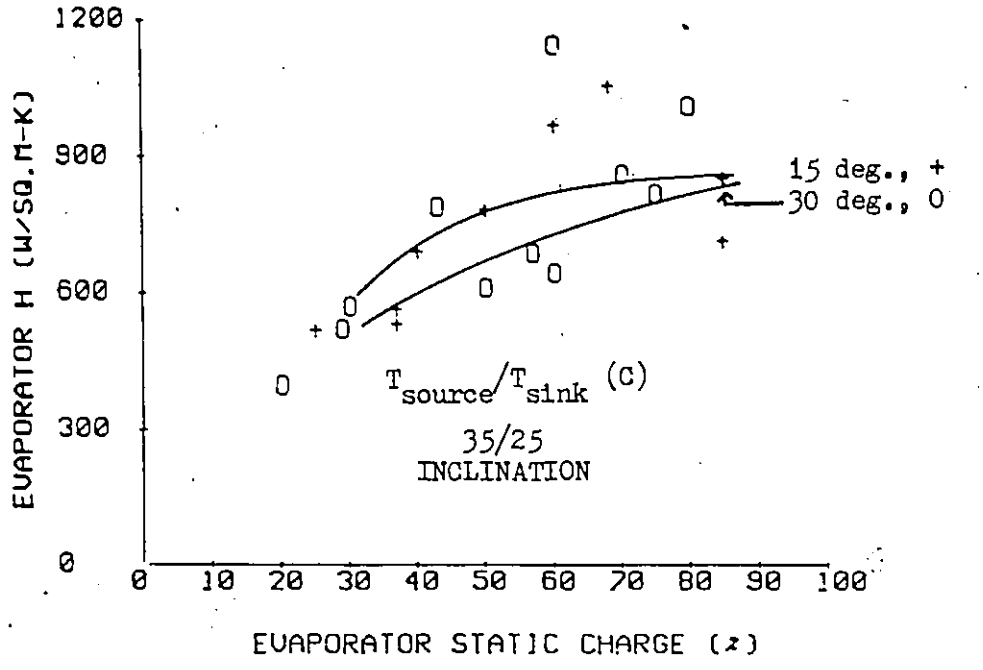

FIG. 4.6 AVERAGE EVAPORATOR HEAT TRANSFER COEFFICIENT VERSUS STATIC CHARGE FOR INCLINED EVAPORATOR TUBES, T_{mean} = 30 C.

C and 10 C source to sink temperature differences. For the 20 C source to sink temperature difference tests the evaporator tubes were inclined at 30 and 45 degrees from the vertical. For the 10 C source to sink temperature difference they were inclined at 15 and 30 degrees from the vertical. The simulated results accurately predicted the effect of tube dryout for source and sink temperature of 40C & 20C with increasing angle for charges below 70 % (figures 4.3 & 4.4), but failed to predict any enhancement above this value. Due to the scatter in the experimental data for 35C/25C (figures 4.5 & 4.6), the simulated data does not agree very well with the experimental data. The improved performance obtained experimentally for higher charges with increased angle of inclination, is a result of the reduced hydrostatic head in the evaporator tube and causes a reduction in the evaporator inlet pressure and hence promotes boiling.

The performance of the evaporator when rotated from the vertical, and hence with unequal charges present in each evaporator tube, are shown in figures 4.7, 4.8, 4.9 and 4.10 for the 40C/20C and 35C/25C source/sink temperatures. Rotation angles of 15, 30 & 45 degrees from the vertical resulted in static charge differences between adjacent tubes of 3 %, 8 % and 13 % respectively. The results are plotted against the average static charge (the value for the center tube). In this case it may be seen that the experimental results show little effect as compared to the inclination of the

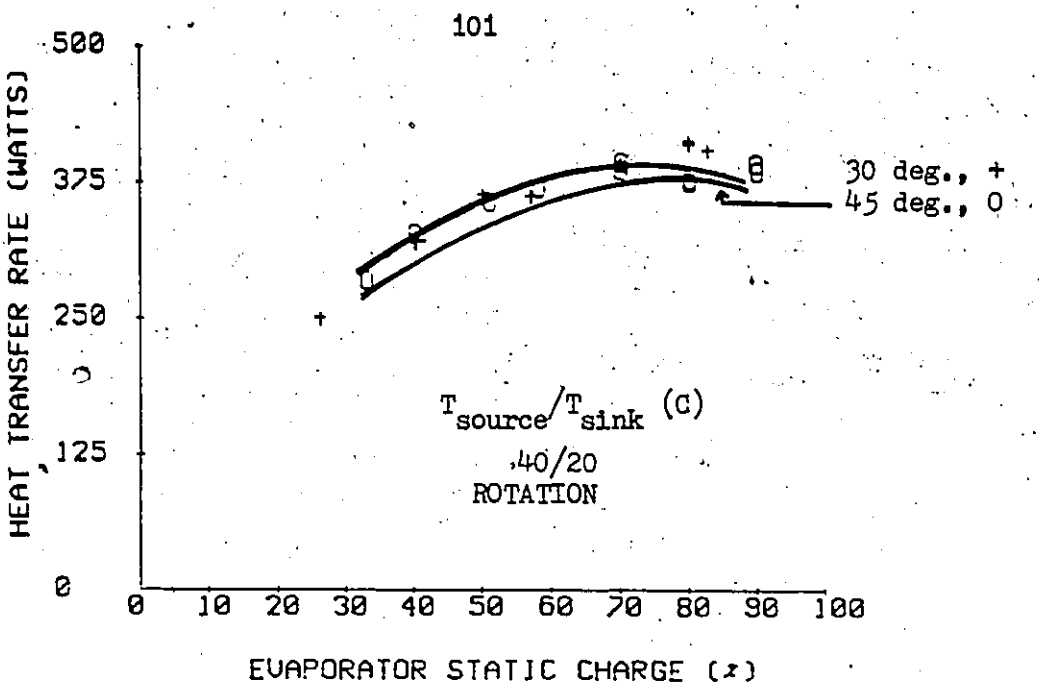

FIG. 4.7 HEAT TRANSFER RATE VERSUS STATIC CHARGE FOR ROTATED EVAPORATOR TUBES, T_{mean} = 30 C.

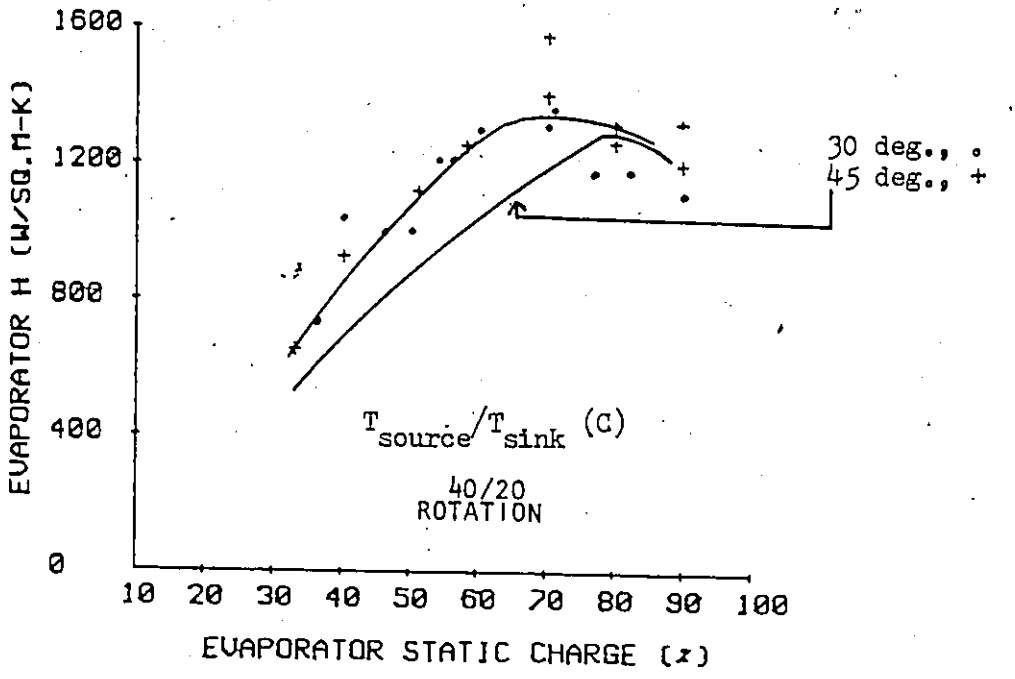

FIG. 4.8 AVERAGE EVAPORATOR HEAT TRANSFER COEFFICIENT VERSUS STATIC CHARGE FOR ROTATED EVAPORATOR TUBES, T_{mean} = 30C.

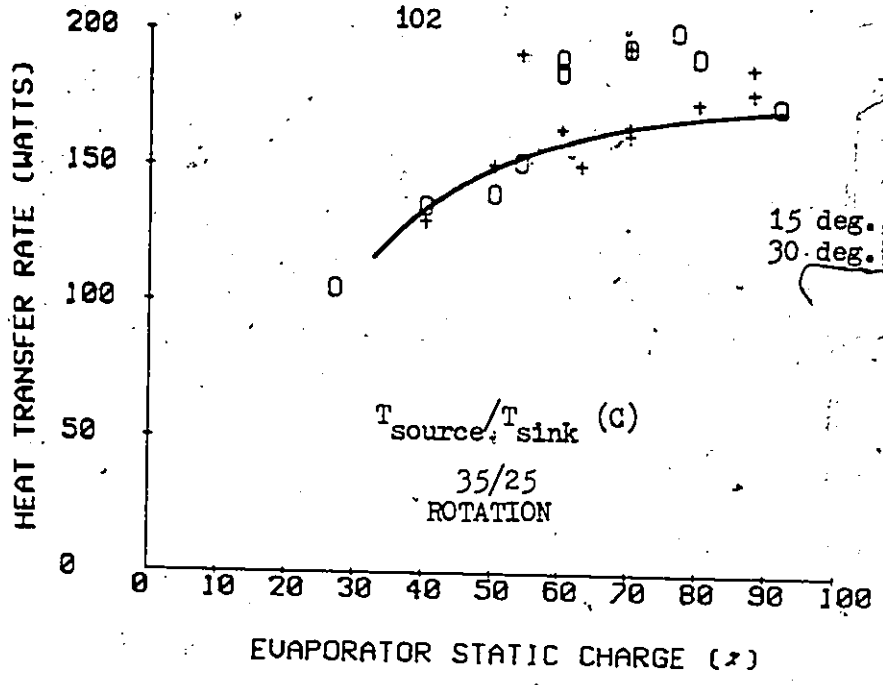

FIG. 4.9 HEAT TRANSFER RATE VERSUS STATIC CHARGE FOR ROTATED EVAPORATOR TUBES, T_{mean} = 30C.

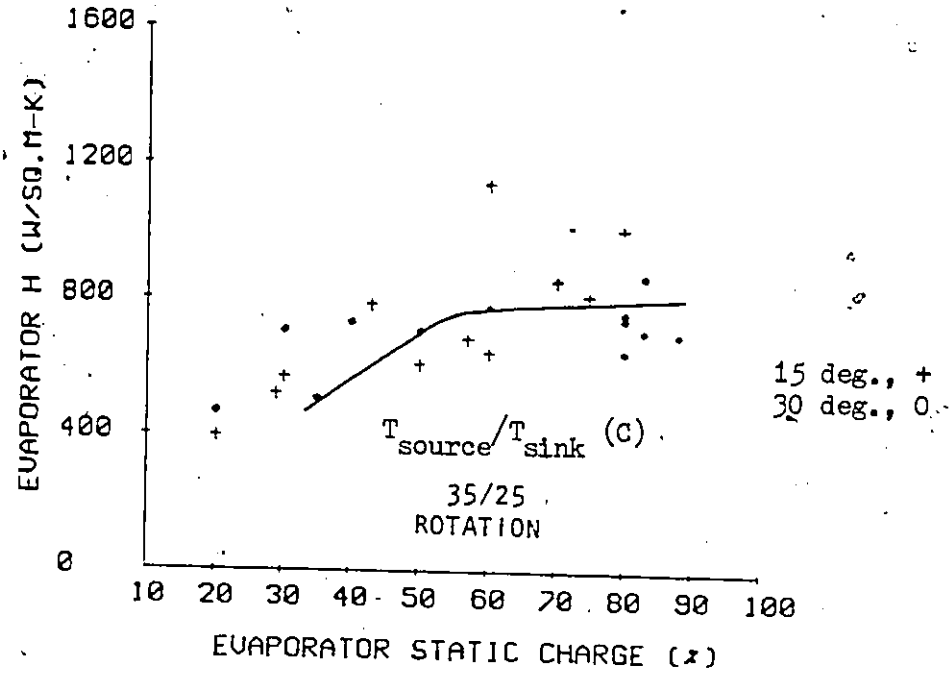

FIG. 4.10 AVERAGE EVAPORATOR HEAT TRANSFER COEFFICIENT VERSUS STATIC CHARGE FOR ROTATED EVAPORATOR TUBES, T_{mean} = 30C.

tubes. The simulated results for 40C/20C (figures 4.7 & 4.8)* indicate that dryout should be much more severe than was found. The only explanation offered for this behaviour is that liquid carried into the evaporator vapour header from the tube with greatest charge may have splashed into the top of the tubes with less charge which would otherwise have dried out. For 35C/25C source/sink temperatures, the simulated data for 15 deg. and 30 deg. is shown by a single curve, since there was very little difference in the values for 15 deg and 30 deg. rotation. The agreement is better for this case.

Figure 4.11 shows a comparison of the values of the overall loop conductance "U" and for the mean wall superheat. For the loop conductance, curves 1 and 2 are for source water jacket temperatures of 40 C and (44, 40, 36 C) respectively, are in very good agreement but curve 3, for source and sink temperatures of 35C and 25C respectively, falls along the lower edge of the experimental scatter. The temperature differences are also in reasonably good agreement with the simulated values.

Figure 4.12 shows the average heat transfer coefficient versus the static charge. The simulated curves are in good agreement with the experimental points within the accuracy of the data. Curve "2" shows the variation of the average evaporator heat transfer coefficient versus static charge for source fluid temperatures of 44, 40 & 36 C with a condensing temperature of 20C. Although, this performance is

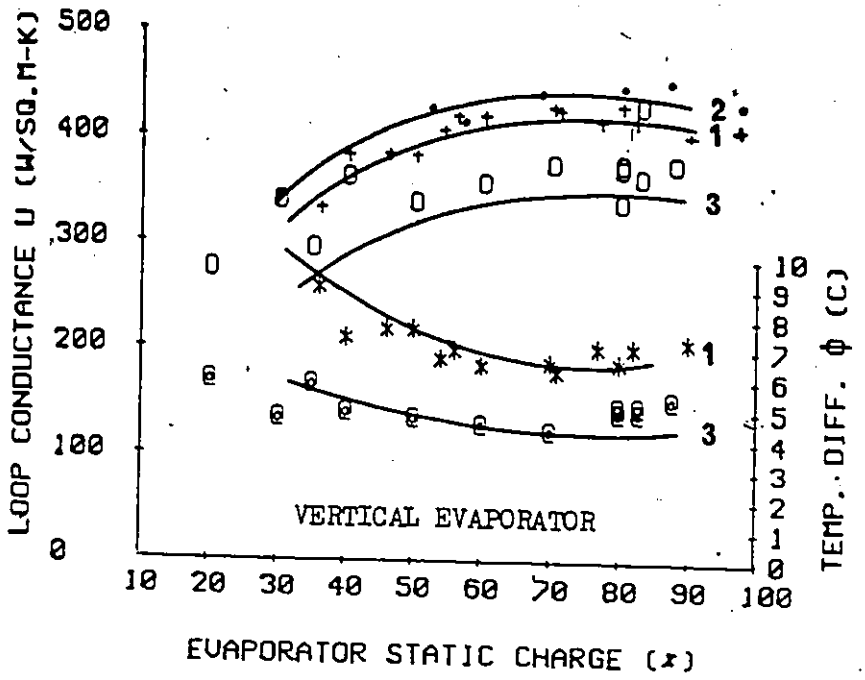

FIG. 4.11 EFFECT ON CONDUCTANCE & WALL SUPERHEAT OF STATIC CHARGE & SOURCE-SINK TEMPERATURES. (1) 40 C SOURCE & 20 C SINK; (2) 44 C, 40 C, 36 C SOURCE & 20 C SINK & (3) 35 C SOURCE & 25 C SINK.

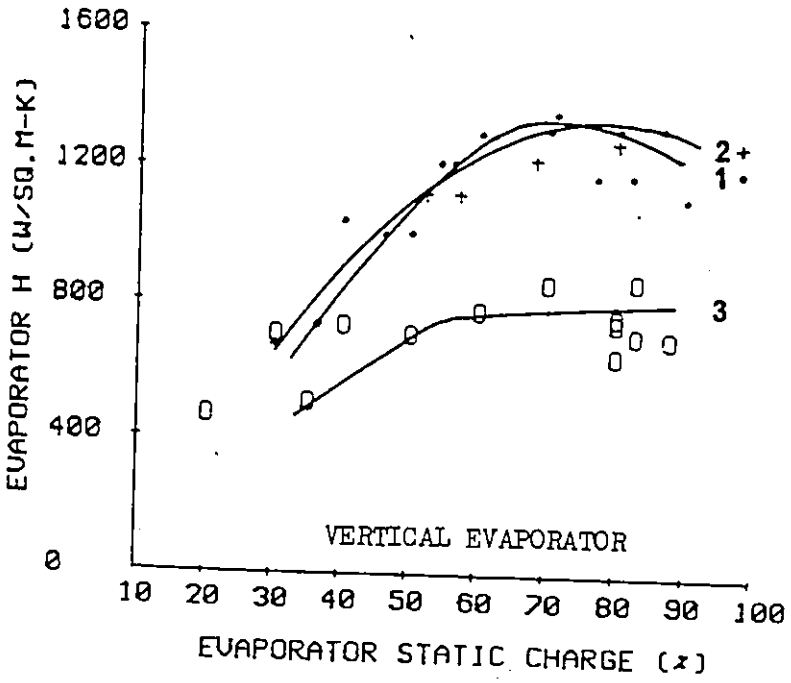

FIG. 4.12 EFFECT OF SOURCE-SINK TEMPERATURES ON THE AVERAGE EVAPORATOR HEAT TRANSFER COEFFICIENTS

very similar to curve "1", in which all three evaporator tubes are equally heated at 40 C, the performance of the individual tubes varies a great deal. Figure 4.13. shows that the simulated curves for the individual tubes were, initially, not in good agreement with the experimental data although the trends are similar. This discrepancy was caused by the hysteresis effect which occurs in real systems due to the fact that a greater wall superheat is required to initiate boiling than to maintain it. As a result, the actual performance of a surface when subjected to low wall superheats is dependent on its past history. To illustrate the effect of this phenomenon the simulation program was rerun with the additional constraint that the fluid could not boil until the wall superheat was equal to 13.3 C (24 F). The result obtained is plotted in figure 4.14. This simulation was in much better agreement with the experimental data. It indicated that the fluid would not boil in the coolest tube (subjected to a source fluid temperature of 36 C), since wall superheats of only 10-12 C occured in that tube. The fact that the fluid did boil in the coolest tube for some of the experimental runs is most likely due to the fact that for those tests the thermal history of the coolest tube was not noted and hence nucleation sites may have already been activated. As a result, the experimental behaviour should fall somewhere between those predicted in figure 4.13 and figure 4.14. With this understanding it may be seen that the simulation program can account for the measured behaviour.

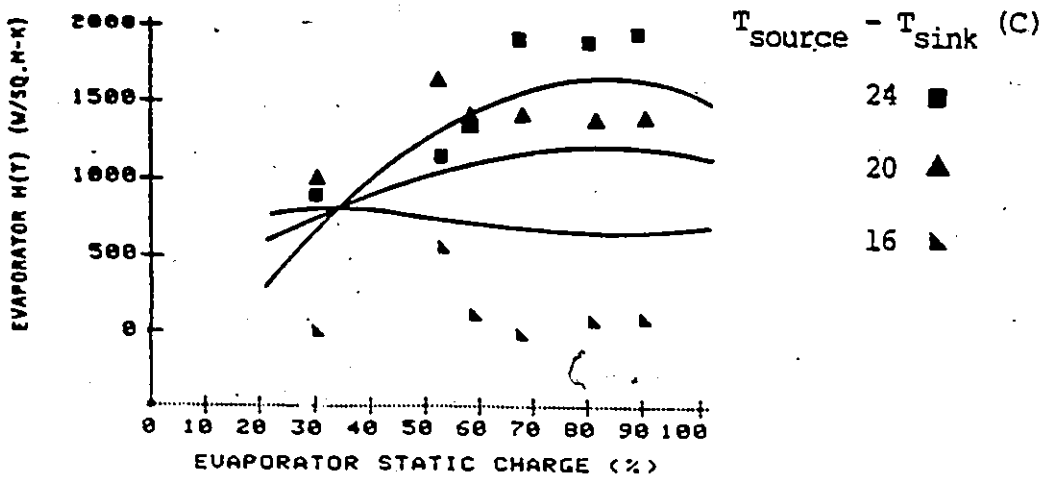

Figure 4.13

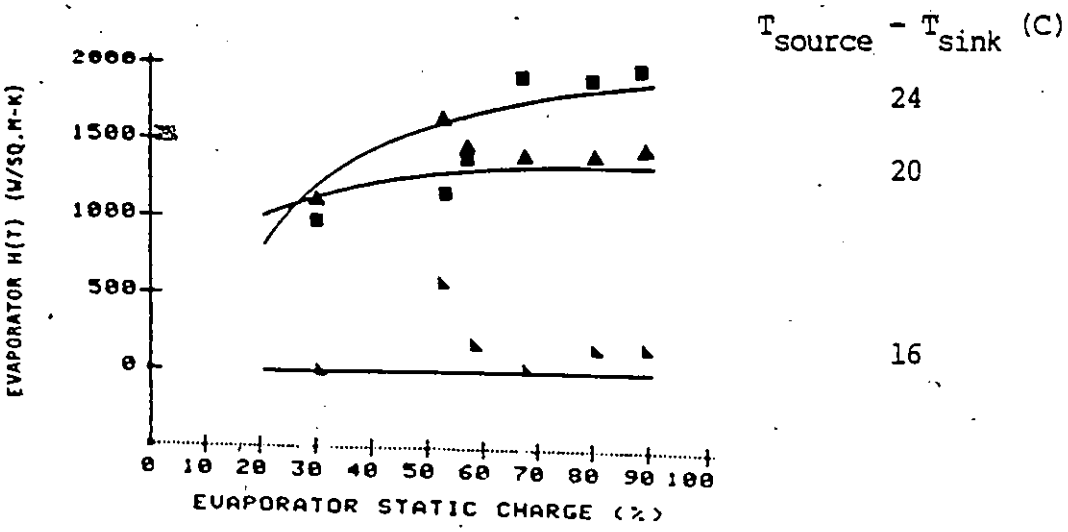

Figure 4.14

Average evaporator heat transfer coefficient in individual tubes versus static charge with source to sink temperature difference of 24, 20 and 16 C and Tsink = 20 C.

4.3 COMPARISON WITH AIR-TO-AIR SYSTEM

For this study, the simulated effectiveness of an air-to-air thermosiphon loop heat exchanger is compared with the corresponding experimental results obtained by Kosnik & Bertoni (15) and Stauder (17).

The air-to-air heat exchanger system of Kosnik & Bertoni and Stauder consisted of a number of thermosiphon loops mounted in a counter flow configuration in the warm and cold air ducts. A schematic diagram of the system is shown in figure 2.4. The heat exchanger coils were fabricated using commercially manufactured finned tube evaporator and condenser coils with wavy aluminum plate fins at a spacing of 12 fins per inch (473/m). The condenser and the evaporator coils each consisted of 8 rows of tubes of 7.9 mm I.D. each with its own separate liquid and vapour header. The evaporator tubes were vertical and 0.915 m long. The condenser tubes were inclined at 45 degrees and were 0.305 m long. The evaporator and the condenser coils had the same face area and were installed in warm and cold ducts having the same air mass flow rates. A complete description of this system is given by Kosnik & Bertoni (15) and Stauder (17). Kosnik & Bertoni used 4 loops for their study of the effect of the static charge on the effectiveness of the system for two different overall temperature differences and two air flow rates. Stauder studied the performance of one and four loop

systems as a function of the hot to cold duct air temperature difference for three different duct air mass flow rates. This temperature difference was first increased (heating process) then decreased (cooling process) in order to study the hysteresis effect caused by the boiling characteristics of R-11. It has been shown by Abdelmessih et. al (120) and others that it requires a much greater wall superheat to initiate nucleate boiling than it does to sustain it. Once initiated, this large temperature difference is not required.

Figure 4.15 shows the performance of single loop systems for both heating and cooling for a coil face velocity of 2.2 m/s. The simulated results are in excellent agreement with the experimental data, both for the heating and cooling processes. The effectiveness is considerably lower for the heating portion of the curve since a larger amount of wall superheat is needed to initiate bubble growth for the system startup. This initiation of the bubble growth for this system started when the overall temperature difference exceeds approximately 13C. When the temperature difference exceeds approximately 40C, the simulated performance curves for heating and cooling merge and become essentially constant over the range studied (up to 65C). When the overall temperature difference is decreased from 40C the effectiveness of the system remains high since the nucleation sites which were established at the higher temperatures are initially not destroyed. Eventually, as the overall temperature difference continues to decrease, some of the nucleation sites are deactivated. All were

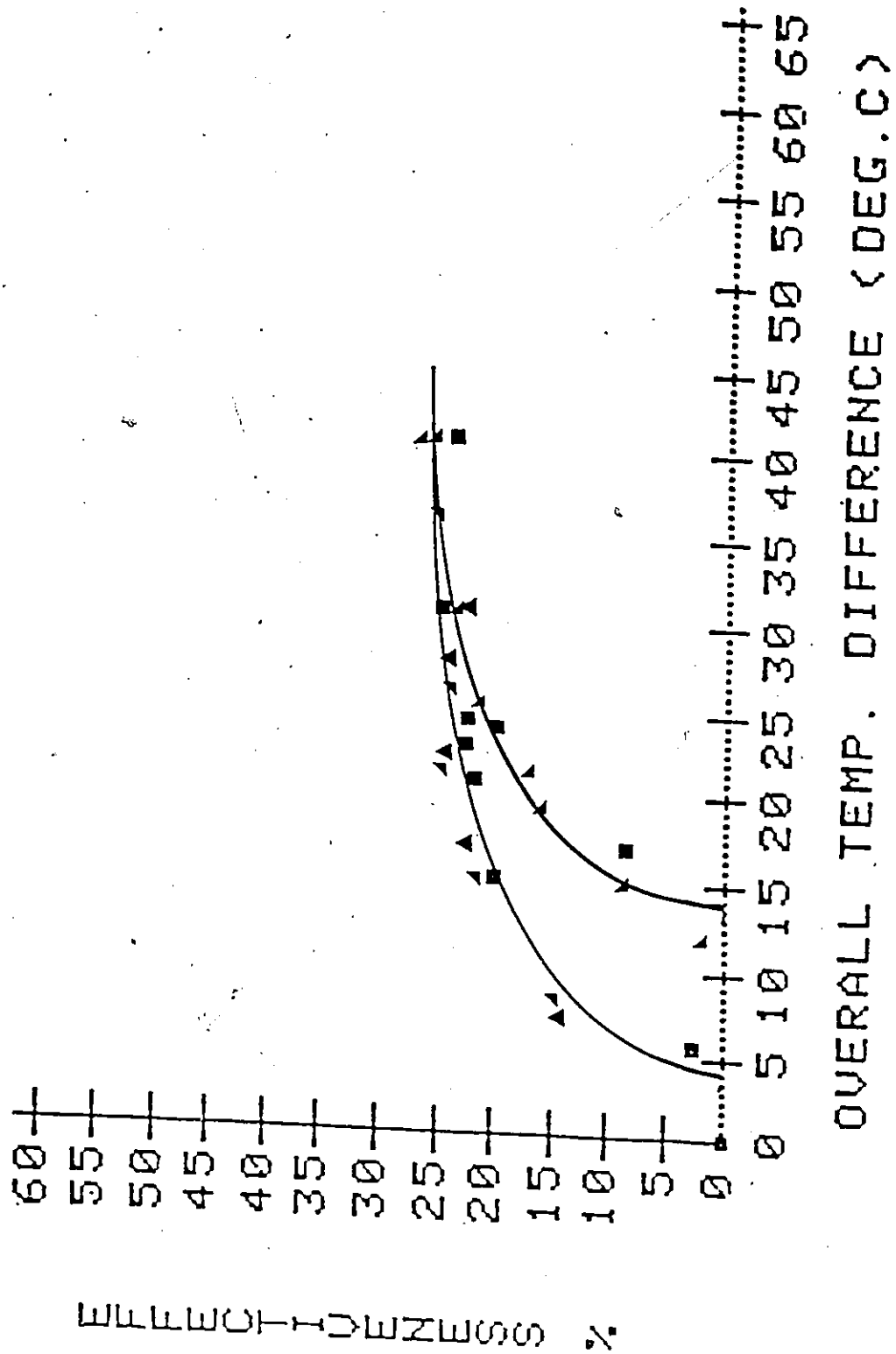

FIGURE 4.15 EFFECTIVENESS VERSUS OVERALL TEMPERATURE DIFFERENCE FOR A SINGLE LOOP

deactivated when the overall temperature difference was decreased below 4C.

In order to use the simulation program to predict the performance of 4 loops it was necessary to make the following relationship. The effectiveness, E(N), for a heat exchanger consisting of "N" loops in a counterflow configuration can be related to one having "M" loops - provided each loop has the same temperature differences (see figure 2.4a). See appendix I for the derivation.

$$E(N) = \frac{N\ E(M)}{M + (N - M)\ E(M)} \qquad \text{--- (1)}$$

$$\theta(N) = \theta(M)[M + (N - M)\ E(M)] \qquad \text{--- (2)}$$

To simulate the experimental data for 4 loops, the program was used to simulate the performance for a range of temperature differences for one loop. The effectiveness and the overall temperature difference for 4 loops were then calculated from equation 1 and 2.

Figures 4.16, 4.17 and 4.18 show the effect of the heating and cooling processes on the performance of the system for the 4 loop configuration for coil face velocities of 1.3, 2.2 and 3.1 m/s respectively. The simulation program is able to predict the

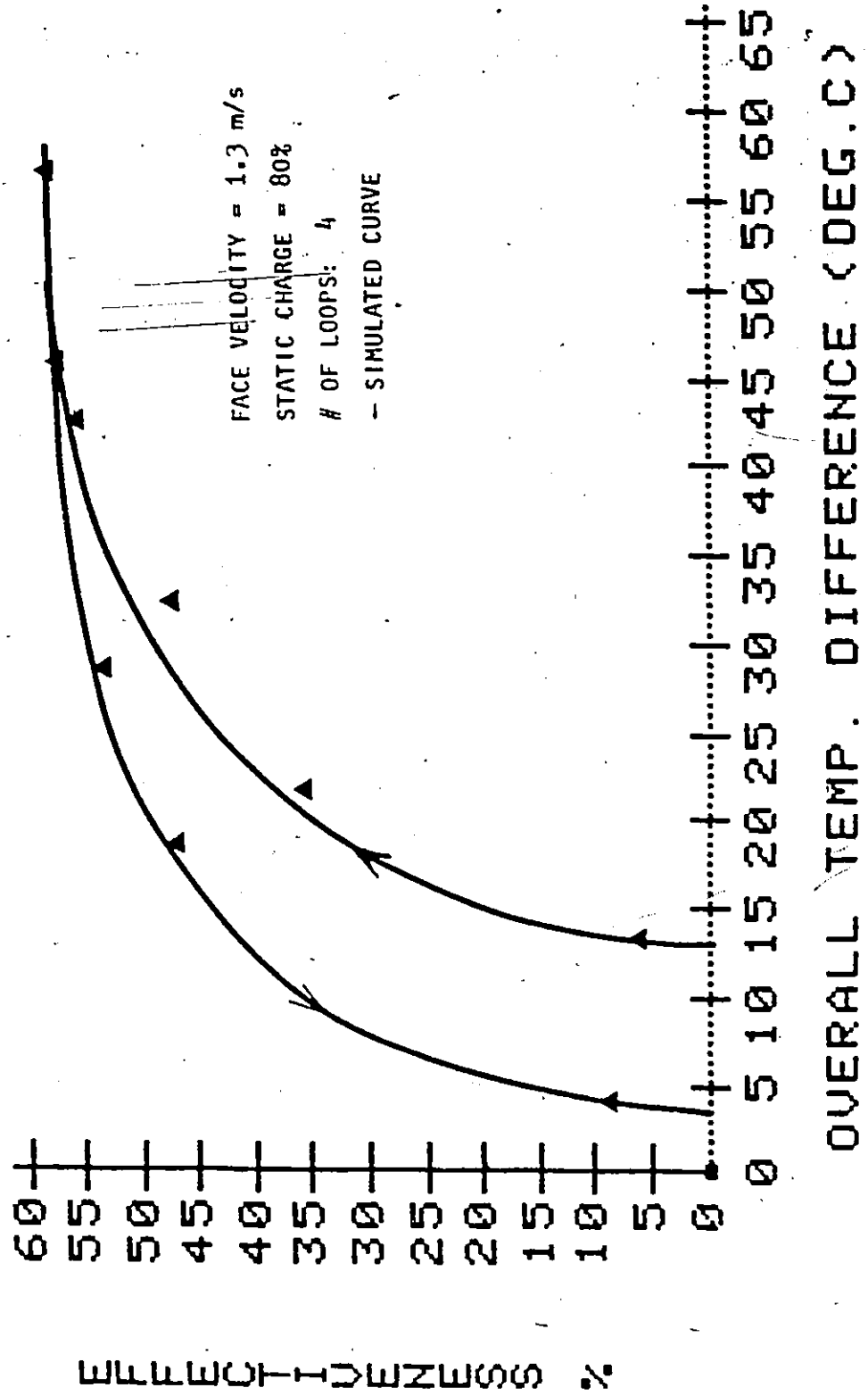

FIG. 4.16 HYSTERESIS ENVELOPE FOR A COIL FACE VELOCITY OF 1.3 M/S

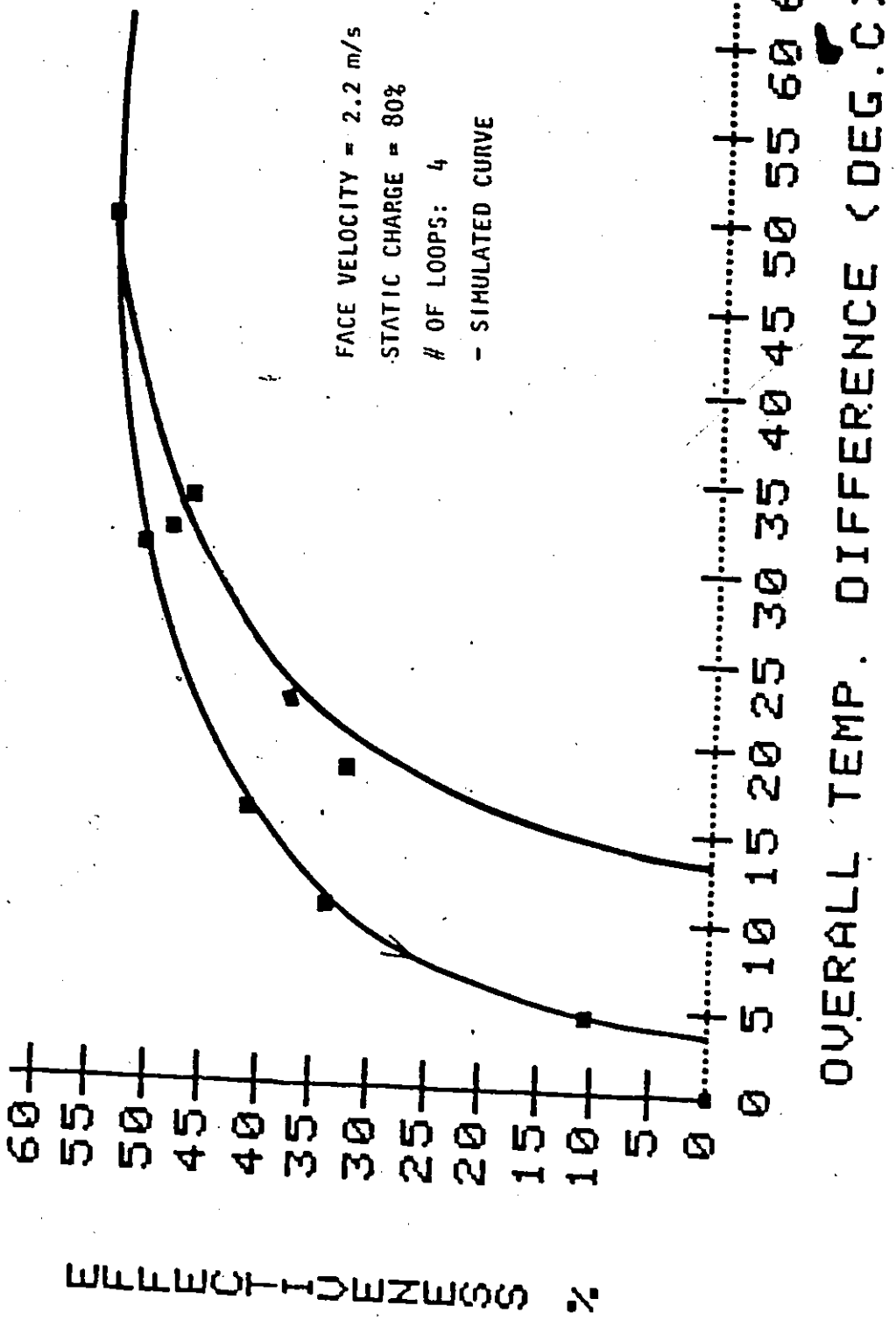

FIG. 4.17 HYSTERESIS ENVELOPE FOR A COIL FACE VELOCITY OF 2.2 M/S

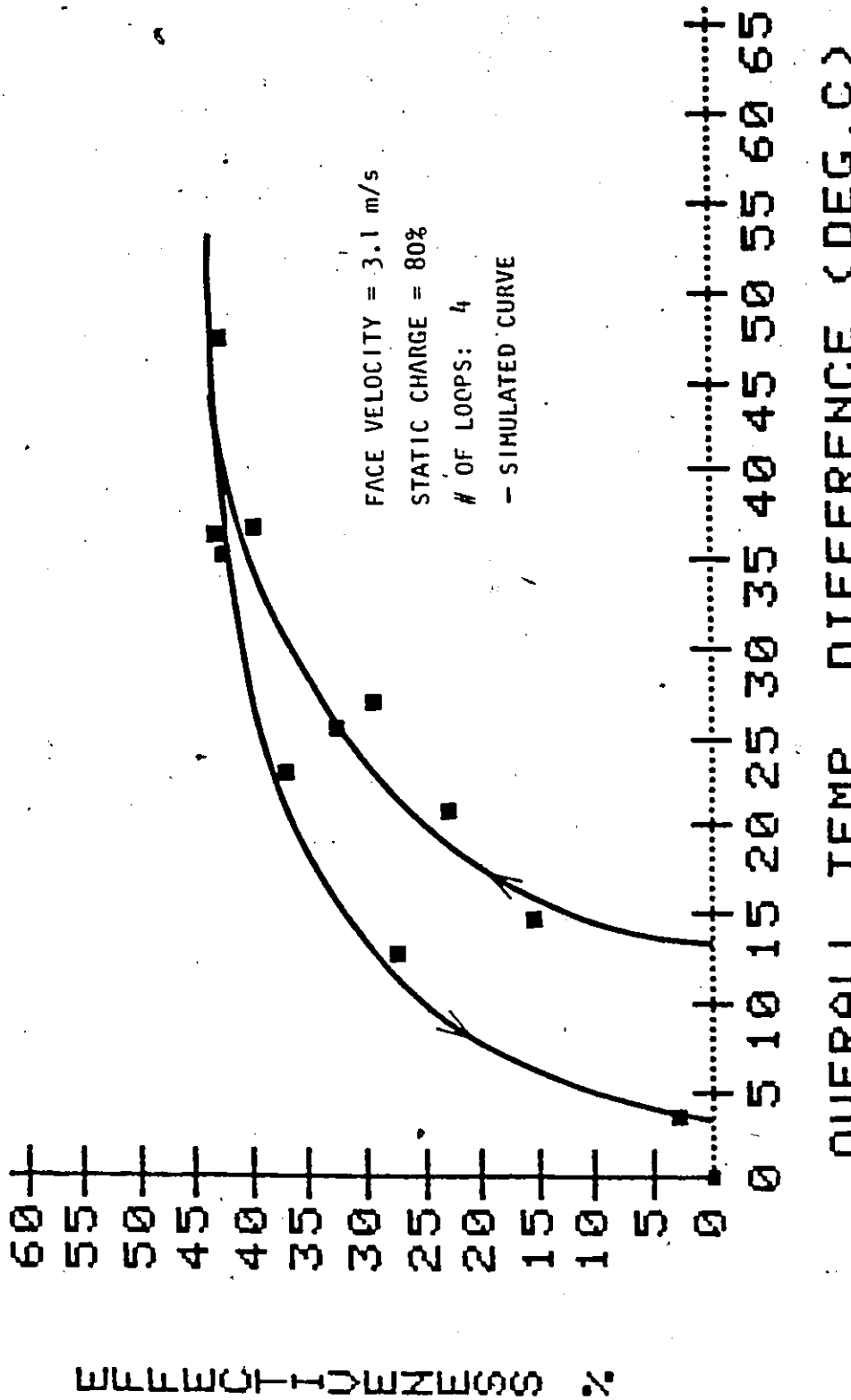

FIG. 4.18 HYSTERESIS ENVELOPE FOR A COIL FACE VELOCITY OF 3.1 M/S

performance of the system very well provided that the external thermal resistance is modeled accurately.

Figure 4.19 shows a comparison of the system effectiveness versus the overall temperature difference between the experimentally obtained results with the corresponding results obtained by the simulation program. These results are for cooling process for three different coil face velocities. The simulation program is able to predict the experimental cooling results very well. The simulated results, which have been extended to temperature differences much higher than could be achieved experimentally, show the effect of dryout which occurs with large temperature differences. This effect is clearly visible for the coil face velocities of 2.2 and 3.1 m/s. The curve also shows that the boiling process is quenched when the overall temperature difference is lowered to approximately 4 C, since below this temperature difference all the nucleation sites are destroyed. The performance of the heat exchanger becomes independent of the temperature difference for temperature differences greater than 40 C, which indicates that nucleation has been initiated at all the readily available sites.

Figures 4.20 and 4.21 show the effect of static charge on the effectiveness of the system for overall temperature differences of 35 and 25C and for a coil face velocities of 2.2 and 3.4 m/s. The

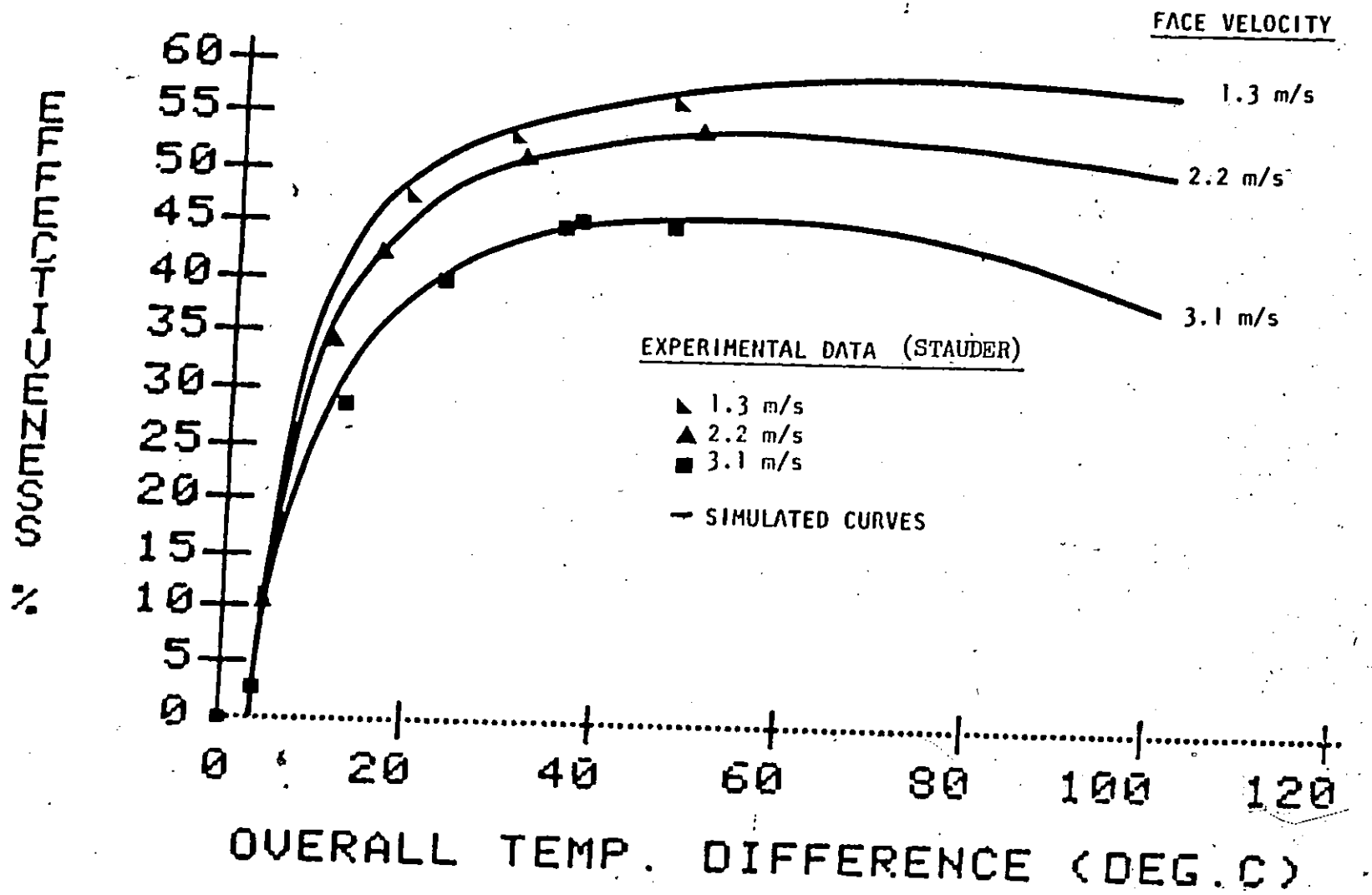

FIG. 4.19 COMPARISON OF EXPERIMENTAL & SIMULATED LOOP PERFORMANCE FOR THE COOLING PROCESS

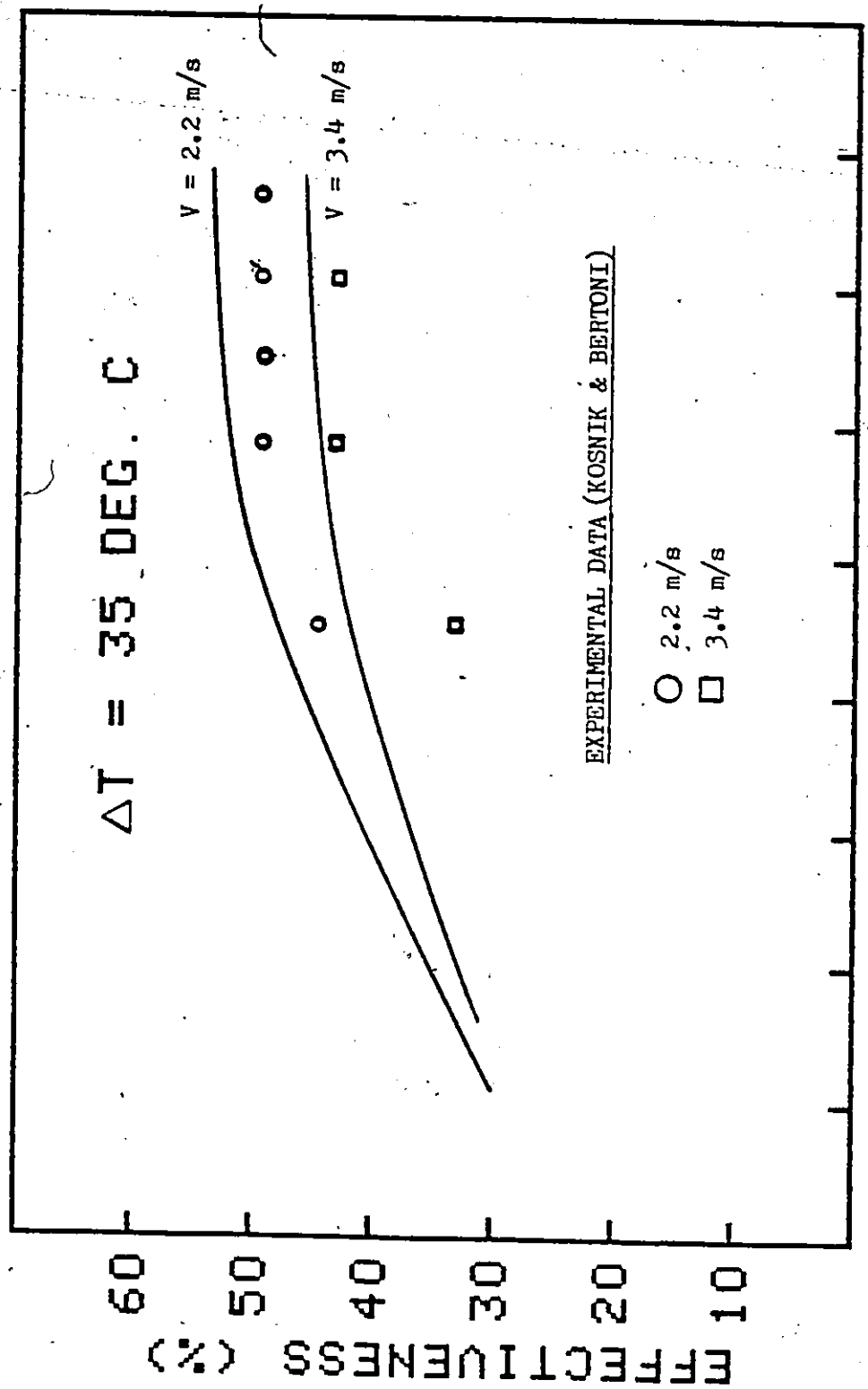

FIG. 4.20 SYSTEM EFFECTIVENESS VERSUS STATIC CHARGE FOR ΔT = 35 C & FACE VELOCITIES OF 2.2 & 3.4 M/S

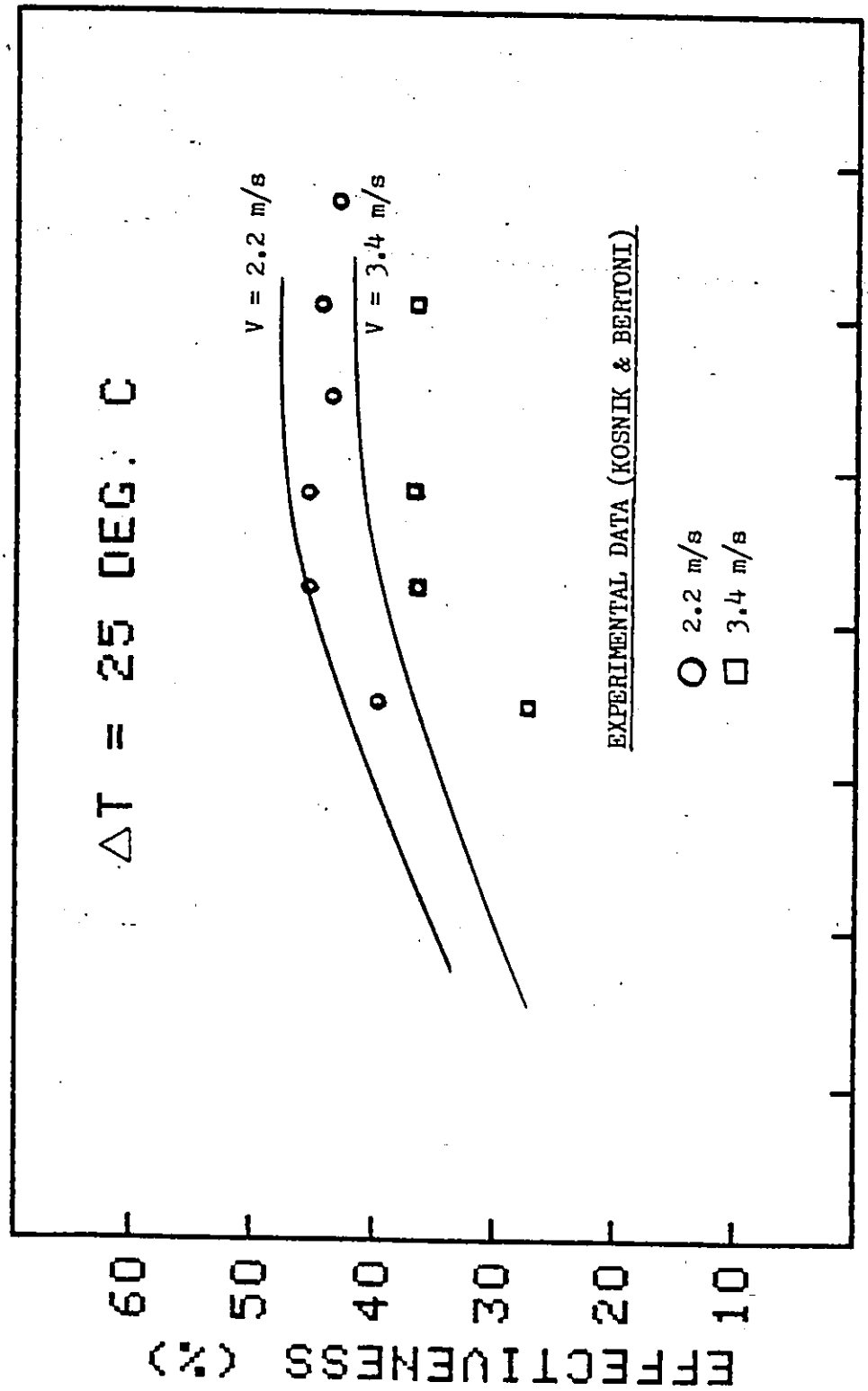

FIG. 4.21 SYSTEM EFFECTIVENESS VERSUS STATIC CHARGE FOR ΔT = 25 C & FACE VELOCITIES OF 2.2 & 3.4 M/S

agreement of the simulated curves with the corresponding experimental data (15) is not as good as for those of Stauder (17), but do generally show the same trends. This difference in the performance between the experimental results and the simulated results could be due to the presence of some air in the system of reference (15). The decrease in performance, noted in both the experimental and simulated results when the charge decreases below 60 %, is caused by dryout.

4.4 COMPARISON WITH CONSTANT HEAT FLUX BOUNDARY CONDITION IMPOSED ON THE EVAPORATOR TUBE

For this study, the simulated values of the average heat transfer coefficient for the boiling region have been compared with the corresponding results obtained by Bergevin et al. (23).

The system used in this experimental study was made of glass. The evaporator tube was inclined at an angle of 60 degrees from the horizontal. The condenser was water jacketed. The lengths of the evaporator and the condenser tubes were 143 and 400 cm respectively, and the internal diameters of both the tubes were 5 mm. The heat flux was varied from 600 to approximately 3400 W/sq.m. The working fluid

was in a subcooled state at the inlet to the evaporator and the inlet temperature was 45 C.

Figure 4.22 shows their experimentally measured values of the average heat transfer coefficient over that portion of the tube where boiling is present. The experimental results can be explained as follows: At low heat flux, the performance is goverened by pool boiling, where the magnitude of the heat transfer coefficient is low. As the heat flux is increased, the two-phase heat transfer mode starts to dominate and the flow becomes annular. With further increase of the heat flux, the two-phase heat transfer dominates over the most of the tube length. When the heat flux is increased sufficiently high, dryout starts, and the performance starts to deteriorate.

To compare the simulated performance with the above experimental data, the computer program was run with the original value of "m" = 0.5 and with m = 0.1 and 0.05. Exponent "m", used in the calculation of the effective heat transfer coefficient in the dryout region, governs how quickly dryout influences the heat transfer coefficient as shown by the following relations.

$$h_{e3} = A\, h_v + B\, h_{e2} \qquad \text{---} \quad (1)$$

where the proportion of dry area $A = ((x - x_c)/(1 - x_c))^m$

and the proportion of wet area $B = (1 - A)$.

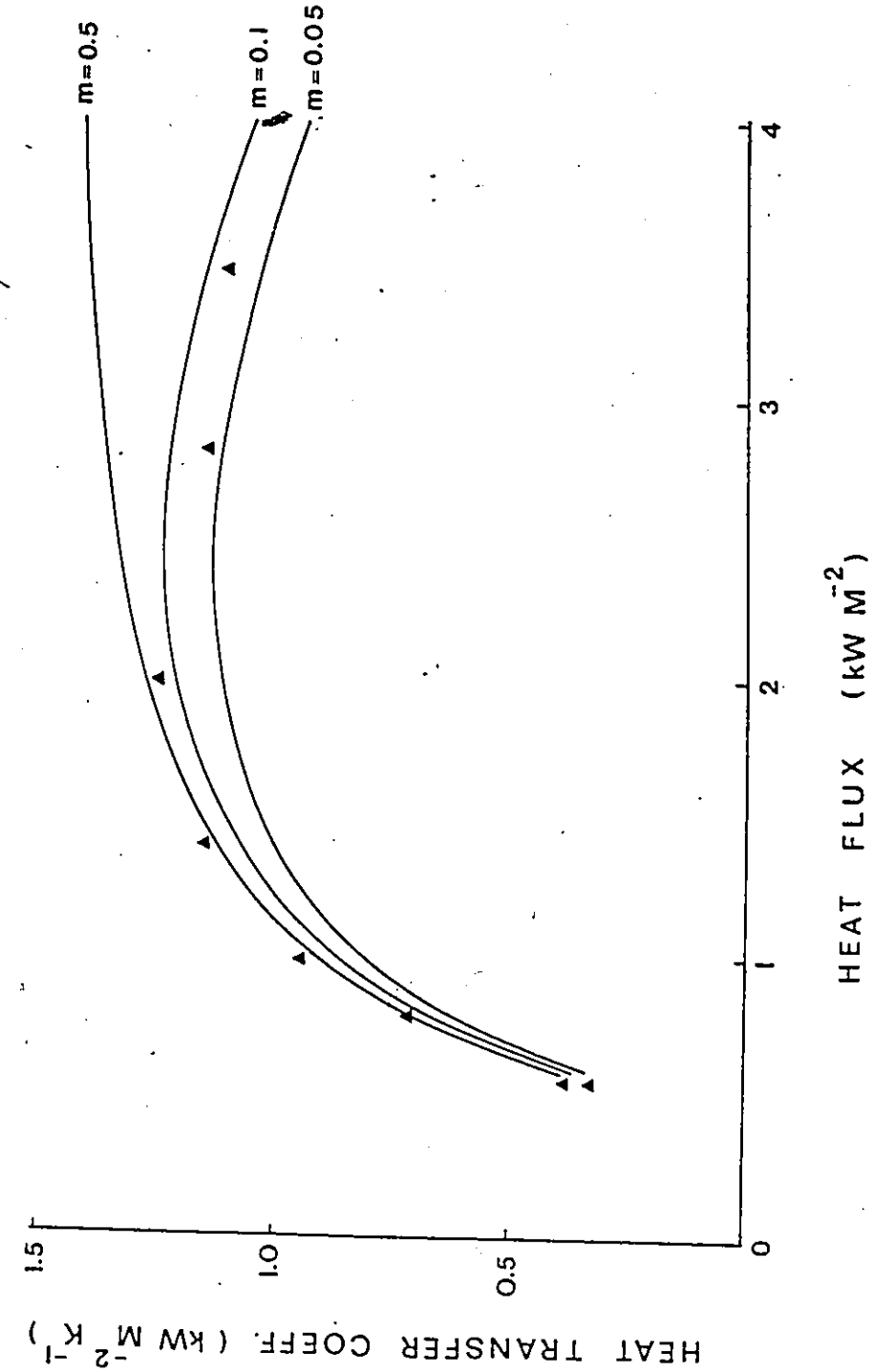

FIG. 4.22 AVERAGE EVAPORATOR HEAT TRANSFER COEFFICIENT FOR THE BOILING REGION VERSUS HEAT FLUX (EXPERIMENTAL DATA OF BERGEVIN ET AL., REF. 23).

For m = 0.5, the value established for prescribed-wall-temperature tubes, comparison with the experimental data was excellent up to 2000 W/sq.m, but failed to predict the drop in performance for higher heat fluxes. This means that the effective heat transfer coefficient, h_{e3}, given by equation 1 was much too high for larger heat fluxes. This would indicate that, for this prescribed-heat-flux boundary condition, the proportion of the surface area subject to dryout increases much more rapidly than is the case for dryout within prescribed-wall-temperature tubes. Figure 4.23 shows the variation of the area proportions "A" and "B" for m = 0.5, 0.01 and 0.05 when x_c = 0.05. The simulated performance curves for the system with m = 0.1 and 0.05 show that the decrease in the value of the average heat transfer coefficients as the heat flux increases above 2000 W/sq.m can be achieved by reducing m.

A value of 0.1 for m indicates that for large inclined evaporator tube lengths (1.43 m for the present case), and for high heat fluxes, the dryout is much more severe in comparison to inclined evaporator tubes of smaller lengths (0.62 m in Raza's system).

It is very important to note that the critical quality, x_c, the quality where dryout starts, has a significant impact on the effective heat transfer coefficient, h_{e3}, for the dryout region. An erroneous value of x_c could change the results drastically.

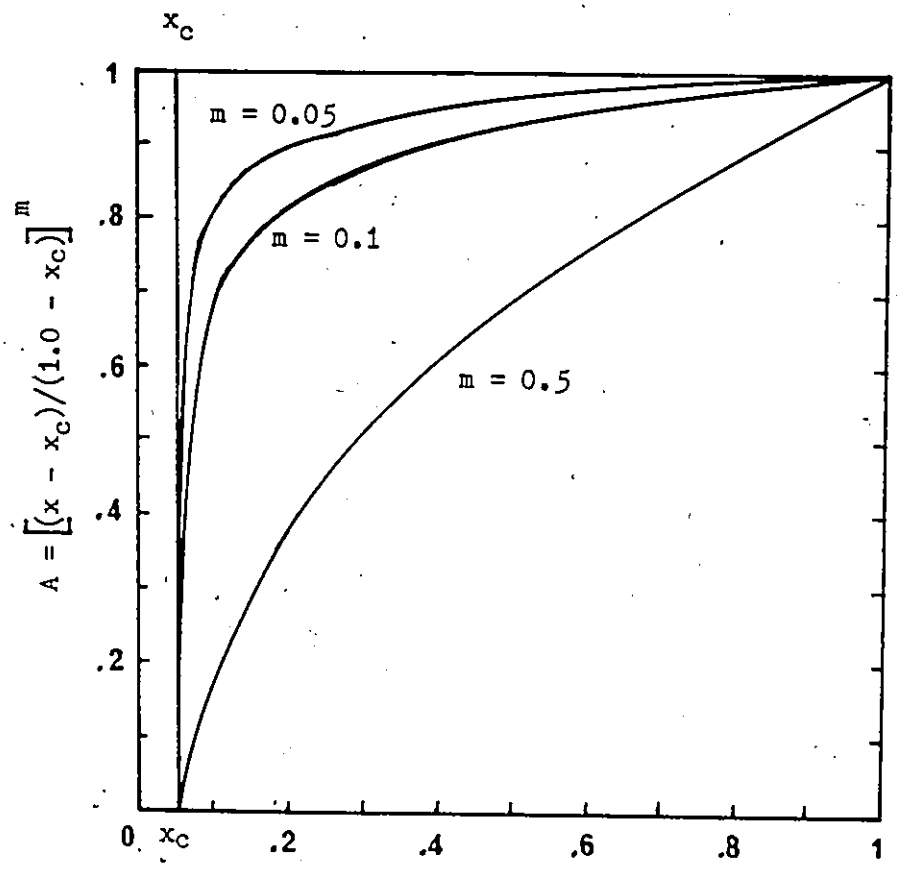

FIGURE 4.23 EFFECT OF POWER "m" ON VARIABLE "A"

B =(1.0 - A)

CHAPTER V

SIMULATED THERMOSIPHON EVAPORATOR PERFORMANCE

5.1 INTRODUCTION

In the last chapter, a comparison between simulated and experimental data was made for three two-phase thermosiphon loop heat exchanger systems having very different geometries and sizes. By comparing the experimental data of Raza (12), Kosnik & Bertoni (15), Stauder (17) and Bergevin et al. (23) with the corresponding simulated results, it was found that they agreed very well over a wide range of operating conditions. As a result, the model developed in chapter 3 could be used as a tool to simulate the performance of fluid-to-fluid two-phase thermosiphon-loop heat exchanger systems of different geometries and sizes.

In a typical application the temperatures and the mass flow rates of the exhaust gas, T_h and m_h and of the intake air T_c and m_c respectively, are known to the designer. The designer has control over the geometry of the exhaust and intake air ducts, the size of the evaporator and condenser tubes, the number of tube rows, and the tube and fin spacing. There are infinite numbers of combinations for which

the system could be studied. This chapter illustrates how a sequence of simulations could be carried out to assist the designer in selecting an optimum length and diameter of a given evaporator coil design for a given overall temperature difference.

Since the factors influencing condenser performance have received much attention in the past and are well documented, attention will be focused on the effect of various parameters on thermosiphon evaporator performance. This study is necessary as the performance of an evaporator in a thermosiphon system, unlike most evaporators is influenced by the complex interaction which occurs between the flow, pressure drop and heat transfer which governs the behaviour of the working fluid within the loop as the fluid is transformed from a subcooled liquid at entry to either a wet or a superheated vapour at the exit.

The following section describes the simulations which were carried out to study the behaviour of these systems.

5.2 PARAMETERS INVESTIGATED

The following table shows the range over which each parameter was investigated in the course of this study.

S.N.	PARAMETERS INVESTIGATED	
1.	Length of the coils	$L_c = 0.5\ L_e$; 0.61 m< L_e <2.44 m
2.	Evap. and cond. tube diameters	$D_c = D_e$ - 1/4", 3/8" and 1/2" nominal size
3.	Overall temp. diff.	- varied between 30 - 160 C
4.	Static charge	30 - 90 %
5.	Pressure drop in vapour header	0, 3.45, 6.90 Kpa

The ambient air temperature T_c was fixed at 20 C. Both coil face velocities and fin spacing were also held constant at 3.1 m/s (600 fpm) and 473/m (12 fins/inch) respectively. For all the simulations, the diameter of both the coil tubes were set equal and the evaporator and the condenser coils were assumed to be in vertical position. The areas of both the coils were taken equal and it was assumed that the condenser coil height was half the size of the evaporator coil (condenser coil width = 2 * evaporator coil width).

The airside resistances for 1/4" and 1/2" tubes were calculated

in a manner similar to that discussed in section 3.2.2.1. The coefficients used for the evaluation of airside resistance in equation 1 (appendix F) for tube diameters of 1/4" and 1/2" are given in Table F1 of appendix F.

The evaporator conductance, U_e, is defined by

$$U_e = \frac{Q}{A_e\,(T_{w,av} - T_{sat})}$$

where Q, A_e, $T_{w,av}$, T_{sat} are the heat transfer rate (W), area of the evaporator (sq.m) average evaporator wall temperature (C) and saturation temperature in the evaporator vapour header (C), respectively. The saturation temperature, T_{sat}, in the evaporator vapour header is a function of the pressure drop in the evaporator tube.

In the following section, the simulated thermosiphon evaporator performance is presented in graphical form. For these simulations, the hysteresis was not accounted for and the performance is based on the cooling curve ,i.e. it was assumed that the heated surface was at a higher temperature before reducing to the current level and thus nucleation sites were already established at a higher temperature.

5.3 RESULTS

The effect of evaporator static charge and tube length on the evaporator performance for a tube diameters of 0.635 cm (1/4") and 0.953 cm (3/8") and 1.270 cm (1/2") are shown in figures 5.1 to 5.8. For low static charges, the evaporator performance is poor due to the presence of dryout in the tubes. With the increase of the static charge and hence the flow rate, the dried out portion of the evaporator tubes decreases which results in better performance. However, when larger evaporator tubes are used, the evaporator conductance starts decreasing (see figures 5.3, 5.4, 5.8) at higher charges. This happens because as the charge and hence flow rate is increased, the increase in the frictional pressure drop in the evaporator causes a decrease in the saturation temperature in the evaporator vapour header and hence an increase in the temperature differences across the evaporator. For these high charges the temperature difference increases more rapidly than the heat flux and hence causes a decrease in the evaporator conductance. The decrease in the evaporator conductance for a tube diameter of 0.635 cm, with the increase of the overall temperature difference is due to dryout. However, the performance increases for larger tube diameters with the increase of the overall temperature difference, since the two-phase heat transfer coefficient and the vigour of the boiling increases. The decrease in the evaporator conductance for the overall temperature

difference lower than 20 C is due to the boiling suppression over large portion of the evaporator tube.

It was found that generally the evaporator performance increased with the increase of the percent static charge except for large evaporator tube lengths and temperature differences where excessive pressure drops occured. It was seen from these results that the evaporator performance is fairly good at static charges greater than 75 %. Hence,in order to analyze these results, the evaporator conductance versus evaporator tube length and overall temperature difference curves shown in figures 5.9 to 5.12, for a static charge of 80 % were constructed by cross-plotting the curves shown in figures 5.1 to 5.8.

Figure 5.9 shows the variation of the evaporator conductance with the length of the evaporator tube for a static charge of 80 % for D_e = 0.635 cm and 0.953 cm. For any source fluid temperature investigated for De = 0.635 cm, the peak performance is obtained at an evaporator tube length of 1.22 m. For an evaporator tube diameter of 0.953 cm and for 60 and 70 C overall temperature differences, the peak performance is obtained at 1.83 m. For an overall temperature difference of 90C the peak occurs at 2.44 m. For overall temperature differences larger than 90C, the peak would be obtained at tube lengths greater than 2.44 m. For the overall temperature difference of

100 C, the evaporator performance for 0.61 and 1.22 m tube length is lower in comparison to 90 and 70C overall temperature differences due to higher pressure drop at 80 % static charge, and dryout. Figure 5.10 shows similar results for a tube diameter of 1.270 cm.

Figure 5.11 shows the variation of the evaporator conductance with the overall temperature difference for a static charge of 80%, D_e = 0.635 and 0.953 cm, L_e = 0.61, 1.22, 1.83 and 2.44 m. For D_e = 0.635 cm, the decrease in the performance with the increase of the overall temperature difference is due to dryout. The decrease in the evaporator conductance for the overall temperature difference lower than 20C is due to the boiling suppression over large portion of the evaporator tube. For D_e = 0.953 and 1.270 cm (Figure 5.12), the performance increases with the increase of the overall temperature difference and peaks off at some higher overall temperature difference. Further increase of the overall temperature difference yields a lower performance due to increased dryout and increased pressure drop. For a given evaporator tube length, the optimum temperature difference can be determined from these graphs - i.e. the optimum temperature difference for L_e = 0.61 m and D_e = 1.270 cm is 100 C (see figure 5.12). However, the optimum length for an overall temperature difference of 100 C is 2.44 m.

In all the graphs shown so far (figure 5.1 - 5.12), the pressure

drop in the vapour header was set equal to zero. The significant effect that a pressure drop in the vapour header can have on the performance is illustrated in figure 5.13. The figure shows the variation of the performance for vapour header pressure drops of 0, 3.45 and 6.90 kPa (0, 0.5 and 1.0 psi). It is very important to keep this pressure drop to a minimum.

Figures 5.9 - 5.12 are plotted for a static charge of 80%. The performance of the thermosiphon evaporator could be very different for charges greater than 80%, especially for larger tube lengths. Hence, care should be taken for proper selection of the static charge, for a given set of condition.

5.4 CONCLUSIONS

Through a careful selection of the coil tube diameter and length as well as the static charge, finned multiple-tube thermosiphon evaporators can provide very good conductance values over a wide range of temperature differences. The range is limited by the evaporator tube dryout for large temperature differences and by boiling suppression for small temperature differences.

For a given overall temperature difference, there exists a tube diameter and length which yield a maximum evaporator performance. The

optimum diameter and length increase with increasing temperature difference as shown in the following table.

TEMPERATURE DIFFERENCE (C)	OPTIMUM	
	DIAMETER (cm)	LENGTH (M)
10	0.635	1.22
20–70	0.953	1.83
80	0.953	1.83/2.44
90–110	0.953	2.44
120–130	1.270	2.44

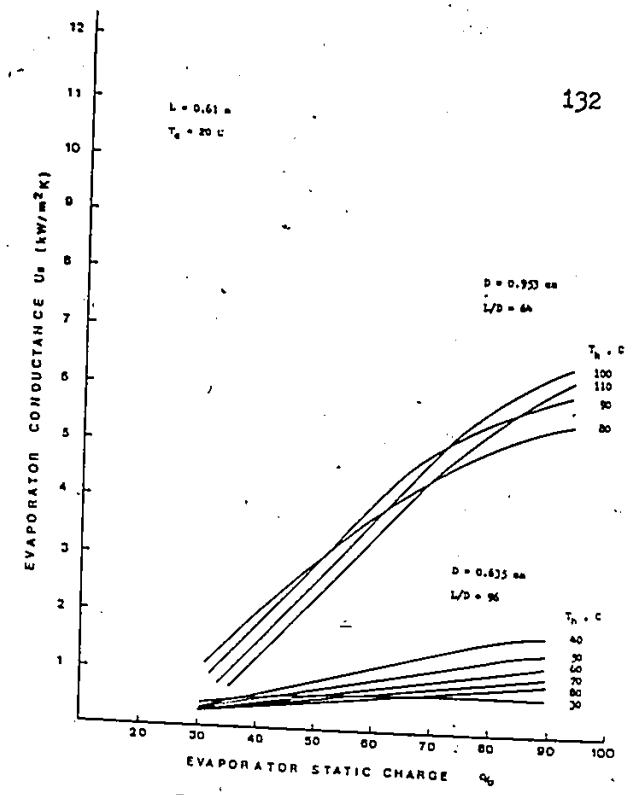

Figure 5.1 L = 0.61 m

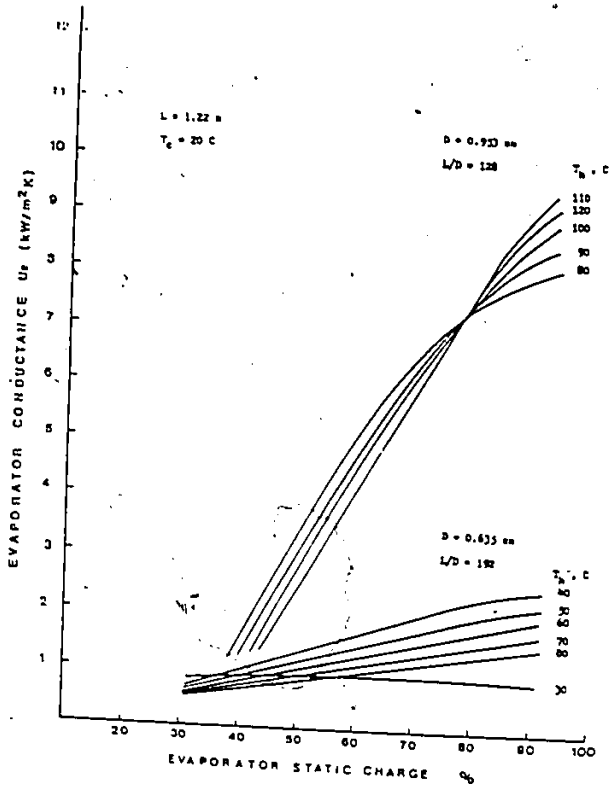

Figure 5.2 L = 1.22 m

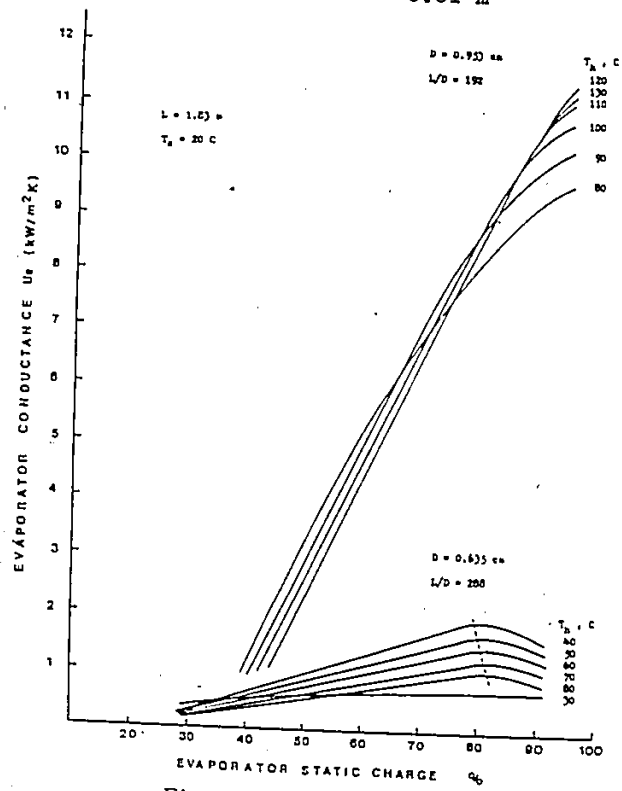

Figure 5.3 L = 1.83 m

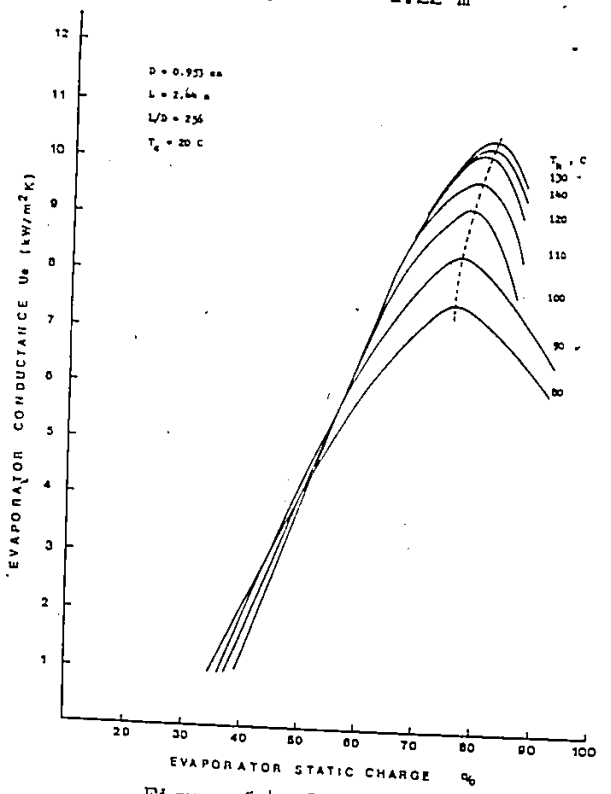

Figure 5.4 L = 2.44 m

Effect of tube length, static charge and source fluid temperature on the evaporator conductance for D = 0.635 and 0.953 cm

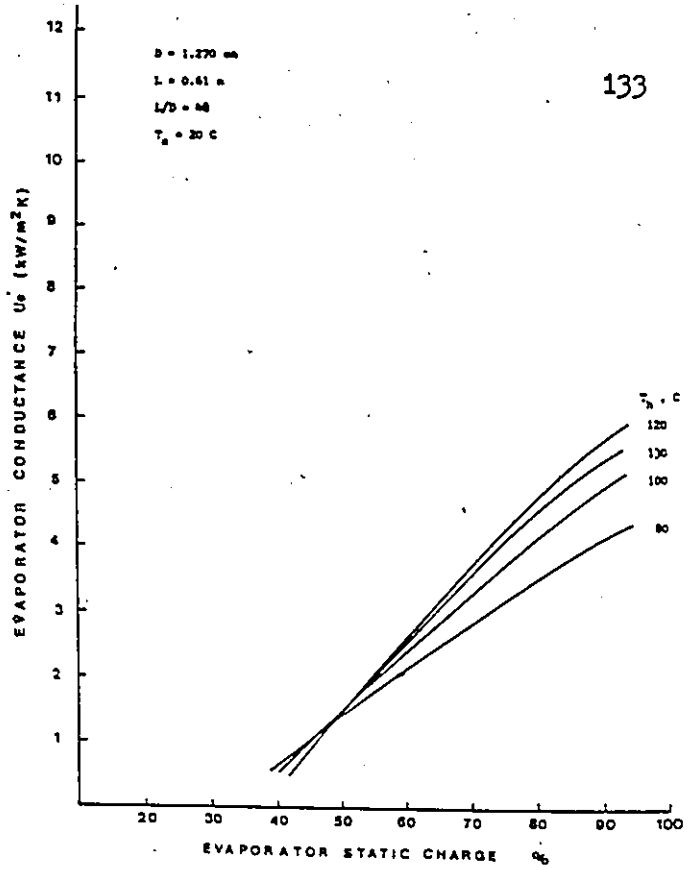

Figure 5.5 L = 0.61 m

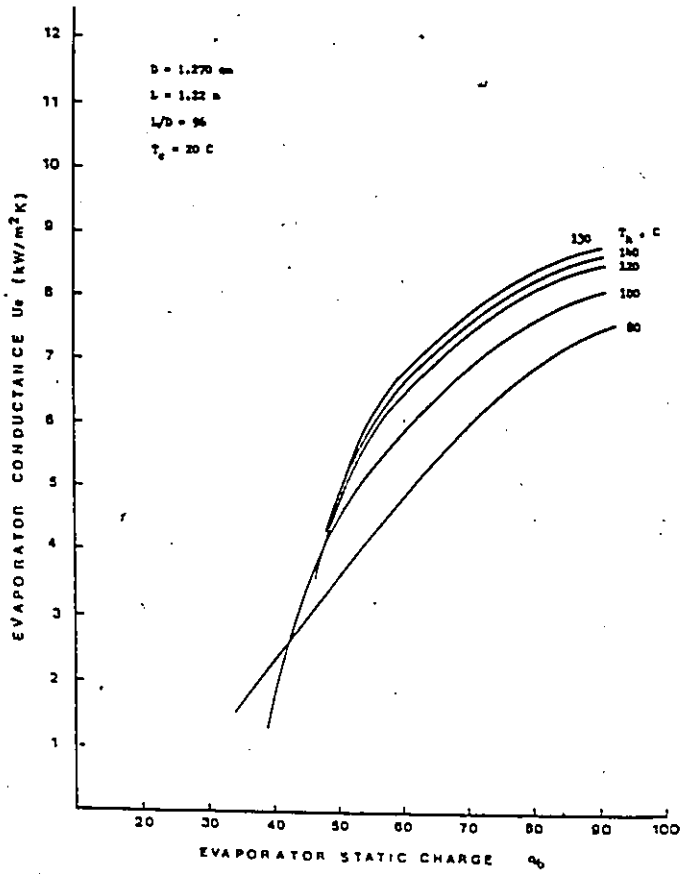

Figure 5.6 L = 1.22 m

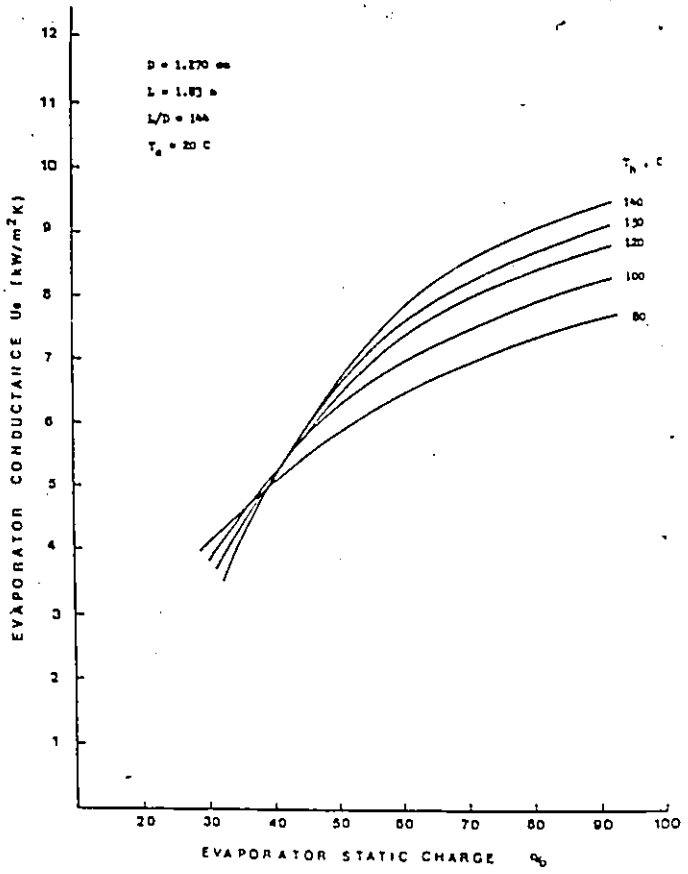

Figure 5.7 L = 1.83 m

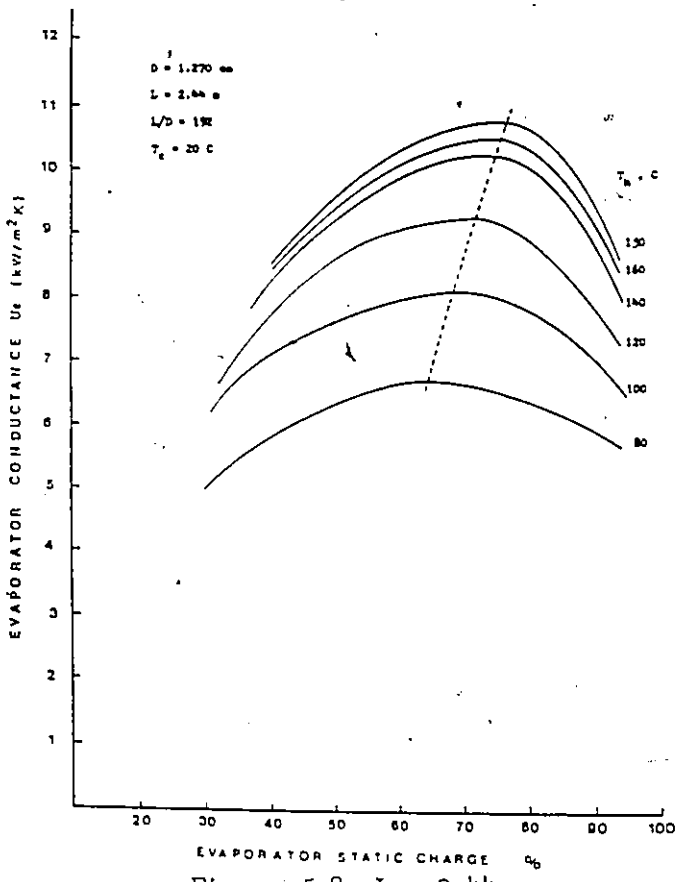

Figure 5.8 L = 2.44 m

Effect of tube length, static charge and source fluid temperature on the evaporator conductance for D = 1.270 cm

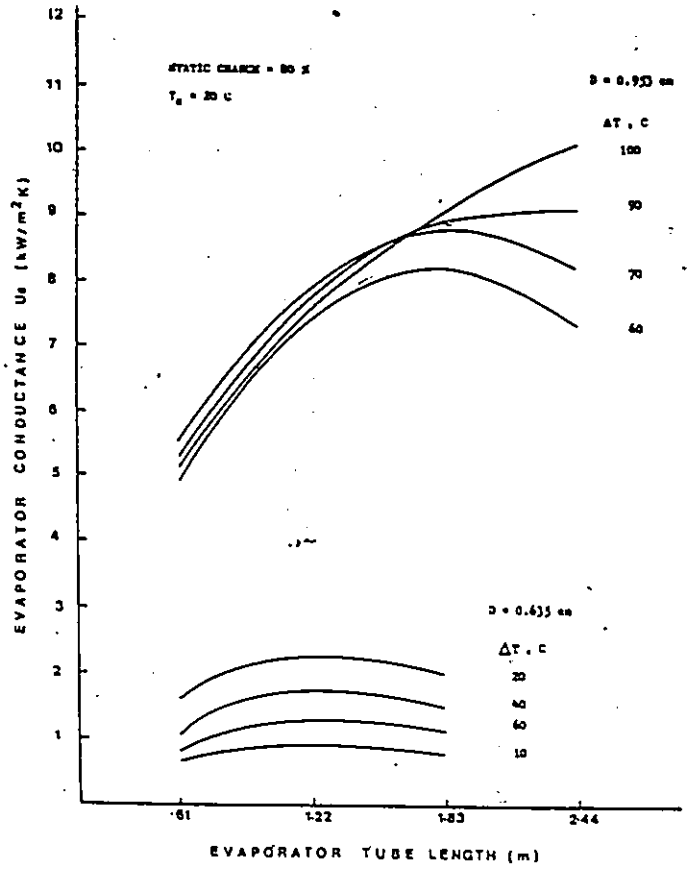

Figure 5.9 D = 0.635, 0.953 cm

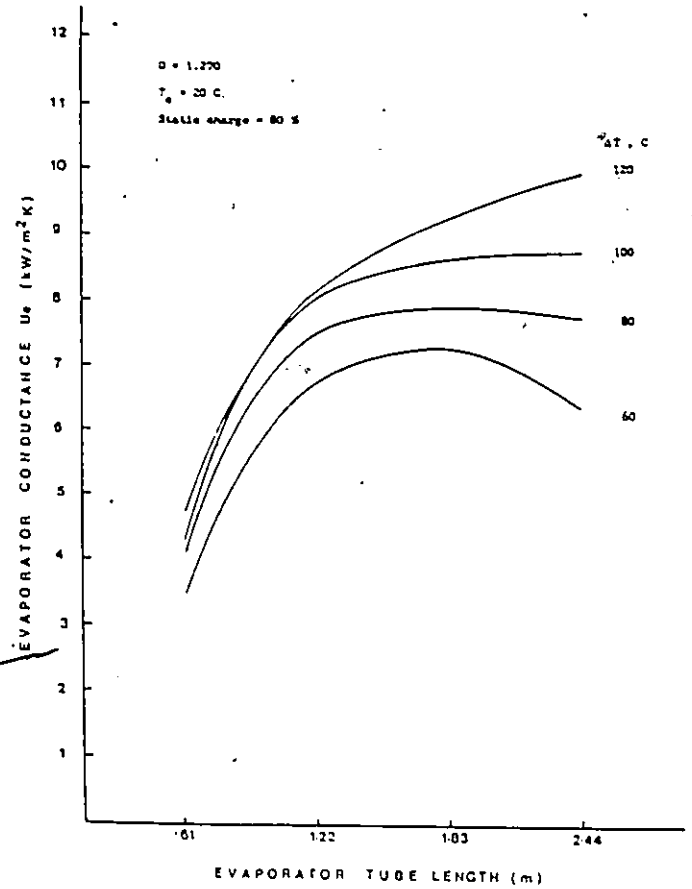

Figure 5.10 D = 1.270 cm

Effect of overall temperature difference and evaporator tube length on the evaporator conductance for a static charge of 80 %

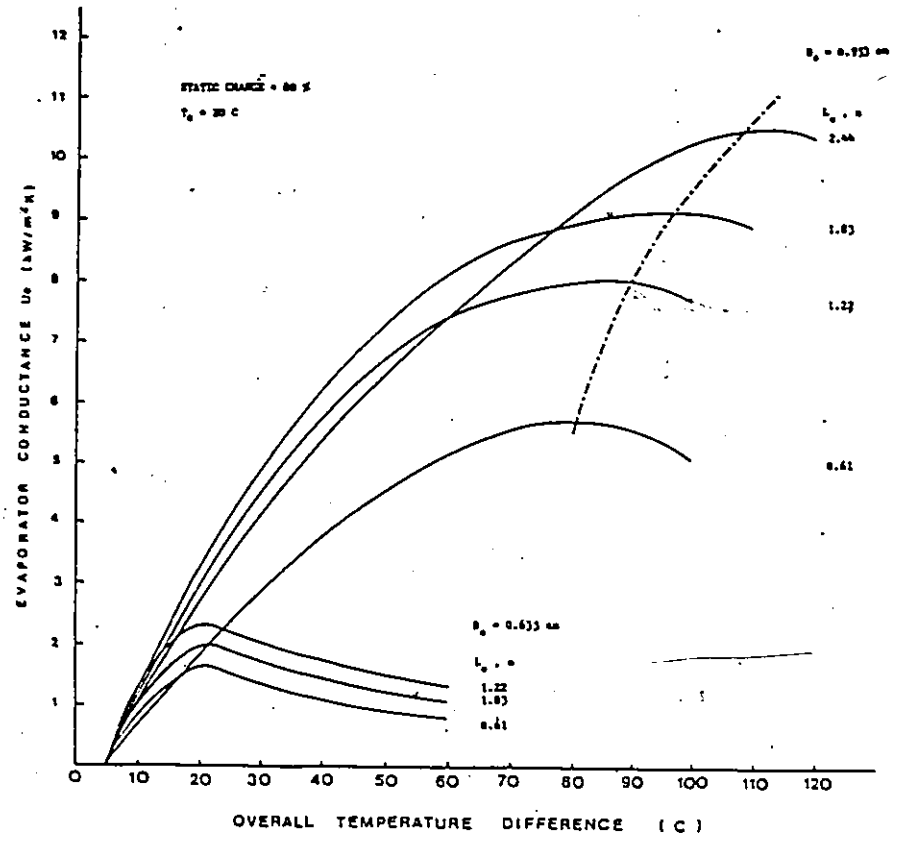

Figure 5.11 D = 0.635, 0.953 cm

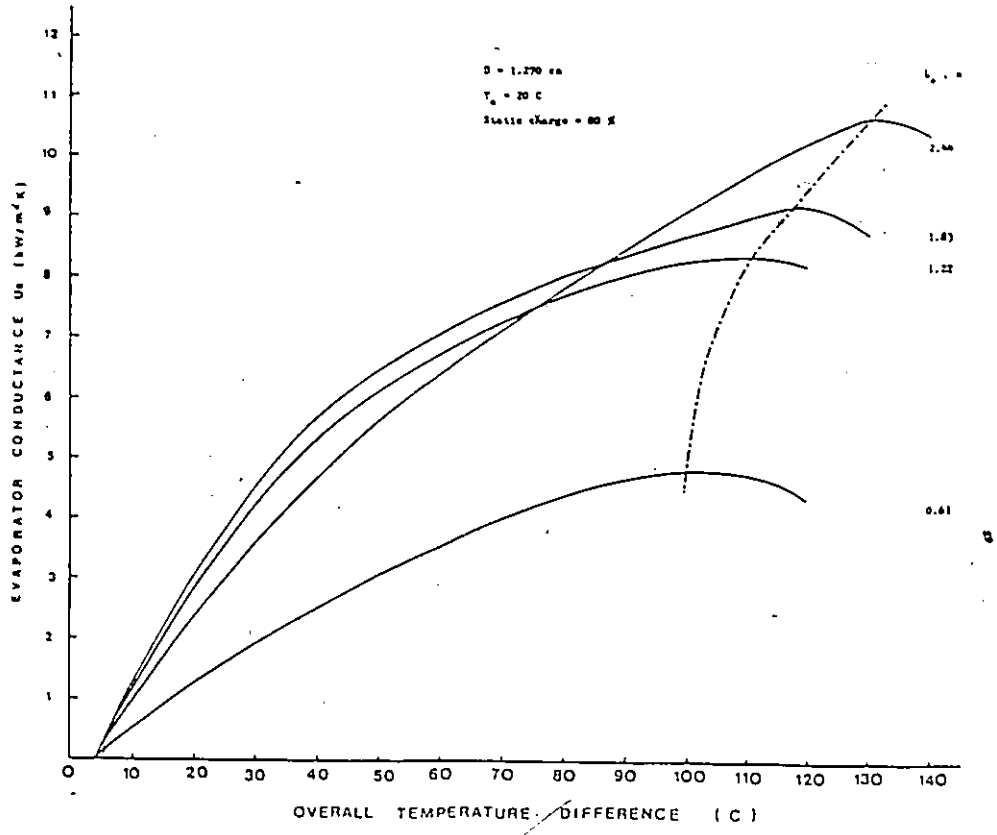

Figure 5.12 D = 1.270 cm

Effect of evaporator tube length and overall temperature difference on the evaporator conductance for a static charge of 80 %

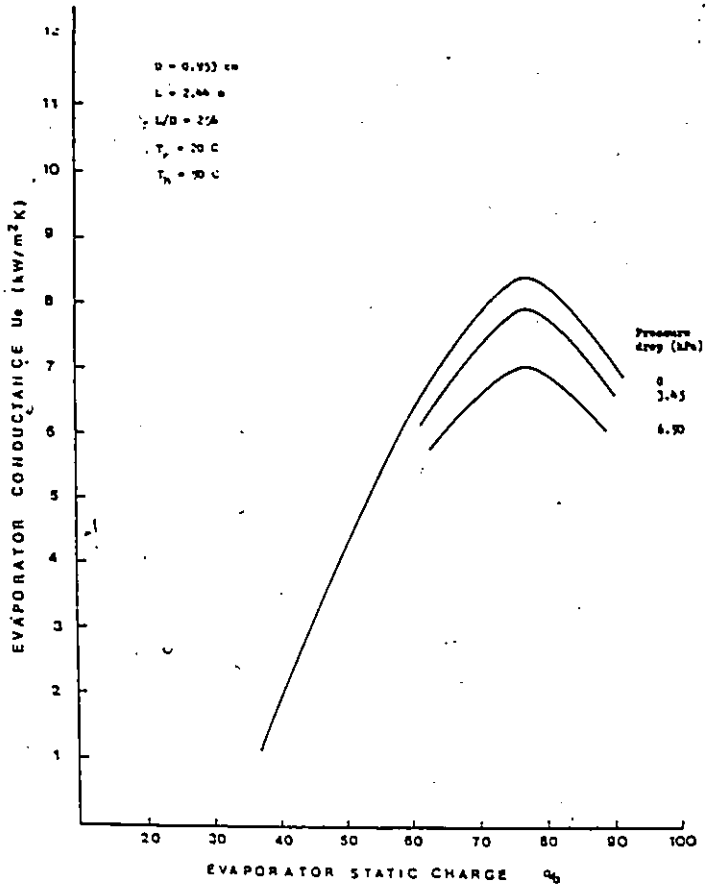

Figure 5.13 Effect of vapour header pressure drop on the evaporator conductance for D = 0.953 cm, L_e = 2.44 m, T_h = 90 C & T_c = 20 C

CHAPTER VI

CONCLUSIONS AND RECOMMENDATIONS

The computer program developed is capable of simulating the performance of fluid-to-fluid two-phase thermosiphon-loop heat exchanger systems in which the evaporator and condenser coils consist of parallel rows of straight tubes running between a common liquid header and a common vapour header. The model developed is based on the assumption of one-dimensional equlibrium flow in the tubes. The program is modular in form and hence may be easily modified to simulate any external boundary conditions. The following external flow and thermal conditions are built into the program:

1. Prescribed surface temperature
2. Source and or sink fluid flowing in an annular jacket
3. Source and or sink fluid flowing over finned tubes
4. Prescribed heat flux

The validity of the program was checked by comparison with experimental results generated in three different systems, one with water annulii jackets on all tubes (12), and one with air flowing over finned evaporator and condenser tubes (15), (17), and one with a constant heat flux boundary condition imposed on the evaporator tube (23). It was found that the computer program is capable of simulating

the behaviour of these two-phase thermosiphon loops with good accuracy.

Since computer program is based on the assumption of one-dimensional equlibrium flow in the tubes it will not be valid for large diameter tubes where two-dimensional effects will be present. The program has accurately simulated the performance of two-phase thermosiphon loops having coils consisting of 1- to 4.7-ft tubes with diameters of 1/4 and 3/8 in. A major limitation at present is the need for a correlation to determine the conditions under which the boiling will initiate during the system startup. Experimental studies should also be carried out for the dryout region so that better correlations can be developed for the estimation of the heat transfer coefficients.

REFERENCES

1. Hwang, K.S. Two-phase thermosiphon loops- part 1 (An experimental study of a 3/8 in diameter 2ft * 4 ft loop). M.Sc. thesis , University of Windsor, 1976.

2. Diciccio, R. Two-phase flow visualization thermosiphon loop. Mechanical engineering report, University of Windsor, HT-1-75.

3. Sampath, S. Two-phase multiple-tube thermosiphon loop (an experimental study). M.S. Thesis, University of Windsor, 1985.

4. Ali,A.F.M. Two-phase thermosiphon loops- Part 2 (development of a computer simulation program), Ph.D. thesis, University of Windsor, 1976.

5. McDonald, T.W., Hwang,K.S. & Diciccio,R. Thermosiphon loop performance characteristics: part 1, experimental study. ASHRAE trans., V 83, Pt. 2, pp 250-259, 1977.

6. Ali, A.F.M. & McDonald,T.W. Thermosiphon loop performance characteristics: part 2, simulation program. ASHRAE trans. V 83, Pt. 2, pp 260-278, 1977.

7. McDonald, T.W. & Ali,A.F.M. Thermosiphon loop performance characteristics: part 3, simulated results. ASHRAE trans., V 83, Pt. 2, pp 279-287, 1977.

8. McDonald, T.W., Ali, A.F.M. & Sampath,S. The unidirectional coil loop thermosiphon heat exchanger. ASHRAE trans, V 84, pt. 2, pp 27-37, 1978.

9. McDonald, T.W. & Sampath, S. The bidirectional coil loop thermosiphon leat exchanger. ASHRAE trans., V 86, pt. 2, pp 37-47, 1980.

10. McDonald, T.W. Development of performance characteristics for two-phase thermosiphon loops. Final report on ASHRAE RP-140, Dec. 1975.

11. McDonald,T.W. Recirculation thermosiphon loops with multiple tube evaporators and condensers. Final report on ASHRAE RP-180, Jan. 1979.

12. Raza, S. A study of the effect of unequal evaporator heating and charge distribution on the performance of a two-phase thermosiphon heat exchanger. M.A.Sc. thesis, University of Windsor, Dec. 1983.

13. Raza, S. & McDonald, T.W. Thermosiphon evaporator performance with unequal tube heating and tube charge conditions. ASME paper 84-HT-90, Aug. 1984.

14. McDonald, T.W. & Raza, S. Effect of unequal evaporator heating and charge distribution on the performance of a two-phase thermosiphon loop heat exchanger. ASHRAE trans., paper # 2853, Vol 90, pt 2, 1984.

15. Kosnik, M. & Bertoni, G. Performance testing of a two-phase thermosiphon loop. Senoir year project, Department of Mech. Eng., University of Windsor, 1984.

16. McDonald, T.W., Kosnik, M. & Bertoni, G. Performance of a two-phase thermoosiphon air-to-air heat exchenger. ASHRAE Trans., v 91, pt. 2, paper # 2901, 1985.

17. Stauder, F.A. Experimental study of an air-to-air two-phase

thermosiphon loop heat exchanger. M.A.Sc. Thesis, University of Windsor, 1985.

18. Mendler, O.J., Rathbun, A.S., Van Huff, N.E. & Weiss,A. Natural circulation tests with water at 800 to 2000 psia under non boiling, local boiling, and bulk boiling conditions. J. of heat transfer, pp 261-273, Aug 1961.

19. Bandy,D.B. Dhuey,J.A., Stevens, W.F. & Bankoff,S.G. Maximization of heat rejection rate to a natural circulation boiling channel. Chemical engg. prog. symp. series, N 92, V 65, pp 231-242.

20. Soin,R.S., Rao, K.S., Rao,D.P. & Rao, K.S. Performance of flat plate solar collector with fluid undergoing phase change. Solar Energy, V 23, pp 69-73, 1979.

21. Tanger,G.E., Lytle,J.H. & Vachon, R.I. Heat transfer to sulphur hexafluoride near the thermodynamic critical region in a natural circulation loop. J. of heat transfer, ASME, pp 37-42, Feb 1968.

22. Cheng, K.C. & Rovang, G.W. Heat transfer characteristics of a closed loop two-phase thermosiphon system for low grade waste heat recovery from liquid heat sources. ASME, HTD-Vol 44, Nov. 1985.

23. Bergevin, B., Jean, B. & Rheault, F. Etude des mecanismes de transfert de la chaleur dans un capteur solaire a changement de phase. Sunfest 83, SESCI, Aug 1-5, 1983.

24. Bezrodnyy, M.K. & Alekseyenko, D.V. Investigation of heat & mass transfer in heat pipes. Teplofiz. vy. temp., v 15, n 12, 370-77, 1977.

25. Casarosa,C, Latrofa,E & Shelginski,A. The geyser effect in a two-phase thermosiphon. Int. JH&MT, V 26, N 6, pp 933-941,1983.

26. Imura,H., Sasaguchi,K., Kozai, H., & Numata,S. Critical heat flux in a closed two-phase thermosiphon, Int. JH&MT, V 26, N 8, pp 1181-1188, 1983.

27. Kashirskiy, V.G., Pechnogov, Y., & Sernov, Y.I. Experimental study of boiling heat transfer to water in a microthermosiphon heated from the end. Heat transfer- Soviet res., V 15, N 2, March-April 1983.

28. Pioro, I.L. Maximum heat transfer capability in two-phase thermosiphons. Heat Transfer- Soviet res., V 15, N 1, Jan-Feb 1983.

29. Bezrodnyy, M.K. & Sakhatskiy, V.A. Relationships governing the limiting heat transfer in inclined evaporative thermosiphons. Teploenergetika, N 3, pp 75-77, 1977.

30. Bezrodnyy, M.K., Volkov, S.S. & Alekseyenko, D.W. Maximum heat transfer in thermosiphons with separated uptake and downtake flows. Heat transfer- Soviet res., V 15, N 2, March-April 1983.

31. Bezrodnyy, M.K. & Elekseyenko, D.V. Boiling heat transfer in closed two-phase thermosiphons. Heat Transfer-Soviet res., V 9, N 5, Sept-Nov 1977.

32. Savchenkov,G.A. 6 Gorbis,Z.R. Boiling heat transfer in low-temperature evaporating thermosiphons. Heat transfer- Soviet res., V 8, N 4, July-Aug 1976.

33. Galaktionov,V.V., Portnov,V.D. & Mironenko,A.V. Investigation of heat and mass transfer in the evaporator zone of a two-phase thermosiphon. Heat transfer-Soviet res., V 9, N 3, May-June 1977.

34. Faynzilberg, S.N. Koloskova,N.Y. & Semena,M.G. Correlation of experimental data on the maximum heat fluxes in two-phase

thermosiphons. Heat transfer-Soviet res., V 11, N 2, March-April 1979.

35. Lee,Y & Mital,U. A two-phase closed thermosiphon. Int.JH&MT, V 15 pp 1695-1707, 1972.

36. Lee,Y & Bedrossian, A. The characteriscis of heat exchangers using heat pipes or thermosiphons, Int. JH&MT, V 21, pp 221-229, 1978.

37. Larkin,B.S. An experimental study of the two-phase thermosiphon tube. paper 70-CSME-6, Trans. of the Engg. Institution of Canada, V 14, N B-6, Aug/Sept 1971.

38. Larkin, B.S. Heat transfer in a two-phase thermosiphon tube, DME/NAE Quarterly bulletin, National research council, Ottawa, pp 45-53, 1976.

39. Larkin, B.S. A computer cooling applications for thermosiphons.

40. Kusuda,H. & Imura,H. Boiling heat transfer in an open thermosiphon. Report 1, JSME, V 16, N 101, pp 1723-33.

41. Kusuda, H. & Imura, H. Boiling heat transfer in an open thermosiphon. Report 2, JSME, V 16, N 101, pp 1734-40.

42. Knoner, R. Dependance of heat transfer efficiency of a thermosiphon on transfer coeifficients. ----------, pp 244-245.

43. Haynes,F.D. & Zarling,J.P. A comparative study of thermosiphons used for freezing soil. ASME paper # WA/HT-40.

44. Chen, K. The influence of loop configuration on closed loop thermosiphons. ASME paper # 82-WA/HT-63.

45. Japikse, D. & Winter, E.R.F.. Single-phase transport processes in an open thermosiphon. IJH&MT, V 14, pp 427-441, 1971.

46. Japikse,D., Jallouk, Winter,E.R.F. Single-phase transport processes in the closed thermosiphon. IJH&MT, V 14, pp 869-887, 1971.

47. Chato, J.C. Natural convection flows in parallel channel systems. J of heat transfer, ASME, pp 339-345, Nov 1963.

48. Alstad, C.D., Isbin, H.S., Amundson, N.R. & Silvers, J.P. Transient behavior of single-phase natural circulation loop systems. A.I.Ch.E.J., V 1, N 4, pp 417-425, Nov 1955.

49. Zvirin, Y., Shitzer, A. & Grossman, G. The natural circulation solar heater - models with linear and nonlinear temperature distribution. IJH&MT, V 20, pp 997-999, 1977.

50. Martin, B.W. & Lockwood, F.C. Entry effects in the open thermosiphon. J of fluid mechanics, V 19, pt 2, pp 246-256.

51. Close,D.J. The performance of solar water heaters with natural circulation. Solar Energy, V 6, pp 33-40, 1962.

52. Jasinski, J. & Buckley, S. Thermosiphon analysis of a thermic diode solar heating system. ASME papere # 77-WA/Sol-9.

53. Mertol, A., Place,W., Webster,T. & Greif,R. Detailed loop model (DLM) analysis of liquid solar thermosiphons with heat exchangers. Solar energy, V 27, N 5, pp 367-386, 1981.

54. Young,M.F. & Bergquam,J.B. Performance characteristics of a thermosiphon solar domestic hot water system. J of solar energy engg., ASME, V 103, N 3, pp 193-200, 1981.

55. Morrison,G.L. & Ranatunga,D.B.J. Thermosiphon circulation in solar collectors. Solar energy, V 24, pp 191-198, 1980.

56. Morrison,G.L. & Ranatunga,D.B.J. Transient response of the thermosiphon solar collector. Solar energy, V 24, pp 55-61, 1980.

57. Grossman, G, Shitzer,A & Zvirin, Y. Heat transfer analysis of a flat plate solar energy collector. Solar energy, V 19, pp 493-502, 1977.

58. Huang, B.J. Similarity theory of solar water heater with natural circulation. Solar energy, V 25, pp 105-116, 1980.

59. Shitzer,A., Kalmanoviz,D., Zvirin,Y. & Grossman, G. Experiments with a flat plate water heating system in thermosiphonic flow. Solar energy, V 22, pp 27-35, 1979.

60. Ong,K.S. A finite difference method to evaluate the thermal performance of a solar water heater. Solar energy, V 16, pp 137-147, 1974.

61. Ong,K.S. An improved computer program for the thermal performance of a solar water heater. Solar energy, V 18, pp 183-191, 1976.

62. Yellot,J.I & Sobotka, R. An investigation of solar water heater performance. ASHRAE Trans., V 70, pp 425-433, 1964.

63. DeSa,V.G. Solar energy utilization at Dacca. Solar energy, V 8, N 3, pp 83-90, 1964.

64. Sternling, V.C. Two phase flow theory and engineering decision. Award lecture presented at AIChE annual meeting, Dec. 1965.

65. Govier, G.W. & Aziz, K. The flow of complex mixtures in pipes. Van Nostrand Reinhold, New York, 1972.

66. Wallis, G.B. One dimensional two phase flow. McGraw Hill, New York, 1972.

67. Hewitt, G.F. & Roberts, D.N. studies of two-phase flow patterns by simultaneous x-ray and flash photography. UKAEA report AERE. - M2159, 1969.

68. Griffith, P. & Wallis, G.B. Two-phase slug flow. J of H. Tr., V 83 C, N 3, 307, 1961.

69. Duns, H. & Ros,N.C.J. Vertical flow of gas and liquid mixtures from borcholes. Proceedings of 6 world petroleum congress, Frankfurt, June, 1963.

70. Gould, T.L. Vertical two-phase steam-water flow in geothermal well. J of pet. tech., V 26, 833, 1974.

71. Spedding, P.L. & Nguyen, V.T. Regime map for air water two-phase flow. Chem. engg. Sci., V 35, 779, 1980.

72. Weisman, J. & Kang, S.Y. Flow pattern transitions in vertical and upwardly inclined tube. I J of Multiphase flow, V 7, pp 271-291, 1981.

73. Dukler, A.E. & Taitel, Y. Flow regime transitions for vertical upward gas liquid flow : a preliminary approach through physical modeling. Progress report N 1, NUREG-0162, 1977.

74. Dukler, A.E. & Taitel, Y. Flow regime transitions for vertical upward gas liquid flow : a preliminary approach through physical modeling. Progress report N 2, NUREG-0163, 1977.

75. Taitel, Y., Bornea, D. & Dukler, A.E. Modeling flow pattern transitions for steady upward gas-liquid flow in vertical tubes.

AIChEJ, V 26, N 3, 345, 1980.

76. Barnea, D., Shoham, O., Taitel, Y. & Dukler, A.E. Gas-liquid flow in inclined tubes : flow pattern transitions for upward flow. Chem engg. sci., V 40, N 1, pp 131-136, 1985.

77. Mishima, K. & Ishii, M. Flow regime transition criteria for upward two-phase flow in vertical flows. IJH&MTr, V 27, N 5, pp 723-737, 1984.

78. Troniewski, L. & Ulbrich, R. The analysis of flow regime of two-phase gas liquid flow in pipes. Chem engg. sci., V 39, N 7/8, pp 1213-1224, 1984.

79. Hashizume, K. Flow pattern, void fraction and pressure drop of refrigerant two-phase flow in a horizontal pipe - 1. IJ multiphase flow, V 9, N 4, pp 399-410, 1983.

80. Crawford, T. & Weisman, J. Two-phase (vapour-liquid) flow pattern transitions in ducts of non circular cross section and under diabatic conditions. IJ of Multiphase flow, V 10, N 3, pp 385-391, 1984.

81. Weisman, J., Duncan, D., Gibson, J. & Crawford, T. Effects of fluid properties & pipe diameter on two-phase flow patterns in horizontal lines. I J of Multiphase flow, V 5, pp 437-462, 1979.

82. Troniewski, L. & Ulbrich, R. Two-phase gas-liquid flow in rectangular channels. Chem. engg. sci., V 39, N 4, pp 751-765, 1984.

83. Stylianou, S.A. & Rose, J.W. Drop to filmwise condensation transition : heat transfer measurements for ethanediol. IJH&MT, V 26,

N 5, pp 747-760, 1980.

84. Barnea, D., Luninski, Y. & Taitel, Y. Flow pattern in horizontal and vertical two-phase flow in small diameter pipes. Can. J of Chem engg., V 61, pp 617-620, 1983.

85. Mandhane, J.M., Gregory, G.A. & Aziz, K. A flow pattern map for gas-liquid flow in horizontal pipes. IJ of Multiphase flow, V 1, pp 537-553, 1974.

86. Palen, J.W., Berber, G. & Taborek, J. Prediction of flow regimes in horizontal tube - side condensation. Heat tr. engg., V 1, N 2, Oct. - Dec. 1979.

87. Soliman, H.M. Correlation of mist-to-annular transition during condensation. Can. J. of Chem engg., V 61, pp 178-182, 1983.

88. Breber, G., Palen, J.W. & Toborek, J. Prediction of horizontal tubeside condensation of pure refrigerant using flow regime criteria. Condensation heat transfer, ASME, Aug. 1979.

89. Baker, C. Design of pipelines for the simultaneous flow of oil and gas. The oil & gas J, V 53, 185, 1954.

90. Scott, D.S. Properties of concurrent gas-liquid flow. Advances in Chem engg., V 4, Academic press, N Y.

91. Graetz, L. Uber die Warmeleitungsfahigkeit von Flussigkeiten. Annalen der Physik Chem, V 25, 335, 1885.

92. Leveque, J. Ann Mines, V 13, N 201, 305, 1928.

93. Lipkis, R. Discussions in reference 74.

94. Norris, R.H. & Stried, D.D. Laminar flow heat transfer for ducts. Trans ASME, V 62, 525, 1940.

95. Kays, W.M. & London, A.L. Convective heat transfer and flow friction behaviour of small cylindrical tubes-circular and rectangular cross section. Trans ASME, V 74, 1179, 1952.

96. Sieder, E.N. & Tate, G.E. Heat transfer and pressure drop of liquids in tubes. Industrial and Eng. Chemistry, V 28, N 12, 1429, 1936.

97. Nusselt, W. Mitt. iber Forsch V 89, 1910.

98. Colburn, A.P. Trans. AIChE, V 29, 174,1933.

99. Dittus, F.W. & Boelter,L.M.K. University of California publishing engineers, V 2, 443, 1930.

100. Skupinski, E.S., Tortel, J. & Vautrey, L. IJH&MT, V 8, 937, 1965.

101. Seban, R.A. & Shimazaki, T.T. Trans ASME, V 73, 803, 1951.

102. Kays, W.M. Numerical solutions for laminar flow heat transfer in circular tubes. Trans ASME, 1265, Nov 1955.

103. McAdams, W.H. Refrigerating Engineering, V 10, N 9, 1924.

104. Hausen, H.Z. VDI Beih. Verfahrenstech, V 4, 91,1943.

105. Mills, A.F. Experimental investigation of turbulent heat transfer in the entrance region of a circular conduit. J of Mechanical Eng. Sc., V 4, N 1, 63, 1962.

106. Aladyev, I.T. Experimental determination of local and mean coeifficients of heat transfer for turbulent flow in pipes. NASA, TM 1356, 1954.

107. Iversion, H.W. Variation of the point unit thermal conductance of entrance to tubes for a fluid flowing turbulently. M.S. Thesis,

Univ of California, 1943.

108. Hsu,Y.Y. On the size range of active nucleation cavities on a heating surface. J of Heat transfer, ASME, Ser. C, V 84, pp 207-216, 1962.

109. Hsu,Y.Y. & Graham, R.W. An analytical and experimental study of the thermal boundary layer and ebullition cycle in nucleate boiling. NASA TN-D-596,1961.

110. Berglés, A.E. & Rohsenow, W.M. The determination of forced convection surface boiling heat transfer. J of heat transfer, ASME, Ser. C, V 86, pp 365-372,1964.

111. Han,C.Y. & Griffith, P. The mechanism of heat transfer in nucleate pool boiling- part 1 bubble initiation, growth and departure. IJH&MT, V 8, pp 887-904,1965.

112. Sato, T. & Matsumura, H. On the conditions of incipient subcooled boiling and forced convection. JSME, V 7, N 36, pp 392-398, 1964.

113. Davis,E.J. & Anderson, G.H. The incipience of nucleate boiling in forced convection flow. AIChEJ, v 12, pp 774-780,1966.

114. Murphy, R.W. & Bergles,A.E. Subcooled flow boiling of fluorocarbons-hysteresis and dissolved gas effects on heat transfer. Proceedings of the 1972 heat transfer & fluid mechanics institution, Standford University press, pp 400-416, 1972.

115. McAdam, W.H., Kennel, W.E., Minden, C.S., Carl, R., Pieornell, P.M. & Dw,J.E. Heat transfer at high rates to water with surface

boiling. Industrial & Engineering Chem., V 41, N 9, 1945.

116. Discussed in reference 85.

117. Chen, J.C. Incipient boiling superheats in liquid metals. J of heat transfer, ASME, pp 303-312, Aug. 1968.

118. Corty, C. & Foust, A.S. Surface variables in nucleate boiling. Chem eng. prog. symp. ser., V 51, N 16, pp 1-12, 1955.

119. Turton, J.S. The effects of pressure and acceleration on the pool boiling of water and arcton-11. IJH&MT, V 11, pp 1295-1310,1968.

120. Abdelmessih, A.F., Fakhri, A. & Yin, S.T. Hysteresis effects in incipient boiling superheat of freon-11. Fifth international heat transfer conf., JSME, V 4, pp 165-169, 1974.

121. Hodgson, A.S. Hysteresis effects in surface boiling of water. J of heat transfer, ASME, pp 160-162, 1969.

122. Marto, P.J. & Rohenow, W.M. Effects of surface conditions on nucleate pool boiling of sodium. J of heat transfer, ASME, Ser. C, V 86, pp 196-204, 1966.

123. Joudi, K.A. & James, D.D. Incipient boiling characteristics at atmospheric and subatmospheric pressure. J of heat transfer, ASME, V 99, pp 398-403, Aug. 1977.

124. Clarke,R.H. & Robertson, J.M. Investigation into the onset of convective boiling with liquid nitrogen in plate fin heat exchanger passages under constant wall temperature boundary conditions. AIChE symp. ser., Heat transfer- Niagara Falls, V 80, N 236, pp 98-103, 1984.

125. Bankoff, S.G. On the nature and location of bubble nuclei in

boiling from surfaces. J of applied physics, 29, pp 1739-1741.

126. Sakurai, A. & Shiotsu, M. Temperature controlled pool boiling heat transfer. Intl. heat transfer conf. Tokyo, V 4, B 3.1, JSME, 1974.

127. Yin, S.T. & Abdelmessih, A.F. Prediction of incipient flow boiling from a uniformly heated surface. AIChE symp. ser., Solar & nuclear heat transfer, V 73, N 164, pp 236-243, 1978.

128. Nishikawa, K., Fujita, Y., Uchida,S, & Ohta, H. Effect of surface configuration on nucleate boiling heat transfer. IJH&MT, V 27, N 9, pp 1559-1571,1984.

129. Han, C. & Griffith, P. The mechanism of heat transfer in nucleate pool boiling- part 1. IJH&MT, V 8, pp 887-904, 1965.

130. Han, C. & Griffith, P. The mechanism of heat transfer in nucleate pool boiling- part 2. IJH&MT, V 8, pp 905-914, 1965.

131. Singh, A., Mikic, B.B. & Rohsenow, W.M. Active sites in boiling. J of heat transfer, ASME, pp 401-406, Aug 1976.

132. Winterton, R.H.S. Flow boiling: prediction of bubble departure. IJH&MT, V 27, N 8, pp 1422-1424, 1984.

133. Howell, J.R. & Siegel,R. Incipience, growth and detachment of bubbles in saturated water from artificial nucleation sites of known geometry and size. 3 Intl heat transfer conf., V 4, p 12, 1966.

134. Hsu,Y.Y. On the size range of active nucleation cavaties on a heating surface. J of heat transfer, ASME, pp 207-216, Aug. 1962.

135. Srinivas, N.S. & Kumar, R. Prediction of bubble growth rates

and departure volumes in nucleate boiling at isolated sites. IJH&MT, V 27, N 8, pp 1403-1409, 1984.

136. Ibrahim, E.A. & Judd, R.L. An experimental investigation of the effect of subcooling on bubble growth and waiting time in nucleate boiling. J of heat tr., ASME, pp 168-174, Feb. 1985.

137. Vachon, R.I., Tanger, G.E., Davis, D.L. & Nix, G.H. Pool boiling on polished and chemically etched stainless steel surfaces. J of heat transfer, ASME, pp 231-238, May 1968.

138. Glaser, H. Equlibrium radii of small vapour bubbles and liquid droplets. IJH&MT, V 27, N 9, pp 1439-1443, 1984.

139. Marcus, B.D. & Dropkin, D. Measured temperature profiles within the superheated boundary layer above a horizontal surface in saturated nucleate pool boiling of water. J of heat transfer, ASME, pp 333-341, Aug. 1965.

140. Marto, P.J. & Rohsenow, W.M. Nucleate boiling instability of alkali metals. J of heat transfer, ASME, pp 183-195, May 1966.

141. Bhat, A.M., Prakash, R. & Saini, J.S. On the mechanism of macrolayer formation in nucleate pool boiling at high heat flux. IJH&MT, V 26, N 5, pp 735-740, 1983.

142. Bartolini, R., Guglielmini, G & Nannel, E. Exprimental study on nucleate boiling of water in vertical upflow and downflow. IJ Multiphase flow, V 9, N 2, pp 161-165, 1983.

143. Thermohyhraulics of two-phase systems for industrial design and nuclear engineering. Edited by: Delhaye, J.M., Giot, M., Riethmuller, M.L., McGraw-Hill Book Company, 1981.

144. Two-phase flow and heat transfer in the power & process industries. Edited by: Bergles, A.S., Collier, J.G., Delhaye, J.M., Hewitt, G.F. & Mayinger, F., Hemisphere Publishing Corporation, 1981.

145. Two-phase flow and heat transfer. Edited by: Butterworth, D. & Hewitt, G.F., University Press, 1977.

146. Heat transfer in boiling. Edited by: Hahne, E., Grigull, U., Academic Press, Hemisphere Publishing Corporation, 1977.

147. Boiling heat transfer and two-phase flow. By: Tong, L.S., John Wiley & Sons, 1965.

148. Shah, M.M. Generalized prediction of heat transfer during subcooled boiling in annuli. Heat transfer engineering, V 4, N 1, pp 24-31, Jan-Mar. 1983.

149. Shah, M.M. A generalized correlation for heat transfer during subcooled boiling in pipes and annuli. ASHRAE Trans., paper # 2443, V 83, part 1, pp 202-217, 1977.

150. Stephan, K. & Auracher, H. Correlations for nucleate boiling heat transfer in forced convection. IJH&MT, V 24, pp 99-107, 1981.

151. Stephan, K. & Abdelsalam, M. Heat transfer correlations for natural convection boiling. IJH&MT, V 23, pp 73-87, 1980.

152. Rohsenow, W.M. A method of correlating heat transfer data for surface boiling of liquid. ASME Trans, V 74, 939, 1952.

153. Chang, Y.P. An emperical modification of nucleation theory and its application to boiling heat transfer. ANL-6304, 1961.

154. Nishikawa, K. An experiment of nucleate boiling under reduced

pressure- memoirs of faculty of engineering, Kyushu UniversitY, V 19, N 3 63, 1960.

155. Forster, H.K. & Greif, R. Heat transfer to a boiling liquid mechanism and correlation. J of heat transfer, V 81, series C, 43, 1959.

156. Levy, S. Generalized correlation of boiling heat transfer. J of heat transfer, series C, 37, 1959.

157. McNelly, J.J. A correlation of the rate of heat transfer to nucleate boiling liquids. J Imp. College Chem. Engg. Soc., V 7, 18, 1953.

158. Piret, E.L. & Isbin, H.S. Natural circulation evaporation two phase heat transfer. Chem Engg. Progress, 306, June 1954.

159. Gilmour, C.H. Nucleate boiling- a correlation. Chem engg. progress, V 54, N 10, 77, 1958.

160. Mikic, B.B. & Rohsenow, W.M. A new correlation of pool boiling data including the effect of heating surface characteristics. J of heat transfer, pp 245-250, May 1969.

161. Davis, E.J. & David, M.M. Heat transfer to high quality sream-water mixtures flowing in a horizontal rectangular duct. Canadian J of Chem. engg. ,19, June,1961.

162. Dengler, C.E. & Addoms, J.N. Heat transfer mechanism for vaporization of water in a vetrical tube. Chem. Eng. Prog Symp series, V 52, N 18, 95, 1956.

163. Guerrieri, S.A. & Talty, R.D. A study of heat transfer to organic liquids in single-tube, natural circulation, vertical tube

boilers. Chem Eng. Prog. Symp. series, V 52, N 18, 69, 1956.

164. Schrock, V.E & Grossman, L.M. Forced convection boiling studies. Final report on forced convection vaporization project, Lawrence Radiation Lab report # TID-14632.

165. Wright, R.M. Downflow forced convection of boiling in uniformly heated tubes. UCRL-9744, Aug 21, 1961.

166. Somerville, E.F. Downflow boiling of n-butunol in a uniformly heated tube. Lawrence Radiation Lab report # UCRL 10527.

167. Collier, J.G. & Pulling, D.J. Heat transfer to two phase gas liquid systems: part 2- further data on steam-water mixtures in the liquid dispersed region in an annulus. Trans Inst. Chem. Engr. V 42, pp 127-139, 1964.

168. Pujol, L. & Stenning, A.W. Effect of flow direction on the boiling heat transfer coefficient in vertical tubes. Int symp. research in cocurrent gas-liquid flow. Edited by E. Rhodes & D.S. Scott, Plenum press, New York, 1969

169. Sani, R.L. Downward boiling & non-boiling heat trasfer in a uniformly heated tube. Lawrence radiation lab report # UCRL 9023.

170. Chaddock, J.B. & Brunemann, H. Forced convection boiling of refrigerants in horizontal tubes- part 3. Report # HL-113. School of Engg., Duke University, Nort Carolina.

171. Kvamme, A. M.S. Thesis, University of Minnesota, 1959.

172. Groothuis & Hendal, Chem Engg. Science, 11, 222, 1959.

173. Sachs, P. & Long, A.K. A correlation for heat transfer in

stratified two-phase flow with vaporization. IJH&MT, V 2, 222, 1961.

174. Shah, M.M. Generalized prediction of heat transfer during two-component gas-liquid flow in tubes and other channels. A.I.Ch.E. Sym. Series, V 77, N 208, 140, 1981.

175. Chaddock, J. & Noerager, J.A. Evaporation of refrigerant 12 in a horizontal tube with constant wall heat flux. ASHRAE Trans., Jan 1966.

176. Coulsen, J.M. & McNelly, M.J. Heat transfer in a climbing film evaporator-part 2. Trans. Instn. Chem. Engrs., V 34, 247, 1956.

177. Pierre, Bo. The coefficient of heat transfer for boiling R-22 in horizontal tubes. S.F. Review, V 2, N 1, 1955.

178. Altman, M., Norris, R.H. & Staub, F.W. Local & average heat transfer and pressure drop for refrigerants evaporating in horizontal tubes. Trans of ASME, J. of Heat Tr., V 82, 189, Aug., 1960.

179. Ananiev, E.P. & Boyko, L.D., Kruzhilin, G.M. Heat transfer in the presence of steam condensation in a horizontal tube. Intl heat transfer conf., Boulder, Colarodo. Int. developments in heat transfer, Pt. II, paper 34, 290-295, 1961.

180. Lavin, J.G. & Young, H.Y. Heat trasnfer to evaporating refrigerants in two-phase flow. A.I.Ch.E.J., V 11, N 6, 1124, Nov. 1956.

181. Rhee, B.W. & Young, H.Y. Heat transfer to boilng refrigerants flowing inside a plain copper tube. A.I.Ch.E. Symp. series, 64, 1974.

182. Chen, J.C. Correlation for boiling heat transfer to saturated fluids in convective flow. I&EC process design & development, V 5, N

3, 322, July 1966.

183. Bennett, D.L. A study of internal forced convective boiling heat transfer for binary mixtures. Ph.D. Thesis, LeHigh, University, 1975.

184. Bennett, D.L. & Chen., J.C. Forced convective boiling in vertical tubes for saturated pure components and binary mixtures. A.I.Ch.E.J, V 26, N 3, May 1980.

185. Uchida, H. & Yamaguchi, S. Heat transfer in two-phase of refrigerant-12 through horizontal tube. Proceeding of 3 international heat transfer conf., V 5, 69, 1966.

186. Chawla, J.M. Warmeubergangund Druckabfall in Waagrechten Rohren Bei Der Stromung Von Verdamfenden Kaltemitteln. VDI-Forschungsheft 523, 1967.

187. Steiner, D. & Schlunder, E.U. Heat transfer and pressure drop for boiling nitrogen flowing in a horizontal tube. Heat transfer in boiling. edited by Hahne, E & Grigull, U., Hemisphere publishing corp., 263-306, 1977.

188. Shah, M.M. A new correlation for heat transfer during boiling flow through pipes. ASHRAE Trans., V 82, Pt. 2, 66-86, 1976.

189. Kandlikar, S.G. & Thakur, B.K. A new correlation for heat transfer during flow boiling. Proceedings of 16 south eastern seminar on Thermal Science, Miami, Florida, 1982.

190. Purcupile, J.C., Riedle, K., Schmidt, F.K. Experimental investigation: boiling heat transfer in evaporator tubes vertical

flow. AIChE Symp. series, N 138, V 70, pp 91-97, 1978.

191. Elamvaluthi, G., Srinivas, N.S. Two-phase heat transfer in two-component vertical flows. Int J. Multiphase flow, V 10, N 2, pp 237-242, 1984.

192. Mobarak, A., Abdel-Salam, M.S., Morcos, S.M. & El-Sallak, M.S. Boiling flow characteristics in inclined circular tubes under low heat flux. Fundamentals of phase change: Boiling & Condensation, HTD-Vol38, pp 19-25, 1984.

193. Sthapak, B.K., Varma, H.K. & Gupta, C.P. Mass vapour fraction at the onset of dryout in a horizontal tube evaporator. Paper B 1.39, XIV Intl congress of refrigeration, Moscow, 1975.

194. Roko,K., Takitani, K., Yoshizaki,A. & Shiraha, M. Dryout characteristics at low mass velocities in a vertical straight tube of a steam generator. 6 Intl heat transfer conf., Toronto, Canada, Aug 7-11, 1978.

195. Jones, J.H. & Altman, M. Chem. Eng. prog. symp. series, V 61, N 51, 205, 1965.

196. Bassi, L., Clerici, G.C. & Sala, R. A non-equlibrium description of two-phase annular flow - application to the burnout prediction. IJH&MT, V 12, pp 319-331, 1969.

197. Chein, S.F. & Ibele, W. Pressure drop & liquid film thickness of two-phase annular and annular-mist flows. J of Heat transfer, pp 89-96, Feb. 1964.

198. Unal, H.C. & Gasselt, M.L.G. Post dryout heat transfer in steam generator tubes at high pressures. IJH&MT, V 26, N 3, pp 459-

464, 1983.

199. Heinman, J.B. ANL 6213, 1960.

200. Varma, H.K. A model for heat transfer coefficients in dryout region of forced convection evaporation. 6 Intl. heat transfer conf., Toronto, Canada, Aug 7-11, pp 417-422, 1978.

201. Zahn, W.R. A visual study of two-phase flow while evaporating in horizontal tubes. J of heat transfer, pp 417-429, Aug. 1964.

202. Sthapak, B.K., Varma, H.K. & Gupta, C.P. Heat transfer coefficients in dryout region of horizontal tube water heated R-12 evaporator. ASHRAE Trans. V 82, Pt. 2, paper # 2405, 1976.

203. Varma, H.K. & Chaddock, J.B. Wall dryout transition in forced convection evaporation of R-22. XIV Intl. congress of refrigeration, Moscow, paper # B 1.38, 1975.

204. Varma, H.K. & Chaddock, J.B. An experimantal investigation of dryout with R-22 evaporating in a horizontal tube. ASHRAE Trans., V 85, Pt. 2, Paper # 2534, 1979.

205. Robertson, J.M. Dryout in horizontal hairpin waste-heat boiler tubes. AIChE symp. series, Heat Transfer, pp 55-62, V 69, N 131, 1973.

206. Jenson, M.K., Cooper, P.E. & Bergles, A.E. Boiling heat transfer and dryout in restricted annular geometries. AIChE symp. series, Solar & nuclear heat transfer, pp 205-214, 1977.

207. Rao, V.D. & Sarma, P.K. Condensation heat transfer on laminar, falling film. J of Heat transfer, V 106, pp 518-523, Aug. 1984.

208. Lee, W.C., Rahbar, S. & Rose, J.W. Film condensation of refrigerant-113 and ethanediol on a horizontal tube - effect of vapour velocity. J of H Tr., V 106, pp 524-530, Aug. 1984.

209. Rao, D.S. & Murthy, M.S. Heat transfer during dropwise condensation. Chem Engg. J., V 26, pp 1-12, 1983.

210. Soliman, M., Schuster, J.R. & Berenson, P.J. A general heat transfer correlation for annular flow condensation. J of H. Tr., Trans ASME, pp 267-276, May 1968.

211. Altman, M., Staub, F.W., Norris, R.H. Local heat transfer and pressure drop for refrigerant-22 condensing in horizontal tubes. Chem engg. prog. symp. series, Heat transfer - Storrs, N 30, pp 151-159, 1960.

212. Akers, W.W. & Rosson, H.F. Condensation inside a horizontal tube. Chem. engg. prog. symp. series ,Heat transfer - Storrs, pp 145-149, 1960.

213. Akers, W.W., Deans, H.A. & Crosser, O.K. Condensing heat transfer within horizontal tubes. Chem. engg. symp. series, Heat transfer - Chicago, V 55, N 29, pp 171-176.

214. Chato, J.C. Laminar condensation. ASHRAE Journal, pp 52-60, Feb. 1962.

215. Tepe, J.B. & Mueller, A.C. Condensation and subcooling inside an inclined tube. Chem. engg. prog., V 43, N 5, pp 267-278, May 1947.

216. Matsuki, R., Yaamaguchi, H. & Satomura, M. Refrigerant flow condensation in annulus passage. Basic aspect of two-phase flow & heat transfer, HTD-Vol 34, 1984.

217. Honda, H. & Nozu,S. A prediction method for heat transfer during film condensation on horizontal low integral fin tubes. Fundamentals of phase change: Boiling & condensation, HTD-Vol 38, 1984.

218. Wanniarachchi, A.S., Marto, P.J. & Rose, J.W. Filmwise condensation of steam on externally finned horizontal tubes. Fundamentals of phase change: Boiling & condensation, HTD-Vol 38, 1984.

219. Morgan, C.D. An analysis of condensation heat transfer with noncondensable gases present in a vertical tube at high pressure. Heat exchangers for two-phase applications, HTD-Vol 27, 1983.

220. Morgan, C.D. & Rush, G.C. Experimental measurements of condensation heat transfer with noncondensable gases present in a vertical tube at high pressure. Heat exchangers for two-phase applications, HTD-Vol 27, 1983

221. Lee, W.C., Rahbar,S. & Rose, J.W. Forced convection film condensation of refrigerant 113 and ethanediol on a horizontal tube. Heat excahnagers for two-phase applications, HTD-Vol 27, 1983.

222. Sernas, V., Varma, V.C. & Fletcher, L.S. Condensation of steam inside a horizontal tube. Condensation heat transfer, ASME, 1979.

223. Blangetti, F. & Schlunder, E.U. Local heat transfer coefficients in film condensation at high Prandlt number. Condensation heat transfer, ASME, 1979.

224. Fujii, T., Honda, H. & Oda, K. Condensation of steam on a

horizontal tube - the influence of oncoming velocity and thermal conductivity at the tube wall. Condensation heat transfer, ASME, 1979.

225. Tanasawa, I. & Utaka, Y. Measurement of condensation curves for dropwise condensation heat transfer. Condensation heat transfer, ASME, 1979.

226. Tanasawa, I. & Shibata, Y. Dropwise condensation at low heat flux and small surface subcooling. Condensation heat transfer, ASME, 1979.

227. Traviss, D.P., Rohsenow, W.M. & Baron, A.B. Forced convection condensation inside tubes : ..a heat transfer equation for condenser design. ASHRAE Trans., V 79, Pt 1, paper 2274, pp 157-165, 1973.

228. Ali, A.F.M. & McDonald, T.W. Laminar film condensation on horizontal elliptical cylinders - a first approximation for condensation on inclined tubes. ASHRAE Trans., V 83, pt. 2, 1977.

229. Nusselt, W. Die oberflachen kondensation des wasserdamfeg. Zietschrift des vereines deutscher ingenieure, V 60, 541, 1916.

230. Bromley, L.A., Brodkey, R.S. & Fishman, N. Heat transfer in condensation. Ind. & engg. chem, V 44, N 12, 2962, 1952.

231. Rohsenow, W.M. Heat transfer and temperature distribution in laminar film condensation. Trans ASME, 1645, Nov 1956.

232. Meyers, J.A. & Rosson, H.F. Condensing coefficients inside a horizontal tube near atmospheric pressure. Chem engg. prog. symp. series, V 57, N 32, 150, Heat transfer - Buffalo, 1961.

233. Hassan, K. & Jakob, M. Laminar film condensation of pure

saturated vapours on inclined circular cylinders. Trans. of ASME, 887, May 1958.

234. Blasius, H. Mitt Fonsehungsarb, 131, 1 1913.

235. Rouet, A. A note on the Lockhart-Martinelli correlation in the turbulent-turbulent case. IJH&MT, V 26, N 1, pp 145-146, 1982.

236. Taitel, Y. & Dukler, A.E. A theoretical approach to the Lockhart-Martinelli correlation for stratified flow. I J of multiphase flow, V 2, pp 591-595, 1976.

237. Idsinga, W., Todreas, N. & Bowring, R. An assessment of two-phase pressure drop correlations for steam-water systems. I J of multiphase flow, V 3, 401-413, 1977.

238. Stepanek, J.B. & Kasturi, G. Two phase flow - 1. Pressure drop and void fraction measurements in concurrent gas-liquid flow in a coil. Chem. engg. sci., V 27, pp 1871-1880, 1972.

239. Stepanek, J.B. & Kasturi, G. Two phase flow - 2. Parameters for void fraction and pressure drop correlations. Chem. engg. sci., V 27, 1881-1891, 1972.

240. Spedding, P.L., Chen, J.J.J. & Nguyen, V.T. Pressure drop in two-phase gas liquid flow in inclined pipes. I J of multiphase flow, V 8, N 4, pp 407-431, 1982.

241. Chen, J.J.J. & Spedding, P.L. An extension of Lockhart-Martinelli theory of two-phase pressure drop & holdup. I J of multiphase flow, V 7, N 6, pp 659-675, 1981.

242. Laurinat, J.E., Hanratty, T.J. & Dallman, J.C. Pressure drop and film heights measurements for annular gas-liquid flow. I J of

multiphase flow, V 10, N 3, pp 341-356, 1984.

243. Ishihara, K., Palen, J.W. & Taborek, J. Critical review of correlations for predicting two-phase flow pressure drop across tube banks. Heat transfer engg., V 1, N 3, Jan.- Mar. 1980.

244. Johnston, A.J. An investigation into the interficial shear stress contribution in two-phase stratified flow. I J of multiphase flow, V 10, N 3, pp 371-383, 1984.

245. Dukler, A.E., Wicks, M. & Cleveland, R.G. Frictional pressure drop in two-phase flow: A- Comparison of existing correlations for pressure loss and holdup. AIChEJ, V 10, N 1, pp 38-43, 1964.

246. Dukler, A.E., Wicks, M. & Cleveland, R.G. Frictional pressure drop in two-phase flow: B- An approach through similarity analysis. AIChEJ, V 10, N 1, pp 44-51, 1964.

247. Hughmark, G.A. & Pressburg, B.S. Holdup & pressure drop with gas-liquid flow in a vertical pipe. AIChEJ, V 7, N 4, pp 677-682, Dec. 1961.

248. Beattie, D.R.H. & Whalley, P.B. A simple two-phase frictional pressure drop calculation method. I J of multiphase flow, V 8, N 1, pp 83-87, 1982.

249. Lockhart, R.W. & Martinelli, R.C. Proposed correlation of data for isothermal two-phase, two component flow in pipe. Chem. engg. prog., V 45, N 1, pp 39-48, Jan 1949.

250. Martinelli, R.C., Nelson, D.B. & Schenectady, N.Y. Prediction of pressure drop during forced circulation boiling of water. ASME

Trans., pp 695-702, Aug. 1948.

251. Owens, W.L. & Schrock, V.E. Local pressure gradients for subcooled boiling of water in vertical tubes. ASME 60-WA-249, 1960.

252. Anderson, G.H. & Mantzouranis, B.G. Two-phase (gas-liquid) flow phenomena- 1. Chem engg. sci., V 12, pp 109-126, 1960.

253. Thom, J.R.S. Prediction of pressure drop during forced circulation boiling of water. IJH&MT, V 7, pp 709-729, 1964.

254. Levy, S. Prediction of two-phase pressure drop and density distribution from mixing length theory. J of heat transfer, ASME trans., pp 137-152, May 1963.

255. Bergles, A.E. & Dormer, T. Subcooled boiling pressure drop with water at low pressure. IJH&MT, V 12, pp 459-470, 1969.

256. Jordan, D.P. & Leppert, G. Pressure drop & vapour volume with subcooled nucleate boiling. IJH&MT, V 5, pp 751-761, 1962.

257. Levy, S. Steam slip - theoretical prediction from momentum model. J of heat transfer, ASME Trans., pp 113-124, May 1960.

258. Fujie, H. A relation between steam quality and void fraction in two-phase flow. AIChEJ, V 10, N 2, pp 227-232, March 1964.

259. Spedding, P.L. & Chen, J.J.J. Holdup in two-phase flow. I J of multiphase flow, V 10, N 3, pp 307-339, 1984.

260. Tandon, T.N., Varma, H.K. & Gupta, C.P. A void fraction model for annular two-phase flow. IJH&MT, V 28, N 1, pp 191-198, 1985.

261. Madsen, N. A void fraction correlation for vertical & horizontal bulk boiling of water. 5 Intl. heat transfer conf., Toronto, V IV, pp 185-189, 1974.

262. Larsen, P.S. & Tong,L.S. Void fractions in subcooled flow boiling. J of heat transfer, Trans, ASME, pp 471-476, Nov 1969.

263. Staub, F.W. The void fraction in subcooled boiling - prediction of the initial point of net vapour generation. J of heat transfer, Trans. ASME, pp 151-157, Feb. 1968.

264. Levy, S. Forced convection subcooled boiling - prediction of vapour volumetric fraction. IJH&MT, V 10, pp 951-965, 1967.

265. Rouhani, S.Z. Calculation of steam volume fraction in subcooled boiling. J of heat transfer, Trans. ASME, pp 158-163, Feb 1968.

266. Zuber,N. & Findley,J.A. Average volumetric concentration in two-phase flow systems. J of heat transfer, Trans. ASME, pp 453-464, Nov 1965.

267. Beggs, H.D. An experimental study of two-phase flow in inclined pipes. Ph.D. thesis, Univ. of Tulsa, 1972.

268. Bonnecaze,R.H., Erskine,W. & Greskovich,E.J. Holdup & pressure drop for two-phase slug flow in inclined pipes. AIChEJ, V 17, pp 1109-1113, 1969.

269. Armand, A.A. The resistance during the movement of two-phase system in horizontal pipes. Izv. V.T.I., V 1, pp 16-23, AERE Trans., 828, 1946.

270. Bankoff, S.F. J of heat transfer, Trans. ASME, V 82, 265, 1960.

271. Simth, S.L. Proc. Instn. of Mech. Eng., 184, pt 1, 647, 1970.

A P P E N D I X - A

TABLE OF CORRELATIONS

TABLE 2.3 Correlations to predict the flow transitions

Investigators	Correlation
Barnea et al. (76)	For bubble to slug flow transition $U_{ls} = \frac{1-\alpha}{\alpha} U_{gs} - 1.53 (1-\alpha)$ * $\frac{g (\rho_l - \rho_g) \sigma^{1/4}}{\rho_l^2}$ Sin β where $\alpha = 0.25$; U is the superficial velocity.
Mishima & Ishii (77)	For bubble to slug flow transition $J_f = (\frac{3.33}{Co} - 1) J_g - \frac{0.76}{Co} (\frac{\sigma g \Delta\rho}{\rho_f^2})^{1/4}$ where $Co = 1.2 - 0.2 (\rho_g/\rho_l)^{0.5}$
Taitel & Dukler (236)	For bubble to slug flow transition $\frac{J_l}{J_g} = 2.34 - 1.07 \frac{[g (\rho_l - \rho_g) \sigma]^{1/4}}{J_g \rho_l^{1/2}}$ For slug to annular flow transition $\frac{J_g \rho_g^{1/2}}{[g (\rho_l - \rho_g) \sigma]^{1/4}} = 30.9 X^{-1}$ for $X \gg 1$; $X = \left[(dp/dz)_l / (dp/dz)_g\right]^{1/2}$

TABLE 2.3 CONTINUED

Investigators	Correlation
Soliman (87)	For mist to annular flow transition during condensation $Re_l = 72.0 \left(\frac{\mu_l^2}{\rho_l \sigma D}\right)^{-0.38} \left(\frac{\rho_l}{\rho_g}\right)^{-0.073} * \left(\frac{\mu_g}{\mu_l}\right)^{0.141} X_{tt}^{0.9} \phi_g^{0.506}$ for $Re > 1250$ $Re_l = 37.6 \left(\frac{\mu_l^2}{\rho_l \sigma D}\right)^{-0.469} \left(\frac{\rho_l}{\rho_g}\right)^{0.0867} * \left(\frac{\mu_g}{\mu_l}\right)^{0.173} X_{tt}^{1.11} \phi_g^{0.625}$ for $Re \leq 1250$

TABLE 2.4.1 Correlations to predict Nusselt number for the single-phase region

Investigators	Correlation
	A LAMINAR FLOW
Graetz (91)	$Nu_z = \dfrac{\sum_{n=0}^{\infty} Gn \exp(-fn\, z^*)}{2 \sum_{n=0}^{\infty} Gn/fn^2 \exp(-fn^2 z^*)}$
	$Nu_d = 4.36$ for constant heat flux for fully developed flow
	$Nu_d = 3.66$ for constant wall temperature for fully developed flow
Leveque (92)	For uniform wall temperature $Nu_z = 1.3565\ (z^*)^{-1/3}$
	For constant heat flux $Nu_z = 1.6393\ (z^*)^{-1/3}$
	For linearly varying wall temperature $Nu_z = 2.0348\ (z^*)^{-1/3}$
Lipkis (93)	For constant wall temperature $Nu_z = \dfrac{1.3565\ (z^*)^{-1/3}}{1.0 - 4.07\ (z^*)^{2/3}}$ for $z^* \leq 0.001$

Investigators	Correlation
Hausen (104)	$Nu_m = 3.66 + \dfrac{0.0668\,(D/L)\,Re\,Pr}{1+0.04[(D/L)\,Re\,Pr]^{2/3}}$
	B TURBULENT FLOW
Nusselt (97)	$Nu_m = a\,Re^n\,Pr^m$ where $a=0.036$, $n=0.764$, $m=0.355$
Colburn (98)	$Nu_d = 0.023\,Re^{0.8}\,Pr^{0.33}$
Dittus & Boelter (99)	$Nu_d = 0.023\,Re^{0.8}\,Pr^n$ where n= 0.4 for heating n= 0.3 for cooling $0.7 \le Pr \le 160$ $Re \ge 10{,}000$ $L/D \ge 60$
Sieder & Tate (96)	$Nu_d = 0.027\,Re^{0.8}\,Pr^{0.33}\,(\mu/\mu_s)^{0.14}$ $0.7 \le Pr \le 16{,}700$ $Re \ge 10{,}000$ $L/D \ge 60$
McAdams (103)	$Nu = 0.0272\,(1+50\,D/L)\,Re^{0.8}$ for $34 \le L/D \le 100$ for developing flow
Mills (105)	$Nu = 0.0397\,Re^{0.73}\,Pr^{0.33}$ $10^5 < Re < 10^6$ (turbulent flow)

TABLE 2.4.1 CONTINUED

Investigators	Correlation
	$Nu_z = 1.3565\ (z^*)^{-1/3} - 1.7$ for $z^* \leq 4 * 10^{-3}$
Norris & Streid (94)	$Nu_m = 2.035\ (z^*)^{-1/3}$ for $z^* < 0.1$
Kay & London (95)	$(h_m/Gc)\ Pr = 3.66/Re + 0.05\ Pr/(L/D)$ where Gc is the Graetz number = Re Pr D/L
Sieder & Tate (96)	$Nu_m = 1.86\ [Re\ Pr/(L/D)]^{1/3}\ (\mu/\mu_s)^{0.14}$ $0.48 < Pr < 16{,}700$ $0.0044\ (\mu/\mu_s) < 9.75$
Kay (102)	For constant wall temperature $Nu_m = 3.66 + \frac{0.208/z^*}{1 + (0.028/z^*)}$ For constant heat flux $Nu_m = 4.36 + \frac{0.072/z^*}{1 + (0.0022/z^*)}$ both correlations valid for Pr=0.7

TABLE 2.4.2 Correlations to predict the wall superheat to sustain boiling

Investigators	Correlation
Hsu (108), Hsu & Graham (109)	$[q\delta / k_l - (Tsat-Tb)]^2 > \dfrac{8\sigma\, Tsat\, Cl}{h_{fg}\, \rho_v\, k_l}\, q$
Bergles & Rohsenow (110)	$q = 15.6\, p^{1.156}\, (Tw-Tsat)^{2.3/p0.0234}$
Han & Griffith (111)	$(Tw-Tsat)^2 = \dfrac{12\sigma\, Tsat}{h_{fg}\, \rho_v\, k_l}\, q$
Sato & Matsumura (112)	$(Tw-Tsat)^2 = \dfrac{8\sigma\, Tsat}{h_{fg}\, \rho_v\, k_l}\, q$
Davis & Anderson (113)	$(Tw-Tsat)^2 = \dfrac{8\sigma\, Tsat\, Cl}{h_{fg}\, \rho_v\, k_l}\, q$
Murphy & Bergles (114)	$q=(k_l/8\sigma) * [Tw-Tsat(p_l)]^2 \left.\dfrac{dp}{dT}\right]_{pl,sat}$
McAdam et al. (115)	$(Tw-Tb)_q = [\dfrac{0.026\, k_l\, (Tw-Tb)}{Cl\, D}\dfrac{q}{} * (DG/\mu)^{0.8}\, Pr^{1/3}\, (\mu/\mu_w)^{0.14}]^{0.259}$

TABLE 2.4.2 CONTINUED

Investigators	Correlation
Buchberg et al. (116)	$q = 0.0027 \frac{G^{0.8}\, Tb^{0.32}}{D^{0.2}} (646-Tb)$ $q = 0.00083 \frac{G^{0.8}\, Tb^{0.53}}{D^{0.2}} (487-Tb)$ The first equation is valid for pressures upto 140 ata. and the second upto 35 ata.
Chen (117)	$P_s = \frac{\sigma(P'-P_v')}{\sigma'} - \frac{G_o}{r_d^3} * [T + \frac{\sigma}{\sigma'} T']$ where ' represents the deactivation conditions, G_o is the dimensional variable measuring the amount of gas (lbf.in/R) , r_d is the deactivation radius (inches)

TABLE 2.4.3 Correlations to predict nucleate boiling heat transfer coefficients

Investigators	Correlation
Shah (148, 149)	A graphic correlation for subcooled nucleate boiling. See ref. 122, 123.
Stephan & Auracher (150)	For refrigerants in forced convection $\frac{h_b D}{K_l} = 207 \left(\frac{q D}{K_l T_s}\right)^{0.745} \left(\frac{\rho_g}{\rho_l}\right)^{0.581} * \left(\frac{\mu}{K_l}\right)^{0.55}$ for $0.003 \leq p/p_{cr} \leq 0.78$ see ref. 124 for correlations for water, hydrocarbon, cryogenics fluids.
Stephan & Abdelsalam (151)	For refrigerants in natural convection boiling. $h = C_4 \, q^{0.745}$ C_4 is calculated from a plot in ref. 124. See ref. for correlations for water, hydrocarbons and cryogenics fluids.
Rohsenow (152)	$\frac{C_{p_l} \Delta T}{h_{fg}} = Csf \left[\frac{q}{\mu_l h_{fg}} \sqrt{\frac{g_c \sigma}{g(\rho_l - \rho_v)}}\right]^r Pr_l^{1.7}$
Chang (153)	For feeble boiling $q = 0.145 \frac{K_l}{D} \left(1 + \frac{\varepsilon}{\alpha_l}\right)^{2/3} \Delta T * (Gr \cdot Pr)^{2/3}$

TABLE 2.4.3 CONTINUED

Investigators	Correlation
Nishikawa (154)	$\frac{h\,D}{K_l} = 8.0 \left[F_s^{0.5} \left(\frac{P}{P_{atm}}\right) \left(\frac{C_{pl}\,\rho_l^2}{C_5^2\,P\,K_l\,h_{fg}\,\rho_v}\right)^{0.5} * D^{1.5}\,q \right]^{2/3}$ where F_s is the foamability factor; $F_s = 1$ for smooth pipes; $= 3.6$ for rough pipes; C_5 is a constant & is equal to 900 m^{-1}.
Forster & Grief (155)	$q = 4.3 * 10^{-5} \left(\frac{\alpha_l\,C_{pl}\,\rho_l\,T_s}{\sigma^{0.5}\,(h_{fg}\,\rho_v)^{1.5}}\right) * (C_{pl}\,T_s\,\alpha_l^{1/2})^{0.25} \left(\frac{\rho_l}{\mu_l}\right)^{5/8} Pr^{0.33}\,\Delta P^2$
Levy (156)	$q = \frac{K_l\,C_{pl}\,\rho_l^2}{\sigma\,T_s\,(\rho_l - \rho_v)} \left(\frac{1}{B_l}\right) (T_w - T_s)^3$ where B_l is a dimensionless parameter, a function of $\rho_v\,h_{fg}$.
McNelly (157)	$\frac{h\,D}{K_l} = 0.225 \left(\frac{D\,q}{h_{fg}\,\mu_l}\right)^{0.67} \left(\frac{P\,D}{\sigma}\right)^{0.31} * \left(\frac{\rho_l}{\rho_v} - 1\right)^{0.33} \left(\frac{C_{pl}\,\mu_l}{K_l}\right)^{0.69}$

TABLE 2.4.3 CONTINUED

Investigators	Correlation
Piret & Isbin (158)	$\frac{h\,D}{K_l} = 0.0086 \left(\frac{D\,V_m\,\rho_l}{\mu_l}\right)^{0.8} Pr_l^{0.6} \left(\frac{\sigma_w}{\sigma}\right)^{0.33}$
Gilmour (159)	$\left(\frac{h}{Cp_l\,G}\right) Pr_l^{0.6} \left(\frac{\rho_l\,\sigma}{P^2}\right)^{0.425} = \text{Const} * \left(\frac{D\,G}{\mu}\right)^{-0.3}$ where $G = \frac{V_v\,\rho_l}{A\,.\,\rho_v}$ Const term depends on the characteristics of the heating surface.
Mikic & Rohsenow (160)	$q = C_1 \frac{C_2\,C_3^{1/2}\,r_s^m}{\pi\,2^{m-1}} \left(K_l\,Cp_l\,\rho_l\right)^{1/2} * \left(\frac{h_{fg}\,\rho_v}{T_{sat}\,\sigma}\right)^m \left[\frac{\sigma\,g_o\,g\,(\rho_l - \rho_v)}{\rho_l^2}\right]^{1/8} * Ja^{15/8}\,\Delta T^{m+1}$ where r is the radius of an active cavity Ja is the Jacob number. For C_1 , C_2 , C_3 & m see ref 134.
Lavin & Young (180)	$\frac{h_b\,D}{K_l} = 0.225 \left(\frac{q\,D}{h_{fg}}\right)^{0.69} Pr_l^{0.69} *$

TABLE 2.4.3 CONTINUED

Investigators	Correlation
	$\left(\frac{\rho_l}{\rho_v} - 1\right)^{0.31} \left(\frac{P\ D}{\sigma}\right)^{0.31}$
Rhee & Young (181)	$Nu = 0.023\ Re_l^{0.8}\ Pr_l^{0.4} + 0.3\ Re_{th}^{0.69} * \left(\frac{\rho_l}{\rho_v} - 1\right)^{0.31} \left(\frac{P\ D}{\sigma}\right)^{0.31}$

TABLE 2.4.5A Correlations to predict two-phase heat transfer coefficients

Values of the coefficients a and b found by various workers

$$(h_{tp}/h_{lo}) \text{ or } (h_{tp}/h_l) = a\ (1/X_{tt})^b$$

Authors	a	b	h_l base	Working fluid	Maximum exit x(%)
Dengler & Addoms (162)	3.5	0.5	h_{lo}	Water	70
Guerrierri & Talty (163)	3.4	0.45	h_l	varius organics	12
Schrock & Grossman (164)	2.5	0.75	h_{lo}	Water	59
Wright(165)	2.721	0.581	h_l	Water	19
Somerville (166)	7.55	0.328	h_l	n-Butanol	31
Collier & Pulling (167)	2.167	0.699	h_l	Water	66
Pujol & Stenning (168)	4.0	0.37	h_{lo}	Fr-113	70

TABLE 2.4.5B Correlations to predict two-phase heat transfer coefficients

Values of constants C_1, C_2, n_1 and n_2 found by various workers

$$(h_{tp}/h_l) = C1[\ Bo + C2\ (1/X_{tt})^{n1}\ ]^{n2}$$

Authors	C_1	C_2	n_1	n_2	h_l base	Fluid/ Max.exit x(%)
Schrock & Grossman (164)	7.39	1.5	0.67	1	h_{lo}	Water/59
Sani(169)	14.8	1.5	0.67	1	h_l	Water/14
Wright (165)	6.7	3.5	0.67	1	h_l	Water/19
Somer-ville (166)	24.5	1.5	0.67	1	h_l	n-Butanol/31
Chaddock & Brunemann (170)	19.1	1.5	0.67	0.6	h_{lo}	varius cholorinated paraffins/75
Pujol & Stenning (168)	9.0	4.45	0.37	1	h_{lo}	Fr-113/70
Pujol & Stenning (168)	5.3	7.55	0.37	1	h_{lo}	Fr-113/70

TABLE 2.4.5C Correlations to predict two-phase heat transfer coefficients

Investigators	Correlation
Kvamme (171)	$h_{tp} = 1.5 \left[\frac{(1 - x)}{R_l} \right]^{0.8}$ R_l is the Martinelli holdup
Groothuis & Hendal (172)	$h_{tp} = 0.029 \left(\frac{K_l}{D}\right) \left(\frac{D\, G_t}{\mu_{tp}}\right)^{0.87} Pr_l^{0.33} \left(\frac{\mu_b}{\mu_w}\right)^{0.14}$
Sachs & Long (173)	Working fluid R-11 $h_{tp} = 0.023 \left(\frac{K_l}{D}\right) Re_{tp}^{0.8} Pr_l^{0.33}$ where $Re_{tp} = (V_v D_v \rho_l / \mu_l)$
Shah (174)	$h_{tp} = h_l \left(1 + \frac{V_g}{V_l} \right)^{0.25}$ V_g & V_l are superficial vapour & liquid velocities.
Chaddock & Noeranger (175)	Working fluid R-12 $h_{tp} = 1.85 \left[10^4 Bo + 1.5 (1/X_{tt}) \right]^{2/3} h_l$ (modified correlation of Schrock & Grossman) $h_{tp} = 3.0\ h_l\ (1/X_{tt})^{0.667}$ (modified correlation of Dengler & Addoms)

TABLE 2.4.5C CONTINUED

Investigators	Correlation
Coulson & McNelly (176)	$h_{tp} = \left(1.3 + \frac{D}{A} \right) \left(\frac{K_l}{D}\right) \left[Pr_l^{0.9} \cdot Re_l^{0.23} * Re_v^{0.34} \left(\frac{\rho_l}{\rho_v}\right)^{0.23} \left(\frac{\mu_v}{\mu_l}\right) \right]$ A is a constant & is equal to 12 m^{-1}.
Bo Pierre (177)	$h_{tp} = 0.0009 \left(\frac{K_l}{D}\right) \left(\frac{D\,G}{\mu_l}\right) A^{0.5}$ valid for x> 90 % $h_{tp} = 0.0082 \left(\frac{K_l}{D}\right) \left(\frac{D\,G}{\mu_l}\right)^{0.8} A^{0.4}$ can be used for superheats upto 6 C at the exit of the evaporator. $A = \frac{h_{fg}\, J\, \Delta x}{L}$ both equations valid for $10^9 < Re_l^2 A < 7*10^{11}$.
Altman (178)	Working fluid R-22 $h_{tp} = h_l \left[0.0225 \left(\frac{K_l}{D}\right) \left(Re_l^2\, A \right)^{0.375} \right]$

TABLE 2.4.5C CONTINUED

Investigators	Correlation
Ananiev (179)	$h_{tp} = h_l \left(\frac{\rho_l}{\rho_{av}}\right)^{0.5}$ $\rho_{av} = \frac{1.0}{\frac{x}{\rho_g} + \frac{(1-x)}{\rho_l}}$ The average coefficient for complete evaporation is approximately given by; $\bar{h}_{tp} = (h_l/2)\left[1 + \left(\frac{\rho_l}{\rho_g}\right)^{0.5}\right]$
Lavin & Young (180)	Working fluid R-12 & R-22 $h_{tp} = A\, h_l\, Bo^{0.1} \left[\frac{1+x}{1-x}\right]^{1.16}$ where A = 3.79 for vertical tubes & A = 6.59 for horizontal tubes
Rhee & Young (181)	Working fluid R-12 & R-22 For annular-mist flow regime $h_{tp} = 59.03\ h_l \left[\frac{1+x}{1-x}\right]^{0.81} \cdot Fl^{-0.30}$

TABLE 2.4.5C CONTINUED

Investigators	Correlation
	For stratified flow regime $h_{tp} = 313.76\ h_l \left[\frac{1+x}{1-x}\right]^{-0.542} Fl^{-0.448}$ For annular (no mist) flow regime $h_{tp} = 140.80\ h_l \left[\frac{1+x}{1-x}\right]^{0.565} Fl^{0.41}$ where $Fl = 1/Bo$
Chen (182)	$h_{tp} = h_{mac} + h_{mic}$ where $h_{mac} = h_l\ F\ (1/X_{tt})$, & $h_{mic} = \frac{0.00122\ K_l^{0.79}\ Cp_l^{0.45}\ \rho_l^{0.47}\ g_c^{0.25}}{\sigma^{0.5}\ \mu_l^{0.29}\ h_{fg}^{0.24}\ \rho_v^{0.24}} * \Delta T_s^{0.24}\ \Delta P_s^{0.75}\ S\ Re_{tp}$ S is the boiling suppression factor
Bennett (183)	Presented a relation for S for Chen's correlation $S = \Phi_{ltt}^{0.89} \left[\frac{Pr_l + 1}{2}\right]^{0.44}$ $\Phi_{ltt} = 1 + 20/X_{tt} + 1/X_{tt}^2$

TABLE 2.4.5C CONTINUED

Investigators	Correlation
Bennett & Chen (184)	Working fluids: distilled water & ethylene glycol $h_{tp} = h_{mac} + h_{mic}$ $h_{mac} = 0.023\ Re_l^{0.8}\ Pr_l^{0.4}\ \frac{K_l}{D}\ \left[\frac{(dp/dz)_{tp}}{(dp/dz)_l}\right]^{0.44} * F(Pr_l)\ (\frac{\Delta T}{\Delta T_s})_{mac}$ where h_{mic} is same as in Chen's correlation $(\frac{\Delta T}{\Delta T_s})_{mac} = 1.0$ for pure components $F(Pr_l) = Pr_l^{0.296}$ for pure components
Uchida & Yamaguchi (185)	Working fluid R-12 $h_{tp} = 17.5\ Bo^{0.2}\ (1/X_{tt})^{1.67}$
Chawla (186)	Working fluid R-11 $h_{tp} = (\frac{K_l}{D})\ C_1\ (\ Re_l\ Fr_l\ )^{C_2}\ (\frac{x}{1-x})\ * (\frac{\rho_l}{\rho_g})^{0.8}\ Re_l^{0.35}\ Pr_l^{0.45}$ see reference 160 for C_1 & C_2.

TABLE 2.4.5C CONTINUED

Investigators	Correlation
Steiner & Schlunder (187)	Working fluid nitrogen $Nu_{tp} = 1.05 * 10^{-2} K_1^a K_2^b K_3^c K_4^d K_5^e K_6^f F_{wet}$ where K_1 - K_6 are dimensionless group & a,b,c d,e,f & F_{wet} are constants. See reference 161 for these values.
Shah (188)	Working fluids: water, refrigerant cyclohexane Graphic correlation presented in paper.
Kandlikar & Thakur (189)	Working fluids: water, refrigerant cyclohexane $h_{tp} = B1 \ CO^{B2} \ (25 \ Fr_l)^{B5} \ h_l + B3 \ Bo^{B4} \ Fr_l^{B6} \ h_l$ where $CO = \left(\frac{1 - x}{x}\right)^{0.8} \left(\frac{\rho_g}{\rho_l}\right)^{0.5}$ B1 - B6 are constants. See reference 163.
Purcupile et al. (190)	Working fluids: R-11, R-12 & R-113 $T_w - T_s = 22.8 \left(\frac{\rho_l}{\rho_v}\right)^{-0.25} q^{0.3} D^{0.6}$
Elamvaluthi & Srinivas (191)	$h_{tp} = 0.5 \left(\frac{K_l}{D}\right) Re_m^{0.7} Pr^{0.33} \left(\frac{\mu_g}{\mu_l}\right)^{0.25} * \left(\frac{\mu_b}{\mu_w}\right)^{0.14}$

TABLE 2.4.5C CONTINUED

Investigators	Correlation
	where Re_m is the Reynolds number of mixed flow $Re_m = \frac{D V_l \rho_l}{\mu_l} + \frac{D V_g \rho_g}{\mu_g}$
Mobarak et al. (192)	For $x < 0.1$ $Nu_{tp} = 0.8 \left(\frac{Re_{tp}}{Re_l^{0.75}}\right)^{1.15}$ For $x > 0.1$ $Nu_{tp} = 2.75 \left(\frac{Re_{tp}}{Re_l^{0.75}}\right)^{0.75}$ where $Re_{tp} = G D / \mu_{tp}$ & $\frac{1}{\mu_{tp}} = \frac{x}{\mu_v} + \frac{1 - x}{\mu_l}$
Davis & David (161)	Working fluid; water & steam For separated annular flow model $h_{tp} = 0.06 \left(\frac{K_l}{D}\right) \left(\frac{D G_t}{\mu_l}\right)^{0.87} Pr_l^{0.4} \left(\frac{\rho_l}{\rho_g}\right)^{0.28}$ For homogenous flow model $h_{tp} = 0.0333 \left(\frac{K_l}{D}\right) \left(\frac{D G_t}{\mu_{tp}}\right)^{0.87} Pr_l^{0.4}$

TABLE 2.4.6 Correlations to predict the critical quality

Investigators	Correlation
Sthapak et al. (193)	Working fluid: R-12 $x_{cr} = 7.943 \left[Re_g \, (2.03 * 10^4 \, Re_g^{-0.81} \quad \Delta T - 1) \right]^{-0.161}$ $\Delta T = T_{wall} - T_{sat}$
Lavin & Young (180)	Working fluids: R-12, R-22 $We = 3.07 * 10^{-8} \, Re_g \, (1/Bo)^{0.06} \, (\frac{\rho_l}{\rho_v})$
Rhee & Young (181)	Working fluids: R-12, R-22 $We = 1.89 * 10^{-7} \, Re_g \, (\frac{\rho_l}{\rho_v})^{0.6} \, (\frac{D}{0.0608})^{-0.48}$ D is in ft.
Roko et al. (194)	Working fluid: steam & water $\frac{1 - x_{cr}}{x_{cr}} = \left[12.01 \, (\frac{p}{p_{cr}})^2 - 5.628 \, (\frac{p}{p_{cr}}) + 0.8623 \right] \, (\frac{G}{1000})$
Jones & Altman (195)	$x_{cr} = 1.04 - 1.14 * 10^{-5} \left[(\frac{D \, G}{\mu_l}) * \frac{J \, \Delta x \, h_{fg}}{L} \right]^{3/8}$

TABLE 2.4.6 CONTINUED

Investigators	Correlation
Biasi et al. (196)	$\frac{dG_{lf}}{dx} = -G + 2.3 \frac{\rho_g^{1.5} \tau_c^{0.5} S_{mc} h_{fg}}{\rho_l \phi x} * (G_{lfeq} - G_{lf})$ By integrating this equation, the dryout point can be determined as a point in which the liquid film flowrate reduces to zero. lf = liquid in the film c = film core interface mc = mean in the core
Chien & Ibele (197)	$\left(\frac{4 \dot{m}_g}{D_g}\right) \left(\frac{4 \dot{m}_l}{D_l}\right)^{0.301} = 1.199 * 10^6$

TABLE 2.4.7 Correlations to predict the heat transfer coefficients in the liquid deficient region

Investigators	Correlation
Unal & Gasselt (198)	$Nu = 0.0091\ a1\ a2\ a3\ a4\ a5\ a6\ a7\ a8$ where a1 - a8 are constants. see ref. 172
Lavin & Young (180)	$h = 0.0162 \left(\frac{K_g}{D}\right) Re_g^{0.84} Pr_g^{0.33} (1 - x)^{0.1}$
Rhee & Young (181)	Working fluid: R-12, R-22 $Nu = 0.023\ Re_g^{0.8}\ Pr_g^{0.4}\ x^{-1.23}$ (for R-12) $Nu = 0.038\ Re_g^{0.8}\ Pr_g^{0.4}\ x^{-1.23}$ (for R-22)
Heinman (199)	$Nu = 0.0157\ Re_l^{0.84}\ Pr_l^{0.33}\ \left(\frac{L}{D}\right)^{-0.04}$ for $6 < L/D < 60$ $Nu = 0.0133\ Re_l^{0.84}\ Pr_l^{0.33}$ for $L/D > 60$
Varma (200)	$\frac{h}{h_g} = f(\eta, \dot{m})$ where $\eta = \frac{x - x_{cr}}{1 - x_{cr}}$; $\dot{m}$ is the mass velocity

TABLE 2.5 Correlations to predict the condensation coefficients

Investigators	Correlation
Soliman et al. (210)	For annular flow condensation $\frac{h_z \mu_l}{K_l \rho_l^{0.5}} = 0.036 \ Pr_l^{0.65} \ Fo^{0.5}$ Fo is the wall shear stress
Altman et al. (211)	For horizontal tubes $\frac{h_z \mu_l}{K_l \rho_l^{0.5}} = 0.057 \ Pr_l^{0.5} \ F^{0.5}$ F is the shear stress in laminar condensate sublayer
Akers & Rosson (212)	$Nu = 13.8 \ Pr_l^{0.33} \ \left(\frac{h_{fg}}{Cp_l \ \Delta T}\right)^{1/6} \ Re_g^{0.2}$ for $1000 < Re_g < 20,000$ $Nu = 0.1 \ Pr_l^{0.33} \ \left(\frac{h_{fg}}{Cp_l \ \Delta T}\right)^{1/6} \ Re_g^{0.67}$ for $20,000 < Re_g < 100,000$
Akers et al. (213)	$Nu = 0.0265 \ Pr_l^{0.33} \ \left(\frac{D \ G_t}{\mu_l}\right)^{0.8}$ for $Re > 5 * 10^4$

TABLE 2.5 CONTINUED

Investigators	Correlation
	$Nu = 5.03\ Pr_l^{0.33} \left(\frac{D\ G_t}{l}\right)^{1/3}$ for $Re < 5 * 10^5$
Chato (214)	For horizontal tubes $h_m = 0.357\ C_5 \left[\frac{K_l^3 \rho_l\ (\rho_l - \rho_v)\ h_{fg}\ g\ X}{\mu_l\ D\ \Delta T}\right]^{0.25}$ where $X = 1 + 0.68\ (Cp_l\ \Delta T/h_{fg})$ C_5 is a constant & is a function of angle. see reference for C_5 (in graphical form).
Matsuki et al. (216)	For horizontal annulus $Nu_m = 1.69 * 10^{-3}\ Pr_l^{0.33}\ Re_{eq}^{1.25}$ where $Re_{eq} = (Re_g + Re_l)/2$
Honda & Nozu (217)	See reference for details.
Meyers & Rosson (232)	$Nu = C_4\ Re^{-0.14} \left(\frac{D^3 \rho_l^2\ g}{\mu_l^2}\right)^{1/3}$ where $C_4 = 1.3$ for methanol. For other fluids see the paper.

TABLE 2.5 CONTINUED

Investigators	Correlation
Traviss et al. (227)	$Nu_z = F_2^{-1}\ 0.15\ Cp_l\ \mu_g^{0.1}\ K_l\ x^{0.9}\ \left(\frac{\rho_l}{\rho_g}\right)^{0.5} * \frac{G^{0.9}}{D^{1.1}}\ A$
	where $A = 1 + 2.85\left[\left(\frac{\mu_l}{\mu_g}\right)^{0.1}\left(\frac{1-x}{x}\right)^{0.9} * \left(\frac{\rho_g}{\rho_l}\right)^{0.523}\right]$
	$F_2 = 0.707\ Pr_l\ Re_l^{0.5}$ for $Re_l < 50$
	$F_2 = 5\ Pr_l + 5 \ln\left[1 + Pr_l\ (0.09636\ Re_l^{0.585} - 1)\right]$ for $50 < Re_l < 1125$
Ali & McDonald (228)	$\bar{h}_c = B_1 \left[\frac{K_l^3 \rho_l^2 h_{fg}\ g}{\mu_l\ D\ (T_s - T_w)}\right]^{1/4}$
	for $0^\circ < \beta < 40^\circ$; $B_1 = 0.727$
	for $40^\circ < \beta < 90^\circ$; $B_1 = 0.727\left[\cos\left(\frac{\beta - 40}{50}\right) 90\right]^{0.25}$
Nusselt (229)	For horizontal tube $h_m = 0.725\ \left(\frac{K_l^3 \rho_l^2 h_{fg}\ g}{\mu_l\ D\ \Delta T}\right)^{1/4}$

TABLE 2.5 CONTINUED

Investigators	Correlation
	For vertical plates (also valid for vertical tubes for small film thickness) $h_m = 0.943 \left[\frac{\rho_l (\rho_l - \rho_v) K_l^3 h_{fg} g}{L \mu_l \Delta T}\right]^{1/4}$
	For inclined surfaces (also valid for vertical tubes for small film thickness) $h_m = 0.943 \left[\frac{\rho_l (\rho_l - \rho_v) K_l^3 h_{fg} g \sin\beta}{L \mu_l \Delta T}\right]^{1/4}$ where β is the inclination angle.
Bromley et al. (230)	For horizontal tubes $h_m = 0.728 \left[\frac{K_l^3 \rho_l (\rho_l - \rho_v) h_{fg} g \left(1 + 4 \frac{Cp_l \Delta T}{hfg}\right)^2}{D \mu_l \Delta T}\right]^{0.25}$
	For vertical tubes $h_m = 0.943 \left[\frac{K_l^3 \rho_l (\rho_l - \rho_v) h_{fg} g \left(1 + 4 \frac{Cp_l \Delta T}{hfg}\right)^2}{D \mu_l \Delta T}\right]^{0.25}$

TABLE 2.5 CONTINUED

Investigators	Correlation
Rohsenow (231)	$h_m = 0.943 \left[\frac{K_l^3 \rho_l (\rho_l - \rho_v) h'_{fg} X}{L \mu_l \Delta T \left(1 - \frac{Cp \Delta T}{10 h_{fg}} \right)^4} \right]^{1/4}$
	where $X = 1 - \frac{Cp_l \Delta T}{h'_{fg}} - 0.0328 \left[\frac{\Delta T}{h'_{fg}} \right]^2$
	$h'_{fg} = h_{fg} + 3/8 \; Cp_l \Delta T$
	$h_m = 0.943 \left[\frac{K_l^3 \rho_l (\rho_l - \rho_v) h_{fg} g \left(1 + 0.68 \frac{Cp_l \Delta T}{hfg}\right)}{L \mu_l \Delta T} \right]^{1/}$
	for $0 < (Cp_l \Delta T / h_{fg}) < 1.0$
Hassan & Jakob (233)	For inclined cylinders
	$h_m = 0.727 \left[\frac{\rho_l^2 h_{fg} K_l^3 \cos\beta}{\mu_l D \Delta T} \right] 1/4$
Rao & Murthy (209)	For dropwise condensation
	See reference for details

TABLE 2.6.2 Correlations to predict the pressure drop and void fraction for two-phase region

Investigators	Correlation
Lockhart & Martinelli (249)	For two-phase frictional pressure drop $\phi^2 = \frac{(dp/dz)_{tp}}{(dp/dz)_l}$
	For turbulent - turbulent flow condition $X_{tt} = \left(\frac{1-x}{x}\right)^{0.9} \left(\frac{\rho_v}{\rho_l}\right)^{0.5} \left(\frac{\mu_l}{\mu_v}\right)^{0.1}$
	$\phi_{tt} = \left(1 + X_{tt}^{-0.49} \right)^{2.05}$
	For turbulent - laminar flow condition $X_{tl} = 0.054\ Re_l^{0.4} \left(\frac{1-x}{x}\right) \left(\frac{\rho_v}{\rho_l}\right) \left(\frac{\mu_l}{\rho_v}\right)^{0.5}$
	$\phi_{tl} = \left(1 + X_{tl}^{-0.56} \right)^{1.80}$
	For laminar - laminar flow condition $X_{ll} = \left(\frac{1-x}{x}\right) \left(\frac{\rho_v}{\rho_l}\right) \left(\frac{\mu_l}{\mu_v}\right)^{0.5}$
	$\phi_{ll} = \left(1 + X_{ll}^{-0.70} \right)^{1.43}$
	For laminar - turbulent flow condition $X_{lt} = 18.65\ Re_v^{-0.4} \left(\frac{1-x}{x}\right) \left(\frac{\rho_v}{\rho_l}\right) \left(\frac{\mu_l}{\mu_v}\right)^{0.5}$
	$\phi_{lt} = \left(1 + X_{lt}^{-0.56} \right)^{1.80}$

TABLE 2.6.2 CONTINUED

Investigators	Correlation
	$\alpha = (1 + X^{0.8})^{-0.378}$
Levy (254)	For two-phase frictional pressure drop $\left(\frac{dp}{dz}\right)_{tp} = \left(\frac{dp}{dz}\right)_l \left[\frac{1}{(1-\alpha)^2}\right]$
Larsen & Tong (262)	For two-phase frictional pressure drop $f_{tp} = 16.5 \left[\frac{V D \rho_l}{(1-\alpha)\mu_l}\right]^{-0.6}$
Owens & Schrock (251)	For two-phase frictional pressure drop $\Delta P_{tp} = f \left(\frac{L}{D}\right) \left(\frac{V_{tp}^2}{2 g_c}\right) \rho_{tp}$ where $V_{tp} = G_t v_{tp}$ $v_{tp} = v_l + x (v_v - v_l)$
Bonnecaze et al. (268)	For total pressure drop in slug flow $\left(\frac{dp}{dz}\right) = \left(\frac{R_l - R_{lf}}{1 - R_{lf}}\right) \left[g \rho_l \sin\beta + \left(\frac{2 \rho_l f_{sf} V_t^2}{D}\right) \right]$ where $f_{sf} = 0.0048 + 3980/Re^{1.285}$

TABLE 2.6.2 CONTINUED

Investigators	Correlation
	$R_{lf} = (1/\pi)\left[\cos^{-1}(1-n_s) - (1-n_s)\sqrt{(n_s(2-n_s))}\right]$ n_s = ratio of liquid depth to pipe radius R_l = liquid holdup
Beggs (267)	For two-phase frictional pressure drop $f_{tp} = \left(\frac{2D}{G_t V_t}\right)\left[\frac{dp}{dz}\left(1 - \frac{\rho_{tp} V_t V_{sg}}{P}\right) - (\rho_{tp} g \sin\beta)\right]$
Beattie & Whalley (248)	For two-phase frictional pressure drop $\left(\frac{dp}{dz}\right)_{tp} = f\left(\frac{2G^2}{\rho_{av} D}\right)$ Reynolds number is based on ρ_{tp}.
Rouet (235)	For turbulent - turbulent flow condition (for Lockhart - Martinelli correlation) $\alpha = 1 - (m/2) X_{tt}^{2/(2-b)} - \left[(1+(m/2) X_{tt}^{2/(2-b)})^2 - 1\right]^{0.5}$ where $m = 0.054$ $\alpha = 1 - (1/\Phi_{tt})$; $\Phi_{tt}^2 = 1 + 2/X_{tt} + 1/X_{tt}^2$

TABLE 2.6.2 CONTINUED

Investigators	Correlation
Spedding & Chen (259)	For vertical upward flow

$$\frac{\bar{R}_g}{\bar{R}_l} = \frac{1}{(0.2 + K1\ Q_l/Q_g)}$$

for $\bar{R}_g/\bar{R}_l \leq 4.0$

$$\frac{\bar{R}_g}{\bar{R}_l} = K2\left[1 - \exp(-K3\ Q_g/Q_l)\right]\ (Q_g/Q_l)^{0.65}$$

for $\bar{R}_g/\bar{R}_l > 4.0$ - 275

For horizontal flow

$$\frac{\bar{R}_g}{\bar{R}_l} = 0.45\ (Q_g/Q_l)^{0.65}$$

where Q_g and Q_l are the flow rates of liquid and gas respectively.

$$\ln K1 = -1.44 \ln V_{sl} - 0.007$$

$$K2 = 0.14 \ln V_{sl} + 1.0$$

$$\ln K3 = 0.97 \ln V_{sl} - 3.0$$

TABLE 2.6.2 CONTINUED

Investigators	Correlation
Smith (271)	$\alpha = \dfrac{1}{1 + \dfrac{1-x}{x}\dfrac{\rho_g}{\rho_l}\left[K - (1-K)\left\{\dfrac{\dfrac{\rho_l}{\rho_g} + \dfrac{1-x}{x}}{1 + \dfrac{1-x}{x}}\right\}^{1/2}\right]}$ where K is a function of ρ_l/ρ_g
Hashizume (79)	$\alpha = \dfrac{\rho_l - \dfrac{\rho_{sh}(V1 + V2 + Vo) - \rho_l V2}{V1}}{\rho_l - \rho_g}$ where ρ_{sh} is the density of refrigerant in superheated gas phase under ambient condition. V1, V2 & Vo are the volumes of different test sections for Hashizume's apparatus.
Fujie (258)	$x = \dfrac{\alpha}{m(1-\alpha)}\left[1 + \dfrac{\alpha^{1/4}}{1 - \sqrt{\alpha}}\sqrt{K1}\right]$ where $m = \rho_l/\rho_g$; $K1 = \dfrac{f}{2}\dfrac{\rho_l}{D}\dfrac{A}{C1}$ A & D are the cross sectional area and diameter of the tube & C1 is a constant.

TABLE 2.6.2 CONTINUED

Investigators	Correlation
Armand (269)	For bubble & slug flow $\frac{\bar{R}_g}{\bar{R}_l} = \frac{1}{0.2 + 1.2\,(Q_l/Q_g)}$
Madsen (261)	$\alpha = \frac{1}{1 + (\frac{\rho_l}{\rho_g})^{0.5} \left(\frac{1-x}{x}\right)^m}$ where $m = \frac{0.5 \log(\rho_l/\rho_g) - \log[\alpha_o/(1-\alpha_o)]}{\log(\rho_l/\rho_g) - \log[\alpha_o/(1-\alpha_o)]}$ where α_o is the value of void fraction at $V_l = V_g$
Bankoff (270)	$\alpha = \frac{B}{1 + \frac{1-x}{x}\frac{\rho_v}{\rho_l}}$ where $B = 0.71 + 0.001\,p$
Thom (253)	$\alpha = \frac{1}{1 + \frac{1-x}{x}\frac{1}{A}}$ where A is a function of ρ_l/ρ_g.

TABLE 2.6.2 CONTINUED

Investigators	Correlation
Chen & Spedding (241)	For horizontal annular flow $\bar{R}_g = \frac{1}{1 + X^{1.5}}$ $\bar{R}_l = \frac{X^{1.5}}{1 + X^{1.5}}$ For two-phase frictional pressure drop $(\frac{dp}{dz})_{tp} = Re_{sg}^{1.8} f (\phi_g^2 - 1) + (\frac{dp}{dz})_{sg}$
Tandon et al. (260)	For annular two-phase flow $\alpha = \left[1 - 1.928\ Re_l^{-0.315}\ F(X_{tt})^{-1} + 0.9293\ Re_l^{-0.63}\ F(X_{tt})^{-2}\right]$ for $50 < Re_l < 1125$ $\alpha = \left[1 - 0.38\ Re_l^{-0.088}\ F(X_{tt})^{-1} + 0.0361\ Re_l^{-0.176}\ F(X_{tt})^{-2}\right]$ for $Re_l > 1125$

APPENDIX B

Experimental data of Yin & Abdelmessih (reference 127) for increasing and decreasing heat fluxes.

q (W/m^2)	$\left[\frac{(T_w - T_{sat})^2}{\left(\frac{2\sigma T_{sat}}{K_l h_{fg} \rho_v}\right)}\right]$ (W/m^2)	
	Increasing	Decreasing
1000	46870	2500
3000	128250	7500
5000	194112	12500
7000	245580	17500
9000	283793	22500
11000	309888	27500
13000	325000	32500
15000	330266	37500
17000	326822	42500
19000	315804	47500
21000	298349	52500
23000	275591	57500
25000	248669	62500
27000	218715	67500
29000	186870	72500

APPENDIX C

EQUATIONS USED IN THE SIMULATION PROGRAM OF ALI (4)

Heat Transfer Coefficient Calculations

Single-phase forced Convection (point value) (1).

For laminar flow

$$h_a = 1.24 \frac{kF_1}{D} (Re\ Pr\ D/Z)^{1/3} \left(\frac{\mu}{\mu_w}\right)^{0.14} \quad (A1)$$

For turbulent flow

$$h_a = 0.027 \frac{kF_2}{D} Re^{0.8}\ Pr^n \left(\frac{\mu}{\mu_w}\right)^{0.14}$$

where

n = 0.4 for heating, n = 0.3 for cooling (A2)

Two-phase forced convection (point value)

$$Re_f = \frac{V_g D_g \rho_m}{\mu_L} \quad (A3)$$

where

V_g is the actual vapor velocity, D_g is the diameter of the vapor core, μ_L is the viscosity of liquid, and

$$\rho_m = \alpha\ \rho_g + (1-\alpha)\rho_L \quad (A4)$$

For laminar flow

$$h_f = 1.24 \frac{k_L}{D} (Re_f\ Pr_L \frac{D}{Z})^{1/3} \quad (A5)$$

For turbulent flow

$$h_f = 0.023 \frac{k_L}{D} Re_f^{0.8}\ Pr_L^{0.4} \quad (A5)$$

Entrance effect factors (3,4).

$$F_1 = 1 + 5 \exp\left(\frac{-Z}{100}\right) \quad (A7)$$

$$F_2 = 1 + 7 \frac{D}{Z} \quad (A8)$$

$$F_3 = 0.344\ Re^{-0.078153} \left(\frac{D}{Z}\right)^{1.93/Re^{0.3}} \quad (A9)$$

$$F_4 = 1 + 3.5 \exp\left(\frac{-Z}{100}\right) \quad (A10)$$

Boiling (5).

$$q = \mu_L\ \lambda \left[\frac{g(\rho_L-\rho_g)}{\sigma}\right]^{1/2} \left[\frac{C_L(T_w-T_s)}{\lambda(CSF)\ Pr^{1.7}}\right]^r \quad (A11)$$

where

CSF and r are dependent on the fluid and surface properties

$$h_b = q/\ (T_w-T_s) \quad (A12)$$

Combined boiling and two-phase convection.

$$h_{fb} = (h_f^2 + h_b^2)^{1/2} \tag{A13}$$

Combined boiling and two-phase forced convection with dryout (6).

Criterion for transition to dryout:

$$x > xc \tag{A14}$$

where

$$xc = \left[\frac{We\ \sigma\rho_g}{G_L\mu_L\ (\frac{Re_\ell}{1-\alpha})^{0.125}}\right]^{0.5} \tag{A15}$$

and

$$We = 3.07 \times 10^{-8}\ Re_g\ (\frac{G_L\ \lambda}{q})^{0.06}\ (\frac{\rho_L}{\rho_g}) \tag{A16}$$

$$h_{bfd} = C_1 h_d + C_2 h_{fb} \tag{A17}$$

where

$$C_2 = (\frac{1-x}{1-xc})^a \tag{A18}$$

and

$$C_1 = 1-C_2 \tag{A19}$$

and $h_d = h_a$ for complete dryout at $T = T_s$

Subcooled boiling (7).

If $T \leq T_s$ and if $q > q_{IB}$, then

$$h_{fb} = (h_f^p + h_b^p)^{1/p} \tag{A20}$$

where

$$p = 2 - (T_s-T_x)/(T_s-T_x)_{IB} \tag{A21}$$

and for turbulent flow,

$$q_{IB} = \frac{k_L\ \lambda}{8\sigma T_s(v_g-v_L)}\left[\frac{D^{0.2}\nu_L^{0.8}q}{0.023\ Pr_L^{0.4}k_L v_L^{0.8}} - (T_s-T)\right]^2 \tag{A22}$$

for laminar flow,

$$q_{IB} = \frac{k_L\ \lambda}{8\sigma T_s(v_g-v_L)}\left[\frac{(D\nu_L Z)^{1/3}\ q}{1.86\ v_L^{0.33}\ Pr_L^{0.33}\ k_L} - (T_s-T)\right]^2 \tag{A23}$$

Condensation (8,9).

For an inclined tube

$$h_c = B\ (\frac{k_L^3\ \rho_L^2\ \lambda}{\mu_L\ D\ (T_s-T_w)})^{1/4} \tag{A24}$$

where

B is a function of tube diameter and angle.

For a vertical tube

$$h_c = \frac{k_L}{\delta} \tag{A25}$$

where

$$\delta = \left\{\frac{3\mu_L \Gamma}{\rho_L^2}\right\}^{1/3} \tag{A26}$$

Pressure Drop Calculations

Friction factor (10).

For laminar flow

$$f = 64/Re \tag{A27}$$

For turbulent flow

$$f = .316\ Re^{-.25} \tag{A28}$$

Frictional pressure drop.

For single-phase flow

$$\Delta P_a = f \frac{Z}{D} \frac{\rho V^2}{2} \tag{A29}$$

For two-phase flow (11)

$$\Delta P_f = \Delta P_{lp}\ \phi^2 \tag{A30}$$

For liquid-phase laminar and vapor-phase laminar

$$\phi = [1 + \chi^{-.70}]^{1.43} \tag{A31}$$

where

$$\chi = \left\{\frac{1-x}{x}\right\} \left\{\frac{\rho_g}{\rho_L}\right\} \left\{\frac{\mu_L}{\mu_g}\right\}^{0.5} \tag{A32}$$

For liquid-phase laminar and vapor-phase turbulent

$$\phi = [1 + \chi^{-.56}]^{1.80} \tag{A33}$$

where

$$\chi = 348\ Re_g^{-0.4} \left[\left\{\frac{1-x}{x}\right\} \left\{\frac{\rho_g}{\rho_L}\right\} \left\{\frac{\mu_L}{\mu_g}\right\}\right]^{-0.5} \tag{A34}$$

For liquid phase turbulent and vapor phase laminar

$$\phi = [1 + \chi^{-.56}]^{1.80} \tag{A35}$$

where

$$\chi = .054\ Re_L^{0.4} \left[\left\{\frac{1-x}{x}\right\} \left\{\frac{\rho_g}{\rho_L}\right\} \left\{\frac{\mu_L}{\mu_g}\right\}\right]^{0.5} \tag{A36}$$

For liquid phase turbulent and vapor phase turbulent

$$\phi = [1 + \chi^{-.49}]^{2.05} \tag{A37}$$

where

$$X = \left\{\frac{\mu_L}{\mu_G}\right\}^{0.1} \left\{\frac{\rho_g}{\rho_L}\right\} \left\{\frac{1-x}{x}\right\}^{0.9} \quad \text{(A38)}$$

Acceleration pressure drop (11).

For separated flow

$$\Delta P = \frac{G_L^2 \Delta x}{\rho_g \alpha} \{2x + \Delta x\} - \frac{G_L^2 \Delta x}{\rho_L \{1-\alpha\}} \{2-2x-\Delta x\} \quad \text{(A39)}$$

For homogeneous flow

$$\Delta P = \frac{G_t^2}{\rho_L} (1-x) + x\left(\frac{\rho_L}{\rho_g}\right) - 1 \quad \text{(A40)}$$

Hydrostatic pressure drop

$$\Delta P = \rho g Z \quad \text{(A41)}$$

Liquid Fraction Calculation

$$R = (1 + X^{-.42})^{-2.38} \quad \text{(A42)}$$

NOMENCLATURE

c - Specific heat, J/kgK

CSF- Surface-liquid combination constant in Rohsenhow's boiling equation

D - Tube diameter, m

F_1 - Entrance effect factor for laminar flow in the evaporator as defined in Eq. 7

F_2 - Entrance factor for turbulent flow in the evaporator as defined in Eq. 8

F_3 - Entrance effect factor for turbulent flow in the condenser as defined in Eq. 9

F_4 - Entrance effect factor for laminar flow in the condenser as defined in Eq. 10

f - Fanning friction factor

G - Mass flow rate at a point per unit of flow cross-sectional area, kg/m^2s

g - Acceleration due to gravity, m/s^2

h - Heat transfer coefficient, W/m^2K

k - Thermal conductivity, W/mK

P - Pressure, N/M^2

p - exponent used to combine boiling heat transfer coefficient with single-phase convection as defined in Eq. (20)

Pr - Prandtl number

q - Heat flux, W/m^2

R - Liquid fraction

r - Exponent used in Rohsenow's boiling equation (function of surface-liquid combination)

Re - Reynolds number

Reg - Superficial vapor Reynolds number defined as GxD/μ_g

Reℓ - Superficial liquid Reynolds number defined as $G(1-x)D/\mu_L$

T - Temperature (with no subscript, bulk fluid temperature (K))

V - Velocity, M/s

v - Specific volume, M^3/kg

We - Weber number

x - Quality

xc - Quality at which partial dryout starts to occur

Z - Distance along the evaporator or condenser from its entrance, m

---

λ - Latent heat of vaporization, J/kg

μ - Dynamic viscosity, kg/m-s

σ - Surface tension, N/m

α - Void fraction

ρ - Fluid density, kg/m^3

δ - Liquid film thickness, m

Γ - Condensate mass flow rate per unit perimeter, kg/s-m

ν - Kinematic viscosity, m^2/s

χ - Lockhart-Martinelli parameter defined in Eq. (A32)

Subscript

a - Single-phase liquid

b - Nucleate pool boiling

c - Condensation

d - Single-phase vapor

f - Two-phase flow

g - Saturated vapor state

IB - Incipient boiling

L - Liquid

s - Saturation

t - Total

w - Wall

APPENDIX D

LIST OF PHYSICAL PROPERTIES AND CONSTANTS USED IN THE PROGRAM

In order to calculate the performance characteristics of a thermosiphon loop, the computer program requires subroutines to estimate the following physical properties of the working fluid:

1. Saturation pressure as a function of temperature
2. Saturation temperature as a function of pressure
3. Enthalpy of saturated liquid as a function of temperature
4. Density of liquid as a function of temperature
5. Latent heat of vaporization as a function of temperature
6. Surface tension for the liquid-vapor interface
7. Viscosity of liquid as a function of temperature
8. Thermal conductivity of liquid as a function of temperature
9. Specific heat of liquid as a function of temperature
10. Viscosity of vapor as a function of temperature
11. Specific heat of vapor as a function of temperature

The constants supplied to the program are dependent on the surface-liquid combination. They are

1. CSF: A constant used in Rohsenow's boiling equation (Eq. A11).
2. r: An exponent used in Rohsenow's boiling equation (Eq. A11).

The accuracy with which these subroutines calculate the required properties should be compatible with the tolerances which are specified by the user in the main program.

Also see appendix H2.

APPENDIX E

EQUATIONS FOR ESTIMATING HEAT TRANSFER COEFFICIENT IN ANNULI

To estimate the convective heat transfer coefficient in annulus, the correlations by Sieder-Tate and Monrad & Pelton (also used by Ali - see reference 2) for laminar and turbulent flow respectively were utilized.

For laminar flow:

$$Nu_m = 1.86\ (Re\ Pr\ D/z)^{1/3} \qquad \text{---} \quad (C1)$$

For turbulent flow:

$$Nu_m = 0.02\ Pe^{0.8}\ Pr^{0.33}\ (D_o\ /\ D_i)^{0.53} \qquad \text{---} \quad (C2)$$

In both cases Nu_m and Re were based on the equivalent diameter. However, it was also necessary to enhance the heat transfer coefficient in the entrance region. It was observed that if equations C1 and C2 were multiplied by the following entrance effect factors, satisfactory estimation of the heat transfer data in this region was possible.

For laminar flow:

$$M = 1 + 3.5\ \exp\ (\ -z/90D\ ) \qquad \text{---} \quad (C3)$$

For turbulent flow:

$$M = 1 + 3.0\ \exp\ (\ -z/30D\ ) \qquad \text{---} \quad (C4)$$

APPENDIX F

ESTIMATION OF AIR SIDE RESISTANCE

The airside resistance was calculated by using data from McQuay coil catalog. (McQuay Inc., Minneapolis, Minnesota)

A plot of effectiveness versus the face velocity for 3/8 " O.D. copper tubes is shown in figure F1, which was taken from the McQuay coil catalog. For a specified number of fins/inch (12) and number of row deep (1), the effectiveness for the whole heat exchanger can be found for a given coil face velocity.

The data from this graph and other similar ones for $\frac{1}{4}$ " and $\frac{1}{2}$ " O.D. copper tube were correlated by the following equation:

$$E_{he} = B0 + B1\ V + B2\ V^2 + B3\ V^3 \qquad \text{--- (1)}$$

where V is the velocity of air in ft/sec and the values of B0, B1, B2, B3 are shown in the Table F1.

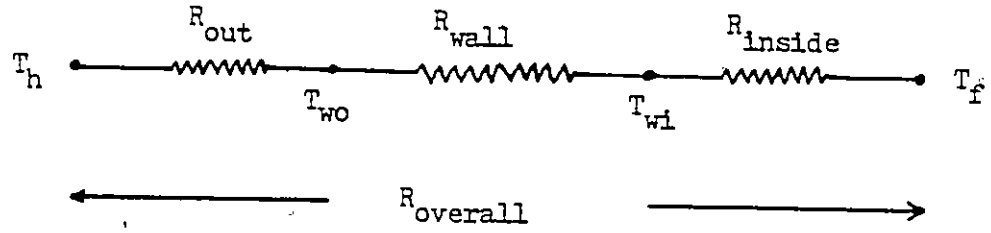

Using an electrical analogy for the heat transfer resistance through the tube, as shown, the overall resistance, $R_{overall}$, can be calculated from

$$R_{overall} = R_{out} + R_{wall} + R_{inside}$$

The outside resistance , R_{out}, can be determined from the above equation if the other three resistances are known. The wall and the inside resistances can be determined easily by standard relations of heat transfer. R_{out} can be determined if the magnitude of $R_{overall}$ is known. The overall resistance, $R_{overall}$, was evaluated as follows.

Effectiveness is related to the number of transfer units by the following relation;

$$E_{he} = 1 - \exp (-NTU)$$

$$= 1 - \exp \left[-(U\ A)_{he}/(m\ Cp)_{he}\right]$$

$$= 1 - \exp \left[-(U\ dA)_e/(dm\ Cp)_e\right]$$

$$\exp\ (-U\ dA/dm\ Cp)_e = 1 - E_{he}$$

$$\exp\ (U\ dA/dm\ Cp)_e = 1/(1 - E_{he})$$

$$(U\ dA/dm\ Cp)_e = \ln \left[1/(1 - E_{he})\right]$$

$$(U\ dA)_e = (dm\ Cp)_e\ \ln \left[1/(1 - E_{he})\right] \quad \text{---} \quad (2)$$

where subscript he and e stands for the heat exchanger and element respectively.

$$R_{overall} = 1/(U\ dA)_e$$

$$R_{wall} = \ln (D_o/D_i) \left[1/(2\ \pi\ dL\ K_m)\right]$$

$$R_{inside} = 1/(h_{cond}\ D_i\ dL)$$

$$R_{out} = R_{overall} - (R_{wall} + R_{inside}) \quad \text{---} \quad (3)$$

R_{inside} was calculated by using the properties of R-22, since the graph shown (Figure F1) is for condensation of R-22.

Equation 3 was used for the calculation of the air side resistance.

TABLE F1

The following data was used in the evaluation of airside resistance.

Description	DIAMETER (NOMINAL SIZE)		
	1/2"	3/8"	1/4"
Pattern	1.25 * 1.082 Staggered	1.0 * 0.866 Staggered	1.0 * 0.866 Staggered
I.D.	0.436 "	0.311 "	0.190 "
Thickness	0.032 "	0.032 "	0.030 "
Coefficients for equation (=D1) (appendix F)			
B0	0.619453164	0.59718992	0.673042579
B1	-0.082210817	-0.08137122	-0.096060295
B2	$5.8274575/10^3$	$5.8313175/10^3$	$6.52356854/10^3$
B3	$-1.5016166/10^4$	$-1.5054689/10^4$	$-1.56466564/10^4$

DRY SURFACE CONDENSER COIL RATINGS - R22
3/8 TUBE STANDARD COILS - 3CX
10, 12, 14 & 15 FPI

TUBES: 3/8 O.D. Copper
PATTERN: 1 x .866 Staggered

FINS: Rippled & Corrugated
10, 12, 14 & 15 FPI-.006 Alum.

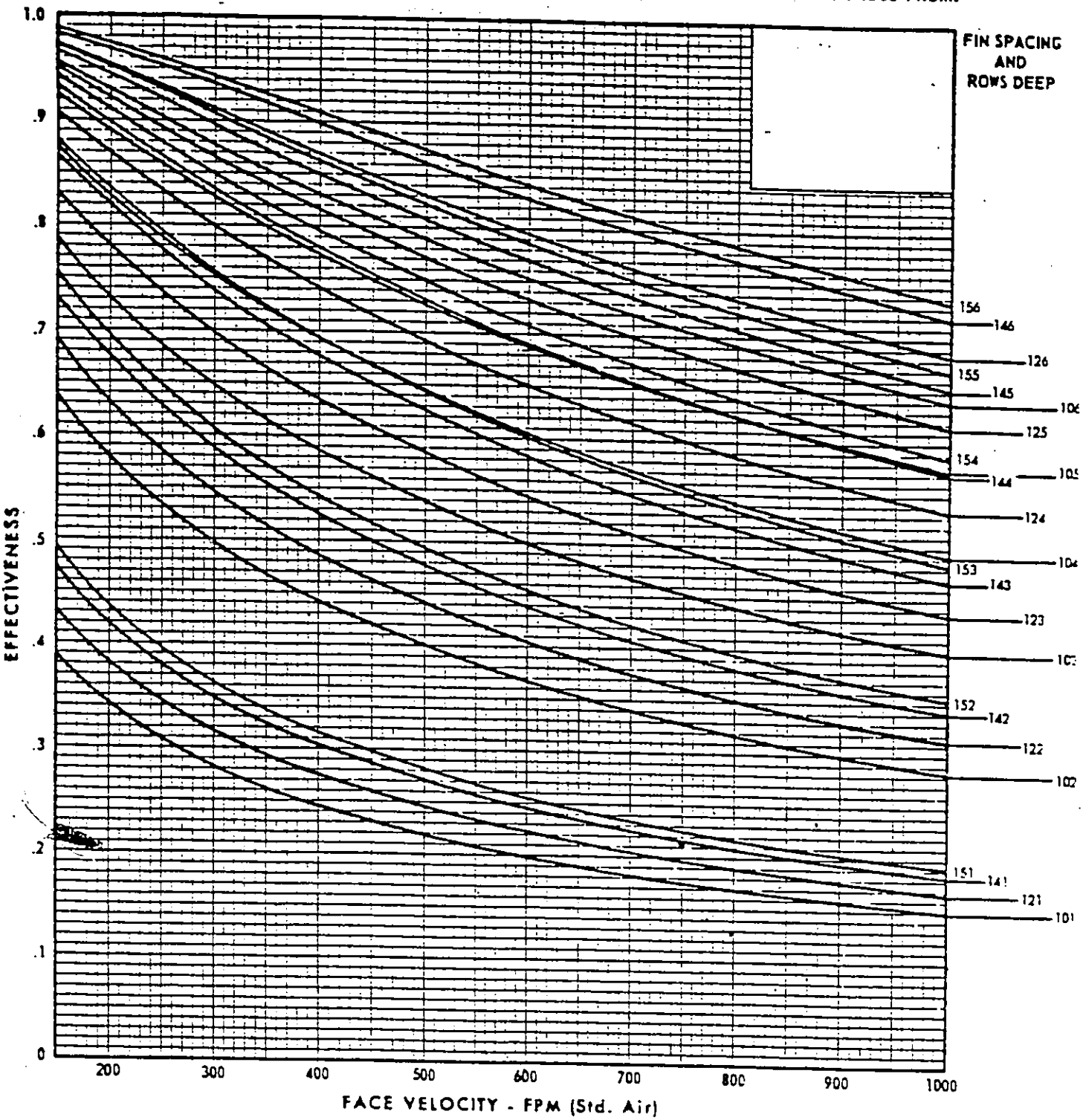

FIGURE F1

APPENDIX G

The friction factors for fully developed laminar and turbulent flow are given by the following relations.

Laminar flow $f = 64/ Re$ --- (1)

Turbulent flow $f = 0.316/ Re^{1/4}$ --- (2)

The continuity equation is given by

$$\dot{m} = \rho A V \quad \text{--- (3)}$$

The pressure drop over a distance L, associated with fully developed flow is given by

$$\Delta P = \frac{f L V^2 \rho}{2 g D} \quad \text{--- (4)}$$

The Reynold's number is given by

$$Re = (\rho V D/\mu) \quad \text{--- (5)}$$

DERIVATION FOR THE LAMINAR FLOW:

Substituting f from equation 1 in equation 4

$$\Delta P = \frac{64}{Re} \cdot \frac{L V^2 \rho}{2 g D}$$

$$= \frac{64}{\left(\frac{\rho V D}{\mu}\right)} \cdot \frac{L V^2 \rho}{2 g D}$$

$$= 64 \frac{L V \mu}{2 g D^2}$$

Substituting for V from equation 3

$$\Delta p = 64 \left[\frac{L \dot{m} \mu}{2 g A D^2 \rho} \right]$$

$$\text{or} \quad \dot{m} = \left[\frac{2 g A D^2 \rho}{64 L \mu} \right] \Delta p$$

for a given state and size of a tube

$$\left[\frac{2 g A D^2 \rho}{64 L \mu} \right] = \text{Constant}$$

Therefore;

$$\dot{m} = \text{Constant} [\Delta p] \qquad \text{--- (A)}$$

DERIVATION FOR THE TURBULENT FLOW:

By following the same method as discussed for laminar flow

$$\left[\frac{2 g A D^{5/4} \rho^{1/4}}{0.316 L \mu^{1/4}} \right] = \text{Constant}$$

Therefore;

$$\dot{m} = \text{Constant} [\Delta p]^{4/7} \qquad \text{--- (B)}$$

Combining equations A and B

$$\dot{m} = \text{Constant} [\Delta p]^{n} \qquad \text{--- (C)}$$

where $n = 1$ for laminar flow

$n = 0.571$ for turbulent flow

Using equation C

For evaporator first tube row

$$\dot{m}_1 = \text{Constant } \Delta p_1^{\,n} \qquad \text{--- (D)}$$

For evaporator second tube row

$$\dot{m}_2 = \text{Constant } \Delta p_2^{\,n} \qquad \text{--- (E)}$$

From equations D & E

$$\dot{m}_2 = \dot{m}_1 \left[\frac{\Delta p_2}{\Delta p_1}\right]^n \qquad \text{--- (F)}$$

Equation F was used in the program to calculate the mass flow rate in the evaporator second and the successive tube rows.

A P P E N D I X H

DETAILS OF THE COMPUTER PROGRAM

APPENDIX H1

PROGRAM NOMENCLATURE

A(1) - Vapour flow rate for the evaporator (lb/hr)

A(2) - Recirculation rate for the evaporator (lb/hr)

A - Power used in the calculation of effective heat transfer coefficient in the dryout region

ACNDEL - Inside surface area of condenser tube element in the flooded region (sq. ft)

AHTCND - Inside surface area of non flooded portion of each condenser tube (sq. ft)

AGAM - GAM (degrees)

ALFMIN - Minimum angle of inclination of the condenser tubes from the vertical (deg) used in the calculation of CF

ALPA - ALPHA (degrees)

ALPHA - Angle of inclination of the plane of the condenser tubes from the vertical (read in degrees then converted to radians) see figure H2

AREAC - Inside surface area of a condenser tube (sq. ft)

AREAH - Inside surface area of an evaporator tube element (sq. ft)

AREAP - Inner surface area of an evaporator tube (sq.ft)

AVEVT(I) - Average evaporator wall temperature for Ith row (F)

AVTC(K) - Average condenser wall temperature for Kth row (F)

AVFLTH - Average film thickness in the condenser (ft)

AVLIQF - Average liquid fraction for the entire loop

AVTSC - The local average value of the condenser tube inner and outer surface temperatures (F)

AVTSCS - Average value of AVTSC for the entire condenser (F)

AVTSH - The local average value of the evaporator tube inner and outer surface temperatures (F)

AVTSHS - Average value of AVTSH for the entire evaporator tube (F)

AVVOID - Average void fraction for the entire loop

AVWATH - Average water side heat transfer coefficient in the annulus (Btu/hr/sq.ft/F)

BETA - Angle of inclination of vapour header from the horizontal (radian) See figure H2

BEX - Exponent in Rohsenow's boiling equation, a function of the fluid-surface combination

BITA - BETA (degrees)

B1 - Total vapour flow rate for an evaporator tube row (lb/hr)

B2 - Total recirculation rate for an evaporator tube row (lb/hr)

BL - Flag used to correct the wall temperature in boiling heat transfer coefficient calculations

---

CF - Factor used in the condensation heat transfer coefficient, a function of the angle of the condenser tube

CG - Entrance effect factor for the heat transfer coefficient in the turbulent developing flow

CONDQ(K) - Rate of heat transfer for entire Kth row for the condenser (Btu/hr)

CPAIR - Specific heat of air (Btu/lb/F)

CSE - A constant in Rohsenow's boiling equation, a function of fluid-surface combination

---

DELP - Pressure drop in a differential element in the condenser (lbf/sq.ft)

DELT - Difference between the average evaporator and condenser tube temperatures (F)

DENSG - Density of vapour (lb/ft3)

DENSM - Mean density of the two-phase mixture (lb/ft3)

DENSW - Water density (lb/ft3)

DEQVC - Equivalent diameter of condenser (inch)

DEQVE - Equivalent diameter of evaporator (inch)

DIST - Distance of the midpoint of a differential element from the entrance of the evaporator (ft)

DIVCON - Number of divisions for the condenser, one for the vapour region, the balance for the liquid region

DIVN - Total number of divisions into which the evaporator is divided for the sequential calculations

DENEVP - Density of air in the evaporator (lb/ft3)

DISCND - Air flow rate approaching the condenser (cu-ft/hr)

DISEVP - Air-flow rate approaching the evaporator (cu-ft/hr)

DOWNST - Summation of all the source fluid temperatures downstream of each tube element (F)

DLNGTH - Differential length along the evaporator (ft)

DNSLO - Density of liquid in condensate return line (lb/ft3)

DPA - Acceleration pressure drop along an element (lbf/sq.ft)

DPAC - Acceleration pressure drop from the tube entrance to the end of the tube element (lbf/sq-ft)

DPCOND - Hydrostatic head corresponding to the pressure difference between the condenser top and the evap. bottom (ft)

DPDL - Pressure gradient along a tube (lbf/ft3)

DPF - Frictional pressure drop along an element (lbf/sq.ft)

DPFG - Frictional pressure drop along an element based on the vapour flow (lbf/sq.ft)

DPH - Hydrostatic pressure drop along an element (lbf/sq.ft)

DQ - Heat flow rate into a differential element of the evaporator (Btu/hr)

DT - Local difference between bulk fluid temp. and condenser tube inner surface temperature (F)

DTA - Local difference between the saturation temperature and the evaporator tube inner surface temperature (F)

DYNPER - True dynamic charge in the evaporator tube (%)(the ratio of vol of liquid to the total vol of the tube)

DUCTXS - Cross sectional area of the evaporator duct (sq.ft)

DX - Change in vapour quality along a differential element of length for the evaporator tube

---

EFLOP(I) - Effectiveness for I number of loops

ELEV - Elevation of bottom of condenser tubes relative to the bottom of the evaporator tube (ft). See figure H2

EVAPST - Average evaporator wall temperature for the present row (F)

EX - Exponent used in correlating void fraction with Xtt, in evaporator and vapour header

EXTIDC - Exterior diameter of condenser annulus (inch)

EXTIDE - Exterior diameter of evaporator annulus (inch)

F - Friction factor

FBL - Distance along the evaporator tube beyond the point where transition to mist flow has occurred (ft)

FC - Entrance effect factor for laminar flow in the annulus

FCT - Entrance effect factor for turbulent flow in the annulus

FLCOUN - If =1, the program uses the read in value for FLRATE; for = 0, the program generates an estimate for FLRATE

FL(K) - Vapour flow rate for Kth row for the condenser (lb/hr)

FLAG2 - Counter for number of iterations where the evaporator tube flow rate has been reduced in order that ZRECRC < ZMAX

FLDCND - The length of the condenser which is flooded (ft)

FLDEV(I) - Length of evaporator recirculation tube flooded for Ith row (ft)

FLPR - Evaporator tube flow rate in previous iteration (lb/hr)

FLRATE - Flow rate inside the loop (lb/hr)

FM - Entrance effect factor for the heat transfer coefficient in a laminar developing flow

FOULNF - Fouling factor - tube inside surface (hr-sq.ft-F/Btu)

FOULNW - Fouling factor - tube outside surface (hr-sq.ft-F/Btu)

FRCPO - Head loss per unit length along the flooded portion of the condenser tube

FRECRC - Total mass flow rate in the evaporator and condenser recirculation tubes (lb/hr)

FTEF - Friction factor

GAM - Rotation of the plane of the condenser tubes from the horizontal (read in degrees then converted to radians) See figure H2

GC - Gravitational constant

GF - Mass flux (lb/sq.ft/sec)

HDIAMC - Diameter of vapour header on the condenser (inch)

HDIAME - Diameter of vapour header on the evaporator (inch)

HCON(K) - Condensation coefficient for the Kth row (Btu/hr/sq.ft/F)

HEDVLC - Volume of the vapour header on condenser (ft3)

HEDVLE - Volume of the vapour header on evaporator (ft3)

HIC - Convective heat transfer coefficient for the working fluid in the condenser (Btu/hr/sq.ft/F)

H1PC - Single-phase liquid heat transfer coefficient for the working fluid (Btu/hr/sq.ft/F)

H2P1 - Two-phase heat transfer coeff. (Btu/hr/sq.ft/F)

H2P2 - Single-phase vapour heat transfer coeff. (Btu/hr/sq.ft/F)

HEITB - Length of evaporator tubes (ft)

HEITC - Length of condenser tubes (ft)

HF - Enthalpy of saturated liquid at any point around the loop (Btu/lb)

HFBOT - Initial enthalpy of liquid at the bottom of the evaporator (Btu/lb)

HFBOTN - The new value of HFBOT calculated by the program (Btu/lb)

HFG - Latent heat of vaporization (Btu/lb)

HFLOLD - Previous enthalpy of the saturated liquid (Btu/lb)

HFOLD - Previous enthalpy of the fluid (Btu/lb)

HFTOP - Enthalpy at the top of the condenser (Btu/lb)

HG - Enthalpy of the saturated vapour at the top of the condenser (Btu/lb)

HIL - Single-phase liquid heat transfer coefficient for the

working fluid in the evaporator (Btu/hr/sq.ft/F)

HITP - Effective heat transfer coefficient for the inside surface of an element in the evaporator (Btu/hr/sq.ft/F)

HITP2 - Effective heat transfer coefficient for the inside surface of an element in the condenser (Btu/hr/sq.ft/F)

HITPB - Boiling heat transfer coefficient (Btu/hr/sq.ft/F)

HTCFNT - Condensation coefficient (Btu/hr/sq.ft/F)

HTFLUX - Heat flux (Btu/hr/sq.ft)

HW - Water side heat transfer coefficient in evaporator annulus (Btu/hr.sq.ft/F)

HW2 - Water side heat transfer coefficient in condenser annulus (Btu/hr/sq.ft/F)

ICNDSB - Number of elements in the submerged portion of the condenser

ICNHOT - If all source fluid temperatures are identical = 1, otherwise = 0

IDC - Inside diameter of the condenser tube (inch)

IDH - Inside diameter of the evaporator tube (inch)

IDLC - Inside diameter of the liquid return line (inch)

IDUC - Inside diameter of vapour header (inch)

IHYSTR - A counter set = 0 for increasing temperature differences, set = 1 for decreasing overall temperature differences

IPCOND - Ith element in the submerged portion of condenser for which printout is required

IPRI - A flag which if set = 0, suppresses the printing of the transition points in the evaporator

IPRINT - A flag which if set = 0, suppresses the printing of data for

the vapour header/liquid return line

KF - Thermal conductivity of fluid (liquid or vapour) (Btu/hr/ft/F)

KG - Thermal conductivity of vapour (Btu/hr/ft/F)

KL - Thermal conductivity of liquid (Btu/hr/ft/F)

K(I) - Total recirculation rate for evaporator Ith row (lb/hr)

KW - Thermal conductivity for water (Btu/hr/fr/F)

L - Counter which detects the initiation of subcooled boiling

LCNDSN - Non flooded length of condenser (ft)

LEM - Inclination of the condensate return tube from the horizontal (radians) See figure H2

LENGTH - Distance to the downstream end of an element in the evaporator or condenser (ft)

LFB - A flag which is set equal to 1 when transition to mist flow occurs in the evaporator (otherwise = 0)

LH - Length of liquid column in the condensate return tube (ft)

LHDEVP - Length of evaporator header (ft)

LHDCND - Length of condenser header (ft)

LLOXO - Length of the condensate return line (ft)

LN - New LENGTH calculated in subroutines BULKPT or SBCOOL which locates where bulk or subcooled boiling starts

LO - Length to the upstream end of an element (ft)

LUPXO - Length of the vapour header (ft)

LQFR(I) - Liquid fraction for the evaporator Ith row

MAIREV - Mass flow rate of source air in the evap. duct (lb/hr)

MAIRCN - Mass flow rate of sink air in the cond. duct (lb/hr)

MCLWTR - Mass flow rate for the sink water (lb/hr)

MHOTW(I) - Mass flow rate for the source water for Ith row (lb/hr)

MODE - A counter set = 1, for water jacketed evap. and cond. tubes; set = 2, for a prescribed heat flux; set = 3, for air-to-air system

MWT - Molecular mass of the working fluid (lbm); 137.37 for R-11 and 187.4 for R-113

MX - A flag which is set equal to 1 at the beginning of all vapour flow (otherwise = 0)

NBEND - Number of bends in the vapour header

NCC - Number of printouts desired along the length of the condenser

NCP - Number of printouts desired along the length of the evaporator

NROWC - Number of rows in the condenser

NROWE - Number of rows in the evaporator

NSCB - Exponent used in equation when combined boiling and convective heat transfer takes place in subcooled boiling

NTUBEC - Number of tubes in a condenser row

NTUBEE - Number of tubes in an evaporator row

NTU - Number of transfer units (UA/mcp)

NVALVE - Number of valves in the condensate line

NUW - Nusselt number for the water in the evap. annulus

NUW2 - Nusselt number for the water in the cond. annulus

ODC - Outside diameter of the condenser (inch)

ODH - Outside diameter of the evaporator (inch)

P - A counter which detects the onset of bulk boiling

PAR - Parachor of working fluid; 193.4 for R-11 and 249.6 for R-113

PEBEST - Estimated pressure at the entrance to the evaporator tube (psia)

PEB(I) - Pressure at the bottom of the evaporator Ith tube row (psia)

PET - Pressure at the top of the evaporator first row (psia)

PMAX - Maximum pressure possible for the loop (psia)

PMIN - Minimum pressure possible for the loop (psia)

PERLNG - Percent of evaporator length flooded under static conditions (%)

PERDY(I) - True dynamic charge for the evaporator Ith tube row (%)

PEVTOP - Pressure at the top of the evaporator tube (psia)

PI - 3.1428571

PO - Value of PRESS at the upstream end of an element (psia)

POWER - Power used in the calculations for the mass flow rate

PR - Prandtl number (either liquid or vapour)

PRCFL - Percent of evaporator recirculation tube flooded under dynamic conditions (%)

PRESS - Pressure at a particular location along the loop (psia)

PRESOL - Pressure at the bottom of the evaporator from the previous iteration (psia)

PRF - Prandtl number of liquid

PRG - Prandtl number of vapour

PRLNGO - Previous value of PERLNG

PRCOUN - If = 1, the program uses the read in value of PEBEST
if = 0, the program generates an estimate for PEBEST

PRW - Prandlt number for water in evaporator annulus

PRW2 - Prandtl number for water in condenser annulus

Q - Heat flow rate (Btu/hr)

QA - Heat flux (Btu/hr/sq.ft)

QAVFLX - Average heat flux for both evap. and condenser (Btu/hr/sq.ft)

QC(K,KK) - Rate of heat transfer for KKth element for Kth row for condenser (Btu/hr)

QCFLUX - Average heat flux for all condenser tubes (Btu/hr/sq.ft)

QCOND - Heat transfer rate per condenser tube (Btu/hr)

QCS - Total heat transfer rate in the condenser coil (Btu/hr)

QEFLUX - Average heat flux for all the evaporator tubes (Btu/hr/sq.ft)

QES - Total heat transfer rate in the evaporator coil (Btu/hr)

QLOXO - Heat loss from the condensate tube (Btu/hr)

QO - Total heat flow rate to the start of current element (Btu/hr)

QROWE - Heat transfer rate for an evaporator row (Btu/hr)

QQ - Minimum heat flux necessary to sustain boiling (Btu/hr/sq.ft)

QRECRC - Heat loss from the recirculation tube (Btu/hr)

QUPXO - Heat loss from the vapour header (Btu/hr)

QULTY(I) - Quality at the top of the Ith evaporator row

QINPT(I) - Heat transfer rate for the evaporator Ith row (Btu/hr)

RECID - Recirculation tube inside diameter (inch)

RECRCL - Recirculation tube length (ft)

REN - Reynold number (either liquid or vapour)

RENF - Reynold number of liquid

RENG - Reynold number of vapour

RENW - Reynold number for water in evaporator annulus

RENW2 - Reynold number for water in condenser annulus

RINSID - Inside tube resistance for evaporator or condenser (hr.sq.ft.F/Btu)

RESLO - Resistance per unit length of the recirculation and condensate return line (hr.ft.F/Btu)

RESUP - Resiatance per unit length of the vapour header (hr.ft.F/Btu)

ROUT - Outside evaporator or condenser resistance (hr.sq.ft.F/Btu)

RWALL - Tube wall resistance (hr.sq.ft.F/Btu)

SATC - AVTSCS (C)

SATCON - Saturation temperature of the condenser (F)

SATH - AVTSHS (C)

SAAT(I) - Saturation temperature at the bottom of the evaporator Ith tube row (F)

SCB - Distance from the entrance of the evaporator to the point where bulk boiling initiates (ft)

SCL - Distance from the entrance of the evaporator to the point where subcooled boiling initiates (ft)

SDT - DELT (C)

SELEV - ELEV (m)

SFLRT - FLRATE (Kg/sec)

SGMA - SIGMA (degrees)

SHEITB - HEITB (m)

SHEITC - HEITC (m)

SIDC - IDC (m)

SIDH - IDH (m)

SIDLC - IDLC (m)

SIDUC - IDUC (m)

SIGMA - Angle of inclination of the plane of each row of evaporator tubes from the vertical (read in degrees then converted to radian) See figure H2

SQA - QAVFLX (W/sq.m)

SQC - QCFLUX (W/sq.m)

SQCS - QCS (W)

SQE - QEFLUX (W/sq.m)

SQES - QES (W)

SU - UEXPR (W/sq.m/K)

SWIDE - LUPXO (m)

SWIDER - LLOXO (m)

SYSTVL - Volume of entire thermosiphon loop (ft3)

SUEVT(I) - Sum of the evaporator wall temperatures for all elements for Ith row (F)

TAIR - Temperature of the sink air temperature approaching the

condenser coil (F)

TEB - Estimated temperature of the fluid in the evaporator liquid header (F)

TEMRMX - Temperature of the recirculation fluid entering the evaporator liquid header (F)

TC1 - TCOLD, condenser air approach temperature calculated by the program from the previous iteration (F)

TCNDWL - Condenser tube inner surface temperature (F)

TCR - Critical temperature of the working fluid (F); 388.4 for R-11 and 417.4 for R-113

TCWOUT - Condenser tube inner surface temperature (F)

TEM - Temperature of the bulk fluid at the inlet of an element in the condenser (F)

TEMP - Temperature of the bulk fluid at the inlet of an element in the evaporator (F)

TEMPF - Temperature of the bulk fluid (F)

TEMPLO - Temperature required at the exit of the liquid return line to satisfy the initial assumption (F)

TEVTOP - Temperature of the fluid at the top of the evaporator (F)

THETA - Rotation of the evaporator tubes from the horizontal (read in degrees then converted to radian) See figure H2

THICKC - Thickness of condenser tubes (inch)

THICKH - Thickness of evaporator tubes (inch)

THOT(I) - Temperature of hot air approaching the Ith evaporator row (F)

THIN(I,II)- Source fluid temperature for Ith row and IIth element (F)

TOUT(I,II)- Source fluid temperature leaving IIth element for Ith row (F)

TCOUT(K,KK)- Sink fluid temperature leaving KKth element for Kth row (F)

TOTALQ - Total heat input in the evaporator coil (Btu/hr)

TOTALF - Total mass flow rate for the evaporator coil (lb/hr)

TOTALR - Total recirculation rate for the evaporator coil (lb/hr)

TRECRC - Temperature of the liquid at the end of the recirculation tube (F)

TSATEB - Saturation temperature at the bottom of evaporator (F)

TSAT1 - Value of TSATEB from the previous iteration (F)

TSATO - Value of TSAT from the previous iteration (F)

TSCF - Local inside surface temperature for the condenser tube (F)

TSCS - Sum of condenser tube temperatures for all elements (F)

TSCSCN - Local average condenser wall temperature (F)

TSHF - Inside wall temperature of an element in the evaporator (F)

TSHFO - Previous value of TSHF

TUSPCE - Center-to-center distance between two evaporator tubes in the same row (inch)

TSP - Degree of superheat (F)

TST - Superheat temperature (F)

TWIN - Temperature of heating fluid at the inlet of an element (F)

TROOM - Room temperature (F)

U - Overall (inside to outside fluid) heat transfer coefficient (Btu/hr/sq.ft/F)

U2 - Overall (inside to outside fluid) heat transfer

coefficient (Btu/hr/sq.ft/F)

UOUT - Evaporator outside heat transfer coefficient (Btu/hr/sq.ft/F)

UOUTC - Condenser outside heat transfer coefficient (Btu/hr/sq.ft/F)

UF - Evaporator tube inside surface heat transfer coefficient taking into consideration FOULNF (Btu/hr/sq.ft/F)

UF2 - Condenser tube inside surface heat transfer coefficient taking into consideration FOULNF (Btu/hr/sq.ft/F)

UOA - Loop conductance based on average evaporator heat flux and overall temperature difference between the source and the sink fluid (Btu/hr/sq.ft/F)

VDFHDC - Volume of vapour in the condenser outlet header (ft3)

VDFHDE - Volume of vapour in the evaporator outlet header (ft3)

VDFR(I) - Void fraction for Ith evaporator tube row

VF - Velocity of fluid (either liquid or vapour) (ft/s)

VELAIR - Velocity of air in condenser or evaporator duct (ft/s)

VFCOP - Liquid velocity in flooded condenser tube (ft/s)

VG - Vapour velocity in the evaporator (ft/s)

VISC - Viscosity (either liquid or vapour) (lb/ft/s)

VL - Liquid velocity in the evaporator (ft/s)

VODC(K) - Condenser tube void fraction for Kth row

WATH(I) - Average water side heat transfer coefficient for Ith row in the annulus (Btu/hr/sq.ft.F)

X - Vapour quality along the loop

XACOND - Cross sectional area of the condenser tube (ft2)

XAEVAP - Cross sectional area of the evaporator tube (ft2)

XALORX - Cross sectional area of the liquid return tube (ft2)

XARCRC - Cross sectional area of the recirculation tube (ft2)

XAUPRX - Cross sectional area of the vapour header tube (ft2)

XFB - Critical quality

XP - Lockhart-Martinelli parameter

XSCB - Vapour quality at the exit from an element

XXX - A counter if set = 1 prints the input data cards

Y - A counter used to make viscosity corrections in the convective heat transfer equation

ZCOND - Elevation of the liquid vapour interface in the condensate return line above the bottom of the evap. tubes (ft)

ZMAX - Elevation of the top of the evaporator above the bottom of the evaporator tubes (ft)

ZREC(I) - Elevation of the liquid vapour interface in the recirculation tube from the bottom of the evaporator tube for Ith row (ft)

APPENDIX - H2

USER MANUAL FOR THE PROGRAM

In order to use this program the reader must provide the following input data:

1st Read statement Format (5,*)

IDH, IDC, THICKH, THICKC, HEITB, HEITC, LUPXO, LLOXO, TW2,

SIGMA, THETA, ALPHA, GAM, ELEV, TUSPCE, NROWE, NROWC, IPRI

2nd Read statement Format (5,*)

FOULNW, FOULNF, TCR, PAR, MWT, CSF, BEX, DIVN, DIVCON

3rd Read statement Format (5,*)

DPUPXO, NTUBEE, NTUBEC, RECRCL, RESUP, RESLO, TAIR, XXX

4th Read statement Format (5,*)

LEQAE, LEQAC, LEQRE

5th Read statement Format (5,*)

PEBEST, FLRATE, PRCOUN, FLCOUN, IHYSTR

6th Read statement Format (5,*)

NCP, NCC, IPRINT, FLAGUP, A, NBEND, NVALVE

7th Read statement Format (5,*)

MCLWTR, SPHTW, EXTIDE, EXTIDC, IDUC, IDLC

8th Read statement Format (5,*)

DUCTXS, MAIREV, MAIRCN, CPAIR, THOTG, RECID, TROOM

9th Read statement Format (5,*)

MODE, QFLUX

10th Read statement Format (5,*)

HDIAME, HDIAMC, LHDEVP, LHDCND, LEM

11th Read statement Format (5,*)

THOT(1)

THOT(I)

12th Read statement Format (5,*)

MHOTW(1)

MHOTW(I)

The following physical properties of the working fluid should be provided in subroutines.

1. Saturation pressure as a function of temperature (psia, F)
   SUBROUTINE SAT PR(TEMPF, PSAT)
2. Saturation temperature (F) as a function of pressure (psia)
   SUBROUTINE SAT TEM(PRESS, TSAT)
3. Enthalpy (Btu/lb) of saturated liquid as a function of temperature (F)
   SUBROUTINE LIQ HF(TEMPF, HFL)
4. Density of liquid (lb/ft^3) as a function of temperature (F)
   SUBROUTINE LIQ DEN(TEMPF, DENSL)
5. Latent heat (Btu/lb) of vaporization as a function of temperature (F)
   SUBROUTINE LAT HT(TCR,TEMPF,HFG)
6. Surface tension (lbf/ft) for the liquid-vapour interface
   SUBROUTINE SUR TEN(PAR, DENSL, DENSG, MWT, SURFTN)
7. Viscosity of liquid (lb/ft/s) as a function of temperature (F)
   SUBROUTINE LIQ VIS(TEMPF, VISCL)
8. Thermal conductivity (Btu/hr/ft/F) of liquid as a function of temperature (F)
   SUBROUTINE TH COND(TEMPF, KL)

9. Specific heat (Btu/lb/F) of liquid as a function of temperature (F)

   SUBROUTINE LIQ CP(TEMPF, SPHTL)

10. Viscosity (lb/ft/s) of vapour as a function of temperature (F)

    SUBROUTINE GAS VIS(TEMPF, VISCG)

11. Specific heat (Btu/lb/F) of vapour as a functiom of temperature (F)

    SUBROUTINE GAS CP(TEMPF, SPHTG)

The following subroutine is provided in the program to calculate the water properties.

Density (lb/ft3), viscosity (lb/ft/s) and thermal conductivity (Btu/hr/ft/F) as a function of temperature (F).

SUBROUTINE WTRPRP (TEMP, DENSW, VISCW, KW)

The following subroutine calculates the density (lb/ft3) of air as a function of the air temperature (F).

SUBROUTINE AIRDEN (AIRTEM, DENAIR)

The following subroutine calculates the air side resistance (hr.F/Btu) as a function of the air velocity (ft/s).

SUBROUTINE EFF(DISC, AREA, TAIR, PI, INDIA, OUTDIA, CPAIR, GC, ROUT, TCR, DENAIR, CF, DUCTXS, ALPHA, ALFMIN, TUSPCE, LENGTH, UA)

FIGURE H2

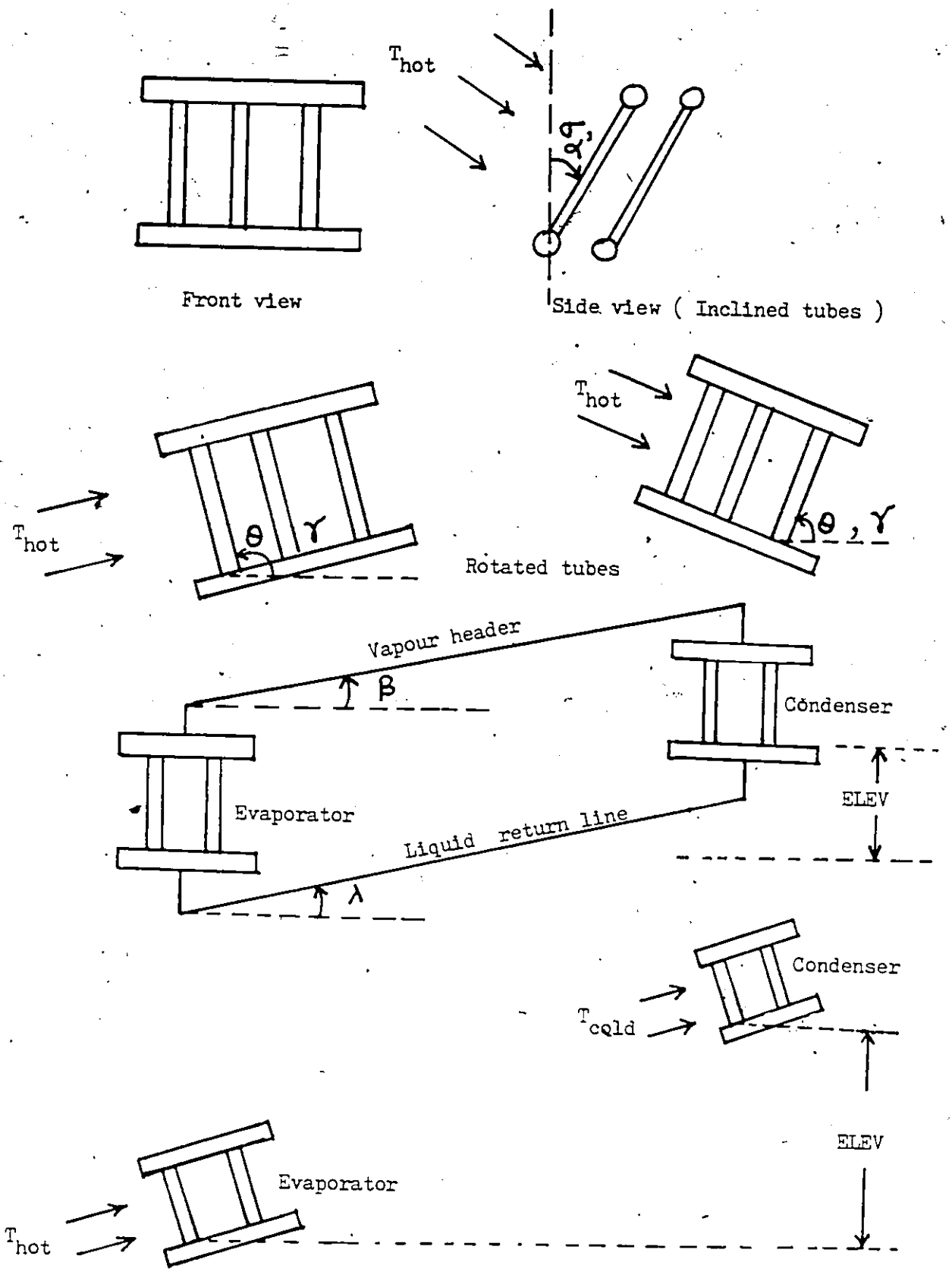

DESCRIPTION OF VARIOUS ANGLES FOR BOTH THE CASES : INTERCEPT

APPENDIX H3

PROGRAM LISTING

```
1.      //MATHUR  JOB (G271,E25,1,4),'DAS',CLASS=Z,MSGLEVEL=(1,1)
2.      //     EXEC  FORTVCLG,FVLANG='LAGLVL(66)'
3.      //FORT.SYSIN  DD  *
4.      C ***************************************
5.      C *  PROGRAM BY:-  GURSARAN DAS MATHUR   *
6.      C ***************************************
7.      C *   PROGRAM NAME :-  ROUTINE          *
8.      C ***************************************
9.      C *  THIS COMPUTER PROGRAM IS CAPABLE OF SIMULATING THE OVERALL PERFORMANCE
10.     C *  OF  FLUID-TO-FLUID TWO-PHASE THERMOSIPHON LOOP HEAT EXCHANGER SYSTEMS
11.     C *  IN WHICH THE COILS CONSIST OF PARALLEL ROWS OF STRAIGHT TUBES RUNNING
12.     C *  BETWEEN A COMMON LIQUID HEADER AND A COMMON VAPOUR HEADER. THIS
13.     C *  PROGRAM CAN SIMULATE MULTIPLE TUBE EVAPORATOR AND CONDENSER COILS
14.     C *  WITH INDEPENDENT HEATING OF EACH TUBE AND SINGLE-PASS, FINNED-TUBE,
15.     C *  MULTIPLE-ROW EVAPORATOR AND CONDENSER COILS WHERE THE SOURCE AND
16.     C *  SINK FLUID IS A GAS. THE TUBE ROWS MAY BE INCLINED FROM THE VERTICAL
17.     C *  AND MAY BE SUBJECT TO DIFFERENT EXTERNAL FLOW AND THERMAL CONDITIONS.
18.     C *  THIS PROGRAM CAN SIMULATE THE FOLLOWING SITUATIONS:-
19.     C *  (A)  AIR-TO-AIR TWO-PHASE THERMOSIPHON LOOP HEAT EXCHANGER
20.     C *  (B)  TWO-PHASE THERMOSIPHON LOOP HEAT EXCHANGER WITH WATER JACKETED
21.     C *  EVAPORATOR AND CONDENSER TUBES
22.     C *  (C)  CONSTANT HEAT FLUX BOUNDARY CONDITION IMPOSED ON THE EVAPORATOR
23.     C *  TUBE
24.     C *
25.     C *  TO RUN THE PROGRAM, THE OPERATOR MAY SPECIFY THE NUMBER OF ELEMENTS
26.     C *  INTO WHICH THE EVAPORATOR TUBES ARE TO BE DIVIDED (THE DEFAULT VALUE
27.     C *  IS 10), AND THE WORKING FLUID FLOW RATE IN A TYPICAL TUBE OF THE
28.     C *  1ST ROW OF THE EVAPORATOR TUBES (A DEFAULT VALUE IS CALCULATED
29.     C *  BASED ON THE OTHER INPUT DATA). AFTER AN INITIAL SOLUTION WHICH
30.     C *  YIELDS A STATIC CHARGE IN THE SYSTEM, THE OPERATOR MAY INCREASE
31.     C *  THE WORKING FLUID FLOW RATE TO YIELD RESULTS FOR LARGER STATIC
32.     C *  CHARGES OR VICE VERSA.
33.     C *
34.     C *  THE CONVERGENCE ROUTINE IS BASED ON THE SINK FLUID TEMPERATURE. THE
35.     C *  PROGRAM CALCULATES THE SINK FLUID TEMPERATURE REQUIRED TO CONDENSE THE
36.     C *  VAPOUR SUPPLIED TO THE CONDENSER. IF THIS SINK FLUID TEMPERATURE IS NOT
37.     C *  CORRECT, VARY THE STATE OF THE WORKING FLUID ENTERING THE EVAPORATOR  UNTIL
38.     C *  CONVERGENCE IS OBTAINED ON THE SINK FLUID TEMPERATURE.
39.     C *
40.     C *  IN ORDER TO USE THE PROGRAM, THE FOLLOWING DATA IS FED TO THE PROGRAM:
41.     C *  READ STATEMENT # 1:-
42.     C *  INSIDE DIA OF THE EVAPORATOR(INCH), INSIDE DIA OF THE CONDENSER(INCH),
43.     C *  THICKNESS OF EVAPORATOR TUBE(INCH), THICKNESS OF THE CONDENSER TUBE(INCH),
44.     C *  LENGTH OF EVAPORATOR TUBE(FT), LENGTH OF THE CONDENSER TUBE(FT),LENGTH
45.     C *  OF THE UPPER CONNECTING PIPE(FT),LENGTH OF LOWER CONNECTING PIPE(FT),
46.     C *  SINK TEMPERATURE (F), EVAP. ANGLE FROM THE VERTICAL(DEG), EVAP. ROTATION
47.     C *  FROM THE HORIZONTAL(DEG), COND. TILT & ROTN ANGLE(DEG), ELEVATION OF THE COND.
48.     C *  BOTTOM FROM THE BASE OF THE EVAPORATOR(FT), TUBE SPACING(INCH), NUMBER
49.     C *  OF EVAP. AND COND. ROWS, COUNTER WHEN=0 SUPRESSES THE PRINTING OF
50.     C *  THE TRANSITION POINTS IN THE EVAPORATOR
51.     C *  READ STATEMENT # 2:-
52.     C *  FOULING FACTOR OUTSIDE EVAPORATOR TUBE(FT2-HR-F/BTU),FOULING FACTOR
53.     C *  INSIDE EVAPORATOR TUBE(FT2-HR-F/BTU), TCR- CRITICAL TEMPERATURE OF THE
54.     C *  WORKING FLUID(F), PAR- PARACHOR OF THE WORKING FLUID, MWT- MOLECULAR
55.     C *  WEIGHT OF THE WORKING FLUID, CSF- A CONSTANT IN ROHSENOWS BOILING EQUATION
56.     C *  BEX-AN EXPONENT IN ROHSENOWS BOILING EQUATION, NUMBER OF LENGTH ELEMENTS
57.     C *  ALONG THE EVAPORATOR , NUMBER OF LENGTH ELEMENTS ALONG
58.     C *  READ STATEMENT # 3:-
59.     C *  ESTIMATE OF THE FRICTIONAL PRESSURE DROP IN THE UPPER CONNECTING TUBES(PSI),
60.     C *  NUMBER OF TUBES IN AN EVAPORATOR ROW, NUMBER OF TUBES IN A CONDENSER ROW,
61.     C *  LENGTH OF THE RECIRCULATION TUBES(FT),  SURROUNDING THERMAL RESISTANCE
62.     C *  PER UNIT LENGTH OF THE RECIRCULATION TUBE, VAPOUR HEADER
63.     C *  AND CONDENSATE RETURN LINE, AIR TEMP(F), A COUNTER WHEN=0 PRINTS THE
64.     C *  DATA CARDS
65.     C *  READ STATEMENT # 4:-
66.     C *  EQUIVALENT LENGTH OF FITTINGS, BENDS ETC. IN VAPOUR HEADER, CONDENSER,
67.     C *  AND RECIRCULATION TUBE
68.     C *  READ STATEMENT # 5:-
69.     C *  ESTIMATED PRESSURE AT THE BOTTOM OF THE FIRST ROW(PSIA), ESTIMATED FLOWRATE IN
70.     C *  THE FIRST ROW OF THE EVAPORATOR (LBM/HR),  A COUNTER IF = 1, THE PROGRAM
71.     C *  USES THE READ IN VALUE OF PBEST, A COUNTER IF = 1, USES THE READ IN
72.     C *  VALUE OF FLRATE, A COUNTER IF = 0, FOR INCREASING OVERALL TEMPERATURE
73.     C *  DIFFERENCES AND 1 FOR DECREASING TEMPERATURE DIFFERENCES
74.     C *  READ STATEMENT # 6:-
75.     C *  NUMBER OF PRINTOUTS DESIRED ALONG THE LENGTH OF THE EVAPORATOR, NUMBER
76.     C *  OF PRINTOUTS DESIRED ALONG THE LENGTH OF THE CONDENSER, A FLAG WHICH
77.     C *  IF=0 SUPPRESSES THE PRINTING OF DATA FOR THE VAPOUR HEADER AND THE LIQUID
78.     C *  RETURN LINE, A FLAG WHICH IF SET=1 USE READ IN VALUE OF THE VAPOUR HEADER
79.     C *  DROP DPVRXD, POWER USED IN  CALCULATION OF THE EFFECTIVE HEAT TRANSFER
80.     C *  COEFF. IN THE DRYOUT REGION, NUMBER OF BENDS IN VAPOUR HEADER, NUMBER
```

```
C *  OF VALVES IN THE LIQUID RETURN LINE
C *  READ STATEMENT # 7:-
C *  SINK WATER FLOW RATE (LBM/HR), SPECIFIC HEAT OF WATER (BTU/LBM/F),
C *  EXTERIOR DIAMETERS FOR THE EVAPORATOR AND CONDENSER ANNULUS (INCH),
C *  DIAMETERS OF UPPER AND LOWER CONNECTING PIPES (INCH).
C *  READ STATEMENT # 8:-
C *  DUCT X-SECTIONAL AREA(FT2), FLOWRATES OF AIR: IN EVAP. IN COND.(LBM/SEC),
C *  SP. HEAT OF AIR(BTU/LB-F), HOT AIR TEMP. APPROACHING THE HEAT EXCHANGER,
C *  DIAMETER OF THE RECIRCULATION TUBE (INCH), SOURROUNDING TEMPERATURE (F):
C *  READ STATEMENT # 9:-
C *  A COUNTER SET = 1 FOR WATER JACKETED TUBES, 2 FOR PRESCRIBED HEAT FLUX,
C *  3 FOR AIR-TO-AIR SYSTEM, HEAT FLUX (BTU/HR/SQ.FT)
C *  READ STATEMENT # 10:-
C *  HEADER DIAMETERS FOR EVAPORATOR AND CONDENSER (INCH), LENGTH OF THE
C *  HEADERS FOR EVAPORATOR AND CONDENSER (INCH)
C *  READ STATEMENT # 11:-
C *  SOURCE FLUID TEMPERATURES FOR EACH OF THE TUBE ROWS (F)
C *  READ STATEMENT # 12:-
C *  SOURCE FLUID FLOW RATE FOR EACH OF THE TUBE ROWS (LBM/HR)
C*****************************************************************************
      DIMENSION WATH(4)
      DIMENSION TCAIR(4),CONDQ(4)
      DIMENSION QC(4,10),FL(4),TCOUT(4,10),VDOC(4),HCON(4),AVTC(4)
      DIMENSION SUEVT(4),VDFR(4),LOFR(4),ELEXT(4),PERDY(4),MHOTW(4)
      DIMENSION QULTY(4),QINPT(4),FLRAT(4),THOT(4),PEB(4),SAAT(4),TFLUD(
     $4),THIN(4,20),TOUT(4,20)
      REAL LBE,LUPXO,LLOXO,LEQAE,LEQRE,LEQAC,LEQBE,LIOFS,LOFR,K1,K2
      REAL IDH,IDC,IDUC,IDLC,NSCB,LCNDSN,LN,LO,LETMCH
      REAL LCON,NBEND,NVALVE,KW,KL,KG,KM,KF,LH,LEM,LEMDA,LHDEVP,LHDCND
      REAL LENGTH,LIOF,MWT,NTU,MASAIR
      REAL LIOHDE,LIOHDC,MHTWTR,MCLWTR,IDBE,MHOTW,MAIREV,MAIRCN
      INTEGER FLAGUP,DIAM,COUNT2,FLAG1,FLAG2,FLAG3,FLAG4,XXX
      READ (5,*)IDH,IDC,THICKH,THICKC,HEITB,HEITC,LUPXO,LLOXO,TW2
     $,SIGMA,THETA,ALPHA,GAM,ELEV,TUSPCE,NROWE,NROWC,IPRI
      READ (5,*)FOULNW,FOULNF,TCR,PAR,MWT,CSF,BEX,DIVN,DIVCON
      READ (5,*)DPUPXO,NTUBEE,NTUBEC,RECRCL,RESUP,RESLO,RESBE,TAIR,XXX
      READ (5,*)LEQAE,LEQAC,LEQRE
      READ (5,*)PEBEST,FLRATE,PRCOUN,FLCOUN,IHYSTR
      READ (5,*)NCP,NCC,IPRINT,FLAGUP,A,NBEND,NVALVE
      READ (5,*)MCLWTR,SPHTW,EXTIDE,EXTIDC,IDUC,IDLC
      READ (5,*)DUCTXS,MAIREV,MAIRCN,CPAIR,THOTG,RECID,TROOM
      READ (5,*)MODE ,QFLUX
      READ (5,*)HDIAME,HDIAMC,LHDEVP,LHDCND,LEM
      NR=NROWE
      NR=NROWC
      DO 41 I=1,NR
   41 READ (5,*) THOT(I)
      DO 43 I=1,NR
   43 READ (5,*)MHOTW(I)
      ICNHOT=0
      PRINT 277
      CALL         DATA(IDH,IDC,THICKH,THICKC,HEITB,HEITC,LUPXO,LLOXO,
     $SIGMA,THETA,ALPHA,GAM,ELEV,XXX,TAIR)
      CALL PRINT(TAIR,THOTG,PEBEST,DENSL,PMIN,PMAX)
      IF(PRCOUN.EQ.1)GO TO 98
      PEBEST=(PMAX+PMIN)/2.0+HEITB*DENSL*COS(SIGMA)/144.0
      DIVN=10.0
   98 PI =3.141596
      GC=32.174
      IF(FLCOUN.EQ.0)CALL  MASS FL(PI,IDH,HEITB,TEMPF,FLRATE,TCR)
      EX=0.21
      ICOUNT=0
      IICOUN=0
      IF(MODE.NE.3) GO TO 1966
      CALL AIRDEN(THOTG,DENEVP)
      DISEVP=MAIREV/DENEVP
      CALL AIRDEN(TAIR,DENCND)
      DISCND=MAIRCN/DENCND
      UNHTL1=UNHTL1/12.0
      UNHTL2=UNHTL2/12.0
      DPFLM1=DPFLM1*(1.4504/10000.0)
      DPFLM2=DPFLM2*(1.4504/10000.0)
      DPFIL1=DPFIL1*(1.4505/10000.0)
      DPFIL2=DPFIL2*(1.4505/10000.0)
 1966 FLAG2=0
      FLAG3=0
      ICNDSB=DIVCON-1.0
      RNCP=NCP
      RNCC=NCC
      IDBE=IDBE/12.0
```

```
      RECID=RECID/12.0
      LHDEVP=LHDEVP/12.0
      LHDCND=LHDCND/12.0
      HEDVLE=(PI*(HDIAME**2.0)/4.0)*LHDEVP
      HEDVLC=(PI*(HDIAMC**2.0)/4.0)*LHDCND
      IDH=IDH/12.0
      IDC=IDC/12.0
      XAEVAP=(IDH**2)*(PI/4.0)
      XACOND=(IDC**2)*(PI/4.0)
      XAUPPX=(IDUC**2)*(PI/4.0)
      XALOWX=(IDLC**2)*(PI/4.0)
      RECID=IDLC
      XARCRC=(RECID**2.0)*(PI/4.0)
      XABE=(IDBE**2.0)*(PI/4)
      THICKH=THICKH/12.0
      THICKC=THICKC/12.0
      ODH=IDH+(2.0*THICKC)
      ODC=IDC+(2.0*THICKH)
      AREAP=PI*(DH*HEITB
      AREAC=PI*IDC*HEITC
      CNROTN=0
      IF(THETA.EQ.90.0)CNROTN=1
      CALL VOL (CNROTN,VSTRAN,THETA)
      EXTIDE=EXTIDE/12.0
      EXTIDC=EXTIDC/12.0
      AANULC=(PI/4.0)*((EXTIDC**2.0)-(ODC**2.0))
      AANULE=(PI/4.0)*((EXTIDE**2.0)-(ODH**2.0))
      DEQVE=EXTIDE-ODH
      DEQVC=EXTIDC-ODC
      WCLWTR=WCLWTR/3.0
      GWC=WCLWTR/AANULC/3600.0
      AGAM=GAM
      ALFA=ALPHA
      THTA=THETA
      SGMA=SIGMA
      ALPHA=PI*ALPHA/180.0
      SIGMA=PI*SIGMA/180.0
      THETA=PI*THETA/180.0
      GAM=PI*GAM/180.0
      ALFMIN=ATAN(IDC/HEITC)
      IF(ALPHA.EQ.0.0)CF=0.0
      IF(ALPHA.EQ.0.0)GO TO 693
      IF(ALPHA.GE.((PI*50.0)/180.0))CF=0.724
      IF(ALPHA.GE.((PI*50.0)/180.0))GO TO 693
      CF=0.724*((COS((((50.0*PI)/180.0)-ALPHA)/((50.0*PI)/180.0)))*
     3(PI/2.0)))**0.25)
  693 BETA=ARSIN(((ELEV+(HEITC*SIN(GAM)*COS(ALPHA)))-(HEITB*SIN(THETA)*
     3COS(SIGMA)))/LUPX0)
      PRESS=PEBEST
      CALL   SAT TEM(PRESS,TSAT)
      TEB=TSAT-0.023*(TSAT-TAIR)
      TA=0.005*(TSAT-TAIR)
      CONST=0.045
      IF(MODE.NE.3)GO TO 308
      TEMPF=TEB
      DENSG=(PRESS*MWT)/(10.730*(TEMPF+460.0))
      VELAIR=DISEVP/DUCTXS
  308 TEMPF=TEB
  307 PEB(1)=PRESS
      PSTART=PEB(1)
      CALL       LIQ DEN(TEMPF,DENSL)
      DO 62 I=1,NR
   62 PEB(I+1)=PEB(I)+(I*TUSPCE*DENSL*COS(THETA))/144
      DO 63 I=1,NR
   63 CALL SAT TEM(PEB(I),SAAT(I))
      IF(ICOUNT.GE.1) GO TO 66
      IF(THETA)64,65,65
   65 TEB=SAAT(1)-CONST*(SAAT(1)-TAIR)
      GO TO 66
   64 TEB=SAAT(NR)-CONST*(SAAT(NR)-TAIR)
   66 FLAG1=0
      TEMPF=TEB
      CALL LIQ HF(TEMPF,HFL)
      HFBOT=HFL
      HF=HFBOT
      PBOT=PRESS
      CALL HFLS(TSAT,HFSTPT)
      CALL LIQ DEN(TEMPF,DENSL)
      CALL LIQ VIS(TEMPF,VISCL)
      TSATEB=SAAT(1)
```

```
      PRINT 277
  277 FORMAT('-','----------------------------------------------------------
     $-------------------------------------------------------------')
      PRINT 1987,NROWE,NTUBEE
 1987 FORMAT('-','EVAPORATOR: TOTAL NUMBER OF ROWS=',I1,3X,'NUMBER OF
     $TUBES IN EACH ROW=',I2)
      PRINT 674,NROWC,NTUBEC
  674 FORMAT('-','CONDENSER : TOTAL NUMBER OF ROWS=',I1,3X,'NUMBER OF TU
     $BES IN EACH ROW=',I2)
      PRINT 277
      PRINT 189,THOTG
  189 FORMAT('-','TEMP. OF HOT AIR APPROACHING THE EVAPORATOR(F)=',F7.3)
      PRINT 190,TAIR
  190 FORMAT(' ','TEMP. OF COLD AIR APPROACHING THE CONDENSER(F)=',F7.3)
      PRINT 1989,TROOM
 1989 FORMAT(' ','ROOM TEMPERATURE (F)=',F7.3)
      PRINT 545,MAIREV
  545 FORMAT('-','MASS FLOW RATE OF AIR IN THE EVAPORATOR(LBM/SEC)=',F10
     $.7)
      PRINT 546,MAIRCN
  546 FORMAT(' ','MASS FLOW RATE OF AIR IN THE CONDENSER(LBM/SEC)=',F10
     $.7)
      PRINT 277
      I=1
   91 IF(MODE.NE.3.AND.I.EQ.2)GO TO 745
      IF(I.EQ.2)GO TO 746
      TWIN=THOT(I)
      TSAT=SAAT(I)
      TEMPF=TEB
      WHTWTR=WHOTW(I)
      GWH=WHTWTR/AANULE/3600.0
      GF=FLRATE/XAEVAP/3600.0
      PLOWR1=PEB(1)+(((2.0/12.0)*DENSL)/144.0)+1.0*(1.0/(GC*2.0))
     $*((GF/DENSL)**2.0)*(1.0/144.0)
      GO TO 745
  746 CALL DELPBE(A1,LBE,LEQBE,GC,ZBE,IDBE,DPEVAP,NTUBEE,PI,
     $DENSL,VISCL,XABE,DLPBE,DPDL,UNHTLI,DENSG,VISCG,IDUC,NELBOW,
     $LETMCH,DPNONH,DPTEE,DPELBO,DPEXIT)
      PRESS=PBOTBE-DLPBE-DPFLW2-DPFIL2
      CALL SAT TEM(PRESS,SAAT(2))
      PEB(2)=PRESS
      PRESS=PEB(2)
      TSAT=SAAT(2)
      PLOWR2=PEB(2)+(((4.0/12.0)*DENSL)/144.0)+1.0*(1.0/(GC*2.0))
     $*((GF/DENSL)**2.0)*(1.0/144.0)
  745 CALL HFLS(TSAT,HFSTRT)
      TEMPF=TEB
      CALL LIQ HF(TEB,HFL)
      HFBOT=HFL
      HF=HFBOT
      DEGSUB=TSAT-TEB
      DLNGTH=HEITB/DIVN
      GF=FLRATE/XAEVAP/3600.0
      DOWNST=0.0
      LENGTH=0.0
      Q=0.0
      HWSUM=0.0
      HW2SUM=0.0
      HW2SM2=0.0
      XTOP=0.0
      VOIDF=0.0
      VOIDFS=0.0
      LIQFS=0.0
      DPA=0.0
      DPAC=0.0
      DPACP=0.0
      HIPC=0.0
      TSHS=0.0
      S=0.0
      HITPB=0.0
      XP=0.0
      PHI=0.0
      VG=0.0
      HITPC=0.0
      MX=0
      TSP=0.0
      LCON=0.0
      PRL=0.0
      H2P1=0.0
      H2P2=0.0
```

```
      XSCR=0.0
      NSCR=0.0
      UAVEV=0.0
      SUMTP=0.0
      ICOUNT=0
      TWOUT=TWIN
      LIQF=1.0
      TSHF=TEMPF
      L=0
      LFB=0
      ICP=1
      M=DIVN
      RM=M
C     ************************************************************
C     *                  START OF EVAPORATOR ELEMENT LOOP        *
C     ************************************************************
      DO 1 II=1,M
      AREAH=PI*IDH*DLNGTH
      IF(MODE.NE.3)GO TO 1973
      CALL AIRDEN(THOTG,DENAIR)
      IF(I.GT.1)CALL AIRDEN(THIN(I-1,II),DENAIR)
      MASAIR=(DENAIR*VELAIR*3600.0)*(DLNGTH*TUSPCE/12.0)
      CALL      EFF(DISEVP,AREAP,TAIR,PI,IDH,ODH,CPAIR,GC,ROUT,
     1TCR,DENAIR,CF,DUCTXS,ALPHA,ALFMIN,TUSPCE,DLNGTH,UA)
      UOUT=(1.0/ROUT)*(1.0/AREAH)
 1973 AREAHO=PI*ODH*DLNGTH
      HFLOLD=HFL
      IF(II.EQ.1)HFLOLD=HFSTRT
      HFOLD=HF
      LO=LENGTH
      TSHFO=TSHF
      TSATO=TSAT
      TEMPFO=TEMPF
      VOIDFO=VOIDF
      PO=PRESS
      IF(H2PI.GT.H1PC)H1PC=0.0
      QL=0.0
      IHBB=0
      IX=0
      PP=0.0
      XBOTOM=XTOP
      X=XBOTOM
      TEMP=TEMPF
      IF(X.GE.1.0)H2PI=0.0
      IF(HITPJ.GT.HITPC)HITPC=0.0
      DENSG=(PRESS*MWT)/(10.730*(TEMPF+460.0))
      PRESS=PRESS*144.0
      DIST=LENGTH+(DLNGTH/2.0)
      LENGTH=LENGTH+DLNGTH
      CG=1.0+(7.0*IDH/DIST)
      FM=(1.0+(5.0/EXP(DIST/(10.0*IDH))))
      FC=((1.0+(3.5/EXP(DIST/(90.0*DEQVE)))))
      FCT=((1.0+(3.0/EXP(DIST/(30.0*DEQVE)))))
      TWIN=TWOUT
      CALL WTPROP(TWIN,DENSW,VISCW,KW)
      RENW=DEQVE*GWH/VISCW
      PRW=VISCW*SPHTW/KW
      IF(RENW-1900.0)650,650,689
  689 NUW=0.02*(RENW**0.8)*(PRW**0.3333)*((EXTIDE/(IDH))**0.53)
      HW=NUW*KW*FCT*3600.0/DEQVE
      GO TO 690
  650 HW=(1.86*KW/DEQVE*(RENW*PRW*DEQVE/DIST)**
     10.333)*3600.0*FC
  690 CALL        LIQ DEN(TEMPF,DENSL)
      CALL        LAT HT(TCR,TEMPF,HFG)
      CALL        SUR TEN(PAR,DENSL,DENSG,MWT,SURFTN)
      VL=GF*(1.0-X)/DENSL
      IF(X.GT.0.0.AND.X.LT.1.0)VL=GF*(1.0-X)/(DENSL*LIQF)
      IF(X.GE.1.0)GO TO 555
      CALL        LIQ VIS(TEMPF,VISCL)
      RENF=IDH*VL*DENSL/VISCL
      POWER=1.0
      IF(RENF.GE.2000.0)POWER=0.571
      CALL        TH COND(TEMPF,KL)
      CALL        HT COND(TEMPF,KW)
      CALL        LIQ CP(TEMPF,SPHTL)
      PRF=SPHTL*VISCL/KL
      RELET=RENF*PRF
      VF=VL
      REN=RENF
```

```
401.            PR=PRF
402.            VISC=VISCL
403.            KF=KL
404.          555 CALL          GAS VIS(TEMPF,VISCG)
405.            CALL          GAS CP(TEMPF,SPHTG)
406.            KG=VISCG*(SPHTG+2.48/MWT)
407.            VG=GF*X/DENSG
408.            IF(X.GT.0.0)VG=GF*X/(DENSG*VOIDF)
409.            IF(X.GT.0.0)RENG=IDH*VG*DENSG/VISCG
410.            RENG=IDH    *GF*X/VISCG
411.            PRG=SPHTG*VISCG/KG
412.            IF(X.LE.0.0)GO TO 1003
413.            IF(H2PI.GT.HIPC.AND.X.LT.1.0)GO TO 5000
414.            IF(X.LT.1.0)GO TO 1003
415.            REN=RENG
416.            PR=PRG
417.            VISC=VISCG
418.            KF=KG
419.            VF=VG
420.         1003 Y=1.0
421.            AA=IDH
422.            BB=DIST
423.            CC=0.4
424.            HH=HIPC
425.         1031 CALL     SPHASE(AA,BB,CC,HH,Y,REN,KF,PR,FN,VISC,VISWAL,CG)
426.            HIPC=HH
427.            HITP=HH
428.            IF(X.GE.1.0)H2P2=HITPC
429.            GO TO 850
430.         5000 CALL   TWOPHE(X,VISCG,VISCL,H2PI,KL,IDH,GF,SPHTL)
431.            IF(X.LE.0.0)GO TO 7300
432.            VAVG=GF/(LIQF*DENSL)
433.            CALL DTINRO(TSHF,TSAT,PECLET,DITI)
434.            CALL     CRITOY(RENG,RENF,HFG,Q,PI,GC,IDH,LENGTH,OLNGTH,FBL,FB,
435.           1DENSL,DENSG,SURFTN,VISCL,LIQF,X,IPRI,PRG,HITPC,HITP,GF,KG,
436.           2H2PI,XFB)
437.            IF(X.GT.XFB)H2P2=HITPC
438.            GO TO 525
439.          850 HITPC=HITP
440.            IF(X.GE.1.0)HITPB=0.0
441.            7  IF (MODE.EQ.2)GO TO 1956
442.            XYZ=IDH/ODH/HW
443.            IF(MODE.EQ.3)XYZ=1.0/UOUT
444.            U =1.0/(1.0/HITP +XYZ+((ALOG(ODH    /IDH    ))*IDH
445.           1/(2.0*KW))  +FOULNW+FOULNF)
446.            IF(MODE.EQ.3)GO TO 1967
447.            DQ=U*AREAH*(TWIN-TEMPF)
448.            GO TO 1957
449.         1967 XY=(U*AREAH)/(MASAIR*CPAIR)
450.            EFFECT=1.0-(EXP(-(XY)))
451.            IF(I.GT.1)GO TO 173
452.            DQ=MASAIR*CPAIR*EFFECT*(THOTG-TEMPF)
453.            TOUT(I,II)=THOTG-DQ/(MASAIR*CPAIR)
454.            GO TO 1957
455.          173 IF(THIN(I-1,II).LE.TEMPF)GO TO 171
456.            GO TO 174
457.          171 WRITE(6,656)
458.          656 FORMAT(' ','****** TEMPERATURE OF INCOMING HOT AIR IS LESS THAN OR
459.           1EQUAL TO TEMPERATURE OF THE FLUID ******')
460.            GO TO 121
461.          174 DQ=MASAIR*CPAIR*EFFECT*(THIN(I-1,II)-TEMPF)
462.            TOUT(I,II)=THIN(I-1,II)-DQ/(MASAIR*CPAIR)
463.            GO TO 1957
464.         1956 DQ=QFLUX*AREAH
465.         1957 UF=1.0/((1.0/HITP)+FOULNF)
466.            TSHF=TEMPF+(DQ/(UF*AREAH))
467.            IF(X.GE.1.0)GO TO 420
468.            IF(BL.GT.0.0)GO TO 5007
469.            GO TO 420
470.         5007 IF(ABS(TSHF-TSHFP)-TA)422,422,136
471.          420 IF(Y.EQ.1.0) GO TO 137
472.            IF(ABS(TSHF-TSHFP)-TA)6000,6000,137
473.         6000 IF(X.GT.0.0.AND.X.LT.1.0)GO TO 5000
474.            GO TO 525
475.          137 IF(X.LT.1.0)GO TO 517
476.            CALL          VISHGW(TSHF,VISWAL)
477.            GO TO 518
478.          517 CALL          VISHLW(TSHF,VISWAL)
479.          518 Y=Y+1.0
480.            TSHFP=TSHF
```

```
      GO TO 1031
  525 REN=RENF
      IF(X.GE.1.0)REN=RENG
      IF(REN -2000.0)813,813,814
  813 F=64.0/REN
      IF(X.GE.1.0)GO TO 422
      GO TO 560
  814 F=4.0*0.079/(REN**0.25)
      IF(X.GE.1.0)GO TO 422
  560 IF(L.EQ.0)GO TO 422
  136 IF(TSHF.GT.TSAT)GO TO 5010
      TSHF=(THPP+TSAT)/2.0
      THPP=TSHF
      IHBR=IHBB+1
      GO TO 5011
 5010 IF(IHBB.GT.0)GO TO 422
 5011 CALL  HPOOLB(DTA,TSHF,TSAT,DITI,HITPB,SPHTL,HFG,CSF,HTFLUX,
     3BEX,VISCL,SURFTN,DENSL,DENSG,TEMPF,PRF,X)
      IF(X.LE.0.0)GO TO 5008
 7300 XSCB=2.0-((TSAT-TEMPF)/DTI)
      HITP=((HITPB**4.0)+(H2P1**4.0))**(1.0/4.0)
      IF(H2P1.GT.HIPC)GO TO 7301
 7302 HITP=((HITPB**NSCB)+(HIPC**NSCB))**(1.0/NSCB)
 7301 IF(LFB.EQ.0)GO TO 6001
      C1=(((X-XFB)/(1.0-XFB))**(1.0/A))
      C2=1.0-C1
      IF(X.GT.XFB)HITP=(C1*H2P2)+(C2*HITP)
 6001 TSHFP=TSHF
      BL=BL+1.0
      GO TO 7
 5008 XSCB=HTFLUX*3600.0*AREAH/(FLRATE*HFG)
      IF(HTFLUX.EQ.0.0)GO TO 7302
      VOIDF=1.0/(1.0+((1.0-XSCB)/XSCB)*(DENSG/DENSL))
      LIQF=1.0-VOIDF
      DENSM=VOIDF*DENSG+(1.0-VOIDF)*DENSL
      VG=GF/DENSM
      RENG=IDH    *VG*DENSG/VISCG
      GO TO 5000
  422 TSHW=TSHF+(DQ*THICKH/XM/AREAH)
      AVTSH=(TSHW+TSHF)/2.0
      TSHS=TSHS+AVTSH
      IF(MODE.EQ.2)GO TO 1963
      UAVEV=UAVEV+(U*AREAH)
 1963 SUMITP=SUMITP+HITP
      TWOUT=TWIN-(DQ/(MMTWTR*SPHTW))
      IF(MODE.EQ.3)TMIN(I,II)=TOUT(I,II)
      IF(MODE.EQ.3)DOWNST=DOWNST+TOUT(I,II)
      Q=Q+DQ
C     FINDING TEMPERATURE AND PRESSURE FOR NEXT HIGHER POINT
      IHBB=0
      HF=HFBOT+Q/FLRATE
      IF(X.GE.1.0)GO TO 931
      IF(X.GT.0.0)GO TO 185
      IF(BL.GT.0.0)GO TO 185
  186 CALL LIQCP(TEMPF,SPHTL)
      TEMPF=TEMPF+(HF-HFBOT)/SPHTL
  453 CALL       LIQ HF(TEMPF,HFCK)
      IF(ABS(HF-HFCK)-0.05)451,451,452
  452 CALL LIQCP(TEMPF,SPHTL)
      TEMPF=TEMPF+(HF-HFCK)/SPHTL
      GO TO 453
  931 TEMPF=TEMPF+DQ/(FLRATE*SPHTG)
  451 TOF=TEMPF
      IF(PP.GT.0.0)GO TO 540
  185 IF(X.GT.0.0.AND.X.LT.1.0)GO TO 16
      IF(X.EQ.0.0.OR.X.GE.1.0)GO TO 17
   16 CALL PRESSP(DPAC,DPA,DPACP,LIQF,DENSL,VOIDF,DENSG,THETA,
     DSIGMA,XBOTOM,F,DLNGTH,IDH,GF,GC,FLRATE,PI,X,XFB,RENF,RENG,XP,
     3VISCL,VISCG,PHI,IX)
      IF(XBOTOM.LE.0.0)GO TO 901
  113 CALL     XPCAL(RENF,RENG,VISCL,VISCG,DENSL,DENSG,X,XP)
      IF(IX.GT.0)GO TO 114
  524 CALL      PHICAL(RENF,RENG,PHI,XP)
      GO TO 21
   17 CALL  SPRESS(DLNGTH,DENSG,THETA,SIGMA,F,IDH,VF,GC,DENSL,X,
     3DPH,DPF,DPA)
   21 PRESS=PRESS-DPH-DPF-DPA
      IF(II.EQ.4)DPDL=(DPH+DPF+DPA)/DLNGTH
      DENSM=(LIQF*DENSL+VOIDF*DENSG)
      IF(II.EQ.4)PRESS=PRESS-0.5*(VF*VF/2.0/GC)*DENSM
```

```
      IF(X.GE.1.0)GO TO 801
      PRESS=PRESS/144.0
      CALL SAT_TEM(PRESS,TSAT)
      CALL HFLS(TSAT,HFL)
      QQ=Q-QQ
      IF(L.GT.0)GO TO 432
      IF(IHYSTR.EQ.0)GO TO 864
      GO TO 865
  864 IF((ABS(TSHF-TEMPF).GE.24.0)GO TO 866
      GO TO 501
  865 IF(TSHF.LT.TSAT)GO TO 501
      IF(TEMPF.GT.TSAT)GO TO 432
  866 CALL          SCOOLS(KL,HFG,SURFTN,TSAT,DENSG,DENSL,PI,IDH,LENGTH,
     3REN,VISCL,PRF,VL,TEMPF,0.0A,QQ)
      IF(QA.GT.QQ)GO TO 427
      GO TO 432
  427 DITI=0.0
      DTA=TSHF-TSAT
      L=L+1
      CALL SBCOOL(TSHF,TSAT,TSHFO,TSATO,LO,LENGTH,PO,PRESS,Q,TEMPFO,
     3TEMPF,HF,HFL,FLRATE,THPP)
      CALL CORECT(TSHS,AVTSH,QQ,Q,QQ,TSHW,TSHF,THICKH,KW,AREAH,
     3DLNGTH,HEITB,LENGTH,RM,II,LO,TEMPFO,IDH,PI,UF)
      MASAIR=(DENAIR*VELAIR*3600.0*(LENGTH-LO)*TUSPCE)/12.0
      TOUT(I,II)=THOTG-QQ/(MASAIR*CPAIR)
      IF(L.EQ.1)DTI=TSAT-TEMPF
      GO TO 501
C     BEGINNING OF TWO PHASE FLOW
  432 TST=TSAT+TSP
      CALL          HFLS(TST,HFL)
      IF(HFL-HF)9,201,201
  201 PP=PP+1.0
      IF(BL.GT.0.0)GO TO 186
  540 TEMPF=TDF
      GO TO 501
    9 DENSG=(PRESS*MWT)/(10.730*(TEMP+460.0))
      CALL GASVIS(TEMPF,VISCG)
      CALL LIQ_DEN(TEMPF,DENSL)
      TEMPF=TSAT
      IF(P.GT.0.0)GO TO 630
      CALL BULKPT(HF,HFL,HFLOLD,HFOLD,LO,LENGTH,PO,PRESS,FLRATE,Q,TSHFO,
     3TSHF,VOIDO,VOIDF,TSAT)
      CALL CORECT(TSHS,AVTSH,QQ,Q,QQ,TSHW,TSHF,THICKH,KW,AREAH,
     3DLNGTH,HEITB,LENGTH,RM,II,LO,TEMPFO,IDH,PI,UF)
      MASAIR=(DENAIR*VELAIR*3600.0*(LENGTH-LO)*TUSPCE)/12.0
      TOUT(I,II)=THOTG-QQ/(MASAIR*CPAIR)
      TEMPF=TSAT
      DTI=1.0
      L=2
      X=XSCB
      IF(XSCB.EQ.0.0)X=1E-10
      GO TO 14
  630 CALL          HFGTS(TCR,TST,HFGO)
      XTOP=(HF-HFL)/HFGO
      DX=XTOP-XBOTOM
      X=XTOP
      IF(X.LT.1.0)GO TO 516
      HG=HFL+HFGO
      LENGTH=LO+((HG-HFL)/(HF-HFL))*DLNGTH
      IF(II.EQ.M)DLNGTH=HEITB-LENGTH
      IF(II.EQ.M)GO TO 345
      DLNGTH=(HEITB-LENGTH)/(RM-II)
  345 Q=Q-(FLRATE*(HF-HG))
      QQ=QQ-(FLRATE*(HF-HG))
      HF=HG
      X=1.0
      VOIDF=1.0
      PRESS=PRESS*144.0
  516 IF(1.0-X)901,801,14
   14 IX=IX+1
  199 CALL     XPCAL(RENF,RENG,VISCL,VISCG,DENSL,DENSG,X,XP)
      IF(IX.GT.0)GO TO 114
      GO TO 199
  114 IX=0
      IF(X.GT.0.0.AND.X.LT.1.0)LIQF=(1.0-(1.0/((1.0+XP**0.8)**0.379)))
      IF(X.GT.0.0.AND.X.LT.1.0)VOIDF=1.0-LIQF
      PRESS=PRESS*144.0
      IF(XBOTOM.LE.0.0.AND.II.EQ.M)GO TO 524
  801 PRESS=PRESS/144.0
      IF(MODE.NE.3)GO TO 1968
```

```
      IF(II.EQ.M)PEXITE=PRESS
      IF(I.EQ.1.AND.II.EQ.M)PVPHR1=PRESS-DPDL*UNHTL1/144.0
      IF(I.EQ.2.AND.II.EQ.M)PVPHR2=PRESS-DPDL*UNHTL2/144.0
 1968 CALL SAT TEM(PRESS,TSAT)
      P=P+1
  501 VOIDFS=VOIDFS+(VOIDF*(LENGTH-LO)*XAEVAP)
      LIQFS=LIQFS+((1.0-VOIDF)*(LENGTH-LO)*XAEVAP)
      IF(MODE.NE.3) GO TO 1969
      IF(I.EQ.1.AND.II.EQ.M)VAPV1=(VOIDF*UNHTL1*XAEVAP)
      IF(I.EQ.1.AND.II.EQ.M)LIQV1=((1.0-VOIDF)*UNHTL1*XAEVAP)
      IF(I.EQ.2.AND.II.EQ.M)VAPV2=(VOIDF*UNHTL2*XAEVAP)
      IF(I.EQ.2.AND.II.EQ.M)LIQV2=((1.0-VOIDF)*UNHTL2*XAEVAP)
 1969 HWSUM=HWSUM+HW
      IF(X.GE.1.0)MX=MX+1
      FLAG4=0
      IF(IPRI.EQ.0)GO TO 120
      IF(MX.EQ.1)PRINT 255,LENGTH,TSAT,TEMPF
  255 FORMAT('-','QUALITY BECAME ONE AT(FT)=',F8.4,3X,'TSAT=',F7.3,3X,
     3'BULK FLUID TEMPERATURE(F)=',F7.3)
  120 XTOP=X
      IF(X.GE.1.0)H1PC=0.0
      IF(X.GE.1.0)H2P2=HIP
      IPEVAP=(ICP*M)/PNCP
      IF(II.EQ.IPEVAP) GO TO 109
      GO TO 110
  109 ICP=ICP+1
      IF(MODE.EQ.3)GO TO 1970
      IF(ICNHOT.EQ.1.AND.CNROTN.EQ.1)GO TO 71
      IF(II.EQ.1) GO TO 71
      IF((ABS(PRESS-PMCHAM)).LE.0.05)GO TO 71
      GO TO 72
 1970 A1=FLRATE*X
      IF(I.EQ.1) GO TO 71
      CALL DELPBE(A1,LBE,LEQBE,GC,ZBE,IDBE,DPEVAP,NTUBEE,PI,
     3DENSL,VISCL,XABE,DLPBE,DPDL,UNHTL1,DENSG,VISCG,IDUC,NELBOW,
     3LETMCH,DPNONH,DPTEE,DPELBO,DPEXIT)
      PRESS=PVPHR2-DPEVAP-((DPTEE+DPELBO+DPEXIT)*DENSG/144.0)
      CALL QLOSS(A1,TEB,TROOM,LBE,RESBE,HFBOT,QBE,HBOTBE)
      IF((ABS(PRESS-PMCHAM)).LE.0.05)GO TO 73
      A1=X*FLRATE
      GO TO 72
   71 CALL DELPBE(A1,LBE,LEQBE,GC,ZBE,IDBE,DPEVAP,NTUBEE,PI,
     3DENSL,VISCL,XABE,DLPBE,DPDL,UNHTL1,DENSG,VISCG,IDUC,NELBOW,
     3LETMCH,DPNONH,DPTEE,DPELBO,DPEXIT)
      PBOTBE=PLOHR1+DLPBE+DPFLM1+DPFIL1
      CALL QLOSS(A1,TEB,TROOM,LBE,RESBE,HFBOT,QBE,HBOTBE)
      PMCHAM=PVPHR1-DPEVAP-((DPTEE+DPELBO+DPEXIT)*DENSG/144.0)
   73 PRESS=PMCHAM
      IF(MODE.EQ.3)AVDOWN=DOWNST/II
      TFLUD(I)=TEMPF
      FLRAT(I)=FLRATE
      QULTY(I)=X
      QINPT(I)=Q
      SUEVT(I)=TSHS
      EVAPST=SUEVT(I)/RM
      A1=FLRAT(I)*QULTY(I)
      A2=FLRAT(I)-A1
      B1=A1*NTUBEE
      B2=A2*NTUBEE
      VOFP(I)=VOIDFS
      LOFP(I)=LIQFS
      DYNPER=((XAEVAP*HEITB-VOFP(I))/(XAEVAP*HEITB))*100.0
      PERDY(I)=DYNPER
      UAVEV=UAVEV/AREAP
      HWAVG=HWSUM/RM
      SUHITP=SUHITP/RM
      WATH(I)=HWAVG
      HEVAP=(QINPT(I)/(HEITB*IDH*PI*((TSHS/RM)-TSAT)))
      GO TO 74
   72 FLRATE=FLRATE*(((PEB(I)-PMCHAM)/(PEB(I)-PRESS))**POWER)
      GO TO 91
   74 FLRAT(I)=FLRATE
      IF(MODE.NE.3)GO TO 1971
      IF(I.EQ.2)GOTO 204
      PRINT 202,PBOTBE
  202 FORMAT('-','PRESSURE IN THE CHAMBER BELOW THE EVAPORATOR(PSIA)=',
     3F7.3)
      PRINT 203,PLOHR1
  203 FORMAT('-','PRESSURE IN THE LIQUID HEADER FOR EVAPORATOR BOX # 1 (
     3PSIA)=',F7.3)
```

```
      GO TO 1971
  204 PRINT 206,PLOHR2
  206 FORMAT('-','PRESSURE IN THE LIQUID HEADER FOR EVAPORATOR RO# # 2 (
     3PSIA)=',F7.3)
 1971 PRINT 256,I
  256 FORMAT('-','FOR EVAPORATOR LIQIUD HEADER TUBE ROW ',I1)
      PRINT 221
  221 FORMAT(' ','----------------------------------------')
      IF(MODE.EQ.2)PRINT 1958,QFLUX
      GO TO 1959
 1958 FORMAT('-','HEAT FLUX PER UNIT AREA (BTU/HR/SQ-F)=',F9.3)
 1959 PRINT 18,PE9(I),TER,SAAT(I),FLRAT(I)
   18 FORMAT('-','AT EVAP TUBE BOTTOM:  PRESSURE(PSIA)=',F7.3,3X,
     3'TEMP(F)=',F7.3,3X,'TSAT(F)=',F7.3,3X,'FLOW RATE(LB/HR)=',F9.3)
      PRINT 998,HFBOT,DEGSUB
  998 FORMAT(' ','ENTHALPY(BTU/LB)=',F7.3,3X,'INLET SUBCOOLING(F)=',F6.3
     3)
      PRINT 257,LENGTH,X,VOIDF
  257 FORMAT('-','DISTANCE FROM BOTTOM OF EVAPORATOR(FT)=',F8.4,3X,
     3'QUALITY=',F6.4,3X,'VOID FRACTION=',F5.4)
      PRINT 258,AVTSH,TEMPF,TSAT
  258 FORMAT(' ','WALL TEMP(F)=',F7.3,3X,'BULK FLUID TEMP(F)=',F7.3,3X,
     3'SATURATION TEMP(F)=',F7.3)
      PRINT 2260,U
 2260 FORMAT(' ','EFFECTIVE HEAT TRANSFER COEFFICIENT "U" (BTU/HR/FT2/F)
     3=',F9.4)
      PRINT 260,HIPC
  260 FORMAT(' ','1-PHASE LIQUID CONVECTIVE HEAT TRANSFER COEFFICIENT
     3(BTU/HR/FT-FT/F)=',F9.4)
      PRINT 261,H291,HITPB
  261 FORMAT(' ','2-PHASE CONVECTIVE COEFFICIENT(BTU/HR/FT-FT/F)=',F9.4
     3,3X,'BOILING COEFFICIENT(BTU/HR/FT-FT/F)=',F9.4)
      PRINT 262,H292,Q
  262 FORMAT(' ','1-PHASE VAPOUR CONVECTIVE COEFFICIENT(BTU/HR/FT-FT/F)
     3=',F9.4,3X,'CUMULATIVE HEAT INPUT(BTU/HR)=',F9.4)
      PRINT 244,HITP
  244 FORMAT(' ','ACTUAL INSIDE "H" USED IN THE CALCULATION(BTU/HR/FT-2/
     3F)=',F9.3)
      PRINT 1988,PEXITE
 1988 FORMAT(' ','PRESSURE(PSIA)=',F7.3)
      IF(MODE.NE.3)GO TO 1972
      PRINT 263,TOUT(I,M)
  263 FORMAT(' ','DOWNSTREAM AIR TEMP.(F)=',F7.3)
      PRINT 188,AVDOWN,EVAPST
  188 FORMAT(' ','AVERAGE DOWNSTREAM AIR TEMP.(F)=',F7.3,3X,'AVERAGE WAL
     3L TEMP.(F)=',F7.3)
      PRINT 900,UOUT
  900 FORMAT(' ','EVAPORATOR AIR SIDE "U" (BTU/HR/SQ-FT/F)=',F9.4)
      IF(I.EQ.1)PRINT 207,PVPHR1
      IF(I.EQ.2)PRINT 208,PVPHR2
  207 FORMAT('-','PRESSURE IN THE VAPOUR HEADER FOR EVAPORATOR RO# # 1 (
     3PSIA)=',F7.3)
      GO TO 209
  208 FORMAT('-','PRESSURE IN THE VAPOUR HEADER FOR EVAPORATOR RO# # 2 (
     3PSIA)=',F7.3)
  209 PRINT 22,PMCHAM
   22 FORMAT('-','MIXING CHAMBER PRESSURE (PSIA)=',F7.3)
 1972 PRINT 289,A2,A1
  289 FORMAT(' ','RECIRCULATION RATE FOR THIS TUBE(LB/HR)=',F9.3,3X,
     3'VAPOUR FLOW RATE(LB/HR)=',F9.3)
      PRINT 19,B2,B1
   19 FORMAT(' ','RECIRCULATION RATE FOR THIS ROW(LB/HR)=',F9.3,4X,
     3'VAPOUR FLOW RATE FOR THIS ROW(LB/HR)=',F9.3)
      PRINT 176,DYNPER
  176 FORMAT(' ','PERCENT OF EVAP. LENGTH FLOODED UNDER DYNAMIC CONDITIO
     3NS=',F5.1)
      SHEVAP=HEVAP*5.6783
      PRINT 187,HEVAP,SHEVAP
  187 FORMAT('-','EVAP.HEAT TRANSFER COEFF.(BTU/HR/FT2/F)=',F10.4,11X,
     3'IN S.I. UNITS(W/M2/K)=',F10.4)
      SUAVEV=UAVEV*5.6783
      SSUHIT=SUHITP*5.6783
      SHWAVG=HWAVG*5.6783
      PRINT 799,SUHITP,SSUHIT
  789 FORMAT(' ','AVERAGE ACTUAL "H" IN THE EVAPORATOR(BTU/HR/FT2/F)=',
     3F10.3,3X,'IN S.I. UNITS(W/M2/K)=',F10.4)
      IF(MODE.NE.1)GO TO 110
      PRINT 577,TWIN
  577 FORMAT('-','INCOMING TEMP. OF THE WATER(F)=',F7.3)
      PRINT 191,TWOUT,HW
```

```
      191 FORMAT(' ','OUTGOING TEMP. OF THE WATER(F)=',F7.3,3X,'WATER SIDE "
     &H" (BTU/HR/FT-2/F)=',F10.3)
          PRINT 981,HWAVG,SHWAVG
      981 FORMAT(' ','AVERAGE WATER SIDE "H" FOR THE EVAP.=',F10.3,17X,
     &'IN S.I. UNITS(W/M2/K)=',F10.4)
          PRINT 198,UAVEV,SUAVEV
      198 FORMAT('-','AVERAGE EVAPORATOR OVERALL "U"(BTU/HR-FT-FT/F)=',F10.4
     &,7X,'IN S.I. UNITS(W/M2/K)=',F10.4)
      110 IF(L.EQ.1)GO TO 410
          GO TO 412
      410 SCL=LENGTH
          IF(IPPI.EQ.0)GO TO 125
          PRINT 414 ,SCL
      414 FORMAT('-','INITIATION OF SUBCOOLED BOILING AT HEIGHT FROM BOTTOM
     &OF HEATER(FT)=',F7.3)
      125 L=L+1
      412 IF(P.EQ.1.0)GO TO 413
          GO TO 1
      413 SCB=LENGTH
          IF(IPPI.EQ.0)GO TO 126
          PRINT 415,SCB
      415 FORMAT('-','BULK BOILING BEGINS AT HEIGHT FROM BOTTOM OF HEATER
     &(FT)=',F7.3)
      126 P=P+1.0
        1 CONTINUE
          IF(ICNHOT.EQ.1.AND.CNROTN.EQ.1)GO TO 919
          I=I+1
          A1=0.5*A1
          FLRATE=FLRATE*(((PEB(I)-PMCHAM)/(PEB(I)-PRESS))**POWER)
          IF(I.GT.NR) GO TO 78
          GO TO 91
C         ***************************************************************
C         *                    END OF EVAPORATOR TUBE CYCLE             *
C         ***************************************************************
       78 TOTALQ=0.0
          TOTALF=0.0
          TOTREC=0.0
          IF(MODE.NE.3)GOTO 1975
          EFLOP1=((THOTG-AVDOWN)/(THOTG-TAIR))*100.0
          EFLOP4=(((4.0*EFLOP1/100.0))/(1.0+(3.0*EFLOP1/100.0)))*100.)
          PRINT 287,EFLOP1,EFLOP4
      287 FORMAT('-','EFFECTIVENESS OF THERMOSIPHON FOR A SINGLE LOOP (%)=',
     &F7.3,3X,'FOR FOUR LOOPS (%)=',F7.3)
     1975 TEMPF=TFLUD(1)
          DO 92 I=1,NR
       92 TOTALQ=TOTALQ+QINPT(I)*NTUBEE
          DO 93 I=1,NR
       93 TOTALF=TOTALF+FLRAT(I)*NTUBEE
          DO 94 I=1,NR
       94 TOTREC=TOTREC+FLRAT(I)*NTUBEE*(1-QULTY(I))
          QIN=TOTALQ
          PRINT 95,QIN
       95 FORMAT('-','TOTAL CUMULATIVE HEAT INPUT(FOR ALL THE TUBES(BTU/HR))
     &=',F14.4)
          IF(MODE.NE.2)GOTO 1998
          DO 96 I=1,NR
       96 AVWATH=AVWATH+WATH(I)
          AVWATH=AVWATH/NR
     1998 QES=TOTALQ
          FLRATE=TOTALF
          FRECRC=TOTREC
          FLRATE=FLRATE-FRECRC
          IF(MODE.EQ.3)GO TO 1982
          VOIDFS=(VOFR(1)+VOFR(2)+VOFR(3))*NTUBEE
          LIQFS=(LQFR(1)+LQFR(2)+LQFR(3))*NTUBEE
          AVEVT1=SUEVT(1)/RM
          AVEVT2=SUEVT(2)/RM
          GO TO 920
     1982 IF(NROWE.EQ.1)GO TO 89
          VOIDFS=(VOFR(1)+VOFR(2)+VAPV1+VAPV2)*NTUBEE
          LIQFS=(LQFR(1)+LQFR(2)+LIQV1+LIQV2)*NTUBEE
          GO TO 90
       89 LIQFS=(LQFR(1)+LIQV1)*NTUBEE
          VOIDFS=(VOFR(1)+VAPV1)*NTUBEE
       90 QES=TOTALQ
          AVEVT1=SUEVT(1)/RM
          PERDY1=PERDY(1)
          IF(NROWE.EQ.1)GO TO 211
          AVEVT2=SUEVT(2)/RM
          PERDY2=PERDY(2)
```

```
      211 PEVTOP=PEXITE
          GO TO 920
      919 QIN=0
          FLRATE=FLRATE*NTUBEE*NR
          LIQFS=LIQFS*NTUBEE*NR
          VOIDFS=VOIDFS*NTUBEE*NR
          QES=QIN*NR*NTUBFE
          AVWATH=HWAVG
          PRINT 95,QES
          AVTSHS=TSHS/RM
          AVEVT1=AVTSHS
          AVEVT2=AVTSHS
          AVEVT3=AVTSHS
          TOTALF=FLRATE
          FRECRC=FLRATE*(1.0-X)
          TOTREC=FRECRC
          FLRATE=FLRATE*X
      920 PEVTOP=PRESS
          TEVTOP=TEMPF
          TSETOP=TSAT
          TOTFLE=FLRATE
          IF(MODE.EQ.3)GOTO 556
          HAVEVP=QES/((((AVEVT1+AVEVT2)/2.0)-TSAT)*NTUBEE*NR*PI*(DH
         2*HEITB)
          HEVPSI=HAVEVP*5.6783
          PRINT 888,HAVEVP,HEVPSI
      888 FORMAT('-','AVERAGE HEAT TRANSFER COEFF. FOR THE EVAP.(BTU/HR-FT2/
         2F)=',F9.4,3X,'IN S.I. UNITS(W/M2-K)=',F10.4)
          IF(ICNHOT.EQ.1.AND.CNROTN.EQ.1)GO TO 557
          ELEXT1=ELEXT(1)
          ELEXT2=ELEXT(2)
          ELEXT3=ELEXT(3)
          PERDY1=PERDY(1)
          PERDY2=PERDY(2)
          PERDY3=PERDY(3)
          GO TO 718
      557 ELEXT1=TWOUT
          ELEXT2=TWOUT
          ELEXT3=TWOUT
          PERDY1=DYNPER
          PERDY2=DYNPER
          PERDY3=DYNPER
          IF(CNROTN.EQ.1.0)GO TO 718
          GO TO 719
      718 CALL LIQVOL(FRECRC,VLIQHE)
          LIQFS=LIQFS+VLIQHE
      719 LIQFS=LIQFS+VSTRAN
      556 HF=HFBOT+QES/TOTALF
C     ***************************************************************
C     *                  START OF SEPARATOR CALCULATIONS            *
C     ***************************************************************
          CALL LIQHF(TEMPF,HFL)
          CALL LIQCP(TEMPF,SPHTL)
          HR=HFL
          CALL GAS CP(TEMPF,SPHTG)
          HF=(TOTALF*HF-TOTREC*HR)/FLRATE
          X=1.0
          VOIDF=1.0
C     ***************************************************************
C     *      VAPOUR HEADER PIPE FLOW AND HEAT TRANSFER CALCULATIONS *
C     ***************************************************************
          CALL FRCSHN(FLRATE,IDUC,DENSG,VISCG,PI,F,VF)
          RENG=VF*IDUC*DENSG/VISCG
          IF(FLAGUP.EQ.1)PRESS=(PRESS*144.0)-(DPUPXO*144.0)
          IF(FLAGUP.EQ.1)GO TO 923
          DPF=F*(LUPXO+LEQAE)/IDUC*((VF**2.0)/2.0/GC)*DENSG
          DPH=LUPXO*SIN(BETA)*DENSG
          PRESS=(PRESS*144.0-DPH-DPF)
      923 PRESS=PRESS/144.0
          CALL SAT TEM(PRESS,TSAT)
          EFFECT=1.0-(EXP(-(LUPXO/(RESUP*FLRATE*SPHTG))))
          QUPXO=EFFECT*FLRATE*SPHTG*(TSETOP-TAIR)
          CALL HFGTS(TCP,TSAT,HFG2)
          CALL HFLS(TSAT,HF2)
          HF=HF-(QUPXO/FLRATE)
          TEMPF=TEMPF-(QUPXO/(FLRATE*SPHTG))
          HG2=HFG2+HF2
          IF(HF.GT.HG2)GO TO 710
          X=(((HF-HF2)/HFG2)+X)/2.0
          TEMPF=TSAT
```

```
      FLUPXO=FLRATE*(1.0-X)
      FRECRC=FRECRC+FLUPXO
      FLRATE=FLRATE*X
      CALL FRCSHN(FLUPXO,IDUC,DENSL,VISCL,PI,F,VF)
      RENF=VF*IDUC*DENSL/VISCL
      CALL     XPCAL(RENF,RENG,VISCL,VISCG,DENSL,DENSG,X,XP)
      LIQF=(1.0-(1.0/((1.0+XP**0.8)**0.378)))
      VOIDF=1.0-LIQF
  710 VOIDFS=VOIDFS+(VOIDF*LUPXO*XAUPRX)
      LIQFS=LIQFS+(LIQF*LUPXO*XAUPRX)
      X=1.0
      VOIDF=1.0
C     ***************************************************************
C     *                                                             *
C     *              RECIRCULATION TUBE CALCULATIONS                *
C     *                                                             *
      IF(FRECRC.LE.0.15)EFFECT=1.0
      IF(FRECRC.LE.0.15)GO TO 500
      EFFECT=1.0-(EXP(-(RECRCL/(RESLO*FRECRC*SPHTL))))
  500 QRECRC=EFFECT*FRECRC*SPHTL*(TEVTOP-TAIR)
      TRECRC=TEVTOP-(EFFECT*(TEVTOP-TAIR))
      IF(FRECRC.LE.0.01)GO TO 502
      HR=HR-(QRECRC/FRECRC)
  502 HELOXO=((TOTALF*HFBOT)-(FRECRC*HR))/FLRATE
      TEMPLO=TEMPF
  666 CALL LIQHF(TEMPLO,HFCK)
      IF((ABS(HELOXO-HFCK))-0.01)667,667,668
  668 CALL LIQCP(TEMPLO,SPHTLO)
      TEMPLO=TEMPLO+((HELOXO-HFCK)/SPHTLO)
      GO TO 666
  667 CALL LIQDEN(TEMPLO,DNSLO)
      CALL LIQVIS(TEMPLO,VSCLO)
      IF(MODE.EQ.3)GO TO 1983
      IF(IPRINT.EQ.0)GO TO 641
      WRITE(6,658)FRECRC
      WRITE(6,177)FLRATE
  658 FORMAT(' ',' TOTAL RECIRCULATION RATE(FOR ALL TUBES(LB/HR))=',F9.2)
  177 FORMAT(' ',' TOTAL VAPOUR RATE(FOR ALL TUBES(LB/HR))=',F9.2)
      GO TO 641
 1983 K1=FLRAT(1)*(1.0-QULTY(1))*NTUBEE
      CALL FRCSHN(K1,RECID,DENSL,VISCL,PI,F,VRECRC)
      FRIC=((VRECRC**2.0)/2.0/GC)*(F/RECID)
      RENF=VRECRC*RECID*DENSL/VISCL
      ZREC1=(((PLQHR1-PVPHR1)*144.0/DENSL)-(FRIC*LEQRE))/(1.0+FRIC)
      ZMAX=(HEITB*COS(SIGMA))+HDIAME
      IF(NROWE.EQ.1)GO TO 212
      K2=FLRAT(2)*(1.0-QULTY(2))*NTUBEE
      CALL FRCSHN(K2,RECID,DENSL,VISCL,PI,F,VRECRC)
      FRIC=((VRECRC**2.0)/2.0/GC)*(F/RECID)
      RENF=VRECRC*RECID*DENSL/VISCL
      ZREC2=(((PLQHR2-PVPHR2)*144.0/DENSL)-(FRIC*LEQRE))/(1.0+FRIC)
  212 IF(ZREC1.LE.ZMAX)GO TO 1637
      FLRATE=FLRAT(1)*(ZMAX/ZREC1)
      WRITE(6,639)
  639 FORMAT('-',' HEIGHT OF LIQUID COLUMN TOO LARGE:REDUCING FLOW RATE')
      FLAG2=FLAG2+1
      TEMPF=TEB
      PRESS=PEB(1)
      GO TO 307
 1637 FLDEV1=ZREC1/COS(SIGMA)
      WRITE(6,636)FLDEV1
  636 FORMAT('-',' LENGTH OF LIQUID COLUMN IN RECIRCULATION TUBE FOR ROW
     1# 1(FT)=',F7.3)
      IF(NROWE.EQ.1) GO TO 213
      FLDEV2=ZREC2/COS(SIGMA)
      WRITE(6,633)FLDEV2
  633 FORMAT(' ',' LENGTH OF LIQUID COLUMN IN RECIRCULATION TUBE FOR ROW
     1# 2(FT)=',F7.3)
  213 SIGHT1=((PLQHR1-PVPHR1)*144.0/DENSL)
      PSIGT1=((SIGHT1-(2.0/12.0))/HEITB)*100.0
      IF(NROWE.EQ.1) GO TO 214
      SIGHT2=((PLQHR2-PVPHR2)*144.0/DENSL)
C     PSIGT2=((SIGHT2-(4.0/12.0))/HEITB)*100.0
  214 CALL VOIHDE(LHDEVP,HDIAME,ZREC1,HEITB,SIGMA,HEDVLE,PI,NTUBEE,
     1VOFHDE,LIQHDE,FLAG3)
      VOIDFS=VOIDFS+VOFHDE+HEDVLC
      LIQFS=LIQFS+LIQHDE
      IF(NROWE.EQ.1)ZREC2=0.0
      VOIDFS=VOIDFS+XARCRC*(NROWE*RECRCL-((ZREC1/COS(SIGMA))-(ZREC2/
     1COS(SIGMA))))
      LIQFS=LIQFS+XARCRC*((ZREC1/COS(SIGMA))+(ZREC2/COS(SIGMA)))
```

```
1041.           GO TO 1984
1042.       641 ZMAX=(HEITB*COS(SIGMA))+HDIAME
1043.           CALL LIQDEN(TEVTOP,DENSL)
1044.           CALL LIQVIS(TEVTOP,VISCL)
1045.           CALL FRCSHN(FRECRC,RECID,DENSL,VISCL,PI,F,VRECRC)
1046.           FRIC=((VRECRC**2.0)/2.0/GC)*(F/RECID)
1047.           RENF=VRECRC*RECID*DENSL/VISCL
1048.           ZRECRC=(((PBOT-PEVTOP)*144.0/DENSL)-(FRIC*LEQRE))/
1049.          3(1.0+FRIC)
1050.           IF(ZRECRC.LE.ZMAX)GO TO 637
1051.           FLRATE=FLRAT(I)*(ZMAX/ZRECRC)
1052.           WRITE(6,639)
1053.           FLAG2=FLAG2+1
1054.           TEMPF=TES
1055.           PRESS=PES(I)
1056.           GO TO 307
1057.       637 FLDEVP=ZRECRC/(COS(SIGMA)*SIN(THETA))
1058.           PRCFL=(FLDEVP/HEITB)*100.0
1059.           WRITE(6,1636)FLDEVP
1060.      1636 FORMAT('-','LENGTH OF LIQUID COLUMN IN RECIRCUL. TUBE(FT)=',F7.3)
1061.           CALL VOIDHDE(LHDEVP,HDIAME,ZRECRC,HEITB,SIGMA,HEDVLE,PI,NTUBES,
1062.          3VDFHDE,LIQHDE,FLAG3)
1063.           VOIDFS=VOIDFS+VDFHDE+HEDVLC
1064.           LIQFS=LIQFS+LIQHDE
1065.           IF(FLAG3.EQ.0)GO TO 681
1066.           VOIDFS=VOIDFS+(XARCRC*(RECRCL-(ZRECRC/COS(SIGMA))))
1067.           LIQFS=LIQFS+(XARCRC*(ZRECRC/COS(SIGMA)))
1068.           GO TO 299
1069.       681 LIQFS=LIQFS+(RECRCL*XARCRC)
1070.      1984 DPCOND=(PBOT-PRESS)*144.0/DNSLO
1071.C          ************************************************************
1072.C          *                START OF CONDENSER CALCULATIONS           *
1073.C          ************************************************************
1074.       299 IF(IPRINT.EQ.0)GO TO 124
1075.           PRINT 222,QUPXO
1076.       222 FORMAT('-','HEAT LOSS BETWEEN EVAP. AND COND. VAPOUR HEADER(BTU/HR
1077.          3)=',F9.4)
1078.           PRINT 77,PRESS,TEMPF
1079.        77 FORMAT(' ','PRESSURE AT THE TOP  OF CONDENSER=' ,F9.5,5X,'
1080.          3TEMPERATURE   AT THE TOP  OF CONDENSER= ',F7.3)
1081.           PRINT 337,X,VOIDF,TSAT
1082.       337 FORMAT(' ','QUALITY AT THE TOP  OF CONDENSER=' ,F7.4,5X,'VOID
1083.          3FRACTION=',F8.5,3X,'SATURATION TEMP=',F7.3)
1084.       124 CALL FRCSHN(FLRATE,IDC,DNSLO,VSCLO ,PI,FTEF,VFTEF)
1085.           FLRATE=FLRATE/(NTUBEC*NP)
1086.           CALL FRCSHN(FLRATE,IDC,DNSLO,VSCLO ,PI,FCOP,VFCOP)
1087.           FRCOP=FCOP/IDC*((VFCOP**2.0)/2.0/GC)
1088.           FRTEF=FTEF/IDUC*((VFTEF**2.0)/2.0/GC)
1089.           ZRECRC=ZREC1
1090.           IF(ZRECRC.LE.ELEV)GO TO 643
1091.           ZCOND=(DPCOND-(FRTEF*((LLOXO*COS(LEM))+ELEV+LEQAC))+((FRCOP*ELEV)/
1092.          3(SIN(GAM)*COS(ALPHA))))/(1.0+(FRCOP/(SIN(GAM)*COS(ALPHA))))
1093.           IF(ZCOND.GT.ELEV)GO TO 649
1094.       643 ZCOND=(DPCOND-(FRTEF*((LLOXO*COS(LEM))+LEQAC)))/(1.0+FRTEF)
1095.       649 FLDCND=(ZCOND-ELEV)/(SIN(GAM)*COS(ALPHA))
1096.           FLDCND=0.0
1097.           IF(FLDCND.LE.0.0)FLDCND=0.0
1098.           CALL THCOND(TSAT,KL)
1099.           CALL LIQ DEN(TSAT,DENSL)
1100.           CALL LIQ CP(TSAT,SPHTL)
1101.           CALL LAT HT(TCR,TSAT,HFG)
1102.           CALL LIQVIS(TSAT,VISCL)
1103.           CALL LIQHF(TSAT,HFL)
1104.           LCNDSN=HEITC-FLDCND
1105.           DLNGTH=LCNDSN/10.0
1106.           HFTOP=HF
1107.           ICP=1
1108.           TSCS=0.0
1109.           WRITE(6,265)FLDCND,LCNDSN
1110.       265 FORMAT('-','FLOODED CONDENSER LENGTH(FT)=',F7.3,3X,'LENGTH AVAILAB
1111.          3LE FOR CONDENSATION(FT)=',F7.3)
1112.           IF(MODE.EQ.3)GO TO 1985
1113.           AHTCND=LCNDSN*PI*IDC
1114.           CALL VTRPRP(TW2    ,DENSW,VISCW,KW)
1115.           RENW2=DEQVC*GWC/VISCW
1116.           PRW2=VISCW*SPHTW/KW
1117.           DO 697 LC=1,10
1118.           RLC=LC-1
1119.           FCT=((1.0+(3.0/EXP((FLDCND+(DLNGTH*(RLC+0.5)))/(30.0*DEQVC))))/EN
1120.          3TFAC
```

```
1121.            IF(RENW2-1900.0)691,691,692
1122.        692 NUW=0.02*(RENW2**0.8)*(PRW2**0.3333)*((EXT(DC/(DDC))**0.53)
1123.            HW2=FCT*KW*NUW*3600.0/DEQVC
1124.            GO TO 1567
1125.        691 FC=((1.0+(3.5/EXP((FLDCND+(DLNGTH*(RLC+0.5)))/(90.0*DEQVC)))))/ENT
1126.           1FAC
1127.            HW2=(1.55*KW/DEQVC*(RENW2*PRW2*DEQVC/(FLDCND+(DLNGTH*(RLC+0.5))))
1128.           1**0.333)*3600.0*FC
1129.       1567 HW2SW2=HW2SW2+HW2
1130.        697 CONTINUE
1131.            HW2=HW2SW2/10.0
1132.            CALL CONCOF(KL,DENSL,HFG,GC,VISCL,LCNDSN,ALPHA,ALFMIN,IDC,
1133.           1HF,HFL,FLRATE,TSAT,AHTCND,HW2,HTCFCN,CF,TCNDWL,QCOND,TCOLD)
1134.            ZZ=1.0/((ALOG(ODC/IDC)*IDC/(2.0*KM))+FOULHW+IDC/ODC/HW2)
1135.            TCOLD=TCNDWL-(QCOND /ZZ/AHTCND)
1136.            DT=TSAT-TCNDWL
1137.            AVFLTH=1.131*(((VISCL*KL*LCNDSN*DT)/(GC*(DENSL**2)*HFG   ))**0.25)
1138.            IF(ALPHA.GT.ALFMIN)AVFLTH=(KL*3600.0)/HTCFCN
1139.            VOID=(((IDC-(2.0*AVFLTH))**2)*(PI/4.0))*LCNDSN
1140.            VOIDF=VOID/(LCNDSN*XACOND)
1141.            CALL   MT  COND(TEMPF,KM)
1142.            RCOND=(1.0/HTCFCN+IDC/ODC/HW2+((ALOG(ODC/IDC))*IDC/
1143.           1(2.0*KM)))/(AREAC*NTUBEC*NR)
1144.            TEMPF=TSAT
1145.            DLNGTH=(HEITC-LCNDSN)/(DIVCON-1.0)
1146.            HW2CN=HW2
1147.            TW2OUT=TCOLD+(QCOND/(MCLWTR*SPHTW))
1148.            LENGTH=LCNDSN
1149.            LCON=0.0
1150.            Q=QCOND
1151.            TCWOUT=TCNDWL-(QCOND*THICKC/KM/AHTCND)
1152.            TSCSCN=(TCNDWL+TCWOUT)/2.0
1153.            AVTSC=TSCSCN
1154.            H1C=0.0
1155.            X=0.0
1156.            SATCON=TSAT
1157.            PCOBOT=PRESS
1158.            IF(IPRINT.EQ.0)GO TO 264
1159.            PRINT 269,LENGTH,X,VOIDF
1160.            PRINT 258,AVTSC,TEMPF,TSAT
1161.            PRINT 270,HTCFCN
1162.            PRINT 271,H1C
1163.            PRINT 272,Q,PRESS
1164.            GO TO 264
1165.       1985 KK=DIVCON
1166.            K=1
1167.       1974 Q=0.0
1168.            L=DIVCON
1169.            FL(K)=FLRATE
1170.            DO 1977 KK=1,L
1171.            AHTCND=LCNDSN*PI*IDC
1172.            HTCFNT=0.943*3600.0*(((KL**3)*(DENSL**2)*HFG*GC/(VISCL*LCNDSN))
1173.           1**0.25)
1174.            IF(ALPHA.GT.ALFMIN)HTCFNT=CF*3600.0*(((KL**3)*(DENSL**2)*HFG*GC/
1175.           1(VISCL*IDC))**0.25)
1176.            IF(K.EQ.1)QC(K,KK)=(HF-HFL)*FL(K)
1177.            CALL AIRDEN(TAIR,DENAIR)
1178.            CALL       EFF(DISCND,AREAC,TAIR,PI,IDC,ODC,CPAIR,GC,ROUT,
1179.           1TCR,DENAIR,CF,DUCTXS,ALPHA,ALFMIN,TUSPCE,HEITC,UA)
1180.            UOUTC=(1.0/ROUT)*(1.0/AREAC)
1181.            UATOT=(UA*NTUBEC)
1182.            NTU=(((UATOT)/(CPAIR*DISCND*DENAIR*3600)))
1183.            EFFECT=1.0-(1.0/EXP(NTU))
1184.            IF(K.EQ.2)GO TO 1990
1185.            TCOLD=TSAT-(((QC(K,KK)*NTUBEC)/(CPAIR*DISCND*DENAIR*3600.
1186.           10*EFFECT))
1187.            TCOUT(K,KK)=TCOLD+(((QC(K,KK)*NTUBEC)/(CPAIR*DISCND*DENAIR*3600)))
1188.            QQCC1=QC(K,KK)
1189.            GO TO 1979
1190.       1990 QC(K,KK)=EFFECT*CPAIR*DISCND*DENAIR*3600.0*(TSAT-TCOUT(K-1,KK))
1191.            TCOUT(K,KK)=TCOUT(K-1,KK)+(QC(K,KK)/(CPAIR*DISCND*DENAIR
1192.           1*3600.0))
1193.            QC(K,KK)=QC(K,KK)/NTUBEC
1194.            QQCC2=QC(K,KK)
1195.       1979 TCNDWL=TSAT-((QC(K,KK)/HTCFNT/AHTCND)**1.33333)
1196.            HTCFCN=HTCFNT/(((TSAT-TCNDWL)**0.25)
1197.            DT=TSAT-TCNDWL
1198.            AVFLTH=1.131*(((VISCL*KL*LCNDSN*DT)/(GC*(DENSL**2)*HFG   ))**0.25)
1199.            IF(ALPHA.GT.ALFMIN)AVFLTH=(KL*3600.0)/HTCFCN
1200.            VOID=(((IDC-(2.0*AVFLTH))**2)*(PI/4.0))*LCNDSN
```

```
1201.            VOIDF=VOID/(LCNDSN*XACOND)
1202.            CALL   MT COND(TEMPF,KM)
1203.            RCOND=(1.0/HTCFCN+(1.0/UOUT)*(IDC/ODC)+((ALOG(ODC/IDC))*IDC/
1204.           $(2.0*KM)))/(AREAC*NTUBEC*NROWC)
1205.            TEMPF=TSAT
1206.            LENGTH=LCNDSN
1207.            LCON=0.0
1208.            Q=Q+QC(K,KK)
1209.            IF(K.EQ.2.AND.KK.EQ.DIVCON)FL(K)=Q/HFG
1210.            TCWOUT=TCNDWL-(QC(K,KK)*THICKC/KM/AHTCND)
1211.            TSCSCN=(TCNDWL+TCWOUT)/2.0
1212.            AVTSC=TSCSCN
1213.            H1C=0.0
1214.            X=0.0
1215.            VODC(K)=VOIDF
1216.            HCON(K)=HTCFCN
1217.            AVTC(K)=AVTSC
1218.            TCAIR(K)=TCOUT(K,KK)
1219.            CONDQ(K)=QC(K,KK)
1220.            SATCON=TSAT
1221.            IF(KK.NE.L)GOTO 1977
1222.       1977 CONTINUE
1223.            K=K+1
1224.            IF(K.GT.NR)GO TO 566
1225.            GO TO 1974
1226.        566 TOTFLC=(FL(1)+FL(2))*NTUBEC
1227.            IF(ABS(TOTFLC-TOTFLE).LE.5.5)GO TO 567
1228.            IF(TOTFLC.GT.TOTFLE)FLRATE=0.9*FL(1)
1229.            IF(TOTFLC.LT.TOTFLE)FLRATE=1.22*FL(1)
1230.            K=1
1231.            GO TO 1974
1232.        567 J=NROWC
1233.            DO 1991 K=1,J
1234.            PRINT 1980,K
1235.       1980 FORMAT('-','FOR CONDENSER TUBE ROW #',I1)
1236.            PRINT 221
1237.            PRINT 1976,FL(K)
1238.       1976 FORMAT('-','VAPOUR FLOW RATE/TUBE FOR THIS ROW(LB/HR)=',F9.3)
1239.            PRINT 269,LENGTH,X,VODC(K)
1240.            PRINT 258,AVTC(K),TEMPF,TSAT
1241.            PRINT 270,HCON(K)
1242.            PRINT 271,H1C
1243.            PRINT 272,CONDQ(K),PRESS
1244.            PRINT 1979, TCAIR(K)
1245.       1979 FORMAT(' ','DOWNSTREAM AIR TEMPERATURE (F)=',F7.3)
1246.       1991 CONTINUE
1247.            PRINT 565,UOUTC
1248.        565 FORMAT('-','CONDENSER AIR SIDE "U" (BTU/HR/SQ-FT/F)=',F9.4)
1249.            CALL CNLQHR(FLRATE,NTUBEC,XACOND,DENSL,VISCL,IDH,GC,LHOCN),VOLUME)
1250.            LIQFS=LIQFS+2*VOLUME
1251.        264 IF(FLDCND.EQ.0.0)GO TO 612
1252.            J=0
1253.            ACNDEL=3.1*IDC*DLNGTH
1254.        235 J=J+1
1255.            Q=0.0
1256.            TW2IN=TW2OUT
1257.            TEM=TEMPF
1258.            LCON=LCON+DLNGTH
1259.            LENGTH=LENGTH+DLNGTH
1260.            FM=(1.0+(9.0/EXP(LCON/10.0*IDC)))
1261.            FC=(1.0+(3.5/EXP((HEITC+(DLNGTH/2.0)-LENGTH)/(90.0*DEQVC))))
1262.            FCT=(1.0+(3.0/EXP((HEITC+(DLNGTH/2.0)-LENGTH)/(30.0*DEQVC))))
1263.            RENW2=DEQVC*GWC/VISCW
1264.            PRW2=VISCW*SPHTW/KW
1265.            IF(RENW2-1900.0)694,694,571
1266.        571 NUW=0.02*(RENW2**0.8)*(PRW2**0.3333)*((EXTIDC/(ODC))**0.53)
1267.            HW2=FCT*KW*NUW*3600.0/DEQVC
1268.            GO TO 1001
1269.        694 HW2=(1.86*KW/DEQVC*(RENW2*PRW2*DEQVC/(HEITC+(DLNGTH/2.0)-LENGTH))
1270.           $**0.3333)*3600.0*FC
1271.       1001 CALL        LIQ DEN(TEM  ,DENSL)
1272.            CALL        LIQ VIS(TEM  ,VISC)
1273.            REN=(IDC   *GF)/VISC
1274.            CG=3.144*(REN**(-0.078153))*((LCON/IDC)**(-1.93/(REN**0.3)))
1275.            VOIDF=0.0
1276.            PRESS=PRESS*144.0
1277.            VF=GF/DENSL
1278.            CALL LIQ CP(TEM  ,SPHTL)
1279.            CALL        TH COND(TEM  ,KF)
1280.            CALL        MT COND(TEM  ,KM)
```

```
1291.           PR=SPHTL*VISC /KF
1292.           CALL          LAT HT(TCR,TEMPF,HFG)
1293.           Y=1.0
1294.           AA=IDC
1295.           BB=LCON
1296.           CC=0.3
1297.           HH=H1C
1298.       141 CALL      SPHASE(AA,BB,CC,HH,Y,REN,KF,PR,FM,VISC,VISWAL,CG)
1299.           H1C=HH
1300.           IF(R.EQ.0.0)GO TO 550
1301.       551 R=R+1.0
1302.           IF(REN -2000.0)817.817.818
1303.       817 F=64.0/REN
1304.           GO TO 591
1305.       818 F=4.0*0.079/(REN**0.25)
1306.       591 HIL2=HITP2
1307.           GO TO 146
1308.       550 U2=1.0/(1.0/HITP2+(1.0/UOUT)*ACNDEL*(IDC/ODC)+((ALOG(ODC /IDC ))
1309.          3*(DC/(2.0*KM))  +FOULNW+FOULNF)
1310.           QQ=U2*ACNDEL*(TEM-TAIR  )
1311.           UF2=1.0/(1.0/HITP2+FOULNF)
1312.           TSCF=TEMPF-QQ/(UF2*ACNDEL)
1313.           IF(Y.EQ.1.0)GO TO 147
1314.           IF((ABS(TSCF-TSCFD))-TA)551.551.147
1315.       147 CALL          VISCL*(TSCF,VISWAL)
1316.           Y=Y+1.0
1317.           TSCFD=TSCF
1318.           GO TO 141
1319.       146 TSCW=TSCF-QQ*THICKC/KM/ACNDEL
1320.           AVTSC=(TSCF+TSCW)/2.0
1321.           TSCS=TSCS+AVTSC
1322.           Q=Q+QQ
1323.           DPF=F*DLNGTH/IDC   *((VF **2.0)/2.0/GC)*DENSL
1324.           DPA=0.0
1325.           DPH=DLNGTH*DENSL*SIN(GAM  )*COS(ALPHA)
1326.           PRESS=PRESS+DPH-DPF+DPA
1327.           PRESS=PRESS/144.0
1328.           PCOBOT=PRESS
1329.           CALL          SAT TEM(PRESS,TSAT)
1330.           SATCO=TSAT
1331.           IPCOND=ICP*(ICNOSB/RNCC)
1332.           IF(J.EQ.IPCOND)GO TO 1000
1333.           GO TO 30
1334.      1000 ICP=ICP+1
1335.           PRINT 269,LENGTH,X,VOIDF
1336.       269 FORMAT('-','DISTANCE FROM CONDENSER TOP(FT)=',F8.4,3X,'QUALITY=',
1337.          3F6.4,3X,'VOID FRACTION=',F6.4)
1338.           PRINT 258,AVTSC,TEMPF,TSAT
1339.           PRINT 270,HTCFCN
1340.       270 FORMAT(1X,'INSIDE CONDENSATION COEFFICIENT(BTU/HR/FT-FT/F)=',F9.4)
1341.           PRINT 271,H1C
1342.       271 FORMAT(' ','1-PHASE LIQUID CONVECTIVE COEFFICIENT(BTU/HR/FT-FT/F)
1343.          3=',F9.4)
1344.           PRINT 272,Q,PRESS
1345.       272 FORMAT(' ','HEAT REMOVED(BTU/HR)=',F9.4,3X,'PRESSURE(PSIA)=',F7.3)
1346.           IF(FLOCND.EQ.0.0)GO TO 612
1347.        30 IF(J.LT.ICNOSB)GO TO 235
1348.       612 QOUT=0
1349.           FLRATE=FLRATE*NTUBEC*NR
1350.           IF(MODE.NE.3)QOUTOT=QOUT*NTUBEC*NROWC
1351.           IF(MODE.EQ.3)QOUTOT=(QOCC1+QOCC2)*NTUBEC
1352.           IF(MODE.EQ.3)FLRATE=TOTFLE
1353.           PRINT 613,QOUTOT
1354.       613 FORMAT('-','TOTAL HEAT REMOVED(BTU/HR)=',F14.4)
1355.           QCS=QOUTOT
1356.           VOIDFS=VOIDFS+(VOID*NTUBEC)
1357.           LIQFS=LIQFS+((FLOCND*XACOND)+((1.0-VOIDF)*XACND*LCNDSN))*NTUBEC
1358.           HF=HFTOP-(QCS/FLRATE)
1359.           AVTSCS=(TSCSCN*LCNDSN/HEITC)+((TSCS/(DIVCON-1.0))*(FLOCND/HEITC))
1360.           IF(MODE.EQ.3)GOTO 1992
1361.           HW2AVG=(HW2CN*LCNDSN/HEITC)+((HW2SUM/(DIVCON-1.0))*(FLOCND/HEITC))
1362.           PRINT 980,HW2AVG
1363.       980 FORMAT('-','AVERAGE WATER SIDE "H" FOR THE COND.(BTU/HR/FT/FT/F)='
1364.          3,F10.3)
1365.C          ************************************************************
1366.C          *                START OF CONDENSATE RETURN LINE CALCULATIONS      *
1367.C          ************************************************************
1368.      1992 EFFECT=1.0-(EXP(-(LLOXO/(PESLO*FLRATE*SPHTL))))
1369.           QLOXO=EFFECT*FLRATE*SPHTL*(TEMPF-TAIR)
1370.           HF=HF-(QLOXO/FLRATE)
```

```
1361.            HFBOTN=((FLRATE*HF)+(FRECRC*HR))/(FLRATE+FRECRC)
1362.            TEMPF=TEB
1363.            TEMPMX=TEMPF
1364.          675 CALL LIQHF(TEMPF,HFCK)
1365.            IF((ABS(HFBOTN-HFCK))-0.01)695,695,698
1366.          698 CALL LIQCP(TEMPF,SPHTL)
1367.            TEMPF=TEMPF+((HFBOTN-HFCK)/SPHTL)
1368.            TEMPMX=TEMPF
1369.            GO TO 675
1370.          695 FLRATE=FLOAT(1)
1371.      C   ***************************************************************
1372.      C   *                    START OF CONVERGENCE ROUTINE             *
1373.      C   ***************************************************************
1374.            IF(IPRINT.EQ.0)GO TO 642
1375.            WRITE(6,603)TCOLD
1376.          603 FORMAT('-','INLET COOLING FLUID TEMP(F)=',F7.3)
1377.          642 IF(ABS(TCOLD-TW2).LE.0.5)GO TO 677
1378.            IF(IPRI.EQ.0)GO TO 679
1379.            WRITE(6,678)TEMPMX,TEB
1380.          678 FORMAT('-','NEW INITIAL TEMPERATURE(F)=',F7.3,5X, 'OLD INITIAL TEM
1381.           1PERATURE(F)=',F7.3)
1382.            GO TO 679
1383.          677 IF(ABS(HFBOT-HFBOTN).LE.0.06)GO TO 679
1384.            ICOUNT=ICOUNT+1
1385.            IF(IPRI.EQ.0)GO TO 224
1386.            PRINT 277
1387.            WRITE(6,734)FLRATE,TEMPMX
1388.          734 FORMAT('-','FLOW RATE=',F7.3,5X,'NEW INITIAL TEMPERATURE=',
1389.           1 F7.3)
1390.            WRITE(6,735)TEB,PEB(1)
1391.          735 FORMAT(' ','OLD INITIAL TEMPERATURE=',F7.3,5X,'OLD PRESSURE=',
1392.           1 F9.5)
1393.            PRINT 277
1394.          224 TEB=TEMPMX
1395.            PEVINN=PEB(1)
1396.            PRESS=PEVINN
1397.          679 IF(FLOCND.GT.0.0)GO TO 1004
1398.            IF(ZCOND.GT.(ELEV-HDIAMC))GO TO 1005
1399.            LIQF=(1.0-VOIDF)*(((IDC**2)*NTUBEC)/(IDLC**2))
1400.            VOIDF=1.0-LIQF
1401.            VOIDFS=VOIDFS+(VOIDF*(ELEV-ZCOND-HDIAMC)*XALORX)+HEDVLC
1402.            LIQFS=LIQFS+(((LIQF*(ELEV-ZCOND-HDIAMC))+ZCOND)*XALORX)
1403.            GO TO 359
1404.         1005 CALL VOIHDC (LHDCND,NTUBEC,HDIAMC,ELEV,ZCOND,PI,HEDVLC,VOFHDC,
1405.           1LIQHDC,NR)
1406.            LIQFS=LIQFS+LIQHDC+((ELEV-HDIAMC)*XALORX)
1407.            VOIDFS=VOIDFS+VOFHDC
1408.            GO TO 359
1409.         1004 LIQFS=LIQFS+HEDVLC+((ELEV-HDIAMC)*XALORX)
1410.          359 IF(IPRINT.EQ.0)GO TO 702
1411.            WRITE(6,1002)ZCOND
1412.         1002 FORMAT('-','LIQUID HEAD IN LOWER CROSS-OVER(FT)=',F9.5)
1413.            PRINT 223,QLOXO
1414.          223 FORMAT(' ','HEAT LOSS IN LOWER HEADER(BTU/HR)=',F9.4)
1415.            PRINT 277
1416.          702 CONTINUE
1417.            IF(VOIDFS.EQ.0.0)GO TO 959
1418.            SYSTVL=(HEITB*NTUBEE*XAEVAP)+(LUPXO*XAUPRX)+(HEITC*NTUBEC*XACOND)
1419.           1+((LLOXO+ELEV)*XALORX)+(RECRCL*XARCRC)+HEDVLE+HEDVLC
1420.            AVVOID=VOIDFS/SYSTVL
1421.            GO TO 957
1422.          959 AV VOID=0.0
1423.          957 AV LIQF=1.0-AV VOID
1424.            CALL   PERCNT(XAEVAP,NR,NTUBEE,XARCRC,XALORX,ELEV,LIQFS,PERLN
1425.           1G,SIGMA,HEITB,XACOND,NTUBEC,ZCOND,FLOCND,THETA,ALPHA)
1426.            QEFLUX=QES/(AREAP*NTUBEE*NROWE)
1427.            QCFLUX=QCS/(AREAC*NTUBEC*NROWC)
1428.            QAVFLX=(QES+QCS)/((AREAC+AREAP)*NTUBEE*NR)
1429.            AVTSHS=(AVEVT1+AVEVT2)/2.0
1430.            IF(MODE.NE.3)GO TO 1996
1431.            IF(NROWE.EQ.1)AVEVT2=0.0
1432.            IF(NROWE.EQ.1)PERDY2=0.0
1433.            AVTSHS=(AVEVT1+AVEVT2)/2.0
1434.            IF(NROWE.EQ.1)AVTSHS=AVEVT1
1435.         1996 DELT=AVTSHS-AVTSCS
1436.            DEXPP=QEFLUX/DELT
1437.            BITA=BETA*(90.0/PI
1438.            CALL           SIUNIT(HEITB,IDH,HEITC,IDC,ELEV,LUPXO,IDUC,LLOXO,
1439.           1IDLC,PEB(1),TOTALF,QEFLUX,QCFLUX,QAVFL,QES,QCS,AVTSHS,AVTSCS,DELT,
1440.           1AVWATH,DEXPP,UOA,SGMA,THTA,ALFA,AGAM,BITA,AVVOID,AVLIQF,PERLNG,
```

```
     1441.          $TEB,QAVFLX,THOT1,THOT2,TW2,AVEVT1,AVEVT2,PRCFL,
     1442.          $TW2OUT,WCLWTR,EXTIDE,EXTIDC,ELEXT1,ELEXT2,ELEXT3,DEQVE,
     1443.          $DEQVC,PERDY1,PERDY2,PERDY3,HW2AVG,WHOTW1,WHOTW2,CNROTN,
     1444.          $MODE,QFLUX,UOUT,UOUTC)
     1445.           PRINT 277
     1446.           IF(FLAG4.EQ.0)GO TO 1006
     1447.           WRITE(6,1007)
     1448.      1007 FORMAT(' ','STATIC LIQUID LEVEL RESTS IN CONDENSER HEADER.')
     1449.      1006 FLAG4=0
     1450.           XX=TW2-TCOLD
     1451.           PRINT 277
     1452.           IF((ABS(TW2-TCOLD)).LE.0.5) GO TO. 3
     1453.           IICOUN=IICOUN+1
     1454.           IF(IICOUN.GE.2)GO TO 128
     1455.           IF(TW2-TCOLD)2,3,2
     1456.     C     CHANGING SATURATION TEMPERATURE IN THE CONDENSER
     1457.        2  CALL SAT PR(SATCON,P1)
     1458.           TEMPF=SATCON+XX
     1459.           CALL SAT PR(TEMPF,P2)
     1460.           PEVINN=PEB(1)+(XX/(RCOND*1500+XX/(P2-P1)))
     1461.           WRITE(6,122) PEVINN
     1462.      122  FORMAT('-','NEW PRESSURE AT THE BOTTOM OF THE EVAPORATOR=',F9.5)
     1463.           WRITE(6,123) PEB(1)
     1464.      123  FORMAT(' ','OLD PRESSURE AT THE BOTTOM OF THE EVAPORATOR=',F9.5)
     1465.           TSAT1=TSATEB
     1466.           PRESS=PEVINN
     1467.           TC1=TCOLD
     1468.           PRINT 277
     1469.           GO TO 308
     1470.      128  TSATEN=TSATEB+((TSAT1-TSATEB)/(TC1-TCOLD))*XX
     1471.           TEMPF=TSATEN
     1472.           CALL SAT PR(TEMPF,PSAT)
     1473.           PEVINN=PSAT
     1474.           PRINT 122,PEVINN
     1475.           PRINT 123,PEB(1)
     1476.           TC1=TCOLD
     1477.           TSAT1=TSATEB
     1478.           PRESS=PEVINN
     1479.           PRINT 277
     1480.           GO TO 308
     1481.        3  WRITE(6,129)
     1482.      129  FORMAT('-','CONVERGENCE OBTAINED ON THE COLD FLUID TEMPERATURE')
     1483.      121  PRINT 277
     1484.           STOP
     1485.           END
     1486.           SUBROUTINE DTINPO(TSHF,TSAT,PECLET,DITI)
     1487.     C     THIS SUBROUTINE ESTIMATES THE TEMPERATURE DIFFERENCE REQUIRED TO
     1488.     C     MAINTAIN BOILING.
     1489.           DITI=(TSHF-TSAT)*((1.0/7000.0)*PECLET-(11.0/7.0))
     1490.           IF(PECLET.LE.11000.0)DITI=0.0
     1491.           IF(PECLET.GE.18000.0)DITI=(TSHF-TSAT)
     1492.           RETURN
     1493.           END
     1494.           SUBROUTINE FRCSHN(FLRATE,DIAM,DENS,VISC,PI,F,VF)
     1495.     C     THIS SUBROUTINE CALCULATES THE FRICTION FACTOR
     1496.           IF(FLRATE.GT.0.0)GO TO 1
     1497.           F=0.0
     1498.           VF=0.0
     1499.           GO TO 2
     1500.         1 VF=FLRATE*4.0/(PI*(DIAM**2.0)*DENS)/3600.0
     1501.           RE=VF*DIAM*DENS/VISC
     1502.           F=0.046*4.0/(RE**0.2)
     1503.           IF(RE.LT.2000.0)F=64.0/RE
     1504.         2 RETURN
     1505.           END
     1506.           SUBROUTINE BULKPT(HF,HFL,HFLOLD,HFOLD,LO,LN,PO,PRESS,FLRATE,Q,
     1507.          $TSHFO,TSHF,VOIDO,VOIDF,TSAT)
     1508.     C     THIS SUBROUTINE CALCULATES THE POINT WHERE BULK BOILING HAS STARTED
     1509.           REAL LO,LN
     1510.           A=(LN-LO)
     1511.           B=HFOLD-(((HF-HFOLD)/A)*LO)
     1512.           C=HFLOLO-(((HFL-HFLOLD)/A)*LO)
     1513.           LN=((B-C)*A)/((HFL-HFLOLD)-(HF-HFOLD))
     1514.           PRESS=PO-(((LN-LO)/A)*(PO-PRESS))
     1515.           CALL SATTEM(PRESS,TSAT)
     1516.           CALL HFLS(TSAT,HFL)
     1517.           HFOLD=HF
     1518.           HF=HFL
     1519.           Q=Q-((HFOLD-HF)*FLRATE)
     1520.           TSHF=TSHFO+(((LN-LO)/A)*(TSHF-TSHFO))
```

```
      VOIDF=VOIDO+(((LN-LO)/A)*(VOIDF-VOIDO))
      RETURN
      END
      SUBROUTINE SBCOOL(TSHF,TSAT,TSHFO,TSATO,LO,LN,PO,PRESS,2,TEMPFO,
     3TEMPF,HF,HFL,FLRATE,THPP)
C     THIS SUBROUTINE CALCULATES THE POINT WHERE SUBCOOLED BOILING HAS STARTED
      REAL LO,LN
      A=LN-LO
      B=TSHFO-(((TSHF-TSHFO)/A)*LO)
      C=TSATO-(((TSAT-TSATO)/A)*LO)
      LN=((B-C)*A)/((TSAT-TSATO)-(TSHF-TSHFO))
      TSHF=B+(((TSHF-TSHFO)/A)*LN)
      TSAT=TSHF
      THPP=TSHF
      PRESS=EXP(((-4623.39)/(TSAT+410.6652))+12.2055)
      TEMPF=TEMPF-((1.0-((LN-LO)/A))*(TEMPF-TEMPFO))
      CALL HFLS(TSAT,HFL)
      HFOLD=HF
      CALL LIQHF(TEMPF,HF)
      Q=Q-((HFOLD-HF)*FLRATE)
      RETURN
      END
      SUBROUTINE SAT PR(TEMPF,PSAT)
C     THIS SUBROUTINE CALCULATES THE SATURATION PRESSURE FOR A
C     GIVEN TEMPERATURE
      PSAT=EXP((-4623.38/(TEMPF+410.6652))+12.2055)
      RETURN
      END
      SUBROUTINE SAT TEM(PRESS,TSAT)
C     THIS SUBROUTINE CALCULATES THE SATURATION TEMPERATURE FOR A
C     GIVEN PRESSURE
      TSAT=(-4623.38/(ALOG(PRESS)-12.2055))-410.6652
      RETURN
      END
      SUBROUTINE LIQ HF(TEMPF,HFL )
C     THIS SUBROUTINE CALCULATES LIQUID ENTHALPY FOR A GIVEN TEMPERATURE
      HFL  =8.1634845+0.1993021*TEMPF+0.000091623*(TEMPF**2)+0.00000042
     31026*(TEMPF**3)+0.0000000012*(TEMPF**4)
      RETURN
      END
      SUBROUTINE LIQ DEN(TEMPF,DENSL)
C     THIS SUBROUTINE CALCULATES DENSITY OF LIQUID FOR A GIVEN TEMPER
      DENSL=98.216372-0.07441*TEMPF-0.0000660245*(TEMPF**2)+0.0000001505
     3*(TEMPF**3)-0.00000000067*(TEMPF**4)
      RETURN
      END
      SUBROUTINE LAT HT(TCR,TEMPF,HFG)
C     THIS SUBROUTINE CALCULATES LATENT HEAT OF EVAPORATION FOR A
C     GIVEN TEMPERATURE
      HFG=2.6154541+0.246939*ALOG(TCR-TEMPF)+0.0095585*((ALOG(TCR-TEMPF
     3))**2)
      HFG=EXP(HFG)
      RETURN
      END
      SUBROUTINE SUR TEN(PAR,DENSL,DENSG,MWT,SURFTN)
C     THIS SUBROUTINE CALCULATES SURFACE TENSION FOR GIVEN PARACHOR,
C     LIQUID DENSITY,GAS DENSITY,MOLECULAR WEIGHT
      REAL MWT
      SURFTN=((PAR*(DENSL-DENSG)*0.01602/MWT)**4)*(2.2481/((10**6)*0.03
     32281))
      RETURN
      END
      SUBROUTINE LIQ VIS(TEMPF,VISCL)
C     THIS SUBROUTINE FINDS LIQUID VISCOSITY FOR A GIVEN TEMPERATURE
      VISCL=-3.9026924+(1640.191052323/(TEMPF+460.0))
      VISCL=EXP(VISCL)*0.000672
      RETURN
      END
      SUBROUTINE TH COND(TEMPF,KL)
C     THIS SUBROUTINE CALCULATES THERMAL CONDUCTIVITY FOR A GIVEN TEMP.
C     TEMPERATURE
      REAL KL
      KL=(0.056-0.000111*(TEMPF-32.0))/3600.0
      RETURN
      END
      SUBROUTINE MT COND(TEMPF,KM)
C     THIS SUBROUTINE FINDS THERMAL CONDUCTIVITY OF METAL FOR GIVEN
C     TEMPERATURE
      REAL KM
      KM=224.0-((TEMPF-32.0)/30.0)
```

```
      RETURN
      END
      SUBROUTINE LIQ CP(TEMPF,SPHTL)
C     THIS SUBROUTINE CALCULATES SP. HEAT OF LIQUID FOR A GIVEN TEMP.
      SPHTL=1.219353-(164.748862/(TEMPF+460.0))
      SPHTL=EXP(SPHTL)
      RETURN
      END
      SUBROUTINE GAS VIS(TEMPF,VISCG)
C     THIS SUBROUTINE CALCULATES GAS VISCOSITY FOR A GIVEN TEMPERATURE
      VISCG=-3.679208963-(454.8512191/(TEMPF+460.0))
      VISCG=EXP(VISCG)*0.000672
      RETURN
      END
      SUBROUTINE GAS CP(TEMPF,SPHTG)
C     THIS SUBROUTINE CALCULATES THE SP. HEAT OF GAS FOR A GIVEN TEMP.
      SPHTG=0.03433333+0.003272*TEMPF-0.000035341*(TEMPF**2)+0.000000155
     3*(TEMPF**3)-0.000000000023022*(TEMPF**4)
      RETURN
      END
      SUBROUTINE VISHGW(TSHF,VISWAL)
C     THIS SUBROUTINE CALCULATES GAS VISCOSITY AT THE WALL TEMPERATURE
C     OF THE EVAPORATOR
      VISWAL=-3.679208963-(454.8512191/(TSHF+460.0))
      VISWAL=EXP(VISWAL)*0.000672
      RETURN
      END
      SUBROUTINE VISHLW(TSHF,VISWAL)
C     THIS SUBROUTINE CALCULATES LIQ. VISCOSITY AT THE WALL TEMPERATURE
C     OF THE EVAPORATOR
      VISWAL=-3.902692+(1640.191052323/(TSHF+460.0))
      VISWAL=EXP(VISWAL)*0.000672
      RETURN
      END
      SUBROUTINE HFLS(TST,HFL)
C     THIS SUBROUTINE CALCULATES THE SATURATED ENTHALPY
      HFL=8.1634845+0.1993021*TS T +0.00091623*(TS T **2)-0.0003304210
     926*(TS T **3)+0.000000012*(TS T **4)
      RETURN
      END
      SUBROUTINE HFGTS(TCR,TST,HFGO)
C     THIS SUBROUTINE CALCULATES THE LATENT HEAT
      HFGO=2.6154541+0.246938*ALOG(TCR-TS T )+0.0095585*((ALOG(TCR-TS T)
     9)**2)
      HFGO=EXP(HFGO)
      RETURN
      END
      SUBROUTINE VISCLW(TSCF,VISWAL)
C     THIS SUBROUTINE CALCULATES LIQ. VISCOSITY AT THE WALL TEMPERATURE
C     OF THE CONDENSER
      VISWAL=-3.902692+(1640.191052323/(TSCF+460.0))
      VISWAL=EXP(VISWAL)*0.000672
      RETURN
      END
      SUBROUTINE VISGW(TSCF,VISWAL)
C     THIS SUBROUTINE CALCULATES GAS VISCOSITY AT THE WALL TEMPERATURE
C     OF THE CONDENSER
      VISWAL=-3.679208963-(454.8512191/(TSCF+460.0))
      VISWAL=EXP(VISWAL)*0.000672
      RETURN
      END
      SUBROUTINE VOOHDE(LNHOR,HEDIAM,ZRECRC,HEITB,SIGMA,HEDVOL,PI,NTUBE
     9E,VOFHDE,LIQHDE,FLAG3)
C     THIS SUBROUTINE CALCULATES THE VOLUME OF LIQUID & VAPOUR IN THE
C     EVAPORATOR OUTLET HEADER
      REAL LIQHDE
      INTEGER FLAG3
      IF(ZRECRC.LE.(HEITB*COS(SIGMA)))GO TO 1
      IF(ZRECRC.GT.((HEITB*COS(SIGMA))+(HEDIAM/2.0)))GO TO 2
      X=(HEDIAM/2.0)-(ZRECRC-(HEITB*COS(SIGMA)))
      CALL TUBVOL(HEDIAM,LNHOR,NTUBES,X,VOL,PI)
      LIQHDE=VOL
      VOFHDE=HEDVOL-LIQHDE
      GO TO 3
    2 X= ZRECRC-(HEITB*(COS(SIGMA)))-(HEDIAM/2.0)
      CALL TUBVOL(HEDIAM,LNHOR,NTUBES,X,VOL,PI)
      VOFHDE=VOL
      LIQHDE=HEDVOL-VOFHDE
      GO TO 3
    1 VOFHDE=HEDVOL
```

```
      LIQHDE=0.0
      FLAG3=1
    3 RETURN
      END
      SUBROUTINE VODHDC(LNHDR,NTUBEC,HEDIAM,ELEV,ZCOND,PI,HEDVOL,VDFHDC,
     3LIQHDC,NR)
C     THIS SUBROUTINE CALCULATES THE VOLUME OF LIQUID & VAPOUR IN THE
C     CONDENSER OUTLET HEADER
      REAL LIQHDC
      IF(ZCOND.GT.(ELEV-(HEDIAM/2.0)))GO TO 1
      X=(ELEV-(HEDIAM/2.0))-ZCOND
      CALL TUBVOL(HEDIAM,LNHDR,NTUBEC,X,VOL,PI)
      LIQHDC=VOL
      VDFHDC=HEDVOL-LIQHDC
      GO TO 2
    1 X=ZCOND-(ELEV-(HEDIAM/2.0))
      CALL TUBVOL(HEDIAM,LNHDR,NTUBEC,X,VOL,PI)
      VDFHDC=VOL
      LIQHDC=HEDVOL-VDFHDC
    2 RETURN
      END
      SUBROUTINE PERCNT(XAEVAP,NR,NTUBEE,XARCRC,XALCRX,ELEV,LIQFS,PERLN
     3G,SIGMA,HEITB,XACOND,NTUBEC,ZCOND,FLDCND,THETA,ALPHA)
C     THIS SUBROUTINE CALCULATES THE % STATIC CHARGE IN THE EVAPORATOR
      REAL LIQFS
      NROWC=NR
      IF(ELEV.EQ.0.0)GO TO 91
      IF(FLDCND.EQ.0)GO TO 93
      GO TO 94
   93 X=LIQFS/(((XAEVAP*NR*NTUBEE)/COS(SIGMA))+2.0*XARCRC+XALCRX)
      GO TO 92
   94 X=LIQFS/(((XAEVAP*NR*NTUBEE)/COS(SIGMA))+2.0*XARCRC+((NR*NROWC*XAC
     3OND)/COS(ALPHA)))
      GO TO 92
   91 X=LIQFS/(((XAEVAP*NR*NTUBEE)/COS(SIGMA))+2.0*XARCRC+((NR*NROWC*XAC
     3OND)/COS(ALPHA)))
   92 PERLNG=((X/(COS(SIGMA)*SIN(THETA)))/HEITB)*100.0
      RETURN
      END
      SUBROUTINE TUBVOL(HEDIAM,LNHDR,NTUBE,X,VOL,PI)
C     THIS SUBROUTINE CALCULATES THE VOLUME OF LIQUID & VAPOUR
      R=HEDIAM/2.0
      THETA=ARCOS(X/R)
      A=(2.0*THETA*PI)/180.0
      B=2.0*THETA
      C=SIN(B)
      VOL=LNHDR*(R**2.0/2)*(A-C)
      RETURN
      END
      SUBROUTINE WTRPRP(TEMP,DENSW,VISCW,KW)
C     THIS SUBROUTINE CALCULATES THE PROPERTIES FOR WATER
      REAL KW
      DENSW=62.3777+(0.003684*TEMP)-(0.0000746*(TEMP**2.0))
      VISCW=(2.2975-(0.02236*TEMP)+(0.00006187*(TEMP**2.0)))*0.000672
      KW=(0.3174239+0.0004397*TEMP)/3600.0
      RETURN
      END
      SUBROUTINE LIQVOL(FRECRC,VLIQHE)
C     THIS SUBROUTINE CALCULATES THE LIQUID VOLUME IN EVAP VAP. HEADER
      VLIQHE=1.4*(FRECRC/210.0)
      VLIQHE=VLIQHE/1728.0
      RETURN
      END
      SUBROUTINE VOL(CNROTN,VSTRAN,THETA)
C     THIS SUBROUTINE CALCULATES THE LIQUID VOLUME IN THE SEPARATOR
      VSTRAN=0.500/1728.0
      IF(CNROTN.EQ.0)VSTRAN=VSTRAN*(1-COS(THETA))
      RETURN
      END
      SUBROUTINE CNLQHR(FLRATE,NTUBEC,XACOND,DENSL,VISCL,IDH,GC,FLHDCND,
     3VOLUME)
C     THIS SUBROUTINE CALCULATES THE LIQUID VOLUME IN THE CONDENSER LIQUID
C     HEADER
      REAL IDH,LHDCND
      FLRATE=FLRATE*NTUBEC
      VEL=((FLRATE/3600.0)/(XACOND*DENSL))
      REN=(DENSL*VEL*IDH)/VISCL
      F=64.0/REN
      IF(REN.GT.2000.0)F=((4.0*0.079)/(REN**0.25))
      DELP=((F*1.5*VEL*VEL*DENSL)/(2.0*GC*IDH))
```

```
      Z=(DELO/DENSL)*12.0
      VOL=Z*(LHOCND*12.0)
      VOLUME=VOL/1728.0
      FLRATE=FLRATE/NTUBEC
      RETURN
      END
      SUBROUTINE PRLIMT(TAIR,THOTG,PEBEST,DENSL,PMIN,PMAX)
C     THIS SUBROUTINE CALCULTES THE MAX. & MIN. PRESSURES FOR THE SYSTEM
      TEMPF=TAIR
      CALL SAT PR(TEMPF,PMIN)
      TEMPF=THOTG
      CALL SAT PR(TEMPF,PMAX)
      CALL LIQ DEN(TEMPF,DENSL)
      PRINT 1,PMIN
    1 FORMAT('-','MINIMUM  PRESSURE LIMIT FOR THE SYSTEM(PSIA)=',F9.5)
      PRINT 2,PMAX
    2 FORMAT('-','MAXIMUM  PRESSURE LIMIT FOR THE SYSTEM(PSIA)=',F9.5)
      RETURN
      END
      SUBROUTINE  MASS FL(PI,IDH,HEITB,TEMPF,FLRATE,TCR)
C     THIS SUBROUTINE CALCULATES THE MASS FLOW RATE OF THE WORKING FLUID
      REAL IDH,KL
      FLRATE=10.0
      X=0.45
      AREAS=PI*IDH*HEITB
      AREAXS=(PI/4.0)*(IDH**2.0)
      TWALL=TEMPF+8.0
      CALL GAS VIS (TEMPF,VISCG)
      CALL LIQ VIS (TEMPF,VISCL)
      CALL TH COND (TEMPF,KL)
      CALL LAT HT(TCR,TEMPF,HFG)
      CALL LIQ CP(TEMPF,SPHTL)
    2 FL=FLRATE
      VIS2P=1.0/(X/VISCG+(1.0-X)/VISCL)
      H2P=0.033*(KL/IDH)*((IDH*GF/VIS2P)**0.87)*((SPHTL*VISCL/KL)**0.4)
      QIN=H2P*AREAS*(TWALL-TEMPF)
      FLRATE=QIN/(HFG*X)
      IF(((ABS(FLRATE-FL))/FL)-0.1)1,1,2
    1 RETURN
      END
      SUBROUTINE AIRDEN(AIRTEM,DENAIR)
C     THIS SUBROUTINE CALCULATES THE DENSITY OF AIR
      B1=0.0860146816
      B2=-1.83631126*(1.0/10000.0)
      B3=2.3819835*(1.0/10000000.0)
      DENAIR=B1+B2*AIRTEM+B3*AIRTEM*AIRTEM
      RETURN
      END
      SUBROUTINE  EFF(DISC,AREA,TAIR,PI,INDIA,OUTDIA,CPAIR,GC,ROUT,
     1TCR,DENAIR,CF,DUCTXS,ALPHA,ALFMIN,TUSPCE,LENGTH,UA)
C     THIS SUBROUTINE CALCULATES THE AIR SIDE RESISTANCE
      REAL INDIA,OUTDIA,KL,KM,MASAIR,LENGTH
      VELAIR=DISC/DUCTXS
      TSAT=120.0
      TWALL=110.0
      TEMPF=(TSAT+TWALL)/2.0
      B0=0.59718992
      B1=-0.08137122
      B2=5.8313175*(1.0/1000)
      B3=-1.5054689*(1.0/10000)
      EFFC=B0+B1*VELAIR+B2*(VELAIR**2)+B3*(VELAIR**3)
      MASAIR=(DENAIR*VELAIR*3600.0)*(LENGTH*TUSPCE/12.0)
      UA=(MASAIR*CPAIR)*(ALOG(1.0/(1.0-EFFC)))
      DENSL=72.708
      DENSG=0.29789
      KL=0.04865/3600.0
      HFG=75.461
      VISCL=0.4645/3600.0
      CALL  HT COND(TEMPF,KM)
   72 HTCFNT=0.943*3600.0*(((KL**3)*(DENSL**2)*HFG*GC/(VISCL*LENGTH))
     1**0.25)
      IF(ALPHA.GT.ALFMIN)HTCFNT=CF*3600.0*(((KL**3)*(DENSL**2)*HFG*GC/
     1(VISCL*INDIA))**0.25)
      HCOND=HTCFNT/((TSAT-TWALL)**0.25)
      RINSID=1.0/(HCOND*PI*INDIA*LENGTH)
      RWALL=(ALOG(OUTDIA/INDIA))*(1.0/(2*PI*LENGTH*KM))
      ROUT=1.0/UA-(RINSID+RWALL)
      Q=MASAIR*CPAIR*EFFC*(TWALL-TAIR)
      TWALLN=TAIR+Q/UA
      IF(ABS(TWALLN-TWALL).LE.0.6)GO TO 77
```

```
      TWALL=TWALLN
      GO TO 72
   77 RETURN
      END
      SUBROUTINE QLOSS(A1,TEB,TROOM,LBE,RESBE,HFBOT,QBE,HBOTBE)
C     THIS SUBROUTINE CALCULATES THE HEAT LOSS FROM THE TUBES BELOW THE EVAP.
      REAL LBE
      CALL LIQCP(TEB,SPHTL)
      EFFECT=1.0-(EXP(-(LBE/(RESBE*A1*SPHTL))))
      IF(EFFECT.EQ.1.0)TEMPBE=TEB
      IF(EFFECT.EQ.1.0)GO TO 356
      TEMPBE=(TEB-(EFFECT*TROOM))/(1.0-EFFECT)
  356 QBE=EFFECT*A1*SPHTL*(TEMPBE-TROOM)
      HBOTBE=HFBOT+(QBE/A1)
      RETURN
      END
      SUBROUTINE DELPBE(FLRATE,LBE,LEQBE,GC,ZBE,IDBE,DPEVAP,NTUBES,PI,
     1DENSL,VISCL,XABE,DLPBE,DPDL,LENGTH,DENSG,VISCG,IDUC,NELBOW,
     1LETMCH,DPNONH,DPTEE,DPELBO,DPEXIT)
C     THIS SUBROUTINE CALCULATES THE PRESSURE DROP FOR THE TUBES BELOW
C     THE EVAPORATOR
      REAL LBE,LEQBE,IDBE,IDUC,LENGTH,LETMCH
      FLRATE=FLRATE*NTUBES
      GFBE=FLRATE/XABE/3600.0
      RENBE=(IDBE*GFBE)/VISCL
      IF(PENBE-2000.0)698,698,699
  698 F=64.0/RENBE
      GO TO 605
  699 F=4.0*0.079/(RENBE**0.25)
  605 DLPBE=((F*(LBE+LEQBE)/IDBE*(((GFBE/DENSL)**2.0)/2.0/GC)*DENSL)+
     1(ZBE*DENSL))/144.0
      DPNONH=DPDL*LENGTH/144.0
      XAVAPH=(IDUC**2.0)*(PI/4)
      GFVAPH=FLRATE/XAVAPH/3600.0
      DPTEE=1.8*((GFVAPH/DENSG)**2.0)*(1.0/(2.0*GC))
      DPELBO=NELBOW*0.9*(1.0/(2.0*GC))*((GFVAPH/DENSG)**2.0)
      DPEXIT=1.0*(1.0/(2.0*GC))*((GFVAPH/DENSG)**2.)
      RENTOP=(IDUC*GFVAPH)/VISCG
      IF(PENTOP-2000.0)98,98,99
   98 F=64.0/RENTOP
      GO TO 7
   99 F=4.0*0.079/(RENTOP**0.25)
    7 DPEVAP=((F*LETMCH/IDUC*(((GFVAPH/DENSG)**2.0)/2.0/GC)*DENSG)/144.0
      RETURN
      END
      SUBROUTINE SCOOLB(KL,HFG,SURFTN,TSAT,DENSG,DENSL,PI,IDH,LENGTH,
     1REN,VISCL,PRF,VL,TEMPF,Q,QA,QQ)
C     THIS SUBROUTINE CALCULATES THE HEAT FLUX REQUIRED TO SUSTAIN
C     BOILING
      REAL KL,IDH,LENGTH
      QA=Q/(PI*IDH    *LENGTH)
      QQ1=QA
      CC=(778.2*KL*3600.0*HFG/(8.0*SURFTN*(TSAT+460.0)*((1./DENSG)-(1./
     1DENSL))))
  117 IF(PEN.LT.2000.0)GO TO 118
      CB=((IDH**0.2)*((VISCL/DENSL)**0.8)*(QQ1/3600.0)/(0.023*(PR**0
     1.4)*KL*(VL**0.8)))
      GO TO 119
  118 CB=(((QQ1/3600.0)/1.86/KL/.667)*((IDH*VISCL*LENGTH/(VL*DENSL*PRF))
     1 **0.3333))
  119 QQ=(CC*((CB-(TSAT-TEMPF))**2)*3600.0)
      IF(ABS(QQ-QQ1)-1.0)112,112,111
  111 QQDT=2*3600*CC*(CB-(TSAT-TEMPF))*CB/QQ1
      QQ1=QQ1+(QQ1-QQ)/QQDT
      GO TO 117
  112 RETURN
      END
      SUBROUTINE CRITQY(RENG,RENF,HFG,Q,PI,GC,IDH,LENGTH,DLNGTH,FBL,LFB,
     1DENSL,DENSG,SURFTN,VISCL,LIQF,X,IPRI,PRG,HITPC,HITP,GF,KG,
     1H2PI,XFB)
C     THIS SUBROUTINE CALCULATES THE CRITICAL QUALITY AND IF XCR>X,
C     SINGLE PHASE VAPOUR "HT" IS CALCULATED
      REAL IDH,LENGTH,LIQF,KG
      IF(LFB.GT.0)GO TO 54
      WEB=((1.39/(10**7))*RENG*((DENSL/DENSG)**0.60))*((IDH/
     1D0.0608)**(-0.48))
      XFB=SQRT(WEB NO*GC*SURFTN*DENSG/(GF*VISCL*((RENF/LIQF)**0.125)))
      IF(X.LE.XFB)GO TO 51
   54 LFB=LFB+1
      IF(IPRI.EQ.0)GO TO 127
```

```
      IF(LFB.EQ.1)PRINT 254,XFB,LENGTH
  254 FORMAT('-','TRANSITION TO MIST FLOW TAKES PLACE AT QUALITY=',F6.4,
     3X,'AND ATA A HEIGTH(FT)=',F8.4)
  127 FBL=FBL+DLNGTH
      IF(RENG.LT.2000.0)GO TO 52
      H2P2=(0.023*KG/IDH    )*(RENG**0.8)*(PRG**0.4)*3600.0
      GO TO 51
   52 H2P2=(1.86*KG/IDH    )*((RENG*PRG*IDH    /FBL)**0.3333)*3600.0
   51 HITPC=H2P1
      IF(X.GT.XFB)HITPC=H2P2
      RETURN
      END
      SUBROUTINE SPRESS(DLNGTH,DENSG,THETA,SIGMA,F,IDH,VF,GC,DENS,X,
     3DPH,DPF,DPA)
C     THIS SUBROUTINE CALCULATES PRESSURE DROP FOR SINGLE PHASE REGION
      REAL IDH
      IF(X.GE.1.0)GO TO 70
      DPA=0.0
      DPH=DLNGTH*DENSL*SIN(THETA)*COS(SIGMA)
      DPF=F*DLNGTH/IDH    *((VF**2.0)/2.0/GC)*DENSL
      GO TO 71
   70 VOIDF=1.0
      LIQF=0.0
      DPA=0.0
      XP=0.0
      PHI=1.0
      DPH=DLNGTH*DENSG*SIN(THETA)*COS(SIGMA)
      DPF=F*DLNGTH/IDH    *((VF**2.0)/2.0/GC)*DENSG
   71 RETURN
      END
      SUBROUTINE PRES2P(DPAC,DPA,DPACP,LIQF,DENSL,VOIDF,DENSG,THETA,
     3SIGMA,XBOTOM,F,DLNGTH,IDH,GF,GC,FLRATE,PI,X,XFB,RENF,RENG,XP,
     3VISCL,VISCG,PHI,IX)
      REAL IDH,LIQF
C     THIS SUBROUTINE CALCULATES TWO-PHASE PRESSURE DROP
   16 DPAC=(GF*GF/(DENSL*GC))*((((1.0-X)**2.0)/(1.0-VOIDF))+(X*X*DENSL/
     3(DENSG*VOIDF))-1.0)
      DPA=DPAC-DPACP
      DPACP=DPAC
      DENSM=(LIQF*DENSL+VOIDF*DENSG)
      DPH=DENSM*DLNGTH*SIN(THETA)*COS(SIGMA)
C     USING LOCKHART & MARTINELLI METHOD TO FIND TWO-PHASE PRESS DROP
      CALL     XPCAL(RENF,RENG,VISCL,VISCG,DENSL,DENSG,X,XP)
      IF(IX.GT.0)GO TO 529
      CALL     PHICAL(RENF,RENG,PHI,XP)
      IF(XBOTOM.LE.0.0)GO TO 529
      DPF=F*DLNGTH/IDH*(((GF/DENSL)**2.0)/2.0/GC)*DENSL
      DPF=DPF*(PHI**2.0)
      RENG1=4.0*FLRATE*X/(PI*IDH*VISCG)/3600.0
      VG1=(RENG1*VISCG)/(IDH*DENSG)
      F=0.046*4.0/(RENG1**0.2)
      IF(RENG1.LT.2000.0)F=64.0/RENG1
      DPFG=F*DLNGTH/IDH*((VG1**2.0)/2.0/GC)*DENSG
      IF(X.GT.XFB)DPF=(((X-XFB)*DPFG)+((1.0-X)*DPF))/(1.0-XFB)
  529 RETURN
      END
      SUBROUTINE TWOPHE(X,VISCG,VISCL,H2P1,KL,IDH,GF,SPHTL)
C     THIS SUBROUTINE CALCULATES THE TWO PHASE HEAT TRANSFER COEFF.
      REAL IDH,KL
      VIS2P=1.0/(X/VISCG+(1-X)/VISCL)
      H2P1=0.033*(KL/IDH)*((IDH*GF/VIS2P)**0.87)*((SPHTL*VISCL/KL)**0.4)
     3*3600.0
      RETURN
      END
      SUBROUTINE CONCOF(KL,DENSL,HFG,GC,VISCL,LCNDSN,ALPHA,ALFMIN,IDC,
     3HF,HFL,FLRATE,TSAT,AHTCND,HW2,HTCFCN,CF,TCNDWL,QCOND,TCOLD)
C     THIS SUBROUTINE CALCULATES THE CONDENSATION COEFFICIENT IN THE CONDENSER.
      REAL KL,LCNDSN,IDC
      HTCFNT=0.943*3600.0*(((KL**3)*(DENSL**2)*HFG*GC/(VISCL*LCNDSN))
     3**0.25)
      IF(ALPHA.GT.ALFMIN)HTCFNT=CF*3600.0*(((KL**3)*(DENSL**2)*HFG*GC/
     3(VISCL*IDC))**0.25)
      QCOND=(HF-HFL)*FLRATE
      TCNDWL=TSAT-((QCOND  /HTCFNT/AHTCND)**1.33333)
      HTCFCN=HTCFNT/((TSAT-TCNDWL)**0.25)
      RETURN
      END
      SUBROUTINE CORECT(TSHS,AVTSH,DO,O,OO,TSHW,TSHF,THICKH,KM,AREAH,
     3DLNGTH,HEITS,LENGTH,RM,II,LO,TEMPFO,IDH,PI,UF)
C     THIS SUBROUTINE MAKES CORRECTION FOR Q,TWALL IN THE SUBCOOL S
```

```
      C     BULK BOILING SUBROUTINES, AFTER THE POINT WHERE SUBCOOLED/
      C     BULK BOILING HAS BEEN LOCATED
            REAL KM,LENGTH,LO,IDH
            TSHS=TSHS-AVTSH
            DQ=Q-QD
            TSHF=TEMPF+(DQ/(UF*(LENGTH-LO)*(DH*PI)))
            TSHW=TSHF+(DQ*THICKH/(KM*(LENGTH-LO)*(DH*PI)))
            AVTSH=(TSHW+TSHF)/2.0
            TSHS=TSHS+AVTSH
            DLNGTH=(HEITB-LENGTH)/(RM-1)
            RETURN
            END
            SUBROUTINE HPOOLB(DTA,TSHF,TSAT,DITI,HITPB,SPHTL,HFG,CSF,HTFLUX,
           BEX,VISCL,SURFTN,DENSL,DENSG,TEMPF,PRF,X)
      C     THIS SUBROUTINE CALCULATES THE HEAT FLUX & THE BOILING HEAT
      C     TRANSFER COEFFICIENT
            DTA=TSHF-TSAT
            IF(DITI.GT.DTA)HITPB=0.0
            IF(DITI.GT.DTA)GO TO 7025
            DTB=DTA-DITI
            HTFLUX=(((SPHTL*DTB)/(HFG*CSF*(PRF**1.7)))**BEX)*((VISCL
           *HFG)/((SURFTN/(DENSL-DENSG))**0.5))
            HITPB=(HTFLUX/(TSHF-TEMPF))*3600.0
       7025 IF(X.LE.0.0)GO TO 508
        508 RETURN
            END
            SUBROUTINE SPHASE(AA,BB,CC,HH,Y,REN,KF,PR,FM,VISC,VISWAL,CG)
      C     THIS SUBROUTINE CALCULATES THE SINGLE PHASE HEAT TRANSFER COEFF.
      C     IN EVAPORATOR & CONDENSER
            REAL KF,AA
            IF(Y.GT.1.0)GO TO 131
        131 IF(REN-2000.0)5,6,6
          5 IF(Y.GT.1.0)GO TO 132
            DD=(1.86*KF/AA    *((REN *PR *AA    /BB)**0.333))*3600.0
            EE=DD *0.6667*FM
            GO TO 416
        132 DD=(1.86*KF/AA    *((REN *PR *AA    /BB )**0.333)*((VISC/VISW
           AL)**0.14))*3600.0 *0.6667
            EE=DD*FM
            GO TO 416
          6 IF(Y.GT.1.0)GO TO 134
            DD=(0.027*KF/AA    *(REN **0.8)*(PR **CC  ))*3600.0
            EE=DD*CG
            GO TO 416
        134 DD=(0.027*KF/AA    *(REN **0.8)*(PR **CC  )*((VISC/VISWAL)**0.14
           ))*3600.0
            EE=DD*CG
        416 HH=EE
            RETURN
            END
            SUBROUTINE XPCAL(RENF,RENG,VISCL,VISCG,DENSL,DENSG,X,XP)
      C     THIS SUBROUTINE CALCULATES THE LOCKHART-MARTINELLI PARAMETER
      C     "XP" AT THE EXIT QUALITY
            IF(RENF.GT.2000.0.AND.RENG.GT.2000.0)XP=((VISCL/VISCG)**0.1)*((
           DENSG/DENSL)**0.5)*(((1.0-X)/X)**0.9)
            IF(RENF.LE.2000.0.AND.RENG.GT.2000.0)XP=(RENG**(-0.4))*(((15.0/0.
           0046)*((1.0-X)/X)*(DENSG/DENSL)*(VISCL/VISCG))**0.5)
            IF(RENF.GT.2000.0.AND.RENG.LE.2000.0)XP=(RENF**0.4)*(((0.05/16.0)
           *((1.0-X)/X)*(DENSG/DENSL)*(VISCL/VISCG))**0.5)
            IF(RENF.LE.2000.0.AND.RENG.LE.2000.0)XP=(((1.0-X)/X)*(DENSG/DENSL)
           *(VISCL/VISCG))**0.5
            RETURN
            END
            SUBROUTINE PHICAL(RENF,RENG,PHI,XP)
      C     THIS SUBROUTINE CALCULATES THE LOCKHART-MARTINELLI PARAMETER "PHI"
            IF(RENF.GT.2000.0.AND.RENG.GT.2000.0)PHI=((1.0+XP**(-2.0*0.2433975
           ))**(1.0/0.2433975))**0.5
            IF(RENF.LE.2000.0.AND.RENG.GT.2000.0)PHI=((1.0+XP**(-2.0*0.2775379
           ))**(1.0/0.2775379))**0.5
            IF(RENF.GT.2000.0.AND.RENG.LE.2000.0)PHI=((1.0+XP**(-2.0*0.2920067
           ))**(1.0/0.2920067))**0.5
            IF(RENF.LE.2000.0.AND.RENG.LE.2000.0)PHI=((1.0+XP**(-2.0*0.3495069
           ))**(1.0/0.3495068))**0.5
            RETURN
            END
            SUBROUTINE DATA(IDH,IDC,THICKH,THICKC,HEITB,HEITC,LUPXO,LLOXO,
           SIGMA,THETA,ALPHA,GAM,ELEV,XXX,TAIR)
      C     THIS SUBROUTINE PRINTS THE DATA FOR THIS RUN IN S.I. & FPS UNIT
            REAL IDH,IDC,LUPXO,LLOXO
            INTEGER XXX
```

```
      PRINT 9020
 9020 FORMAT('1','----------
     @----------')
      WRITE(6,9019)
 9019 FORMAT('-','                                        DATA CARDS FOR THIS RUN
     @')
      PRINT 9022
 9022 FORMAT('-','----------
     @----------')
      IF(XXX.EQ.0)GO TO 7575
      QIDH=(IDH*30.48)/12.0
      QHEITB=HEITB*30.48
      QTHIK=(THICKH*30.48)/12.0
      QIDC=(IDC*30.48)/12.0
      QHEITC=HEITC*30.48
      QTHIC=(THICKC*30.48)/12.0
      QLUPXO=LUPXO*30.48
      QLLOXO=LLOXO*30.48
      QELEV=ELEV*30.48
      QTAIR=(TAIR-32.0)/1.8
      WRITE(6,9000) QIDH,IDH
 9000 FORMAT('-','EVAPORATOR: I.D. OF TUBES(CM)=',F9.5,3X,
     @'I.D. OF TUBES(INCHS)=',F7.3)
      WRITE(6,9001) QHEITB,HEITB
 9001 FORMAT('-','EVAPORATOR: LENGTH OF TUBES(CM)=',F7.2,3X,
     @'LENGTH OF TUBES(FEET)=',F7.3)
      WRITE(6,9002) QTHIK,THICKH
 9002 FORMAT('-','EVAPORATOR: THICKNESS OF TUBES(CM)=',F9.5,3X,
     @'THICKNESS OF TUBES(INCHS)=',F7.3)
      WRITE(6,9003) QIDC,IDC
 9003 FORMAT('-','CONDENSER : I.D. OF TUBES(CM)=',F9.5,3X,
     @'I.D. OF TUBES(INCHS)=',F7.3)
      WRITE(6,9004) QHEITC,HEITC
 9004 FORMAT('-','CONDENSER : LENGTH OF TUBES(CM)=',F7.2,3X,
     @'LENGTH OF TUBES(FEET)=',F7.3)
      WRITE(6,9005) QTHIC,THICKC
 9005 FORMAT('-','CONDENSER: THICKNESS OF TUBES(CM)=',F9.5,3X,
     @'THICKNESS OF TUBES(INCHS)=',F7.3)
      WRITE(6,9006) QLUPXO,LUPXO
 9006 FORMAT('-','LENGTH OF UPPER CROSS OVER TUBE(CM)=',F7.2,3X,
     @'LENGTH OF UPPER CROSS OVER TUBE(FEET)=',F7.2)
      WRITE(6,9007) QLLOXO,LLOXO
 9007 FORMAT('-','LENGTH OF LOWER CROSS OVER TUBE(CM)=',F7.2,3X,
     @'LENGTH OF LOWER CROSS OVER TUBE(FEET)=',F7.2)
      WRITE(6,9008) QELEV,ELEV
 9008 FORMAT('-','CONDENSER ELEVATION(CM)=',F7.2,3X,
     @'CONDENSER ELEVATION(FEET)=',F7.3)
      WRITE(6,9023) SIGMA,THETA
 9023 FORMAT('-','EVAPORATOR: INCLINATION(DEG)=',F6.2,3X,
     @'ROTATION(DEG)=',F6.2)
      WRITE(6,9024) ALPHA,GAM
 9024 FORMAT('-','CONDENSER: INCLINATION(DEG)=',F6.2,3X,
     @'ROTATION(DEG)=',F6.2)
      WRITE(6,9029) QTAIR,TAIR
 9029 FORMAT('-','INCOMING TEMPERATURE OF AIR(C)=',F7.2,3X,
     @'INCOMING TEMPERATURE OF AIR(F)=',F7.2)
      GO TO 9018
 7575 QIDH=(IDH/30.48)*12.0
      QHEITB=HEITB/30.48
      QTHIK=(THICKH/30.48)*12.0
      QIDC=(IDC/30.48)*12.0
      QHEITC=HEITC/30.48
      QTHIC=(THICKC/30.48)*12.0
      QLUPXO=LUPXO/30.48
      QLLOXO=LLOXO/30.48
      QELEV=ELEV/30.48
      QTAIR=32.0+TAIR*1.8
      WRITE(6,9000) IDH,QIDH
      WRITE(6,9001) HEITB,QHEITB
      WRITE(6,9002) THICKH,QTHIK
      WRITE(6,9003) IDC,QIDC
      WRITE(6,9004) HEITC,QHEITC
      WRITE(6,9005) THICKC,QTHIC
      WRITE(6,9006) LUPXO,QLUPXO
      WRITE(6,9007) LLOXO,QLLOXO
      WRITE(6,9009) ELEV,QELEV
      WRITE(6,9023) SIGMA,THETA
      WRITE(6,9024) ALPHA,GAM
      WRITE(6,9029) QTAIR,TAIR
      IDH=QIDH
```

```
      HEITB=OHEITB
      THICKH=OTHIK
      IDC=OIDC
      HEITC=OHEITC
      THICKC=OTHIC
      LUPXO=OLUPXO
      LLOXO=OLLOXO
      ELEV=OELEV
      TAIR=OTAIR
 9018 PRINT 9021
 9021 FORMAT('-','----------------------------------------------------
     $----------')
      RETURN
      END
      SUBROUTINE    SIUNIT(HEITB,IDH,HEITC,IDC,ELEV,LUPXO,IDUC,LLOXO,
     $IDLC,PSTART,TOTALF,QEFLUX,QCFLUX,QAVFL,QES,QCS,AVTSHS,AVTSCS,DELT,
     $AVWATH,UEXPR,UOA,SGMA,THTA,XLFA,AGAM,BITA,AVVOID,AVLIOF,PERLNG,
     $TEB,QAVFLX,THOT1,THOT2,TW2,AVEVT1,AVEVT2,PRCFL,
     $TW2OUT,MCLWTR,EXTIDE,EXTIDC,ELEXT1,ELEXT2,ELEXT3,DEQVE,
     $DEQVC,PERDY1,PERDY2,PERDY3,HW2AVG,MHOTW1,MHOTW2,CNROTN,
     $MODE,QFLUX,UOUT,UOUTC)
C     THIS SUBROUTINE CONVERTS ALL DATA IN S.I. UNITS
      REAL IDH,IDC,LUPXO,IDUC,LLOXO,IDLC,MHTWTR,MCLWTR
      SHEITB=HEITB*30.48
      SIDH=IDH*30.48
      SHEITC=HEITC*30.48
      SIDC=IDC*30.48
      SDEQVE=DEQVE*30.48
      SDEQVC=DEQVC*30.48
      SELEV=ELEV*30.48
      SWIDE=LUPXO*30.48
      SIDUC=IDUC*30.48
      IF(MODE.EQ.3)GOTO 919
      SLEXT1=(ELEXT1-32.0)/1.8
      SLEXT2=(ELEXT2-32.0)/1.8
      STW2OT=(TW2OUT-32.0)/1.8
      SMHT1=(MHOTW1*0.00755988)/60.0
      SMHT2=(MHOTW2*0.00755988)/60.0
      SMCL=(MCLWTR*0.00755988*3.0)/60.0
      SEXIDE=EXTIDE*30.48
      SEXIDC=EXTIDC*30.48
      SHW=AVWATH*5.6783
      SHW2=HW2AVG*5.6783
  919 SWIDER=LLOXO*30.48
      SIDLC=IDLC*30.48
      STEB=(TEB-32.0)/1.8
      STHOT1=(THOT1-32.0)/1.8
      STHOT2=(THOT2-32.0)/1.8
      STCOWA=(TW2-32.0)/1.8
      SPC=(PSTART*6894.8)
      SFLRT=(TOTALF*0.00755988)/60.0
      SQE=QEFLUX*3.152481
      SQC=QCFLUX*3.152481
      SQA=QAVFLX*3.152481
      SQES=QES*0.292875
      SQCS=QCS*0.292875
      SATH1=(AVEVT1-32.0)/1.8
      SATH2=(AVEVT2-32.0)/1.8
      SATC=(AVTSCS-32.0)/1.8
      SATH=(AVTSHS-32.0)/1.8
      SDT=DELT/1.8
      PRINT 920
  920 FORMAT('-','----------------------------------------------------
     $----------')
      WRITE(6,279)
  279 FORMAT('-',' RESULTS IN SI UNITS')
      PRINT 922
  922 FORMAT('-','----------------------------------------------------
     $----------')
      WRITE(6,822)SHEITB,SIDH,SGMA,THTA
  822 FORMAT('-','EVAPORATOR: LENGTH(CM)=',F7.2,3X,'I.D. OF TUBES(CM)
     $=',F9.5,3X,'INCLINATION(DEG)=',F6.2,3X,'ROTATION(DEG)=',F6.2)
      WRITE(6,680)SHEITC,SIDC,ALFA,AGAM
  680 FORMAT(' ','CONDENSER:  LENGTH(CM)=',F7.2,3X,'I.D. OF TUBES(CM)=',
     $F9.5,3X,'INCLINATION(DEG)=',F6.2,3X,'ROTATION(DEG)=',F6.2)
      IF(MODE.EQ.2.OR.MODE.EQ.3)GO TO 1961
      PRINT 968,SDEQVC
  968 FORMAT(' ','EQUIVALENT DIA. OF WATER JACKET OF THE EVAPORATOR(CM)=
     $',F9.3)
      PRINT 969,SDEQVE
```

```
      969 FORMAT(' ','EQUIVALENT DIA. OF WATER JACKET OF THE CONDENSER(CM)='
     3,F9.3)
     1961 WRITE(6,824)SELEV
      824 FORMAT(' ','CONDENSER ELEVATION(CM)=',F7.2)
          WRITE(6,682)SWIDE,SIDUC,BITA
      682 FORMAT(' ','LENGTH OF UPPER CROSS-OVER(CM)=',F7.2,3X,'I.D. OF TUBE
     3(CM)=',F9.5,3X,'INCLINATION(DEG)=',F6.2)
          WRITE(6,826)SWIDER,SIDLC
      826 FORMAT(' ','LENGTH OF LOWER CROSS-OVER(CM)=',F7.2,3X,'I.D. OF TUBE
     3(CM)=',F9.5)
          WRITE(6,602)STER
      602 FORMAT(' ','FINAL FREON TEMPERATURE(C)=',F7.3)
          WRITE(6,946)SPC
      946 FORMAT(' ','FINAL FREON PRESSURE(NEWTON/M2)=',F10.2)
          WRITE(6,807)SFLRT
      807 FORMAT(' ','FINAL FREON FLOW RATE(KGM/SEC)=',F10.7)
          WRITE(6,966)SQA
      966 FORMAT(' ','FINAL HEAT FLUX(WATT/M2)=',F11.3)
          IF(MODE.EQ.2)GO TO 1962
          IF(MODE.EQ.3)GO TO 921
          WRITE(6,299)SMHT1
      299 FORMAT(' ','MASS FLOW RATE OF HEATING FLUID ROW # 1(KGM/SEC)=',F10
     3.7)
          WRITE(6,699)SMHT2
      699 FORMAT(' ','MASS FLOW RATE OF HEATING FLUID ROW # 2(KGM/SEC)=',F10
     3.7)
     1962 WRITE(6,230)SMCL
      230 FORMAT(' ','MASS FLOW RATE OF COOLING FLUID(KGM/SEC)=',F10.7)
          IF(MODE.EQ.2) GO TO 1964
          WRITE(6,828)STHOT1,SLEXT1
      828 FORMAT(' ','INCOMING TEMP OF HEATING FLUID FOR ROW # 1(C)=',F7.3,
     33X,'OUTGOING TEMP OF HEATING FLUID(C)=',F7.3)
          WRITE(6,830)STHOT2,SLEXT2
      830 FORMAT(' ','INCOMING TEMP OF HEATING FLUID FOR ROW # 2(C)=',F7.3,
     33X,'OUTGOING TEMP OF HEATING FLUID(C)=',F7.3)
     1964 WRITE(6,832)STCOWA,STW2OT
      832 FORMAT(' ','INCOMING TEMP OF COOLING FLUID (C)=',F7.3,3X,'OUTGOING
     3 TEMP OF COOLING FLUID(C)=',F7.3)
      921 WRITE(6,834)SATH1
      834 FORMAT(' ','AVERAGE WALL TEMP FOR ROW # 1(C)=',F8.3)
          WRITE(6,835)SATH2
      835 FORMAT(' ','AVERAGE WALL TEMP FOR ROW # 2(C)=',F8.3)
          WRITE(6,811)SATH,SATC
      811 FORMAT(' ','AVERAGE HEATER SIDE WALL TEMP (C)=',F8.3,3X,'AVERAGE C
     3ONDENSER SIDE WALL TEMP(C)=',F8.3)
          WRITE(6,945)SDT
      945 FORMAT(' ','DIFFERENCE BETWEEN AVERAGE HEATER AND CONDENSER WALL T
     3EMPERATURES(C)=',F8.3)
          IF(MODE.EQ.2)GO TO 1965
          IF(MODE.EQ.3)SHW=UOUT*5.6783
          IF(MODE.EQ.3)SHW2=UOUTC*5.6783
          WRITE(6,600)SHW
      600 FORMAT(' ','AVG. OUTSIDE EVAP. HEAT TRANSFER COEF.(WATT/M2/C)=',
     3F10.2)
          WRITE(6,575)SHW2
      575 FORMAT(' ','AVG. OUTSIDE COND. HEAT TRANSFER COEF.(WATT/M2/C)=',
     3F10.2)
     1965 WRITE(6,855)SQES,SQCS
      855 FORMAT(' ','QIN EVAP.(WATT)=',F9.2,3X,'QOUT COND.(WATT)=',F9.2)
          WRITE(6,827)SQE,SQC,SQA
      827 FORMAT(' ','EVAP. FLUX(WATT/M2)=',F10.3,3X,'COND. FLUX(WATT/M2)=',
     3F10.3,3X,'AVG. FLUX(WATT/M2)=',F10.3)
          WRITE(6,941)AVVOID,AVLIQF
      941 FORMAT(' ','AVERAGE VOID FRACTION FOR ENTIRE LOOP=',F6.4,5X,
     3 'AVERAGE LIQUID FRACTION FOR ENTIRE LOOP=',F6.4)
          IF(THTA.NE.90.0)GO TO 711
          WRITE(6,570)PERLNG
      570 FORMAT(' ','PERCENT OF EVAP. LENGTH FLOODED UNDER: STATIC CONDITIO
     3N=',F5.1)
          GO TO 713
      711 WRITE(6,712)PERLNG
      712 FORMAT(' ','AVERAGE STATIC CHARGE IN THE EVAPORATOR=',F5.1)
      713 WRITE(6,970)PERDY1
      970 FORMAT(' ','PERCENT DYNAMIC CHARGE IN ROW # 1=',F5.1)
          WRITE(6,971)PERDY2
      971 FORMAT(' ','PERCENT DYNAMIC CHARGE IN ROW # 2=',F5.1)
          IF(CNROTN.EQ.0)GO TO 967
          IF(MODE.EQ.3)GO TO 967
          WRITE(6,572)PRCSL
      572 FORMAT(' ','APPARENT % DYNAMIC CHARGE(RECIRCULATION TUBE)=',F5.1)
```

```
      967 RETURN
          END
/*
//GO.SYSIN DD *
0.311 0.311 0.032 0.032 3.00 1.00 13.00 20.00  102.191
0.0  90.0  45.0  90.0  4.00  1.0  2  2  0
0.0  0.0  388.4 193.4 137.36854 0.01 1.80 1400  6.0
0.50  12  36  3.00  30.0  70.0  1000  102.191  1
1.0  1.0  1.0
50.333  27.0  1  1  1
1  1  1  1  5.0  2.0  0.0
447.6  1.0  0.545  0.430  1.0  0.311
3.0  0.8739  0.8739  0.24  275.00  0.311  79.08
3  4000.0
1.0  1.0  16.0  40.0  30.0
194.0
122.0
196.6
196.6
//
```

APPENDIX - H4

PROPERTY SUBROUTINES FOR R-113

```
      SUBROUTINE SAT PR(TEMPF,PSAT)
      PSAT=EXP(((-5084.637)/(TEMPF+406.3816))+12.3902)
      RETURN
      END
      SUBROUTINE SAT TEM(PRESS,TSAT)
      TSAT=(-5084.637/(ALOG(PRESS)-12.3902))-406.3816
      RETURN
      END
      SUBROUTINE LIQ HF(TEMPF,HFL )
      HFL  =7.1943386+0.2217*TEMPF-0.0000349*(TEMPF**2)+0.00000012914
     a*(TEMPF**3)+0.000000000026402*(TEMPF**4)
      RETURN
      END
      SUBROUTINE LIQ DEN(TEMPF,DENSL)
      DENSL=101.09509+0.02066*TEMPF-0.00109*(TEMPF**2)+0.0000043665
     a*(TEMPF**3)-0.000000006 2323*(TEMPF**4)
      RETURN
      END
      SUBROUTINE LAT HT(TCR,TEMPF,HFG)
      HFG=0.9198105+0.78294*ALOG(TCR-TEMPF)-0.038114*((ALOG(TCR-TEMPF
     a))**2)
      HFG=EXP(HFG)
      RETURN
      END
      SUBROUTINE SUR TEN(PAR,DENSL,DENSG,MWT,SURFTN)
      REAL MWT
      SURFTN=((PAR*(DENSL-DENSG)*0.01602/MWT)**4)*(2.2481/((10**6)*0.03
     a281))
      RETURN
      END
      SUBROUTINE LIQ VIS(TEMPF,VISCL)
      VISCL=-4.19153+(2030.8041/(TEMPF+460.0))
      VISCL=EXP(VISCL)*0.000672
      RETURN
      END
      SUBROUTINE TH COND(TEMPF,KL)
      REAL KL
      KL=(0.04775-0.0000625*TEMPF)/3600.0
      RETURN
      END
      SUBROUTINE LIQ CP(TEMPF,SPHTL)
      SPHTL=-0.8126-(366.0732/(TEMPF+460.0))
      SPHTL=EXP(SPHTL)
      RETURN
      END
      SUBROUTINE GAS VIS(TEMPF,VISCG)
      VISCG=(-0.9990031-(1992.131/(TEMPF+460.0)))
      VISCG=EXP(VISCG)*0.000672
      RETURN
      END
      SUBROUTINE GAS CP(TEMPF,SPHTG)
      SPHTG=0.16+(0.01/100)*(TEMPF-100)
      RETURN
      END
      SUBROUTINE VISHGW(TSHF,VISWAL)
      VISWAL=(-0.9990031-(1992.131/(TSHF+460.0)))
      VISWAL=EXP(VISWAL)*0.000672
      RETURN
      END
      SUBROUTINE VISHLW(TSHF,VISWAL)
      VISWAL=-4.19153+(2030.8041/(TSHF+460.0))
      VISWAL=EXP(VISWAL)*0.000672
      RETURN
      END
```

APPENDIX I

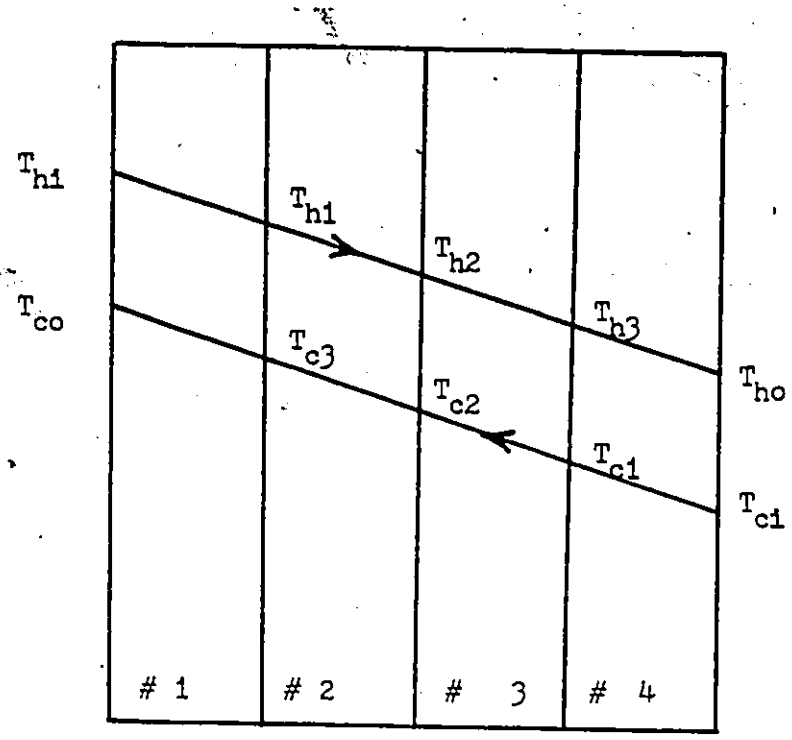

Assumption: Same temperature drop across each loop ($\dot{m}_h = \dot{m}_c$)

Temperature drop across evaporator for loop # 1 $\Delta T_1 = T_{hi} - T_{h1}$

Overall temperature difference for loop # 1 $OTD_1 = T_{hi} - T_{c3}$

Effectiveness for one loop $E_1 = \Delta T_1 / OTD_1$ ... (1)

Effectiveness for "n" loops $$E_n = \frac{n \Delta T_1}{OTD_n} = \frac{n \Delta T_1}{OTD_1 + (n - 1) \Delta T_1}$$

$$E_n = \frac{n E_1}{1 + (n - 1) E_1} \quad \ldots (2)$$

and $$OTD_1 = OTD_n - (n - 1) \Delta T_1$$

$$= OTD_n - (n - 1) E_1 \; OTD_1$$

or $$OTD_n = OTD_1 \left[1 + (n - 1) E_1 \right] \quad \ldots (3)$$

Using equation for the single loop, the effectiveness E_n and the overall temperature difference OTD_n for "n" loops can be predicted in terms of E_1 and OTD_1 from equations 2 and 3 respectively.

PUBLICATIONS WITH DR. T.W. McDONALD

PAPERS

1. Mathur, G.D. and McDonald, T.W. Simulation program for a two-phase thermosiphon-loop heat exchanger. ASHRAE Trans., Vol 92, Pt. 2, paper # 3005, June 1986.

2. Stauder, F.A., Mathur, G.D. & McDonald, T.W. Experimental and computer simulation study of an air-to-air two-phase thermosiphon-loop heat-exchanger. ASME paper # 85-WA/HT-15.

3. Mathur, G.D. & McDonald, T.W. Validation of simulation program for two-phase coil loop thermosiphon heat exchanger systems. Presented at world congress on heating ventilating and air conditioning, CLIMA 2000, Copenhagen, Denmark, Vol 6, pp 557-562, Aug. 1985.

ABSTRACT

1. Mathur, G.D. & McDonald, T.W. Simulation program for a two-phase thermosiphon loop heat exchanger. Presented at 10th Canadian congress of applied mechanics, London, Ontario, June 2-7, 1985.

VITA AUCTORIS

1956 Born in India (Roorkee) on 22nd September.

1974 Completed senior high school from Government Inter College, Roorkee, U.P., India.

1978 Received the degree of Bachelor of Engineering from the Department of Mechanical Engineering, Thapar Institute of Engineering & Technology, Patiala, Pb., India.

1980 Received the degree of Master of Engineering in Applied Thermoscience from the Department of Mechanical Engineering Roorkee University, Roorkee, U.P., India.

1986 Currently a candidate for the degree of Doctor of Philosophy in Mechanical Engineering at the University of Windsor, Windsor, Ontario, Canada.